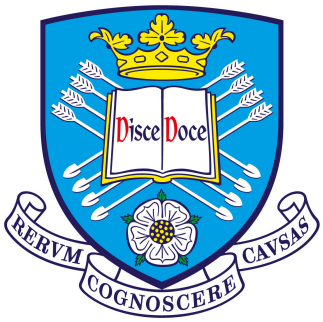

The University Of Sheffield.

Investigating Host Responses to *Salmonella* Typhi in Acute Typhoid Fever

Salma Srour

Department of Biosciences
University of Sheffield

This dissertation is submitted in partial fulfillment
of the requirements for the degree of

Doctor of Philosophy

September 2022

I would like to dedicate this thesis to my late grandfather, my loving parents and siblings whom I would not have achieved anything without their support...

Acknowledgment

I tried to summarize my acknowledgments, but I could not get myself to do that. I would never have achieved anything in my life, including this PhD, without the support of my beautiful community of supporting and nurturing people. So please bare with me as I try to acknowledge some of the people who helped me reach this major goal in my life. I cannot begin to express my gratitude to my amazing supervisor **Dr. Daniel Humphreys**, who is not the typical PhD supervisor, but a mentor to my personal growth journey. Daniel has always been one of the most excited people about my project and it was contagious that I could not talk about my project without a smile on my face. When I met Daniel for the first time I knew I will be investing time in a supervisor who will help me grow as a scientist and a person. Daniel was always there for a quick question and tolerated my unplanned meetings to discuss random results. I am so grateful he was my supervisor through this journey. I am utterly grateful for you Dan, and for everything you taught me and continue to teach me. I would also like to thank my secondary supervisor **Dr. Mark Collins**, for helping me understand and perform complex mass spectrometery and always teaching with passion the most complex of ideas. His passion made it easy on me to understand and enjoy. I would also like to thank **Dr. Andrew Furley** for his constant support and helpful suggestions throughout my PhD.

I would like to especially thank **Dr. Mohamed ElGhazaly**, who has been my immediate mentor since day one, for lending me a helping hand with big samples and datasets, but also in every experiment, random discussion and throughout thesis writing. Mohamed has patiently listened to me ramble and discuss experiments and stress about upcoming work to last him a life-time. I would also like to thank **Dr. Khoa Pham** for patiently teaching me a lot about affinity chromatography and for always giving me a hand with any issues proteomics related, and for always having an optimistic attitude that was contagious.

I would like to thank my supportive colleagues outside our office, who were always up for a quick chat and vent **Ola Shehata** and **Nagham Dous**. I would also like to thank members of the Collin's lab who always lend a listening ear, a supportive statement or a missing reagent **Dr. Hatoon Alamri**, **Weronika Buczek** and **Jorge Ferreira**. My thanks extends to all Humphreys lab members, including alumni, **Dr. Angela Ibler**, **Dr. Zhou Zhu**, **Dr. Mohamed ElGhazaly**, **Daniel Stark**, **Nadia Basser**, **Michelle**

King and **Nataya Deans**. Thank you **Mohamed**, **Daniel** and **Nadia** for being there for a supportive statement when I am being too hard on myself or in Nadia's case a big hug on a low moment. Particular gratitude to my PhD Escape Team or what I like to call my workplace support team, **Mohamed**, **Weronika**, **Jorge**, **Ola**, and **Nadia**. Thank you for your consistent support of me even during the lonely writing stage.

I would like to express my deepest appreciation and love to the biggest assets I made through the years, my chosen family, **Nada Adham**, **Hend ElGhazaly**, **Rania Tarek**, **Ola Shehata**, **Nagham Dous**, **Mark Fahmy**, **Mohamed ElGhazaly**, **Ahmed El-Sawaf**, **Omar Mokhtar**, and **Moataz Swidan**. Thank you **Nada** for always having an open door for a good meal and a refreshing talk after a long day, and for always being there through the lows before the highs. I am greatly indebted to you, grateful beyond words. Thank you **Hend** for always being there with immediate responses despite the 4 hours time difference. Thank you for keeping me company post midnight on long writing nights and for always being there no matter the occasion and regardless of distance, with a daily message checking on me. Thank you **Nada** and **Hend** for being like sisters throughout this journey. Thank you **Rania** and **Mark** for always checking on me with beautiful supportive messages when I need them the most and for always making every holiday back home special. And for being forever by my side since I can remember, no distance ever stopped you. I cannot thank **Mohamed** enough for being my friend, my workmate and my walking to and from work buddy. Whether it was a sudden crazy experimental idea or just needing to ramble, thank you for being there. **Omar**, you have been my company in every all-nighter I ever pulled off in my first year, making sure I remember to smile regardless of the stress. Thank you for always checking up on me despite the distance and being a phone call away. Thank you **Ahmed** for listening to my rambles that do not necessarily make sense, and for your nicely cooked meals during lockdowns. **Moataz**, your offers for driving us all places is only amongst the many reasons I am in gratitude to you. Thank you for making sure we all laugh despite the situation, ensuring no bad vibes.

Words cannot explain how grateful I am that my parents made sure I am never lonely and decided to bring to the world my amazing siblings, whom are forever my pride and joy. They are God's greatest gift to me. Thank you all for listening to me ramble about science when you do not necessarily understand the problem but offering a shoulder to cry on. Thank you for being the motivation for me to be who I am so that I would be a worthy role model for you three. Thank you **Youmna** for forever being the sound of reason in our lives. Thank you for listening to my breakdown moments out of stress and cooking me a meal on stressful days in stressful periods. Utterly grateful for **Ahmed** for being there in my lowest of times, even if it means he travels continents mid exam period on short notice, ensuring I am safe. And last but never least, **Shahd** for keeping me young and reminding me life is quite simple through her young eyes.

I would like to thank my grandfather **Gedo Ahmed Raafat** who is sadly not with us in this physical world but I know he is looking out for me. I want to thank him for giving me the title "Dr" since I was 10 and started to show interest in science. I want to thank him for believing in me so much in his life that it was a driver for me to continue even after his demise.

This dissertation, everything I ever achieved and everything I will achieve could not have been possible without the support of my loving parents **Prof. Dr. Mervat Rafaat** and **Prof. Dr. Hany Srour**. No words can ever capture what I am constantly feeling of utter gratitude and pride that you are my parents. I could not have asked for better parents who are nurturing, supportive both personally and academically. You made me the woman I am today teaching me to defy stereotypes and constantly take on learning opportunities. There is no words to describe how much they helped and continue to help my siblings and I. Thank you **Mum**, for being my safe haven where no actions or words are ever judged. For listening to my post-midnight rambles about work and struggles in life. Thank you for forever teaching us to be ambitious and believing in ourselves. Thank you **Dad**, for always ensuring I am as comfortable as I can be. For having my back in the big moments and forever listening to me ramble about science. Thank you for teaching us by example that no matter what happens, hard work pays off. You are both my role models and for that, this thesis is for you and it is the least I could give you in return to you unconditional love and support. You are the most valuable blessing God has given me, and I pray with gratitude every night for that.

Declaration

I hereby declare that the contents of this dissertation titled **"Investigating host responses to *Salmonella* Typhi in acute Typhoid fever"** are original and have not been submitted in whole or in part for consideration for any other degree or qualification this, or any other university. This dissertation is my own work and contains nothing which is the outcome of work done in collaboration with others, except as specified in the text.

Abstract

Salmonella Typhi causes acute typhoid fever through virulence factors, which includes the typhoid toxin that causes DNA damage in human cells. In 2019, colleagues at the University of Oxford studied the typhoid toxin during typhoid fever by challenging human participants with wild-type (WT) or toxin-negative (TN) strains of *S.* Typhi. In participants' bloodstream, TN *S.* Typhi persisted for up to 96 hours while WT *S.* Typhi were eliminated from the blood by 48 hours. This suggests DNA damage caused by typhoid toxin alerted immune defences in humans that countered bloodstream infection.

To resolve differences in the host response to bacteraemia by WT and TN *S.* Typhi, proteomics identified protein signatures secreted in the plasma of bacteraemic participants with acute typhoid fever ('secretome-WT'). Relative to uninfected participants, the plasma of those infected with WT *S.* Typhi contained significantly regulated proteins by typhoid toxin. Of those proteins, only Apolipoprotein C3 (APOC3) and lysozyme (LYZ) were differentially regulated between WT- and TN-infected indicating a role in mediating clearance of *S.* Typhi. *In vitro* experiments show DNA damage induced by purified recombinant typhoid toxin or infection by toxigenic *Salmonella* elicited DNA damage responses and cell-cycle arrest, which was coincident with increased expression and secretion of APOC3 and LYZ. Importantly, further *in vitro* experiments established that LYZ kills *Salmonella* in a dose dependent manner, which could explain how WT *S.* Typhi are eliminated from blood quicker than TN *S.* Typhi. Ongoing experiments are addressing the putative antimicrobial role of APOC3.

This project sheds light on host innate immune responses activated by bacterial-induced DNA damage and highlights that virulence factors can be viewed as double-edged swords, which promote infection but may also alert host defence.

Contents

List of Figures

List of Tables

Abbreviation

53BP1	p53 Binding Protein
ALAT	alanine aminotransferase
APH	Aphidicolin
APOC3	ApolipoproteinC3
APOF	Apolipoprotein F
APOL3	Apolipoprotein L3
Arp2/3	Actin Related Protein 2/3 complex
ASAT	Aspartate transaminase
ATM	Ataxia telangiectasia mutated
ATR	ataxia telangiectasia and Rad3
ATRIP	ATR-interacting protein
B2M	Beta-2-Microglobulin
BCL2	B-cell lymphoma 2
Caco2	cell line of human colorectal adenocarcinoma cells
CDK	Cyclin dependent kinases
CFU	Colony Forming Unit
cGAS	Cyclic GMP-AMP Synthase
CHK2	Checkpoint kinase 2
CMAH	Cytidine Monophospho-N-Acetylneuraminic Acid Hydroxylase
CRP	C-reactive protein
DDR	DNA Damage response
ΔcdtB	mutant cdtB
dsDNA breaks	Double strand DNA breaks
EDTA	Ethylenediaminetetraacetic acid
ELISA	Enzyme-linked immunosorbent assay
ETP	Etoposide
EU	European Union
GASDMD	Gasdermin D
GBP1	guanylate-binding protein 1
γH2AX	phosphorylated histone 2AX
GI	Gastrointestinal Tract

GMP-AMP	cyclic guanosine monophosphate–adenosine monophosphate
H2A	Histone-2A
H2AX	Histone 2AX
H2B	Histone-2B
H3	Histone-3
H4	Histone-4
HDL	High-density lipoproteins
HepG2	Human liver cancer cell line
HFF1	Foreskin fibroblast cells
HQ	Histone-160-Glutamine mutated
i.e.	The Latin *id est*, or 'that is,'
iBAQ	Intensity based absolute quantification
IFN-γ	Interferon gamma
IL-1B	Interleukin-1B
IL-8	Interleukin 8
IM	Inner membrane
iNTS	Invasisive non-typhoidal Salmonella
kDa	Kilo Dalton
LBP	Lipopolysaccharide binding protein
LC-MS/MS	Liquid Chromatography with tandem mass spectrometry
LDH	lactate dehydrogenase
LDL	Low-density lipoproteins
LFQ	Label-Free Quantification
LPS	Lipopolysaccharide
LRG1	Leucine-rich α-2 glycoprotein 1
LYZ	Lysozyme
LYZ-Chk	Chicken Lysozyme
LYZ-Hu	Human Lysozyme
M-cells	Microfold cells
MARS-14	Multi Affinity Removal Column, Human-14
MDR	Multi-drug resistance
Mg^{2+}	Magnesium ion
MRN	Mre-11 Rad50 and Nbs1
NAG	N-acetylglucosamine
NAM	N-acetylmuramic acid
Neu5Ac	N-acetylneuraminic acid
Neu5GC	N-Glycolylneuraminic acid
NF-κB	Nuclear Factor kappa-light-chain-enhancer of activated B cells
nTPM	Normalized gene expression values
NTS	Non-Typhoidal *Salmonella*

OD	Optical Density
OM	Outer membrane
OMV	Outer membrane vesicles
OVG	Oxford Vaccine group
p-	Phosphorylated
PAMPs	Pathogen-associated molecular patterns
PG	Peptidoglycan
PP	Protein phosphatases
pRb	Phosphorylated retinoblastoma protein
PRR	Pattern recognition receptor
PTGDS	Prostaglandin D synthetas
RING	Response induced by a Genotoxin
RPA	Replication Protein A
S.	*Salmonella*
SAA1	Serum amyloid A1 protein
SASP	Senescence associated secretory phenotype
SCV	*Salmonella* containing vacuole
Secretome-TN	Secretome-Toxin negative
Secretome-WT	Secretome-Wild Type
SNARE	N-ethylmale-imide-sensitive factor-attachment protein receptors
SPI-1	*Salmonella* Pathogenicity Island -1
SPI-2	*Salmonella* Pathogenicity Island -2
ssDNA breaks	single strand DNA breaks
ST	Sequence Types
T3SS	Type-3-secretion system
TFRC	Transferrin Receptor
Th1	T-helper 1 cell
THP1	human monocytic cell line
TLR	Toll-like receptors
TMSB4X	Thymosin
TN	Toxin negtaive
TxHQ	Typhoid toxin cdtB mutant
TxWT	Typhoid toxin Wild Type
TYGER	OVG2016/03 Investigating Typhoid Fever Pathogenesis OVG study
USA	United States of America
WHO	World Health Organization
WT	Wild-Type

Chapter 1

Introduction

The World Health Organization (WHO) leading efforts "to achieve better health for all" has identified *Salmonella* species as a high priority pathogen for research and development in 2017. With respect to human disease, *Salmonella* species can be divided into two groups: typhoidal *Salmonella* and non-typhoidal *Salmonella* (NTS). Typhoidal *Salmonella* cause a systemic disease known as enteric fever while NTS cause diarrheal disease. *Salmonella* is amongst the most common causative agents for enteric fever in the world.[1,2] *Salmonella* is regarded to cause huge global burden on morbidity and mortality. Typhoidal *Salmonella* is reported in developing countries with a mortality rate of 20% if untreated.[3] Typhoidal *Salmonella* It is identified in over 10% of all enteric infections reported in children in different regions around the world.[4–6]

1.1 *Salmonella* - causative agent of enteric fever

1.1.1 *Salmonella* serovars and sequence types

Salmonella is a Gram-negative bacterium that causes gastroenteritis and enteric fever in human and animals. *Salmonella* is divided into two species, *Salmonella* bongori and *Salmonella enterica*, of which, *S. enterica* is of most interest as it causes disease in warm-blooded mammals. *S. enterica* is subdivided into 7 subspecies. *Salmonella enterica* subspecies enterica (also known as *S.* enterica subspecies 1) is the most common subspecies reported in 99% of all human salmonella infections.[7]

Salmonella enterica subsp.1 is divided into ∼2,500 serovars,[8] which are defined by specific antibody recognition (e.g. recognising cell wall, designated O, and phase 1 and phase 2 flagella, designated H antigens). Adding to nomenclature, the advance of genome sequencing has allowed for isolates of *S. enterica* that possess seven identical genetic alleles to be assigned to the same sequence type.[9] For example, *S.enterica* subspecies enterica serovar Typhimurium (henceforth *S.*Typhimurium) can be divided into sequence types (ST) such as ST19 and ST313, which cause distinct diseases.

Salmonella can also be grouped by host-specificity, which relates to the severity of disease manifestation in humans and is introduced below.

1.1.2 Non-typhoidal *Salmonella* (NTS)

The majority of *Salmonella* serovars that infect humans and animals are considered 'host generalists' that infect humans and a broad range of animals. For example, the prototype NTS strain *S.* Typhimurium ST19 infects pigs, cattle, mice and humans, in which different disease manifestations between hosts can be observed.[7,10,11] Host generalists have a diverse genetic repertoire of virulence factors that aid colonisation of different hosts.[12] In humans, host generalists such as *S.* Typhimurium tend to cause self-limiting gastroenteritis and are therefore defined as NTS. NTS serovars that infect humans are zoonotic pathogens, which can be transmitted from food-chain animals. NTS serovars cause 78.7 million cases of disease worldwide and 59,000 fatalities reported annually.[13] In 2016, the European Union (EU) reported salmonellosis incidence rate to be 20.4 cases per 100,000 population. The most prevalent serovars reported in Europe belonged to NTS, e.g. *S.* Typhimurium ST19.[14] The immune status of the host can decide the fate of NTS. Hosts with intact healthy immune defences contain *Salmonella* in the gut and have a localised infection in the form of gastroenteritis typified by inflammatory responses such as neutrophil recruitment. Gastroenteritis is inflammation localised to the intestines and mesenteric lymph nodes, in the first 12-72 hours, followed by symptoms of disease that last less than 10 days. Symptoms include nausea and cramping which is then followed by typical food poisoning symptoms including diarrhoea, fever and vomiting in some cases.[15] It has a relatively short duration of disease due to the recruitment of adaptive immunity defences to the localised site of infection.[16,17]

1.1.3 Invasive non-typhoidal *Salmonella*

The increase in immunocompromised, driven by the HIV pandemic in particular, has sped evolution of invasive NTS (iNTS) serovars that are adapted to the human host and cause more severe systemic disease than NTS.[12] Though capable of infecting animals, the prototype iNTS strain *S.* Typhimurium ST313 has undergone genome degradation, relative to its NTS counterpart *S.* Typhimurium ST19, which contributes to human host-adaptation.[12] When iNTS infect immunocompromised hosts, the *Salmonella* disseminate from the gut into the bloodstream resulting in bacteraemia.[18] While 5% of NTS cases can become invasive, invasive disease is dominated in sub-Saharan Africa by iNTS strains such as *S.* Typhimurium ST313 and are a major cause of morbidity and over 20% fatality.[12,19]

1.1.4 Typhoidal *Salmonella*

Only a small subset of *Salmonella* enterica serovars are host specific, in other words, infect only a single host species. In the case of humans and higher primates, serovars

include, *S.* Typhi, *S.* Paratyphi and *S.* Sendai.[20] These so-called typhoidal serovars result in a more aggressive dissemination of bacteria via bacteraemia that leads to enteric fever with 1-4% fatality.[21] Typhoidal *Salmonella* have undergone significant genome degradation that contributes to their human host-specificity.[22] For example, ∼200 genes that are active in *S.* Typhimurium are inactivated in *S.* Typhi. *S.* Typhi has also acquired unique virulence genes such as those encoding the Vi polysaccharide capsule.[23]

S. Typhi and *S.* Paratyphi are the main causative agents of enteric fever (also referred to as typhoid fever when caused by *S.* Typhi).[24–26] Typhoid dominates and has subsequently captured most attention of researchers and health care professionals. Typhoid fever is a life-threatening enteric disease with about 128,000 fatalities reported in 2018.[24] Typhoid affects 11-20 million humans worldwide most of which are children in areas that lack good sanitation. Low- and middle-income countries including countries in South Asia (∼85% of typhoid cases) and sub-Saharan Africa struggle with maintaining a clean water supply, enabling transmission through the faecal-oral route.

Unlike gastroenteritis, typhoid fever causes a noninflammatory disease which lacks initial inflammatory gastroenteric symptoms, e.g. neutrophil recruitment. Typhoid symptoms present between day 8-14 post infection.[27] The incubation time can vary greatly to develop in as short as 4 days or as long as 33 days post infection.[28] Clinical symptoms of enteric fever usually persist to up to 3 weeks with a high fever (>39°C). Other symptoms include malaise, headaches, chills, weight loss, abdominal pain, cough, and red spots on chest. 50% of cases eventually develop gastroenteritis symptoms of diarrhoea, nausea, and vomiting. Due to the invasive nature of typhoidal salmonella individuals develop bacteraemia related diseases, like osteomyelitis, and septic arthritis.[29–31] Bactereamia reported in typhoid fever can last for years, and develop from primary to secondary infections leading to chronic carriage.[28]

1.1.5 Carriage of typhoidal *Salmonella*

Following typhoid, 2-5% of individuals become chronically infected, which is termed *Salmonella* carriage.[28,32]

In the late 19th and early 20th century chronic carriage came into light with the famous examples of Mary Mallon and Mr. N. Marry Mallon was a private cook in New York city with a bad sense of hygiene. Mary infected over 50 people in nine different epidemics until her case was discovered and she was put in isolation till her demise.[33,34] Meanwhile in England Mr. N was a milker and cowman responsible for 207 cases of typhoid which continued from 1899 to 1909.[35]

In 1902, Robert Koch proposed the idea that the main virulence of *S.* Typhi is humans, not just contaminated water. This makes *S.* Typhi an even bigger concern as some infected

individuals are asymptomatic carriers, like Mary Mallon and Mr. N. They continue to excrete the live pathogen even after the resolution of acute typhoid symptoms.[36]

When left untreated, studies show 10% *S.* Typhi infected patients continue to shed *S.* Typhi bacilli for over 3 months. Meanwhile 1-4% of *S.* Typhi infected patients become asymptomatic and shed bacilli for over a year periodically.[37] Comprehensive studies on *S.* Typhi patients in the span of 28 years post infection showed 11.9% become temporary carriers (3-12 months shedding) and 3.5% become chronic carriers (i.e. more than 12-months).[32]

Bacterial persistence starts off with a breach of intestinal barrier, followed by evasion of host's primary innate immune responses, and finally residence in the proper niche in the host.[38] 60% of typhoid carriers reported gallbladder pathology, thus the gallbladder is the principal niche for individuals who are chronically infected with *Salmonella*.[39] Despite the harsh environments in the gallbladder due to the presence of bile, *S.* Typhi persists.

Salmonella responds to the presence of bile by enhancing expression of bile resistance genes such as *phoP* and *ompA*, which regulate environmental changes and aids in biofilm formation respectively.[40,41] Studies showed the ability of *S.* Typhi to form biofilms on surfaces, such as gallstones and cholesterol coated surfaces.[42] Amongst the bile resistance genes, *Salmonella* produces biofilm which is formed around *Salmonella* aggregates protecting it further from bile conditions.[43]

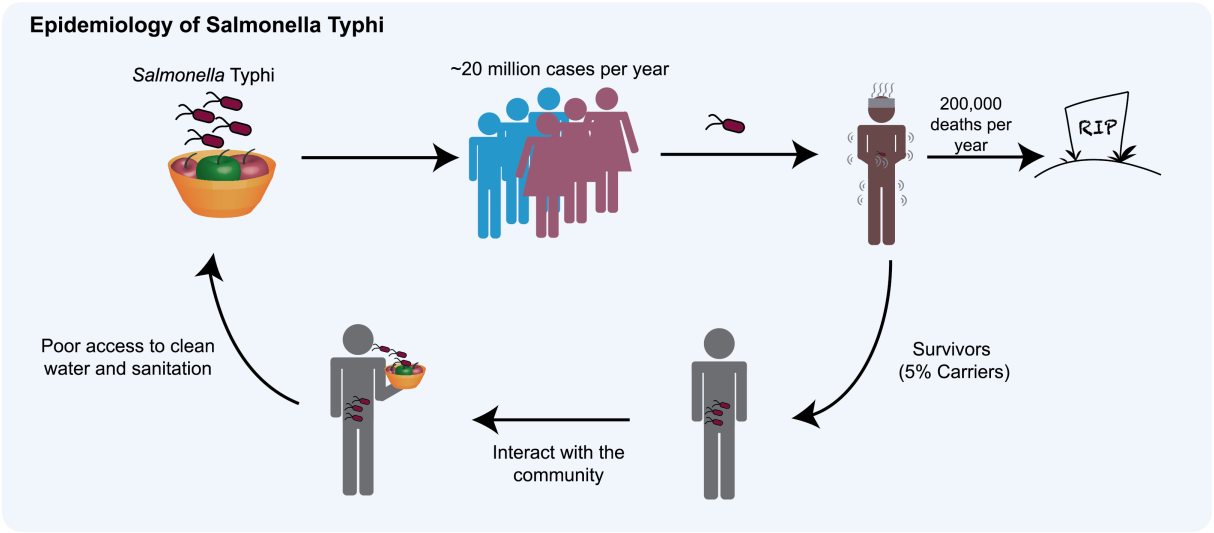

Figure 1.1: Typhoidal disease cycle.
Salmonella Typhi is transmitted through contaminated water and food. It infects about 20 million cases annually. It causes food poisoning like symptoms and can lead to fatality affecting 200,000 cases per year. 5% of surviving *Salmonella* patients exhibit carrier symptoms. Carriers transmit the disease when interacting with the community, and due to the lack of clean water sources the cycle continues.

1.2 Diagnosis, treatment and prevention

1.2.1 Diagnosis

Diagnosis of *Salmonella* infected individuals is crucial. Tests have been developed to identify acute cases, detect carriage and measure disease burden.[44] It has been a field of studies as there is no one test to satisfy all diagnostic needs. Tests are optimized to be performed in endemic regions with lack of laboratories.

Primarily typhoid is diagnosed with clinical symptoms due to the lack of available point-of-care diagnostics in endemic regions. However, clinical diagnosis is problematic and unreliable. Clinical symptoms are indistinguishable from other endemic diseases, for example, influenza, malaria and dengue.[45]

Samples collected from sterile sites, including blood, bone marrow and rose spots provide conclusive evidence of typhoid fever diagnosis. However, this is not a practical approach. In the 19th century, bacterial cultures were first established as a more reliable diagnostic to typhoid than clinical symptoms. Bacterial cultures have proven effective, but takes 1-5 days to get the results. Although effective, misdiagnosis is still probable due to bacterial susceptibility to antimicrobials.[46]

Bone marrow extracted samples are the most accurate diagnostic procedure. It involves extracting a sample of the bone marrow and culturing it on agar plates. However, it is impractical to apply, as it is a painful invasive approach that requires specialised equipment that might not be available in some endemic settings.[47,48]

In the late 19th century, Widal introduced the first serological test for Typhoid fever. Widal developed an antigen aggregation test that is the most common diagnostic to this day. The Widal aggregation test uses *S.* Typhi and Paratyphi antigens to test for their antibodies in patients' serum. Serum dilutions are added to Widal solution and aggregation is noted of flagellar (H) and lipopolysaccharide (O) antibodies.[49] It is simple and rapid and can be used in minimal lab infrastructure. However, it has limited diagnostic sensitivity and specificity early in the course of disease.

Due to their easy application in endemic regions. Companies have been developing serological tests with better efficiency. Amongst those, TUBEX TF (IDL Biotech, Sweden) and Typhidot (Malaysian Biodiagnostic research, Malaysia) are noteworthy. TUBEX TF uses antibodies to *S.* Typhi LPS O-antigen (specifically O9) and quantifies the inhibition in binding between them and LPS-coupled magnetic particles.[50] Meanwhile, Typhidot is a small scale dot-plot ELISA which detects *S.* Typhi outer membrane specific IgM and IgG antibodies.[51] Analysis of both serological tests' specificities showed up to 95% (TUBEX

TF) and 97% (Typhidot).[52] This is higher than the commonly used Widal test with 85% specificity.[53]

Research has been investing in developing more effective tests employing proteomics, transcriptomics, genomics and *in vivo* based technologies. The aim is to provide diagnostics to enhance monitoring and surveillance of disease progression.[44]

1.2.2 Treatment and antimicrobial resistance

Antimicrobial treatment is the most effective treatment of *S.* Typhi. *S.* Typhi and *S.* Paratyphi infections are treated with several antimicrobial classes including Fluoroquinolones, Cephalosporins, Macrolides, and Carbapenems.[54,55] The Quailes strain used in human challenge studies since 1960 is susciptable for ciprofloxacin. However some *S.* Typhi are resistant to ciprofloxacin (H58) and therefore azithromycin is used instead.[56]

Although effective, antimicrobial treatment has become a less reliable option due to the evolution of antimicrobial resistance (AMR) of *Salmonella*.[57] In the span of 4 years, a study in Malawi showed a rise of multi-drug resistant *S.* Typhi from 7% in 2010 to 97% in 2014.[58,59]

Resistance mechanisms. Horizontal gene transfer has been effective in ensuring antimicrobial resistance is maintained across *Salmonella* species. Plasmids are the main agents of horizontal gene transfer causing antimicrobial resistance in *Salmonella*. IncC plasmids are known carriers of antimicrobial resistance genes, transferred between *Salmonella*.[60] They have a large host range and low copy number which allow them to be transferred with ease making them most effective to maintain antimicrobial resistance in *Salmonella*.[60] IncA/C plasmids are carried by *Salmonella* and transfer up to 10 genes of antimicrobial resistance that spans 5 antimicrobial classes.[61] Amongst the antimicrobial resistance genes encoded by IncA/C, the following genes are encoded, trAB, sul2, tetAR, blaCMY-2, and floR. These genes code for resistance against, aminoglycosides, sulfonamides, tetracyclins, β- lactams and chloramphenicols.[62,63] Inc plasmids' acquired resistance targets several of the treatments used to battle *Salmonella*.

Spread of Antimicrobial resistance. Genomic sequencing of *S.* Typhi strains from 63 countries across the globe, where *S.* Typhi is endemic, identified H58 *S.* Typhi strain as the most common strain. H58 *S.* Typhi encodes multidrug resistance (MDR) genes. H58 strains encode MDR genes that establish resistance against a range of antimicrobials.[58] These genes include, blaTEM-1, for ampicillin resistance, dfrA7, sul1 and sul2, for trimethoprim and sulfonamides resistance, respectively, and to trimethoprim-sulfamethoxazole), catA1, for chloramphenicol resistance and strAB, for streptomycin resistance.[59] The excessive prescription of antimicrobials enhances the MDR reported in the H58 strains. H58 strain is found to spread cross-continentally quite rapidly in the last 20

years.[64] H58 strains reported a high prevalence in reported resistance to fluoroquinolones, for example, ciprofloxacin which works by inhibiting bacterial DNA replication.[65] This is due to the high exposure to fluoroquinolones drugs, that have proven most effective against *S.* Typhi in the last 20 years.[66] This poses a problem as the most effective drug is facing resistant organisms of *S.* Typhi against it.[67,68] These organisms are rapidly being common in most *S.* Typhi infections.[59] This led to the WHO reporting fluoroquinolone-resistant *Salmonella* amongst the high priority pathogens in 2018.[24] This calls for further studies into the understanding of the disease mechanism to further aid in its prevention and alternative treatment pathways.

1.2.3 Vaccination programs

Whole cell vaccine. To prevent typhoid, the 1st vaccine was developed in 1896 from an inactivated whole cell *S.* Typhi. *S.* Typhi was either heat killed, and phenol preserved or acetone killed and lyophilized before administration. This vaccine provided 73% efficiency for 3 years before re-administration[69,70] and was discontinued in 1960 due to the undesired side effects that mimicked typhoid symptoms.[71]

Vi Polysaccharide Vaccine. In 1986, Robbins and Robbins developed an injectable subunit vaccine of Vi-polysaccharide (Vi-PS)[72] that provides between 55-75% protection against the pathogen. Unlike the whole cell vaccine, it showed minimal side effects, but is non-immunogeneic in children below 2 years of age.[73,74] Another drawback came into effect when Vi-negative *S.* Typhi organisms emerged in India in the early 2000s rendering the vaccine ineffective.[75]

Live attenuated Ty21 vaccine. Ty21 is a live attenuated vaccine. Live attenuated vaccines elicit more immune response and higher protection up to 96% for 3 years before re-administration. Ty21 is developed from the WT *S.* Typhi Ty2 strain, which is then chemically attenuated.[71,76] This vaccine lacks some functional genes and antigens, most importantly, it lacks the Vi-antigen and is therefore highly attenuated. Clinical studies have reported Ty21 efficiency to be 67% for 7 years, when high doses are administered, 10^9 bacteria per dose. Ty21 is not recommended for children less than 6 years of age.[77] This is not ideal since a majority of typhoid cases are reported in school-age children in endemic regions, between 0.5-15 years.[78,79] In addition, the oral nature of Ty21 vaccine makes it liable to gastric acid induced deactivation.[77] Thus, this vaccine was not approved by the WHO.[80]

Typhoid-conjugate vaccine. A new conjugate vaccine created by Bharat Biotech International in India, Typbar-TCV, showed efficiency in phase 3 trials.[81,82] The conjugate vaccine consists of the Vi-polysaccharide conjugated to tetanus toxin, which elicits a strong Vi-antibody response in serum of vaccinated participants.[83] The vaccine provided efficiency and safety for use in children as young as 6 months of age, and thus was

prequalified by the WHO in 2019.[84] Clinical trials in the UK showed vaccine efficiency of 54.6% against bacteraemia in adult participants.[81] Meanwhile, Typbar-TCV showed 81.6% efficiency in Nepalise children aged 9 months to 16 years.[82] An outbreak of multidrug resistant *S.* Typhi in Pakistan provided a testing ground for the conjugate vaccine, which controlled the outbreak with vaccinated children reported a 95% lower incidence of contracting multidrug resistance (MDR)*Salmonella*.[85]

Current status of typhoid vaccines. The WHO recommends vaccination programs to contain the spread of typhoid fever in endemic and epidemic regions. The typhoid conjugate vaccine Typbar-TCV is licensed and recommended for children from 6-months of age and adults. Conjugate vaccines are prioritized by the WHO in areas of high typhoid fever incidence. Injectable unconjugated polysaccaride vaccines are recommended for children of 2 years and older. Meanwhile the oral live attenuated vaccine Ty21a is recommended for 6 years or older. Although all vaccines are approved by the WHO, the conjugate vaccine is the most recommended as it is most effective and is applicable to all age groups.[84]

1.2.4 Controlled human infection challenge studies on typhoid

As discussed, WHO identifies *Salmonella* as a "priority pathogen" due to the rising risk of antimicrobial resistance.[84,86] In addition, humans are the main reservoirs of typhoid infections, and thus controlled human infection studies are necessary to understand *S.* Typhi pathogenesis.[87,88] A study in the university of Maryland, USA, between 1952 and 1974, allowed for understanding of typhoidal pathogenesis and aided in the development of vaccine development.[30,89,90] However, this program that lasted over 20 years was halted and more progressive challenge study was carried out in the University of Oxford. Over 400 volunteers were challenged in six separate studies. Most notably a trial published in 2017, testing the efficiency of the typhoid conjugate vaccine Typbar-TCV, with Vi polysaccride capusle conjugated to the tetanus toxin carrier protein, which demonstrated 55%- 87% efficiency of the conjugate vaccine. This study investigated the efficiency of the vaccine in several stages of epidemic progression and thus allowed for establishing a vaccination program that was recommended in the a recent WHO position paper,[24] prequalifying Tybar-TCV as a typhoid vaccine in 2018. In addition, current studies are employed in Malawi,[91] Nepal[92] and Bangladesh[93] to test the vaccine efficiency.

Most of what is known about *S.* Typhi pathogenesis is through non-typhoidal *Salmonella* infected mice.[94,95] As previously mentioned, *S.* Typhimurium exhibits similar symptoms in mice to that of typhoid in humans. However, *S.* Typhimurium differs in several virulence factors to *S.* Typhi including the Vi-capsule[96] and typhoid toxin.[97] Even though mouse studies have been effective in explaining how *Salmonella* establishes infection, human challenge studies are necessary in identifying the impact of virulence factors on

disease. Thus, in addition to testing vaccine efficiency, controlled human infection challenges of *S.* Typhi are employed to understand the pathophysiology of the pathogen and the contribution of virulence factors to typhoid fever.[56] For example, human infection challenge with wild-type *S.*Typhi or a strain in which the virulence factor typhoid toxin had been deleted showed that the toxin does not initiate typhoid fever.[56] Establishing human infection challenge studies also provide insight into related pathogens. For example, 15,000 *S.* Typhi were found sufficient to cause typhoid fever in 63% of volunteers while 10-fold fewer *S.* Paratyphi was sufficient to cause paratyphoid in 56% of volunteers.[98] This is consistent with the observation that the Vi capsule, which is specific to *S.* Typhi, reduces invasion into host cells due to enhanced virulence protein secretion.[99] Though in human volunteers, Vi-positive *S.* Typhi was shown to be more virulent than Vi-deficient strains.[90]

1.3 *Salmonella* establishing an infection in host

1.3.1 Invading the intestinal epithelium

Both typhoidal and non-typhoidal serovars invade the intestinal epithelium in the distal ileum section through *Salmonella* pathogenicity islands 1 and 2 that encode virulence genes, which remodel the host cell actin cytoskeleton and endolysosomal pathways (summarised below). M-cells are specialised microfold cells that are the most common cell in which they invade. M-cells are found in Peyer patches which act as a part of the lymphoid structures in the intestinal epithelium. *Salmonella* also invade epithelial cells. Regardless of the cell type, *Salmonella* are thought to trancytose into the lamina propria where they infect resident macrophages in Peyer's patches, activate innate immune responses and/or disseminate by draining into mesenteric lymph nodes.

Salmonella has pathogenicity islands encoding genes for virulence. *Salmonella* serovars encode pathogenicity islands that aid in establishing disease, amongst those most conserved are SPI-1 and SPI-2.

Invasion of host cells via SPI-1 virulence genes. *Salmonella* pathogenicity island-1 (SPI-1) is conserved in all *Salmonella* serovars. Amongst SPI-1 genes, there are genes encoding the structural proteins to make up a type-III secretion system (T3SS), they are amongst the virulence effector proteins of *Salmonella*.[100,101] Low oxygen and high osmotic pressure found in intestinal epithelium is reported to induce SP1-1 expression through regulation of transcriptional activators.[102] SPI-1 encoded T3SS-1 which is an injection like structure that shoots effector proteins into the host.[103] SPI-1 effector proteins aim to hijack the cytoskeleton and thus allow an entry point for *Salmonella*. Examples of SPI-1 coded effector proteins are SpoE and SipA. SopE works by activating a family of GTPases, Rho GTPases, which elicit Arp2/3-dependent actin polymerisation.[104] Meanwhile, SipA

directly binds and stabilises to actin filaments.[105] Together they cause membrane ruffling which enhances the entry point of *Salmonella*. Effectors work by stabilising actin which in turn causes membrane ruffling creating an entry point for *Salmonella*.[106–108]

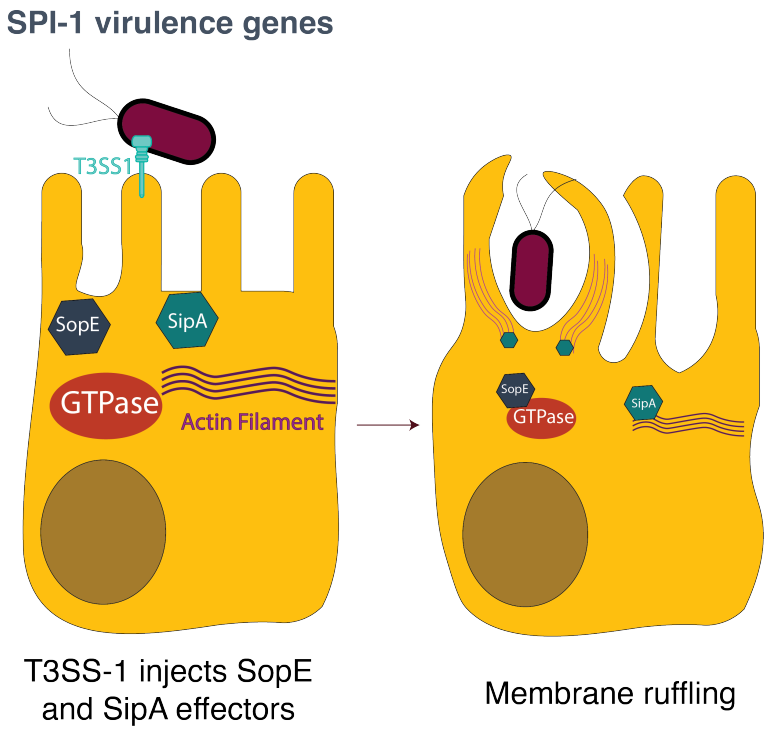

Figure 1.2: SPI1 effectors.
Salmonella expresses T3SS1 effector which acts as injection and injects SPI1 effectors, SopE and SipA into the host cell, where they encounter host proteins like GTPases and actin filaments ***(left)***. SopE interacts with host GTPases, meanwhile, SipA binds to acin filamnets causing membrane ruffling of host cell as shown ***(right)***.

Intracellular survival via SPI-2 virulence genes. Once inside the cell, the pathogen resides within an endosomal compartment referred to as the *Salmonella* containing vacuole (SCV).[109] SCV formation aids *Salmonella* survival, multiplication and spread, which is driven by expression of the SPI-2 T3SS and its substrate virulence effectors. Any pathogen that resides within an endosomal compartment must have a strategy to survive the lysosome. SifA is a SPI-2 effector protein that manipulates lysosomal biogenesis by promoting exocytosis of lysosomal hydrolases such as Cathepsin D.[110] This ensures that the SCV only interacts with attenuated lysosomes lacking their full complement of antimicrobials, for example Cathepsin D, which promotes *Salmonella* survival. Manipulation of endosomal membranes by SifA causes *Salmonella*-induced filament formation, which are thought to ensure nutrients are redirected to the SCV for the pathogen rather than distal cell compartments.[111,112] In addition, SifA detoxifies lysosomes and aids in their exocytosis to the extracellular environment.[113] SPI-2 effectors also mediate SCV transport to the basolateral side of intestinal cells where *Salmonella* can trancytose into the lamina propria, which promotes invasion of the host and dissemination.[114]

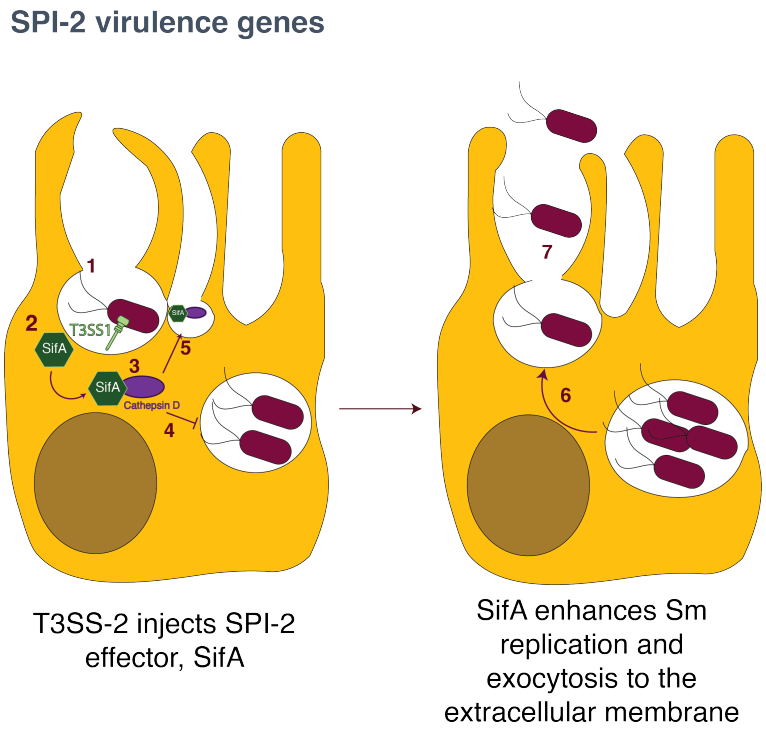

Figure 1.3: SPI2 effectors.
Salmonella expresses SPI2 T3SS effectors which acts as injection and injects SPI2 effector, SifA. SifA binds to host protein Cathepsin D. SifA-Cathepsin D complex prevents Cathespin D binding to SCV and is instead trafficked outside the host cell ***(left)***. This allows for *Salmonella* survival as it prevents the fusion of toxic proteins like Cathepsin D to the SCV. This consequently leads to *Salmonella* proliferating and leaving the cell to infect other cells and ensure persistence ***(right)***.

Systemic dissemination of *Salmonella*. After crossing the intestinal epithelium through M-cells, typhoidal *Salmonella* reside undetected in the lamina propria. This is where the pathogen starts its dissemination routes. Typhoidal *Salmonella* establishes systemic infection through two main routes, (i) free *Salmonella* can surpass the lamina propria and into the mesenteric lymph nodes (MLN) disseminating straight into the bloodstream, and/or (ii) infecting and multiplying through phagosomes in the lamina propria (for example, macrophages), using them as transport vehicles to systemic sites. *S.* Typhi infects macrophages at three primary locations: (1) in the lamina propria, *S.* Typhi can infect intestinal macrophages, (2) or bacteria can be drained into the mesenteric lymph nodes, once they surpass the intestinal epithelium, where they infect macrophages and other mononuclear phagocytes, or finally, (3) free *S.* Typhi invade the bloodstream via mesenteric lymph nodes, which results in primary transient bacteraemia, where they can infect macrophages in the blood.[115]

In the blood, free *S.* Typhi are phagocytosed and cleared from the circulation by mononuclear phagocytes (such as, macrophages). Infected macrophages migrate to organs

of the reticuloendothelial system (e.g. liver, spleen) where *S.* Typhi survives intracellularly due to T3SS-2 effectors. Here, *S.* Typhi resides until onset of typhoid fever (8-14 days), which is typically accompanied by sustained, albeit low level (1–10 organisms/mL), secondary bacteremia lasting several weeks.[116]

During primary bacteremia, *S.* Typhi also reaches the gallbladder, which is critical to establishing chronic carriage - chronic infections that can last up to a lifetime in humans, like the infamous Typhoid Mary (∼5% of typhoid patients). Chronic carriers are responsible for retaining *S.* Typhi in the population and transmitting disease by shedding as many as 10^9 organisms/g faeces.[117,118]

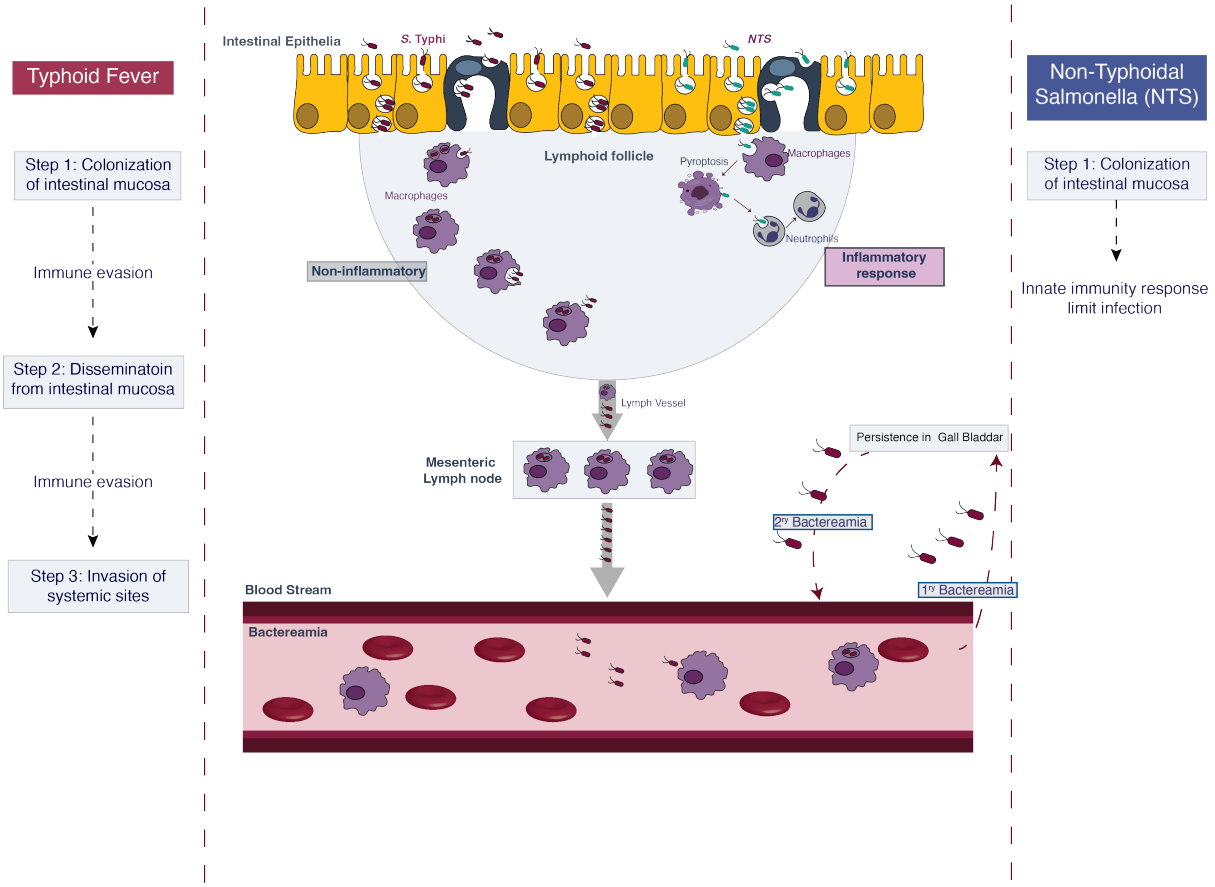

Figure 1.4: *Salmonella* establishing an infection in the gut.
Many of the Non-Typhoidal *Salmonella* (NTS) infects the intestinal epithelium and goes through M-cells in Peyer patches (blue) or epithelial cells (yellow). NTS resides in the lymphoid follicle where it encounters an inflammatory response mediated by macrophages (purple) and neutrophils (gray). Inflammatory response inhibits persistence and ensures NTS is cleared before it becomes a systemic threat. Meanwhile, *S.* Typhi infects the gut epithelium in a similar manner to NTS, but is believed to evade immune responses, which allows it to go into the mesenteric lymph nodes and subsequently to the bloodstream, leading to primary bactereamia. Primary bactereamia causes persistance in systemic sites, like the gallbladder, which consequenty causes secondary bactereamia.

1.3.2 Innate immune response to *Salmonella* and immune evasion

Innate immune responses to NTS. NTS infection of the M-cells followed by invasion of the lamina propria elicits recognition of pathogen associated molecular patterns (PAMP) by host pattern recognition receptors (PRR). For example, *S.* Typhimurium's flagella, LPS and T3SS are PAMPs. Flagella activates TLRs, TLR4 which results in cytokine release such as IL-8.[119] PAMPs release in response to NTS elicits a strong T-helper 1, Th1, immune response, particularly in immunocompromised patients, and recruits phagocytes in an IL-8-dependent manner.[120–122]

Immune evasion by typhoidal *Salmonella*. *S.* Typhi is a stealth pathogen that is highly adapted to evading the innate immune responses activated by NTS (summarised above). Typhoidal serovars induce limited mucosal inflammatory responses and causes diarrheal disease initially.[123–125] This is attributed to the typhoidal virulence factors which include, Vi capsular polysaccride capsule, typhoid toxin and flagella. Although it is unclear which factor causes this evasion of immune response, some studies shed some light into the possible involvement of SPI-7 pathogenicity island coding genes. SPI-7 is unique to the typhoidal serotype genome and contributes to typhoidal virulence factors.[126]

Upon invasion of the intestinal epithelium, *S.* Typhi encounters a reduced osmolarity which in turn results in a rapid induction of TviA expression.[127,128] TviA works with RcsB, together they express the Vi- antigen and represses flagella.[129] Flagella is a major pattern recognition molecule conserved in many pathogens. This allows the pathogen to transit in the epithelium undetected, and thus by the time *Salmonella* is in the lamina propria, major pathogen induced processes and pathogen recognition molecules are no longer detected. *Salmonella* therefore survives in the lamina propria and can disseminate since there is no immune responses to stop it because it simply cannot be seen by immune cells. viaB locus therefore impairs neutrophil recruitment in the intestinal epithelium[130,131] which explains the insufficiency of neutrophils in *S.* Typhi infections[132] and the longer incubations of disease.[27]

The Vi-capsule is restricted to *S.* Typhi and absent in *S.* Paratyphi and *S.* Senai, as previously mentioned, are typhoidal serovars, which cause typhoidal disease. Vi-mutant *S.*Typhi are able to establish typhoid-like illness in humans.[133] This suggests that the Vi-capsule is not the only factor to establish systemic spread and a major focus in recent years has been the typhoid toxin of typhoidal *Salmonella*.

1.4 The typhoid toxin

The typhoid toxin is expressed in 38 serovars including the major typhoidal serovars *S.* Typhi and *S.* Paratyphi A with remaining isolates belonging to non-typhoidal serovars that cause gastroenteritis in humans and animals, for example *S.* Javiana.[97,134–138] It is an A_2B_5 toxin, "A" stands for its enzymatic 'active' subunits, and "B" stands for its host receptor 'binding' subunits. The toxin has a pentameric PltB subunit that binds host receptors linked to two A-subunits, an ADP-ribosyl transferase (PltA) bound by disulfide bonds to DNase (CdtB).[97] The typhoid toxin is implicated in typhoid symptoms, immune evasion, dissemination and bacteraemia, and chronic carriage.[56,97,139–141]

1.4.1 The structure and function of typhoid toxin

Organisation of the toxin pathogenicity islet. The typhoid toxin was discovered when *S.* Typhi exhibited toxigenic effects in a manner dependent upon the cdtB gene, similar to those associated with cytolethal distending toxins (CDT) that also rely on the cdtB gene.[138] CDT is a conserved virulence factor in diverse pathogenic bacteria, usually Gram negative. CDTs are encoded in several organisms of *Escherichia coli*,[142] *Shigella dysenteriae*,[143] *Haemophilus ducreyi*,[144] *actinobacillus actinmycetemcomitas*[145] and *Heliobacter hepaticus*.[146] CDT consists of three moieties, CdtA, CdtB and CdtC. CdtA and CdtC are responsible for uptake of the active catalytic moiety, CdtB.[147] In 2004, researchers puzzled over the observation that *S.*Typhi encoded cdtB but not cdtA and cdtC.[138] In 2008, the toxigenic activity of cdtB in *S.* Typhi was shown to rely on pertussis-like toxin subunits, PltA and PltB to which CdtB was bound, which revealed a novel chimeric typhoid toxin. This leap was based on discovery of a genomic islet encoding the cdtB subunit alongside pltA, and pltB.[134] Pertussis toxin is a key virulence factor of *Bordatella Pertussis* that causes whooping cough syndrome. The typhoid toxin is therefore made up of three subunits, PltB, PltA and CdtB, together they play different roles during intoxication of the host cell.

PltB subunit

PltB subunit of typhoidal serovars. The PltB subunit is made up of 5 PltB proteins that act as the binding moiety of the toxin. Serine 35 on the PltB subunit is very important as it is necessary for binding of sialylated glycans with the terminal acetyl neuraminic acid Neu5Ac2-3Galβ1-3/β1-4Glc/GlcNAc (Neu5Ac). Neu5Ac sialylated glycans are abundantly found in human cells. Unlike other mammals, humans lack the presence of CMP-N-acetylneuraminic acid hydroxylase (CMAH). CMAH is necessary to convert Neu5Ac (found only in human cells) to Neu5GC (found in all other mammalian cells). For example, higher primates express Neu5GC only while mice express a mixture of Neu5GC and Neu5Ac.[148] Due to this evolutionary characteristic, the toxin of typhoidal *Salmonella* are specific for human host cells. More recently, the typhoid toxin CdtB subunit has

been shown complex with homologs of PltB and PltA that broaden the tropism of typhoid toxin: these include the PltB homolog PltC that exhibits preference for immune cells,[149] and the ArtB/ArtC, which can bind Neu5GC found across mammals.[150] PltB is thought to compete with PltC and ArtB to generate toxin variants that depend on CdtB for toxigenic activity.

PltB subunit of NTS serovars. The typhoid toxin was first reported in *S.* Typhi. Recently, studies have shown that it is not unique to *S.* Typhi. 40 serovars of NTS carry the typhoid toxin genes,[151–153] which has been extended to 100 serovars due to widespread expression of artB in NTS serovars.[154] This includes *S.* Javiana, which is responsible for 5% of NTS cases in the USA, and has been used to investigate the effect of the toxin during infection in mice.[152,153,155] Studies have shown that *S.* Javiana activates DNA damage responses through the typhoid toxin.[153] The typhoid toxin of *S.* Javiana (also referred to as Javiana Toxin) suppresses inflammatory immune responses and promotes dissemination of *Salmonella* in mice.[139] The PltB subunit of Javiana Toxin possesses three amino acid changes relative to the PltB of *S.* Typhi, namely N29K, S50G, and T65I.[156] This narrows the receptor tropism of Javiana toxin towards sialylated glycans found in the intestinal mucosa where NTS serovars colonise the host.[156] The substitutions have a profound effect on the toxigenic activity of Javiana toxin, which is non-lethal in mice relative to 100% lethality of typhoid purified typhoid toxin.[156] Amino acid substitutions in PltB are also found in other NTS serovars and may reflect differences in target cell tropism in toxin variants. This led to naming *S.* Javiana toxin as Javiana toxin. In addition, these observations fit with the systemic spread of *S.* Typhi that possesses a promiscuous typhoid toxin, which can bind broader range of human cells than Javiana toxin.[156]

The PltA subunit

PltA is a linker subunit which ties PltB and CdtB together. It has disulfide bonds on each end binding to PltB and CdtB. Consequently, deletion of PltA resulted in a complete loss of CdtB induced toxicity.[134] PltA is thought to have active ADP-ribosyltransferase activity but no targets or toxigenic effects of PltA have been reported.[97,134]

CdtB subunit

The CdtB subunit resembles in sequence and structure the DNase-like moiety of the cytolethal distending toxin family (CDTs), and resembles the nuclease function of mammalian DNase-1.[97,157] Histidine 160 (H160) is a conserved histidine residue in CdtB of typhoid toxin,[97] analogous to histidine 134 in mammalian DNase.[158,159] H134 is required for the catalytic activity of the DNase I enzyme. Similarly, H160 represents the residue responsible for catalytic function of the toxin.[97] When inducing a point mutation in the cdtB subunit of the typhoid toxin, namely histidine 160 to glutamine (H160Q), nucle-

ase activity is attenuated.[97,157] Like the reported effects of CDTs, CdtB causes DNA damage associated with cell cycle arrest in *S.* Typhi infected human cells.[159–166] Once inside the nucleus, CdtB induces DNA strand breaks which in turn activates DNA Damage Responses (DDR)[157,158,167] and resulting cell cycle arrest to allow for repairing of the induced damage.[161,168,169]

1.4.2 Typhoid toxin expression

The expression of the typhoid toxin is carried out intracellularly from 3 hours post-infection when the *Salmonella* reside in their SCV.[134] PhoP-PhoQ is the main positive transcriptional regulator of cdtB, pltA, pltB.[136] PhoP-PhoQ is a two-component system in *Salmonella* activated by a low concentration of Mg^{2+},[170] an acidic pH,[171] alkaline pH,[171,172]the presence of antimicrobials in the environment.[172–174] For example, with endocytosis of *Salmonella* comes a relative reduction in Mg^{2+} concentration within the SCV, which in turn activates the PhoP-PhoQ driving expression of the toxin. Mutations in phoP or phoQ inhibited pltB expression which in turn hindered the expression and secretion of the typhoid toxin.[136] *S.* Typhi with a deleted PhoP-PhoQ created a organism that was proposed as a live attenuated vaccine Ty800.[175]

1.4.3 Typhoid toxin secretion from *Salmonella*

Secretion from *Salmonella*. Typhoid toxin is only expressed intracellularly within an infected cell, which in turn implicates the SCV in toxin trafficking.[176] Two genes are encoded on the same pathogenicity island that encodes the typhoid toxin, *sty1887* and *sty1889*. *Sty1889* encodes ttsA, which is necessary for toxin secretion.[177] TtsA belongs to a family of proteins called muramidases. Muramidases are similar to a family of proteins in bacteriophages calles endolysins. Endolysins interact with holins, which are proteins in the bacterial inner membrane. This interaction allows the toxin to reach the periplasmic space which in turn allows toxin secretion. Unlike endolysins, that interact with holins in bacterial membrane and causes bacterial lysis,[178] TtsA maintains an intact *Salmonella* membrane.[177,179] This suggest TtsA provides a novel protein secretory function for the typhoid toxin.

Toxin exocytosis from the host cell. Once the toxin is secreted from bacteria into the SCV lumen, the toxin is packaged in vesicle carrier intermediates, also known as outer membrane vesicles (OMVs). OMVs are derived from the SCV which is made up from the host membrane. Indeed, PltB mutation prevented toxin packaging and thus inhibited toxin exocytosis.[176] PltB subunit binds to Neu-5Ac sialylated glycans on receptors and creates a vesicle for toxin transport to the extracellular environment[134,176] in a manner dependent on the cation-independent mannose-6-phosphate receptor, coatmer 2/COP2, Sar1 GTPase and Rab GTPases 29 and 11b.[180,181] Fusion of vesicle carrier

intermediates carrying the toxin with the plasma membrane involves SNARE proteins VAMP7, SNAP23, and Syntaxin 4.[181] This results in toxin exocytosis.

1.4.4 Typhoid toxin intoxication of target host cells

The extracellular toxin can intoxicate infected cells (autocrine effects) or non-infected bystander cells (paracrine effects).[134] The typhoid toxin, now free in the extracellular environment, binds to host cells and is then endocytosed by PltB-Neu5AC receptor-mediated endocytosis and trafficked to the Golgi apparatus then the endoplasmic reticulum (ER).[181,182] In the ER, PltA is separated from CdtB by reductase enzymes breaking the disulphide bond holding them together.[182,183] Free CdtB is released into the cytoplasm where it translocates to the nucleus and exerts its toxigenic nuclease activity[97,169,182]

1.5 The role of the typhoid toxin

The role of the typhoid toxin remains unclear. Paramount to understanding the toxin has been *in vivo* studies in mice and humans, which have exploited either purified recombinant toxin or *Salmonella* encoding typhoid toxin.

Toxin studies in mice. Toxin studies in mice. Song *et al.* showed that intravenous injection of purified toxin recapitulated typhoid symptoms in mice, which suffered 100% mortality.[97] Cell-cycle arrest, leukopenia, malaise and weight loss were also observed. Lethality in mice following intravenous administration of typhoid toxin has been observed since.[150,156] However, *Salmonella* infection models in mice do not support the view that typhoid toxin causes the severe symptoms associated with typhoid, e.g. lethality. As *S.* Typhi is a human pathogen, NTS serovars that encode the toxin have been used as a surrogate model to study typhoid toxin. When wild-type mice were infected with *S.* Typhimurium engineered with genes encoding typhoid toxin (*S.* Typhimurium^{TOX}), the toxin suppressed inflammatory responses and enteritis, and promoted host survival to establish asymptomatic chronic carriage.[140] Indeed, while *S.* Typhimurium killed its mouse host within 1-month, *S.* Typhimu-rium^{TOX} persisted, colonising its host at systemic sites in an asymptomatic manner for 6-months at the time of euthanasia. Similarly, the typhoid toxin of *S.* Javiana suppressed inflammatory responses and pathology in mice while promoting bacterial colonisation and systemic spread.[139]

Toxin studies in humans. Human infection challenge studies with wild-type (WT) and toxin-negative (TN) *S.* Typhi demonstrated that typhoid toxin does not initiate typhoid fever but the toxin was found to suppress a pathological symptom, bacteraemia.[56] This agrees with infection models in mice with *S.* Typhimurium^{TOX} or *S.* Javiana.[139,140] The only significant finding in the human infection challenge study was the duration of

bactereamia in human participants, which was extended from a mean of 30 hours with WT to 48 hours with TN S.Typhi (range of 3h - 48h with WT, 29h - 97h with TN).[56]

Collectively, the findings from studies in mice and humans suggest that the *in vivo* role of the toxin is to suppress inflammatory responses and pathology, and regulate phenotypes associated with systemic infection, e.g. dissemination, bactereamia, chronic carriage.[56,139,140] It remains possible that high concentrations of toxin could cause more severe symptoms such as lethality but this has not been recapitulated in a mammalian infection model.[97,156] The mechanism that unites all the phenotypes introduced above is dependence on the nuclease activity of CdtB, i.e. residue H160, which implicates activation of host DNA damage responses in the functional role of typhoid toxin.

1.5.1 Host DNA damage responses

To understand the toxigenic effects of the toxin, the cell cycle and the host DNA damage response must be introduced.

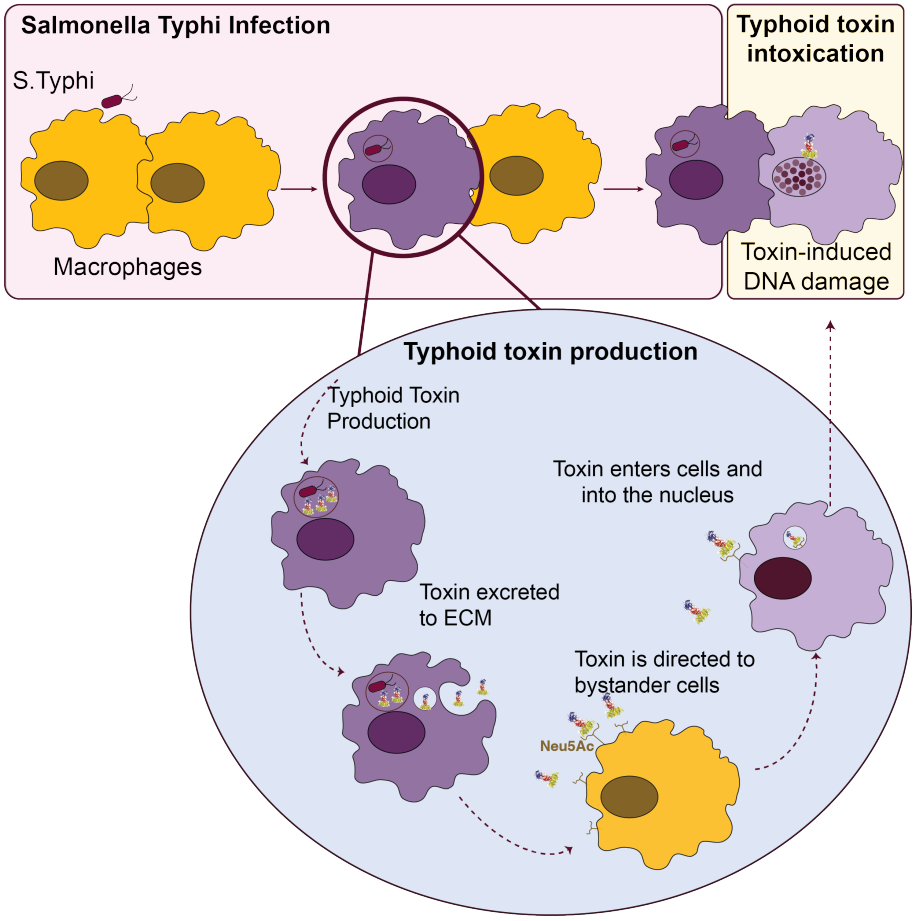

Figure 1.5: *Salmonella* Typhi cellular infection and intoxication.
S. Typhi infects cells, like macrophages. Once inside the cell, it produces the toxin intracellularily and excretes the toxin to the extracellular environment. The toxin binds to Neu5Ac receptors on bystander cells, or even the infected cell. The toxin goes inside a vacuole till it reaches the nucleus. Once inside the nucleus, it causes DNA damage by the action of the toxigenic CdtB subunit.

DNA organisation. Diploid human cells contain 46 chromosomes, 23 pairs of chromosomes containing over 3 billion base pairs.[184] The long chains of DNA double helix wraps around proteins, histones, forming nucleosomes, to ensure compact organisation.[185] Histones are positively charged which allows them to wrap around the negatively charged DNA in an octamer making up the nucleosome.[186] Histone octamer is made up of two copies of each of these four histones, H2A, H2B, H3 and H4.[187] Histone are protein hubs for post translational modifications including ubiquitination, acetylation, methylation and phosphorylation. Post translational modifications play a role in chromatin structure, remodelling and transcription. These post translational modifications aid in the formation of euchromatin and heterochromatin. Euchromatin is a gene dense region that is accessible to translational machinery. It encodes genes that are bound for expression. Meanwhile, heterochromatin are more condensed and inaccessible for transcription. The differences in chromatin structure play a role in cell division, DNA repair and epigenetic cellular processes.[187]

Cell cycle. DNA replication is carried out by undifferentiated cells to allow for cell division. Cell division is necessary for biological processes, for example, regeneration and wound healing. Cell division is divided into 4 cycles, G1, S, G2, M phase.[188] G1 phase prepares DNA replication machinery for DNA synthesis. Following G1, DNA replication occurs in the S phase of the cell cycle, where replication machinery is employed and a copy of the genome is generated. After this, the G2 phase prepares the cell for cell separation mediated by cytokinesis. Finally the M phase where mitosis occurs and the cell splits into two identical cells with the same genomic material. The cell then goes into the G1 phase again if it is undifferentiated, however if it becomes differentiated, it goes to the G0 phase. The G0 phase contains cells that exited the cell cycle and have become quiescent. Quiescent cells do not undergo mitosis and remain in the G0 phase. The cell cycle is regulated by mediated checkpoints that ensure no replication error. These checkpoints include G1, G1/S, intra-S and G2/M checkpoints. Checkpoints are mediated by cyclin and cyclin dependent kinases (CDKs). Both cyclins and CDK initiate a cascade of phosphorylation to progress the cell cycle. When DNA damage occurs, the cell ensures cell division is stopped.[188] This is carried out by CDK inhibitors that are present in response to damage, for example p21. p21 targets p53 (major immunosuppression protein) avoiding the cyclin-CDK complex formation, arresting cell cycle in G2 phase and starting the DNA damage response.[189] p16 is another cell cycle modulator that inhibits CDK4 and cyclin D, preventing their complex formation. This avoids the downstream effect of the CDK-cyclinD complex of phosphorylating retinoblastoma tumour suppressor protein (Rb). Phosphorylated Rb complexes with E2F, which is a transcription factor necessary for cell division. pRb suppresses S-phase by binding E2F. Once pRB is hyperphosphorylated by CDKs, pRB releases E2F, which expresses genes involved in S-phase.[190]

Sensing DNA damage. Cells respond to DNA damage by activating the DDR. To initiate DDRs, DDR kinases ataxia-telangiectasia mutated (ATM) and ATM and rad3-related (ATR) are recruited to sites of DNA damage toregulate DNA repair and cell cycle progression.[191] ATM responds to the more lethal form of DNA damage, double stranded DNA breaks (dsDNA breaks), which are harder to resolve than the single stranded DNA breaks (ssDNA breaks).[192] ATR is recruited to ssDNA breaks.[193] Once activated, ATM/ATR phosphorylate their downstream targets, of which, the best characterised are p53, H2AX, and Chk1/Chk2. For example, p53 is continually degraded via the proteasome following ubiquitination by MDM2.[194] p53 phosphorylation at Ser-15 by ATM/ATR stabilises p53 by preventing ubiquitination by MDM2, which allows p-p53 to orchestrate the DNA damage response and cell fate decisions by controlling expression of p53-target genes, e.g. p21, NOXA, PUMA.[195]

Single strand DNA break repair. Cell-cycle arrest provides time for DNA repair and resulting cell fate decisions to be made. Intrinsic stresses can cause ssDNA breaks. ssDNA breaks are therefore prevented and regulated by several machinery. Replication

protein A (RPA) is a tripartite protein made up of three subunits.[196] It coats the ssDNA breaks and is recognized by ATR-interacting protein (ATRIP). ATRIP recruits ATR and induces ATR autophosphorylation.[197,198] Active ATR phorphorylated RPA at serine 33 and threonine 21 to allow for DNA synthesis and repair.[197] In addition, histone-2AX (H2AX) becomes phosphorylated (γH2AX) avoiding binding of any replication machinery halting the replication fork. In addition, ATR phosphorylates CHK1 which prevents the global DNA replication until ssDNA break is repaired. CHK1 is a checkpoint protein controlling cell cycle progression from S/G2 phase and G2/M phase by recruitment of p53. p53 activates expression of CDK inhibitors like p21, as aforementioned p21 stops replication until the damage is repaired. Inhibition of ATR leads to failed repair machinery which exhaust RPA due to the excessive ssDNA breaks and consequently leads to a permanent cell cycle arrest.[199]

Double strand DNA break repair. Double stranded DNA (dsDNA) breaks are lethal and can affect genes necessary for cell survival. They occur due to intrinsic factors, such as collapsing of replication fork, or extrinsic factors, like chemotherapeutic agents, aphidicolin[200] and etoposide,[201] or genotoxic molecules, typhoid toxin. dsDNA breaks inhibit DNA polymerase activity and cause replication stress.[202]

dsDNA breaks leads to the recruitment of a protein complex, MRN (Mre-11 Rad50 and Nbs1), which detects the damage and subsequently recruits ATM.[203] ATM is autophosphorylated and in turn activates phosphorylate proteins, such as H2AX and checkpoint regulators, such as CHK2, which halts the cell cycle progression. ATM recruits p53 binding protein, 53BP1. 53BP1 binds ATM to the site of dsDNA damage and recruits repair proteins.[204] Similar to the ATR-mediated repair machinery, ATM activates 53BP1 which activates p53 which arrests the cell cycle through driving expression of p21.[205] As the dsDNA break repairs a ssDNA starts forming, this initiates the ATR pathway, allowing both machinery to work to repair the damage.[206]

DNA repair machinery is effective against dsDNA and ssDNA breaks, however excessive DNA damage might not be repaired. In these cases cells try to avoid the mitigated effects of DNA damage so damaged cells undergo senescence or apoptosis.[207]

1.5.2 Cell fate decisions: restart of the cell cycle, apoptosis and senescence.

Re-starting the cell cycle. Once DNA is repaired, cells have to deactivate the DNA damage checkpoint to restart the cell cycle. This process relies on protein phosphatases (PP), PP1, PP4 and Wip. Protein phosphatase PP4 dephosphorylates γH2AX, while PP1 and Wip1 dephosphorylate Chk1 and Chk2, respectively. γH2AX dephosphorylation is necessary for PP1 dephosphorylation of p53, thus, the inactive p53 no longer induces p21

expression and inhibition of CDKs.[208–211] As explained p21, controlled by p53, halts the cell cycle and ensures it is arrested until the DNA damage is repaired.[211] Thus, with a reduction in p21, and a dephosphorylation of checkpoint kinases, cell cycle is restarted after DNA damage repair.

Apoptosis. Cells that do not recover from DNA damage can undergo apoptosis. Apoptosis is a form of programmed cell death initiated after DNA damage. Continuous p53 activation induced by DNA damage through DDR pathways, both ATR and ATM, leads to p53 mediated apoptosis. P53 induces the expression of BH3 proteins such as PUMA and NOXA. Studies showed NOXA and PUMA as critical effectors for apoptosis. Both NOXA and PUMA are directly upregulated by p53 and inhibit the prosurvival proteins such as BCL2, which act as inhibitors of apoptotic effectors BAX and BAK. In addition, p53 activates BAX and BAK which in turn releases cytochrome c from mitochondria and starts a cascade of events leading to apoptotic cell death. Studies showed that a knockout of NOXA and PUMA protects the cell against p53 mediated apoptosis[212–216]

Senescence. Senescence is associated with permanent cell cycle arrest. It is a tumour suppressor mechanism which arrests the cell cycle to stop DNA damage passing on to daughter cells causing catastrophic effects. The main hallmarks of senescence include permanent cell cycle arrest, macromolecule damage, down regulated metabolism and a senescence associated secretory phenotype (SASP).[217] Senescence can be grouped into either acute senescence or chronic senescence (the latter is covered below). Following acute senescence, the cells are thought to be eliminated through immune cells, such as cytotoxic T-cell and macrophages. Therefore, they need to attract immune cells, which they do via an inflammatory secretome that establishes SASP. SASP is amongst the hallmarks of senescence that ensures its persistence. SASP allows for secondary senescence in bystander cells that amplifies mobilisation of immune defences.[218]

SASP is a collection of inflammatory proteins, cytokines, chemokines and growth factors secreted by the senescent cell. There is no signature SASP as it differs between cell types and senescence inducers. Recently, a library of SASP proteins identified between different cell types in response to different inducers was created and thus this library becomes a reference of the known SASP proteins to date.[219]

Inducers of senescence include DNA damage resulting from oncogene expression, irradiation or genotoxins (e.g. chemotherapy, pollutants, typhoid toxin). A pivotal inducer of senescence is p53, which is activated by the DDR, and drives prolonged expression of p21 that contributes to long-lived, often permanent, cell-cycle arrest. It was shown that p21-deficient mice were unable to undergo senescence and instead damaged cells became apoptotic, which in the case of embryos showed severe embryonic deformities.[220]

While the benefits of senescence are clear (i.e. tumour suppression), aberrant accumulation of senescent cells can cause chronic inflammation and disease. This is generally referred to as chronic senescence and can be due to (i) persistent low-grade DNA damage, exacerbated by oncogenes, chemotherapy, and chronic exposure to genotoxins. For example, *E.* coli colibactin toxin is thought to promote chronic senescence resulting in colon tumour growth.[221](ii) Senescence can also be exacerbated by an ageing immune system with declining function that fails to eliminate the senescent cells efficiently.[222] Immune cells are not immune to SASP, although SASP recruits immune cells, SASP can induce senescence in immune cells.[223] Thus, with a senescent immune cell, clearance of senescent cells becomes less effective. This leads to the accumulation of senescence cells and SASPs making it harder for the immune system to clear senescence, which can remodel the tissue environment.[224,225] For example, senescent cells can occupy niches within tissues or cause chronic inflammation through SASP, which causes DNA damage thereby promoting cancer.[217]

Thus, in early life, senescence is a powerful innate defence against diseases such as cancer but when deregulated, particularly ageing organisms, excessive senescence promotes disease.

1.5.3 Activation of host DNA damage responses by typhoid toxin

Studies with *Salmonella* infection showed that the typhoid toxin induces several cellular events. *Salmonella*'s typhoid toxin causes DNA damage in a manner dependent on nuclease activity as substitution of H160Q in CdtB abrogates DDRs.[226] *S.* Typhi infections with an active typhoid toxin produces a γH2AX response as well as cell cycle arrest.[134] This was observed in several studies with direct intoxication with purified typhoid toxin and using toxigenic *Salmonella in vitro*.[56,152,226] Point mutations in the His160 of the CdtB subunit has been shown to disable the DNase activity of the toxin.[147,226] Ibler, *et al.*, showed that the wild-type (WT) toxin caused DNA damage as well as senescence phenotypes in intoxicated cells compared to the His160-Gln mutant toxin (HQ).[226] Both the typhoid toxin and CDTs have been shown to activate ATR and ATM pathways in intoxicated cells following DNA damage and phosphorylate H2AX.[167,168,226,227] Consistent with ATM/ATR activation, the typhoid toxin arrests the cell cycle in G1 and G2 phases of the cell cycle.[226]

The nuclease activity of typhoid toxin was shown to cause distinct γH2AX phenotypes during infection with *S.* Typhi, *S.* Javiana and treatment with purified toxin.[226] γH2AX foci during G1 arrest colocalized with 53BP1 indicating DSBs while γH2AX during G2 arrest localised to heterochromatin at the nuclear periphery, which was uncoupled from 53BP1 marking a novel response induced by a genotoxin (RING).[226] Extensive SSBs

caused by the toxin during S phase resulted in activation of ATR, Chk1 and sequestration of the ssDNA-binding protein RPA, which caused DNA replication stress and DNA damage manifesting as the RING phenotype.[226]

1.5.4 Cell fate decisions in response to typhoid toxin

Apoptotic responses to typhoid toxin. Currently, there is no direct evidence that typhoid toxin causes apoptosis. However, given that CDTs also exert their toxigenic effects through CdtB and CDTs induce apoptosis, it is very likely that typhoid toxin can also induced apoptosis in certains contexts. For example, CDTs have been shown to induce apoptosis in a p53-dependent manner.[228–230] The CdtB subunit of *Haemophilus parasuis* shows p-53 dependent apoptosis *in vitro*.[230] Similarly, the CdtB subunit of *Aggregatibacter actinomycetemcomitans*, causes cell cycle arrest and apoptosis. CdtB active toxin reported increasing levels of p21 in lymphoid cells and primary lymphocytes. Increased p21 expression coincided with an increase in p21 phosphorylation.[228]

Senescence responses to typhoid toxin. *S. enterica* exploits chronic senescence in ageing organisms indirectly: ageing rats were found more susceptible to colonisation by *S.* Typhimurium,[231] which also exhibited enhanced invasion into ageing fibroblasts relative to young fibroblasts from human volunteers.[232] Ageing women have also been associated with increased susceptibility to chronic *Salmonella* carriage.[233] This indicates that senescence due to ageing increases host susceptibility to *Salmonella* infection.

Work on the typhoid toxin indicates that *Salmonella* can cause acute senescence, which can age cells prematurely.[141,226] This fits with the previous observations reporting CDT inducing senescence *in vitro*.[234] DNA replication stress resulting from the typhoid toxin-induced RING phenotype caused acute senescence in fibroblasts and epithelial cells The senescent cells were found to release a secretome in a toxin-dependent manner either during infection or following treatment with purified toxin. The secretome promoted paracrine senescence, DDRs and invasion of bystander cells, a mechanism referred to as toxin-induced SASP (txSASP).[226,235]

Ibler *et al.,* 2019 used cancer cell models to study toxin-induced senescence, which makes the *in vivo* relevance of premature senescence unclear. Publications in back-to-back editions of Cell Reports revealed that the typhoid toxin induced senescence in the intestinal mucosa of mice at 10-days post infection with *S.* Typhimurium^{TOX}.[141,236] Senescence induction by *Salmonella* in humans remains to be established.

1.5.5 The consequences of bacterial activation of host DDRs

Activation of host DDRs promote infection. Ibler et al showed that DDRs can promote infection by toxigenic *Salmonella* and postulated that senescence is hijacked to

accelerate ageing to make the host more susceptible to infections.[226] In support of this view, there are instances where bacterial pathogens have been shown to hijack DDRs for the benefit of infection.[237–239]

Activation of host DDRs counteract infection. DDRs are protective host responses against cancer but there is also evidence that the DDR can counteract infection. p53 has been shown to suppress cell metabolism to counteract the growth of cancerous cells.[240] Similarly, p53-mediated suppression of cell metabolism via the mTOR pathway was reported to suppress the growth of the obligate intracellular bacterial pathogen *Chlamydia Trachomatis*, which relies on host cell metabolism for nutrients.[241]

1.6 Hypothesis

The typhoid toxin activates DDRs and senescence during infection of cultured cells and animal infection models.[139–141,226] The resulting senescence causes release of a host secretome, which remodels bystander cells in the infection niche and enhances infection - referred to as txSASP in Ibler et al 2019.[226] While *Salmonella*-induced senescence has been observed in cultured cells and mice, txSASP has only been observed in cultured cells. Moreover, *S.* Typhi does not cause typhoid in cultured cells or animals. Thus, toxin-induced DDRs need to be examined in clinical samples from humans with typhoid to reveal the significance of senescence responses during *S.* Typhi infection.

The TYGER study by Gibani, *et al.,* 2019 showed that bacteraemia was of significantly shorter duration in human participants with typhoid when infected with wild-type *S.* Typhi relative to toxin-negative *S.* Typhi. Thus, plasma samples from the TYGER study provide a valuable resource to test toxin-dependent responses, which resulted in a measurable response during bacteraemia.

My hypothesis is that (i) the plasma of bacteraemic participants infected with wild-type *S.* Typhi will contain a toxin-specific host secretome, and that (ii) the secretome will influence *Salmonella* infection in one of two ways: firstly, the host secretome may promote infection, which is in agreement with Ibler, *et al.,* 2019.[226] However, this is difficult to interpret with respect to the limited bacteraemia observed with wild-type *S.* Typhi in Gibani, *et al.,* 2019.[56] A second possibility is that the host secretome contains antimicrobial proteins, which counteract *S.* Typhi and could help eliminate the bacteria from the bloodstream.

I addressed my hypothesis with the following project aims:
Aim 1: Resolve the host secretome in plasma samples from bacteraemic human participants infected with either wild-type or toxin-negative *S.* Typhi.
Aim 2: Investigate the significance of the DDR to the identified host secretome and its putative role in *Salmonella* host-pathogen interactions.

Chapter 2

Results Part I

Salmonella Typhi is a strict human pathogen. Cultured human cells are a faithful but a limited model as are humanised mice,[94,95] which have been engineered deficient in innate immune responses. Clinical studies remain the most faithful model to study typhoid fever and the virulence factors of *S.* Typhi. This is exemplified by the human infection challenge model pioneered at the University of Maryland between 1952 and 1974.[90,242] Building on this, the Oxford vaccine group (OVG) established an outpatient *S.* Typhi human challenge model in healthy adult volunteers.[30] The model the human-restricted pathogen to be investigated in its natural human host within an experimental setting and developed the model to look at specific virulence factors including the typhoid toxin. The OVG performed a human infection challenge (TYGER study) using fully antibiotic susceptible *S.* Typhi (Quailes strain) of wild-type (WT) origin or the isogenic toxin-negative (TN) derivative lacking genes for pltB, pltA and cdtB.[56] With a dose of 25,000 CFUs in participants pre-treated with sodium bicarbonate, both WT and TN caused typhoid fever in ∼70% of participants but no significance difference in attack rate or symptom development between WT and TN was observed. Shedding was reported sporadically in the WT infected from day 1 to day 14 post-infection. Alternatively, TN infected reported shedding in a more confined pattern of continuous shedding from days 1 to day 4 but still no significant difference was observed. The most striking result was the significant difference in the duration of bactereamia, which persisted for up to 96h with TN *S.* Typhi (mean of 48h) relative to up to 48h with WT *S.* Typhi (mean of 30h). This was not due to significant differences in circulating *S.* Typhi (TN 0.2 CFU/ml, WT 0.55 CFU/ml). The findings are illustrated in (**Fig.2.1**). The TYGER samples from participants displayed toxin-dependent differences in the duration of bactereamia, providing a valuable resource for investigating the toxin and the hypothesis that the toxin induces a host DDR secretome, which influences host-pathogen interactions. Collaboration with the Oxford vaccine group funded by two HIC-Vac pump priming grants allowed me to utilize plasma samples from these volunteers before and after infection. The aim was to identify proteomic signatures in response to the typhoid toxin associated with infection.

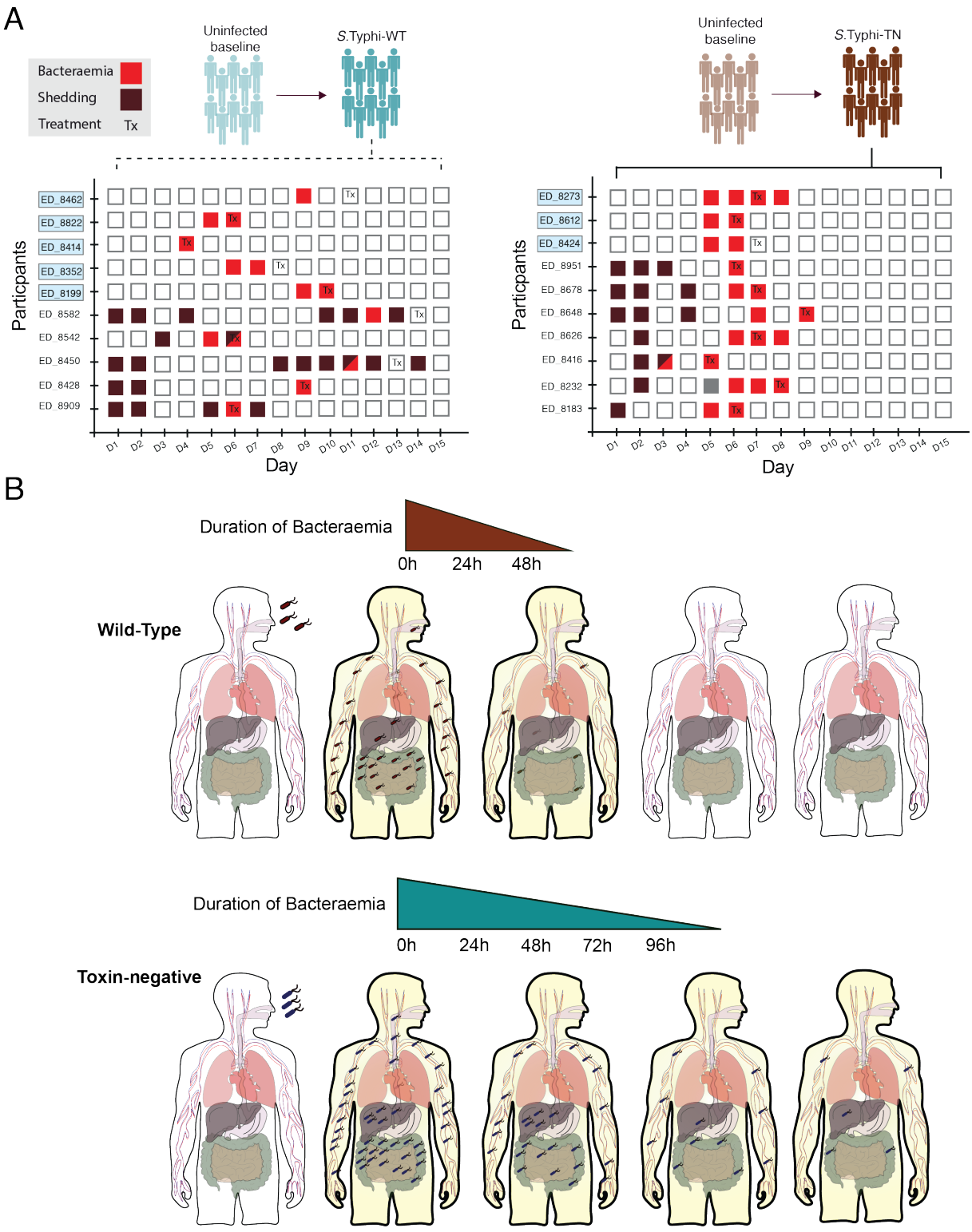

Figure 2.1: Oxford vaccine group shows prolonged bacteraemia in TN infected participants compared to the WT infected counterparts..
(A) Shedding (brown) appears in scattered timepoints, meanwhile bacteraemia (red) shows a more consistent pattern. **(B)** The duration of bacteraemia in the WT infected goes up to 48 hours and 96 hours in the TN infected.

2.1 Immunodepletion removes high abundance proteins from TYGER samples

About 94% of human plasma consists of high abundance proteins conserved between individuals,[243] which mask low abundance proteins of interest in LC-MS/MS experiments. Hence, Agilent MARS-14 and Thermoscientific High Select Top14 immunodepletion columns, were chosen for their selective ability to bind high abundance proteins and elute low abundance proteins using affinity chromatography (**Fig.2.2**). Although proven effective, more tests had to be carried out to investigate which column is more effective for the TYGER study plasma samples.

Theoretically, blood plasma is expected to have high abundant proteins of about 94% and the remaining 6% are proteins of low abundance[243] (depicted in **Fig.2.2C**). Amongst plasma, 14 proteins are the most prominent: Albumin, Immunoglobulin G, A and M, Transferrin, Fibronogen, Haptoglobulin, α1-antitrypsin, α2-Macroglobulin, Apolipoproteins A-I and A-II, α1- acid glycoprotein, complement C3 and Transthyretin (**Fig. 2.2B**). Both immunodepletion columns tested showed a reduction in high abundance proteins from theoretical 94% to 34% by Thermoscientific High select Top-14 mini spin column (**Fig. 2.2D**). Meanwhile, Agilent columns depleted from 94% to 4% significantly more efficiently than Thermoscientific columns (**Fig. 2.2E**). Liquid Chromatography with tandem mass spectrometry (LC-MS/MS) of both eluates from Thermoscientific and Agilent columns, identified 226 proteins and 160 proteins respectively. Further validating the efficiency of Agilent columns compared to their ThermoScientific counterparts. Furthermore, Agilent column, through LC-MS/MS, identified 226 proteins post immunodepletion, while Thermoscientific columns identified 160 proteins (**Fig. 2.2F**). This is evidence of efficiency for the Agilent columns. This encouraged more optimization on the reusable Agilent columns.

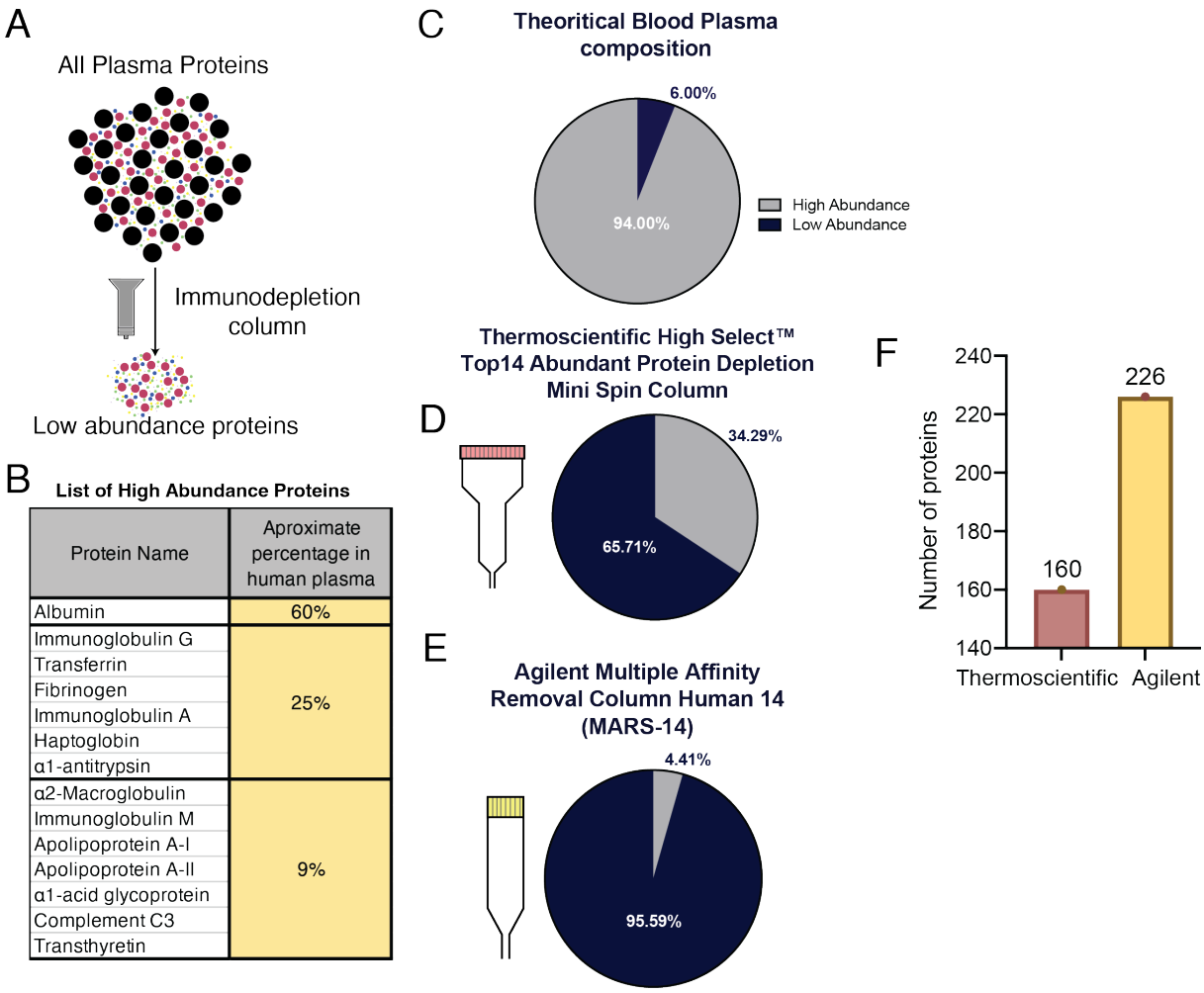

Protein Name	Aproximate percentage in human plasma
Albumin	60%
Immunoglobulin G	25%
Transferrin	
Fibrinogen	
Immunoglobulin A	
Haptoglobin	
α1-antitrypsin	
α2-Macroglobulin	9%
Immunoglobulin M	
Apolipoprotein A-I	
Apolipoprotein A-II	
α1-acid glycoprotein	
Complement C3	
Transthyretin	

Figure 2.2: **(A)** Immunodepletion columns remove high abundance proteins (black) and elute low abundance proteins (coloured). **(B)** List of the 14 most common high abundance proteins in the blood. **(C)** Theoretical composition of high abundance proteins in blood plasma. **(D)** Comparing iBAQ values of high abundance proteins testing efficiency of Themoscientific high select top14 abundant protein depletion mini spin column. **(E)** Comparing high abundance proteins iBAQ of agilent multiple affinity removal column Human-14 (MARS-14). **(F)** Number of detected proteins in elution through Thermoscientific and Agilent columns.

2.2 Pilot experiment shows Agilent columns are efficient in immunodepletion of plas-ma samples.

Plasma purchased from Sigma Aldrich were used to test the efficiency of MARS-14 column. The recommended loading capacity of the MARS-14 column is between 300-500µg per experimental run. Plasma was diluted to five samples 300µg each per run as per manufacturer's instructions (**Fig. 2.3A**). All samples were significantly depleted within the acceptable range (5-12%), identified by BCA analysis post immunodepletion (**Fig. 2.3B**). This provided confidence in column efficiency, thus TYGER plasma were randomly picked from two separate participants (**Fig. 2.3C**). Immunodepletion of TYGER plasma with MARS-14 column was significantly depleted with a depletion efficiency of 90-92%

(**Fig.2.3D**). To test if the reduction in protein concentration is also associated with a reduction in high abundance proteins, samples were digested into peptides before LC-MS/MS analysis .

Pilot experiment generated label-free quantitation (LFQ) intensities and intensity based absolute quantification (iBAQ) values were generated by Max-Quant analysis following LC-MS/MS. iBAQ represents the sum of all peptide intensities divided by the sum of all peptides of a protein. It is used to compare proteins within the same sample. LFQ intensity is very similar to iBAQ however it excludes outliers to represent a better ratio of the protein between different samples. To test the efficiency of the column per sample, iBAQ values of high abundance proteins were compared to the rest of the identified proteins. Depleted Sigma plasma and both TYGER samples were depleted of high abundance proteins to 3.5%, 4.6% and 6.8% respectively (**Fig. 2.3E, F and G**).

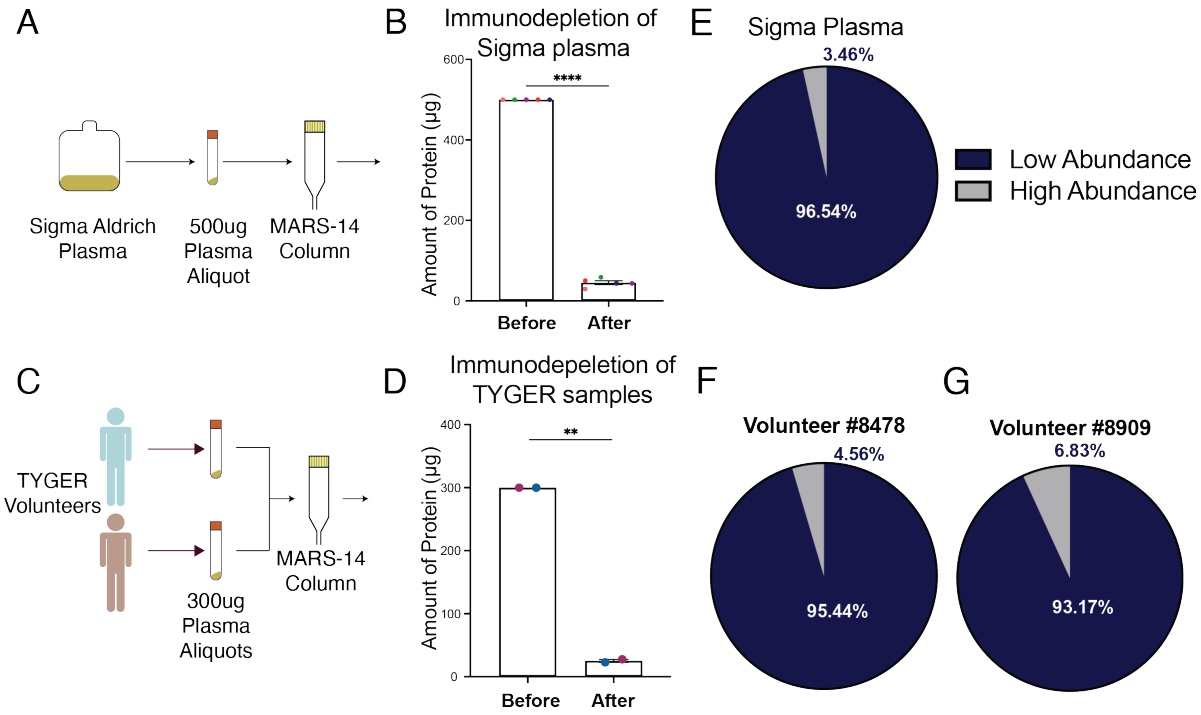

Figure 2.3: Immunodepletion efficiency pilot experiment**(A)**Sigma-Aldrich purchased plasma diluted to 500µg aliquots and depleted using MARS-14 column. **(B)** Bar chart showing final protein concentration post depletion (n=5). **(C)** TYGER plasma samples diluted to 300µg and depleted using MARS-14 column. **(D)** Bar chart showing final protein concentration post depletion. **(E)** Pie chart representing iBAQ values of depleted proteins in Sigma plasma. **(F)** and **(G)** Pie charts of depleted TYGER samples (Participant 8478 and 8909) before infection respectively, comparing high and low abundance proteins.

2.3 Inactivating *Salmonella* in eluted samples

Following elution, steps were carried out to eliminate *S.* Typhi and minimize risk of typhoid transmission from the hazard group 3 pathogen. Based on the strict recruitment criteria set by the TYGER study, participants were all tested for Hepatitis A, B and C,

as well as HIV or any infectious diseases, which leaves *S.* Typhi as the likeliest remaining pathogen in the plasma samples, which were shown to contain *S.* Typhi (TN 0.2 CFU/ml, WT 0.55 CFU/ml)

Acetone is an efficient method to precipitate proteins.[244] In addition, acetone has been shown to kill *S.* Typhi and was approved for the use in whole cell vaccines.[245] Indeed, 4-volumes of acetone killed both a vaccine candidate strain of *S.* Typhi [BRD948] and wild-type *S.* Typhimurium [ST1344] (**Fig.2.4**). (**Fig.2.4A**)and (**Fig. 2.4C**) shows serial dilutions of *S.* Typhi and *S.* Typhimurium, respectively, incubated with Buffer A (elution buffer) or Acetone. Buffer A disturbed the growth of *S.* Typhi and did not affect *S.* Typhimurium growth. No viable *S.* Typhi and *S.* Typhimurium were observed in the presence of acetone (**Fig.2.4**). This led us to conclude that the samples would be pathogen free after acetone incubation. Thus, acetone was to used precipitate eluted proteins whilst also sterilizing any *S.* Typhi contaminating the elution as shown in (**Fig.2.4A**) before proceeding to S-Trap digestion of the elution and identification of proteins using LC-MS/MS mass spectrometry (**Fig.2.5**).

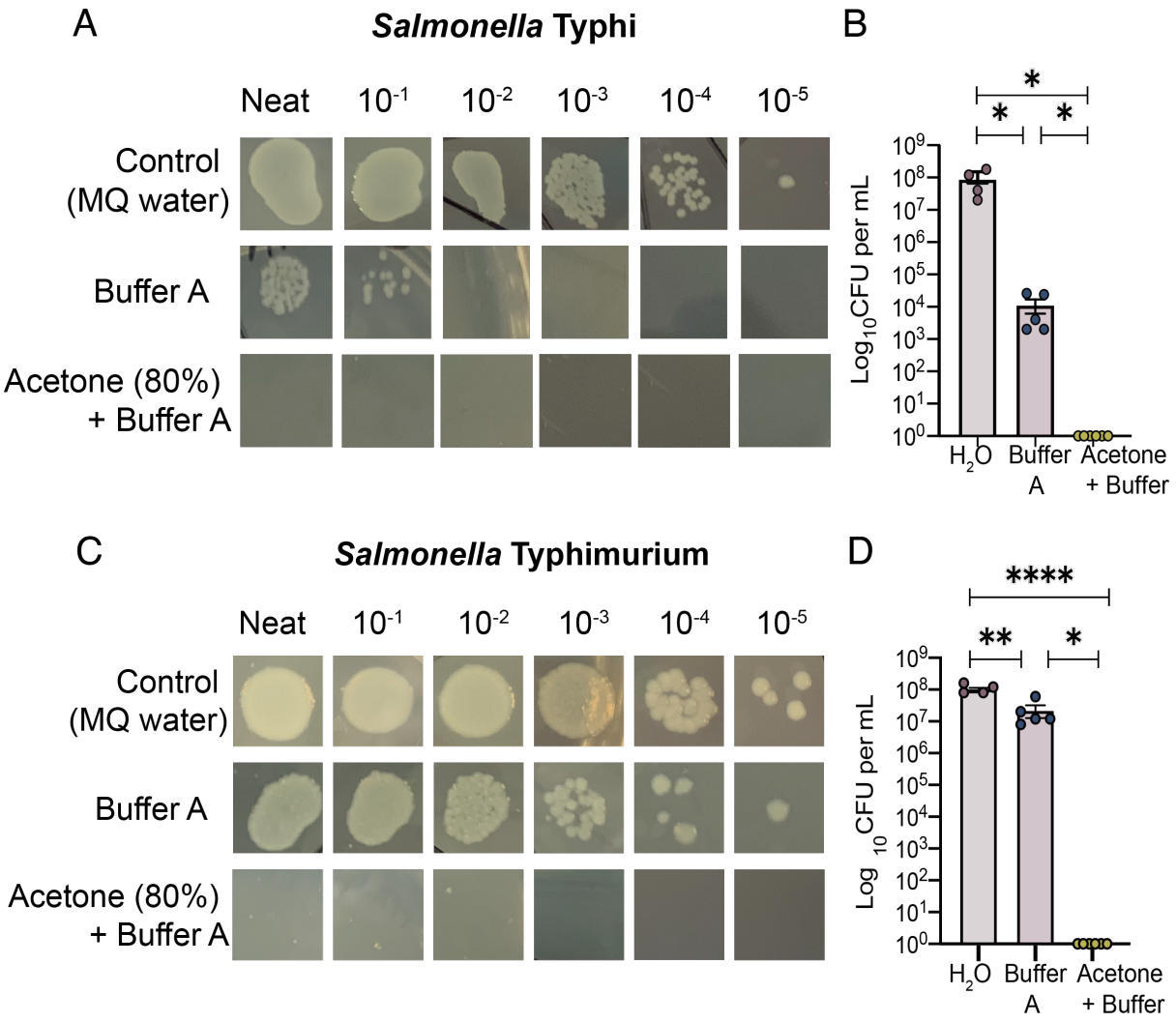

Figure 2.4: Ensuring safety of use of plasma samples. (A) Colony forming unit (CFU) count of *Salmonella* Typhi (BRD948) untreated controls compared to elution buffer (buffer A) and acetone precipitation buffer (Acetone 80% in elution buffer). **(B)** Quantification of Log_{10} CFU counts per ml of *S.* Typhi suspension. **(C)** CFU count of *Salmonella* Typhimurium (ST1344) in response to acetone precipitation buffer. **(D)** Quantification of Log10 CFU counts per ml of *S.* Typhimurium suspension.

2.4 Preparation of all TYGER plasma samples for LC-MS/MS

TYGER sample concentrations were quantified using BCA analysis before and after immunodepletion. Samples were depleted of between 90-98% of plasma proteins (**Fig.2.5A**), which resulted in elution of low abundance proteins at concentrations ranging from 10 µg/ml to 50 µg/ml (**Table 2.1**). To precipitate eluted proteins, samples were incu-

bated in acetone overnight (**Fig.2.5A**) before generation of peptides by S-Trap digestion (**Fig.2.5B**). Once digested, samples were analyzed with LC-MS/MS followed by MaxQuant analysis generating Pearson correlations to assess the similarity between samples (**Fig.2.5C**). Pearson correlation is a way to assess experimental variability thus identifying how reproducible replicates are. In addition, it identifies outliers that can be excluded from the analysis. The closer the Pearson coefficient value to 1 the more similar the samples are to each other. All samples showed positive Pearson values of higher than 0.9 demonstrating a strong positive correlation. Baseline TN samples (red) replicate 1 encountered an error when running the MaxQuant and consequently show the lowest pearson values. This is necessary to determine the process of analysis. Due to the variations in divergence, samples must be correlated between their respective baseline rather than comparing both post-infection groups. This established the analysis method which will be applied to identify significant proteins.

Sample code	Time of extraction	Allocated group	Concentration (µg/µl)	Percentage eluted in ID column
8183	D0	TN	32.90	3.69%
8232	D0	TN	22.08	4.64%
8273	D0	TN	53.14	4.67%
8416	D0	TN	30.55	6.42%
8424	D0	TN	26.78	4.00%
8612	D0	TN	36.20	4.29%
8626	D0	TN	27.73	6.70%
8648	D0	TN	25.84	7.72%
8678	D0	TN	33.84	6.24%
8951	D0	TN	30.55	7.27%
8183	TD	TN	17.20	5.96%
8232	TD	TN	14.80	4.83%
8273	TD	TN	23.40	6.50%
8416	TD	TN	17.70	6.97%
8424	TD	TN	13.60	7.22%
8612	TD	TN	14.40	7.24%
8626	TD	TN	12.30	7.70%
8648	TD	TN	24.40	8.10%
8678	TD	TN	16.00	7.43%
8951	TD	TN	15.60	7.18%
8199	D0	WT	33.37	5.83%
8352	D0	WT	54.08	4.77%
8414	D0	WT	41.37	10.56%
8428	D0	WT	24.43	6.87%
8450	D0	WT	43.89	8.89%
8462	D0	WT	38.32	2.97%
8542	D0	WT	45.92	6.96%
8582	D0	WT	26.68	7.49%
8822	D0	WT	36.20	6.52%
8909	D0	WT	44.40	9.22%
8199	TD	WT	13.50	8.00%
8352	TD	WT	10.60	6.66%
8414	TD	WT	17.40	3.89%
8428	TD	WT	10.60	7.00%
8450	TD	WT	10.90	9.00%
8462	TD	WT	20.70	10.34%
8542	TD	WT	13.60	4.00%
8582	TD	WT	11.70	7.14%
8822	TD	WT	28.30	5.12%
8909	TD	WT	16.60	8.06%

Table 2.1: Immunodepleted elutions concentrations. Sample codes before (D0) and at the time of typhoid diagnosis (TD) due to the toxin negative (TN) and Wild-Type (WT) strains.

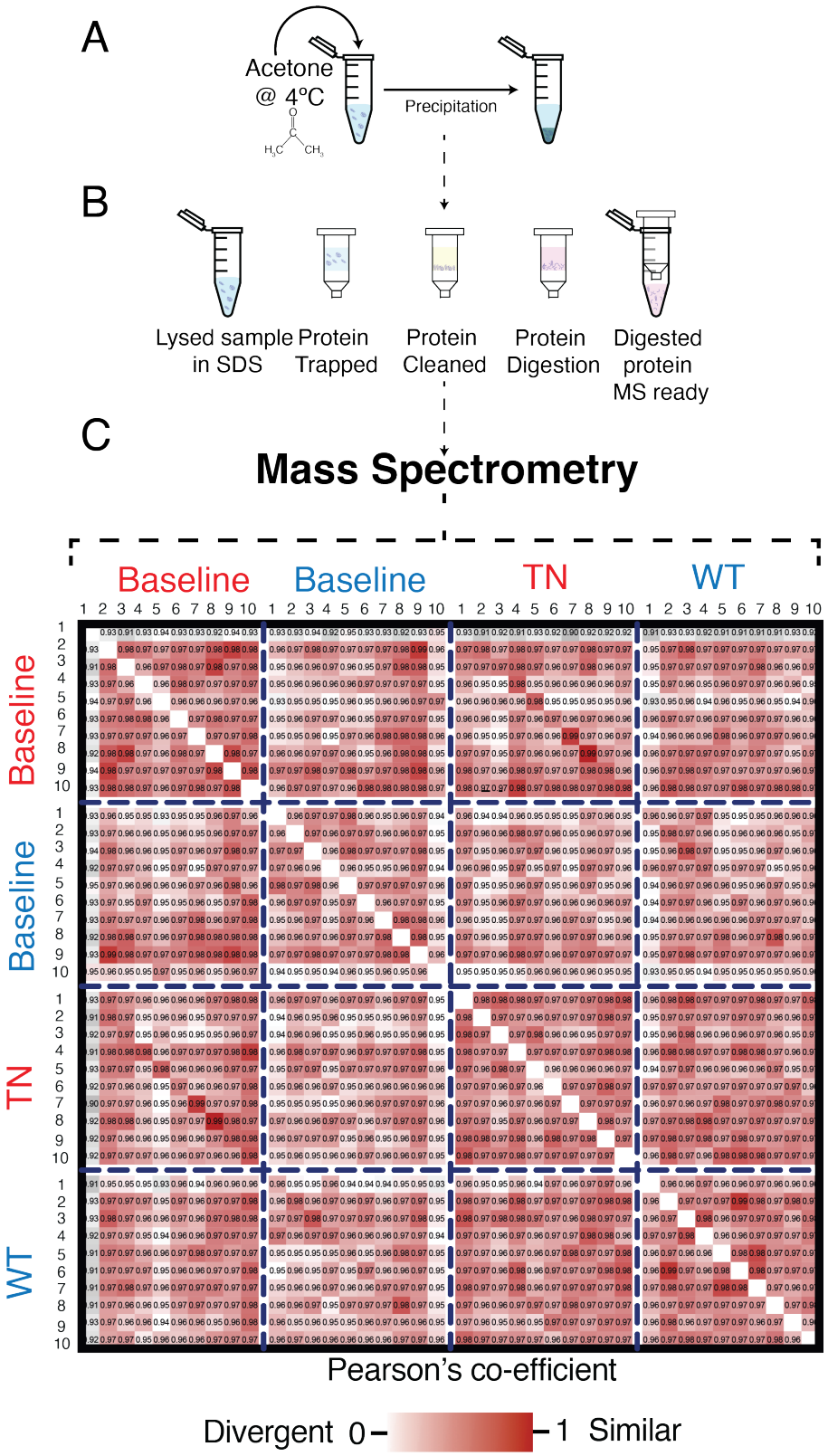

Figure 2.5: TYGER samples immunodepletion. **(A)** Schematic of acetone precipitation process. **(B)** Schematic of S-trap digestion protocol. **(C)** Pearson correlation heatmap, Pearson coefficient=1 represents similar samples, Pearson coefficient = 0 represents most diverse.

2.5 Initial results from Max-Quant analysis show successful preparation of samples.

LFQ-intensities of every sample were plotted against count. All samples show good LFQ counts and thus high protein counts. LFQ intensities varied between 15-35 meanwhile the count of detected proteins at these LFQ intensities would go as high as 100 in most samples (**Fig. 2.6**). Samples were then normalized to fit a normal distribution (**Fig.2.7**). Unidentified protein data with low LFQ intensity and count were imputed generating the final proteomics dataset (**Fig. 2.8**).

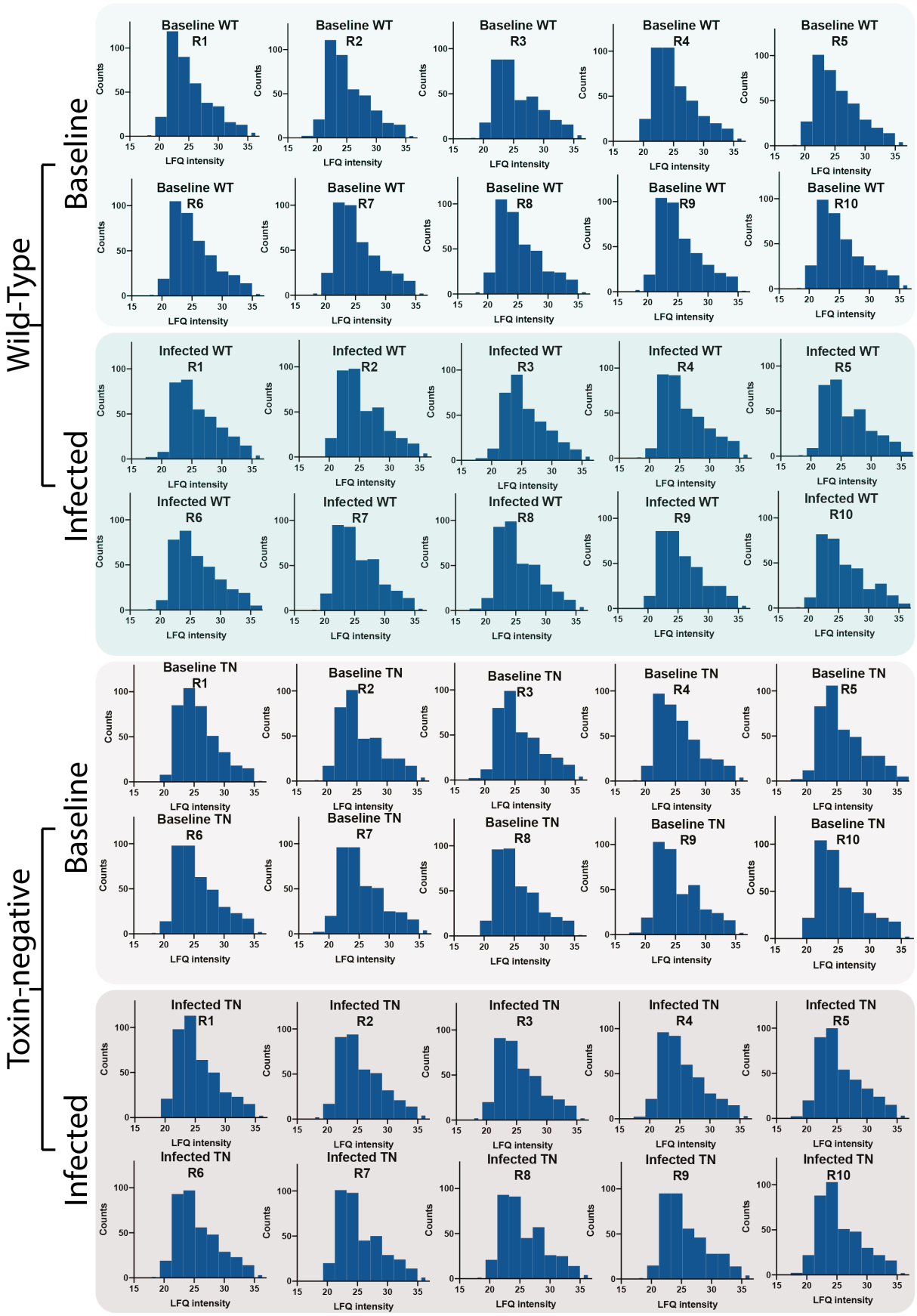

Figure 2.6: Unnormalized LFQ intesnity histograms. Unnormalized LFQ intensity (x-axis) and count (y-axis).

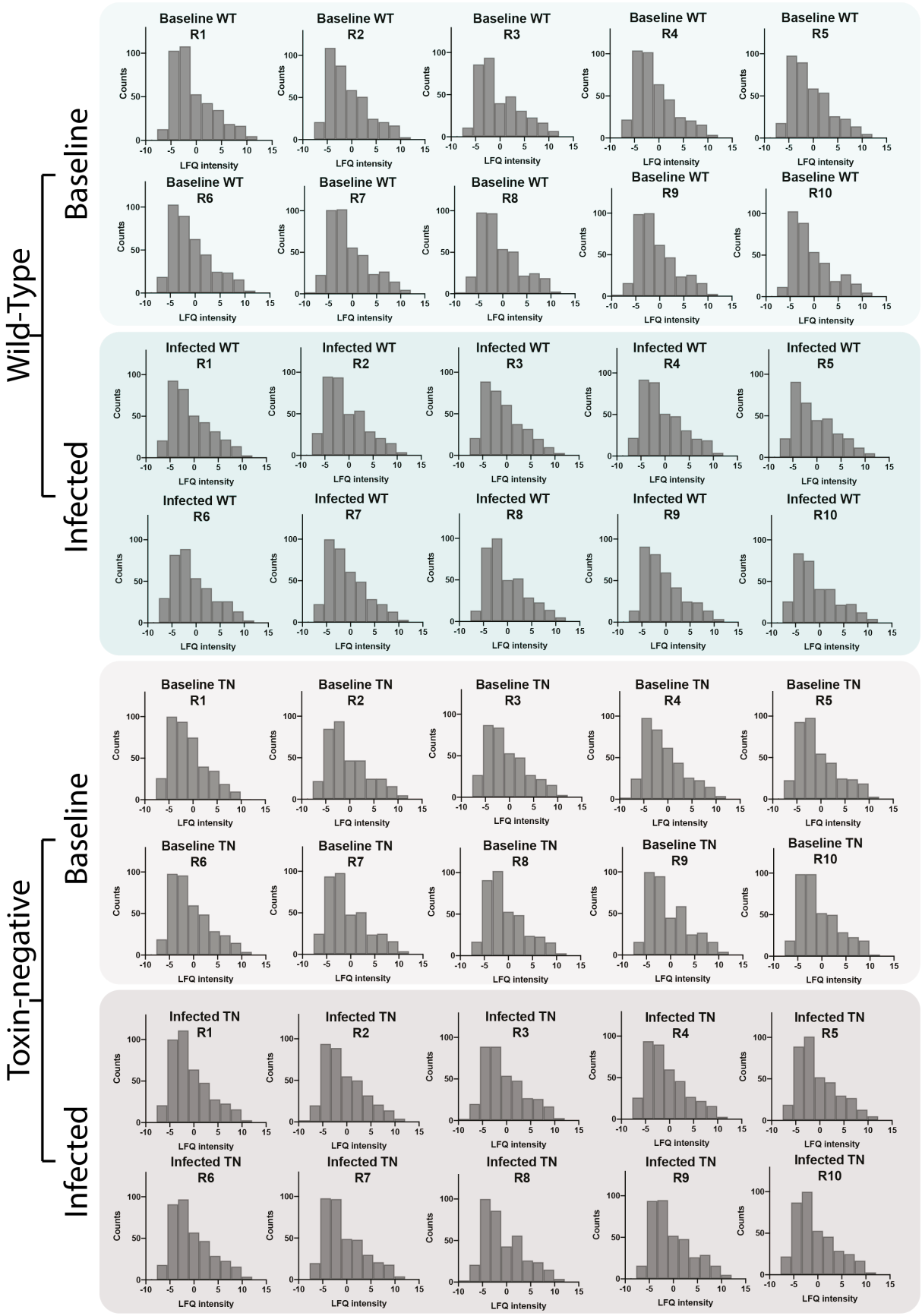

Figure 2.7: Normalized LFQ intesnity histograms. Log2 LFQ intensity values (x-axis) versus count (y-axis) centered around mean intensity per sample.

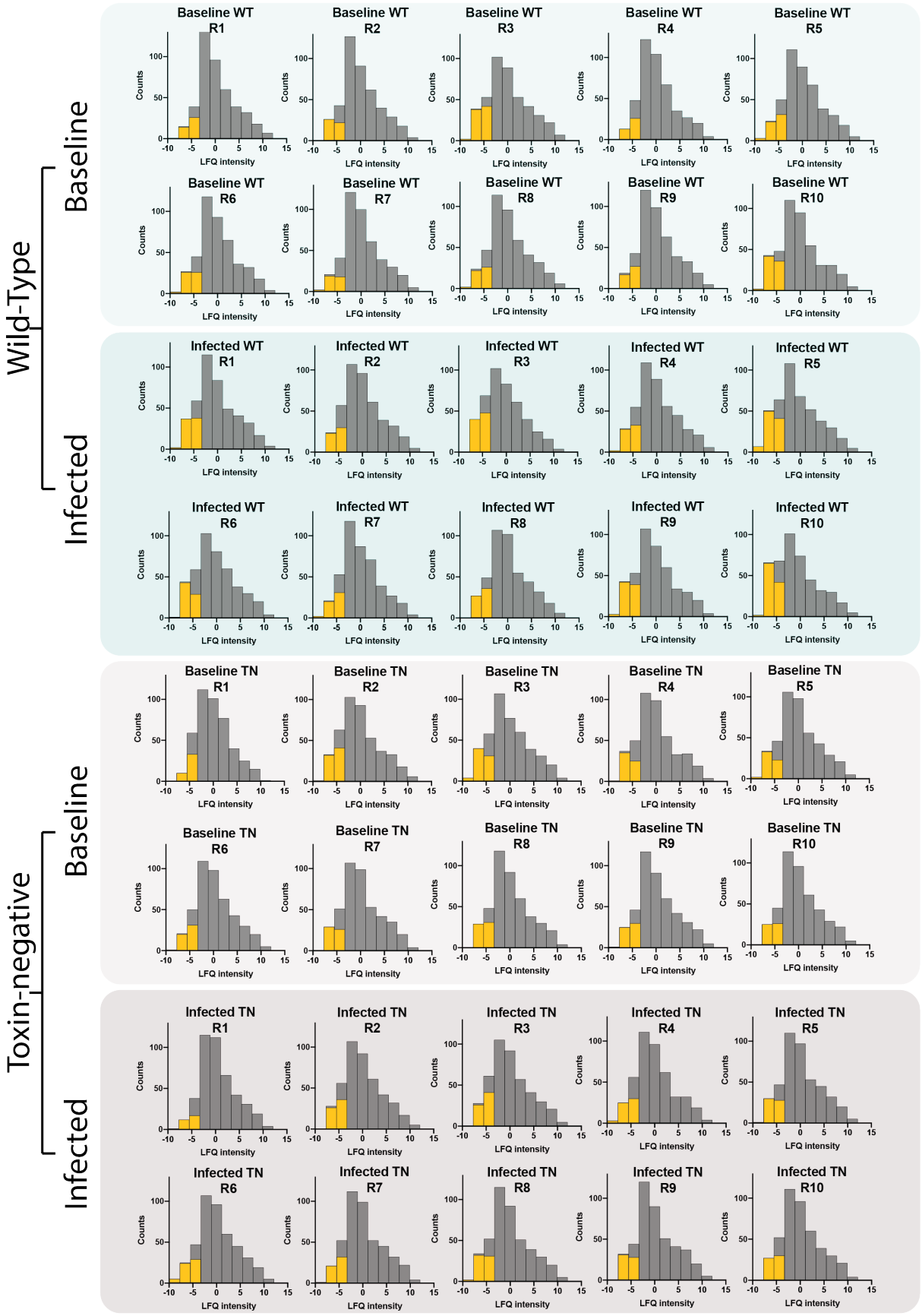

Figure 2.8: Imputed LFQ intensity histograms Log2-transformed intensities across each sample normalized with the mean and variance estimated from observed data set imputing random missing values (Yellow).

.

2.6 Typhoid toxin induces a distinctive host secretome in *Salmonella* WT infected human participants

Human samples are variable and thus each baseline sample had to be compared to its respective individual post infection (**Fig. 2.9A,C**). LC-MS/MS identified 440 proteins across all 40 samples. Statistical analysis employing student t-test identified significantly secreted proteins per sample (*$p<0.05$).* Volcano plots show that 41 proteins were differentially secreted in WT-infected relative to baseline (**Fig. 2.9B**). In the TN group, only 9 proteins were significant relative to baseline (**Fig. 2.9D**).

Of the 9 TN-specific proteins, 6 proteins overlapped in the WT group identifying them as infection-specific toxin-independent proteins **(Black)**. Three proteins were unique to the TN group marking them as TN specific markers **(Blue)**. The WT group showed 5 toxin specific proteins with increased secretions **(Purple)** and 30 toxin specific proteins with decreased secretion**(Yellow)**(**Fig. 2.9D**).

The WT-toxin specific proteins vary in expression and establish a range of secretions from beta-2-micoglobulin (B2M) being the most secreted and Prostaglandin D2 Synthase (PTGDS) the least secreted, with a decrease in its secretion relative to the baseline (**Fig.2.10A**). To identify protein involvement in the secretome, the 440 identified proteins were correlated with the published human proteome database[246] followed by a correlation to the human secretome database[247] (**Fig.2.10B**). It showed that 99% of the identified proteins are known constituents of the human proteome[247] (**Fig.2.10C**). Meanwhile, 73% of the proteins were reported in the human secretome[247] (**Fig.2.10D**) which include 68% of the WT-Toxin specific proteins, making up 5.5% of total secreted proteins, leaving only 32%, as 11 proteins, not reported in the human secretome, making up 2.5% of the secreted proteins[247] (**Fig.2.10E**). Thus, the data showed that the toxin induces a release of a host secretome which could be a signature of the typhoid toxin.

Secretome-WT specific proteins correlated to panther databases of protein classes showed a variety of classes identified (**Fig.2.10F**). Looking at the 5 toxin specific proteins with increased secretions, beta-2-micoglobulin (B2M), Apolipoprotein F (APOF), Lysozyme (LYZ), Thymosin (TMSB4X) and Apolipoprotein C3 (APOC3). TMSB4X is a reported cytoskeletal and cell adhesion protein.[248] It is associated with actin polymerization.[249] B2M is a reported defense protein[250] and displays antimicrobial activity on streptococci pathogens.[251] LYZ is a metabolite interconversion protein[252] which ultimately is responsible for some bacteriolytic functions.[253] Meanwhile, APOC3 and APOF are reported carrier proteins involved in lipid metabolism[254,255] (**Fig.2.9E**). The increased secretion

proteins showed a variety of protein classes, thus further investigations were necessary to identify the proteins to start validations with.

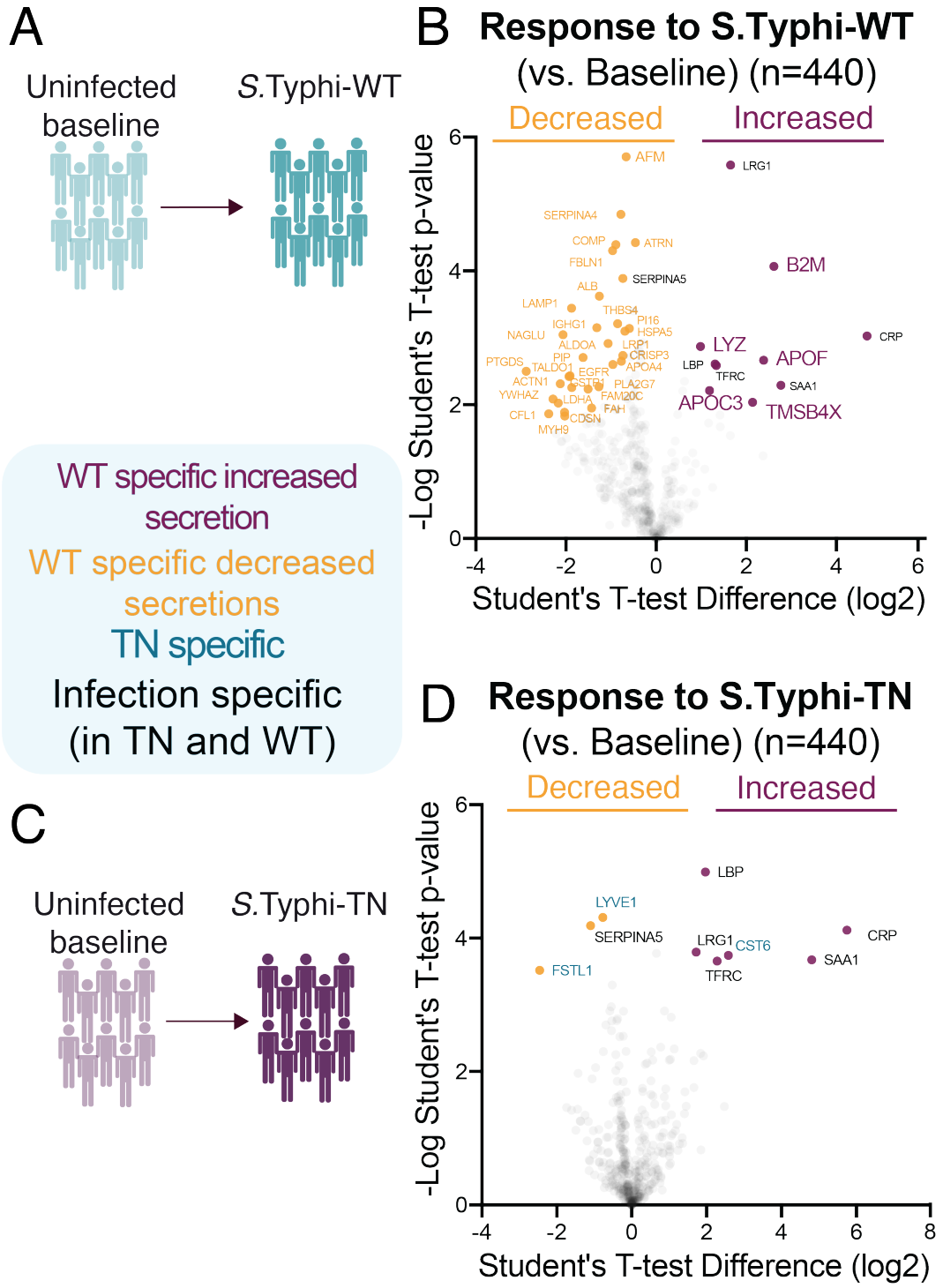

Figure 2.9: Analysis of toxin induced secretome. **(A)** Schematic of plasma samples collected at baseline from uninfected volunteers and at time of diagnosis (TD) of those infected with *S.* Typhi WT or *S.* Typhi TN. **(B)**, **(C)** Volcano plot of significantly secreted proteins in response to infection with *S.* Typhi WT or *S.* Typhi TN respectively; toxin-specific enhanced secretion proteins (Purple), toxin-specific reduced secretion(Yellow) and conserved in both WT and TN (Black). **(D)** Heat-map of enhanced (Purple) to reduced (Yellow) secretion proteins. **(E)** % of toxin specific reported proteins in several protein classes. Increased secretion proteins corresponding to several protein classes are noted on respective bars.

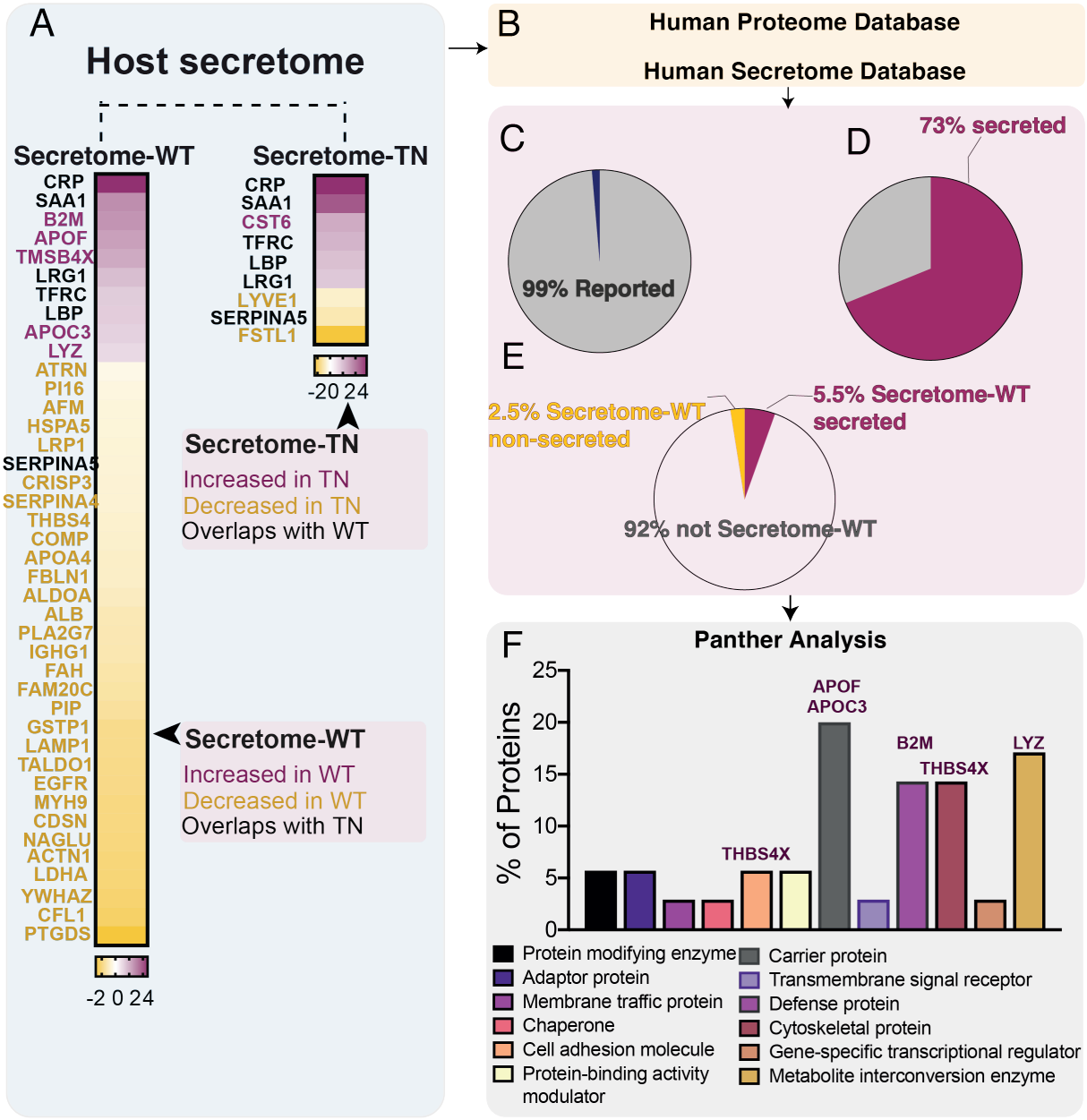

Figure 2.10: Typhoid toxin specific markers are identified in published databases. **(A)** Heatmap of toxin-specific proteins identified in response to *S.* Typhi WT (left) and *S.* Typhi TN (right). **(B)** Correlation to published databases of the human proteome[246] and the human secretome.[247] **(C)** Pie chart of reported (Gray) and unreported (Blue) proteins compared to the human proteome database. **(D)** Pie chart of reported proteins that are also reported secreted (Purple) and non-secreted (Gray) proteins. **(E)** Pie chart of total proteins with WT-toxin specific proteins secreted (Purple) and non-secreted (Yellow). **(F)** Panther analysis of *S.* Typhi WT specific proteins with increased secretion hits labeled corresponding to their protein class.

2.7 Secretome-WT correlates SASP ATLAS thus implicating a toxin-induced senescence phenotype

Previous findings showed that typhoid toxin induced DNA damage in HT1080 fibrosarcoma cells lead to a senescence response marked by SA-β-Gal and γH2AX[226] (**Fig.2.11A**). The secretome from the senescent cells caused paracrine senescence in bystander cells termed the senescence associated secretory phenotype (SASP). Indeed, toxin induced senescence was substantiated using primary Human Foreskin Fibroblasts (HFF1) cells intoxicated with a purified WT typhoid toxin (**Fig.2.11B**). HFF1 cells exhibited a significant increase in γH2AX and SA-β-Gal activity (**Fig.2.11B-D**) further implicating a senescence response to the typhoid toxin in a primary cell line, which was not previously observed. Senescence was observed with the DNA polymerase inhibitor aphidicolin (APH) but not the DNase mutant toxin TxHQ. Thus, to investigate a connection with senescence in human participants, proteins in secretome-WT were correlated to the SASP atlas database[219] (**Fig.2.12A**). The search showed that 54% of proteins in secretome-WT have been identified as SASPs in response to senescence-inducing stimuli ranging from irradiation, oncogene expression, and chemotherapy induced stress via atazanavir treatment (ATV)(**Fig.2.12A,C**). In contrast only 22% of secretome-TN were identified in the SASP atlas (**Fig.2.12B,C**).

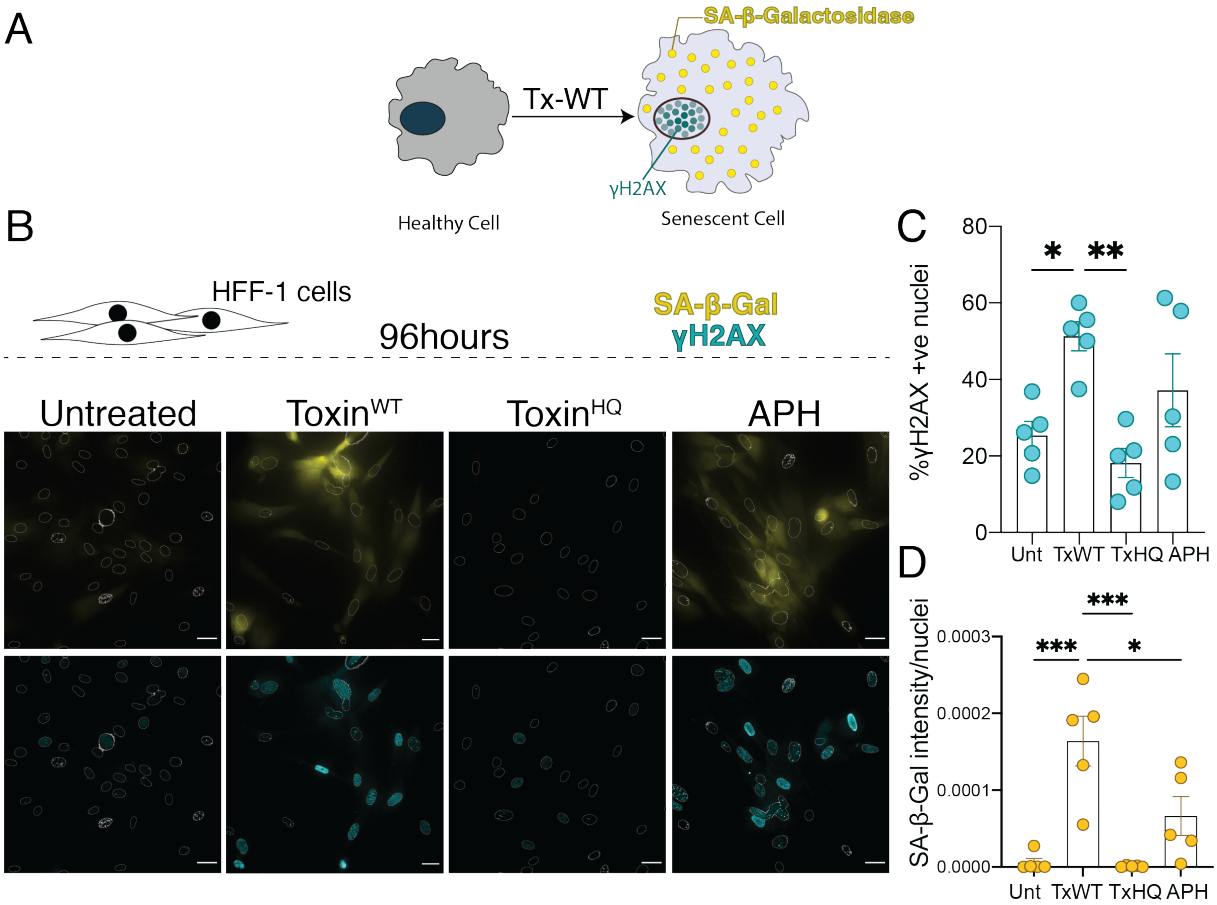

Figure 2.11: The typhoid toxin induces DNA damage and senescence in primary fibroblasts. **(A)** Schematic of the effects of typhoid toxin-WT on healthy cells (inspired by Ibler et al., 2019[226]). **(B)** Intoxicated HFF1 cells at 96 hours exhibiting senescence marker senescence associated betagalactosidase (SA-β-Gal; yellow) and DNA damage marker (γH2AX; cyan). **(C)** Quantification of γH2AX positive cells per field of view. **(D)** Quantification of SA-β-gal intensity per field of view. *n=1 One-way ANOVA statistical analysis was carried out*

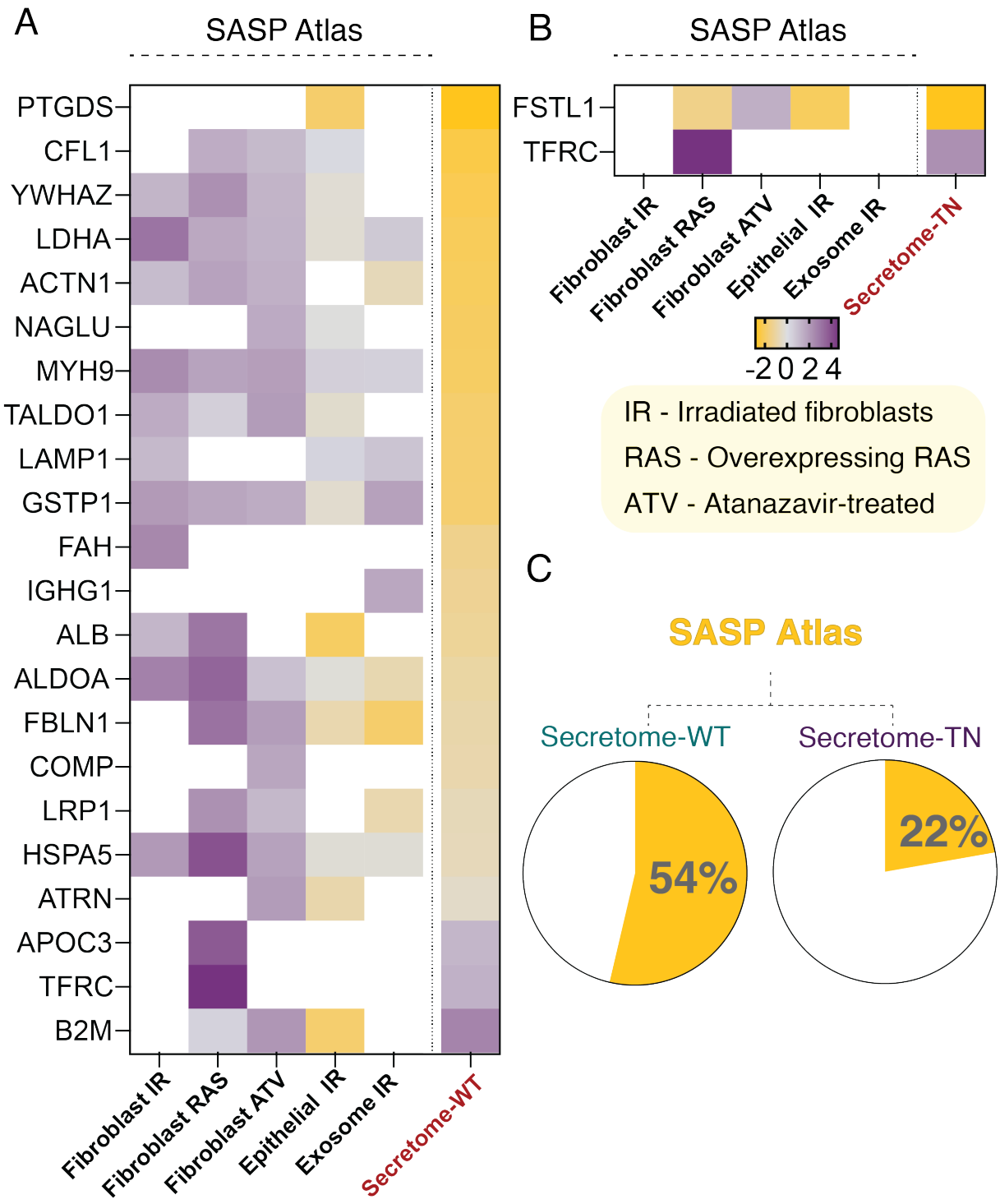

Figure 2.12: Secretome-WT correlated with SASP Atlas proteins[219] (A) and **(B)** Heatmap of SASP reported proteins, in secretome-WT and secretome-TN respectively, expression across different cell lines with different inducers of senescence, IR; irradiation, RAS; RAS oncogene overexpression, ATV; Atanazavir treatment. **(C)** percentage of SASP reported proteins in secretome-WT and secretome-TN respectively (Yellow).

2.8 Protein secretion between WT and TN groups

The WT infected group reported 41 proteins, 6 of which were common between secretome-WT and secretome-TN and therefore labeled "infection specific". Meanwhile the TN group reported 3 secretome-TN proteins, but the WT group reported 35 secretome-WT **Fig.2.13A**. By considering individual fold changes in LFQ intensity, the individual trend of increased/reduced secretion can be determined and correlated with individual participants in the WT and TN group.

To begin with, the 6 infection-specific proteins, 5 proteins (CRP, SAA1, LRG1, TFRC, LBP) showed increased secretion in both groups while SERPINA5 was reduced in secretion in both TN and WT. This will be referred to as "similarly secreted" in **Fig.2.13B**. Amongst the secretome-TN proteins, FSTL1 was significantly reduced in secretion in the secretome-TN and increased secretion in 80% of WT volunteers, showing a trend of "differential secretion" (**Fig.2.13C**). Additionally, differentially secreted secretome-TN proteins included CST6 (reduced secretion in WT, increased secretion in TN) and LYVE1 (increased secretion in WT, reduced secretion in TN). The secretome-WT proteins were divided into increased secretion secretome-WT (**Fig.2.13D**) and reduced secretion secretome-WT (**Fig.2.13G**). The secretome-WT increased secretion proteins, B2M and APOF were also secreted in TN too but were not significant (**Fig.2.13E**). In contrast, TMSB4X, APOC3 and LYZ were differentially secreted (**Fig.2.13F**). For example, LYZ and APOC3 displayed a prominent fold change decrease in the TN ($\log2<-0.5$) and a significant fold change increase in the WT group ($\log2<0.5$) in at least 90% of participants (**Fig.2.13F**).

Meanwhile between the reduced secretion proteins, there was some differentially secreted, namely, CRISP3 which shows reduced secretion in secretome-WT and increased secretion in TN group. The effects in secretions amongst secretome-WT reduced secretion proteins, although noteworthy, were not as drastically different from the TN group (**Fig.2.13G**).

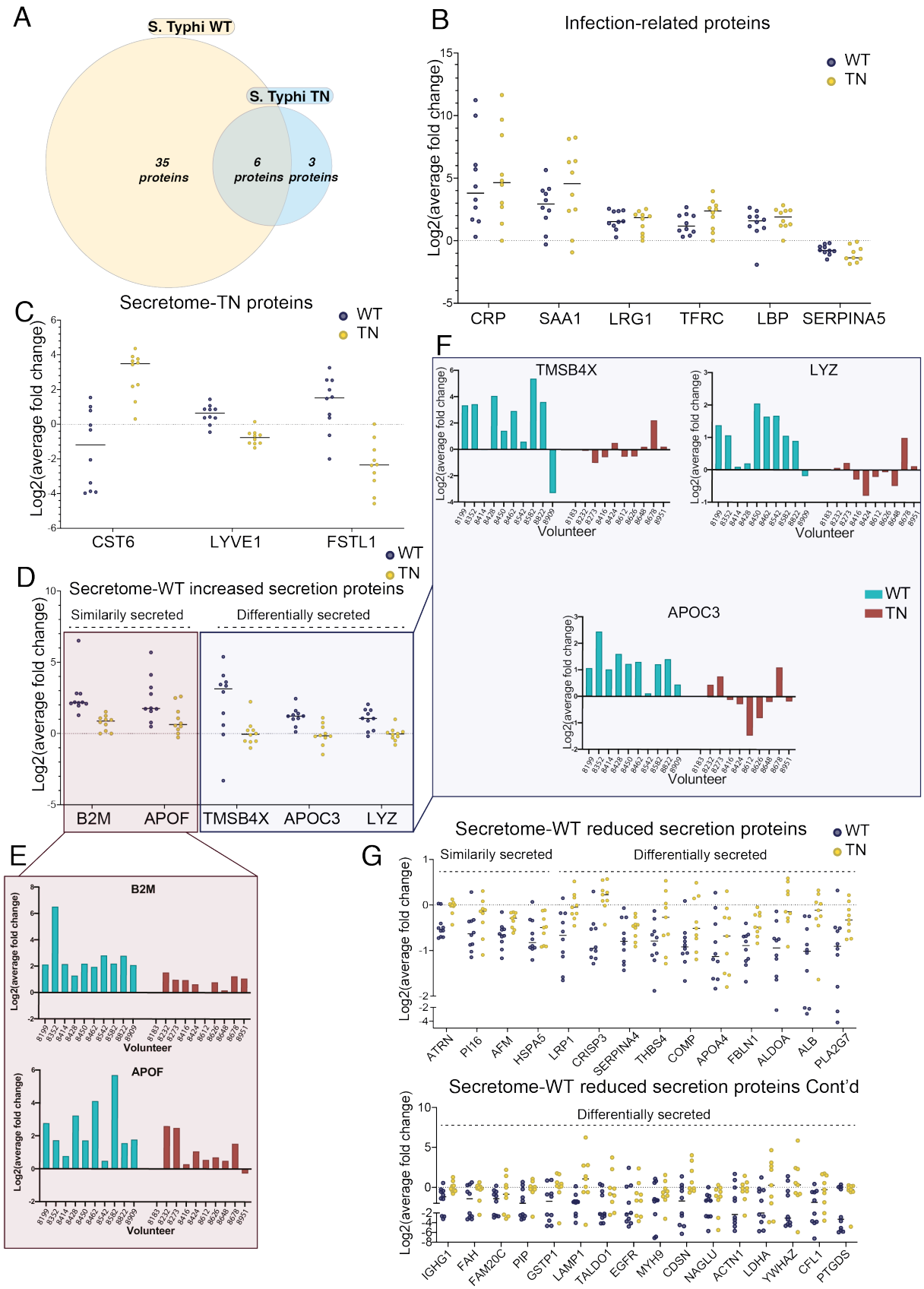

Figure 2.13: Protein secretion by fold change between WT and TN groups.(A) Venn Diagram depicting the common proteins between WT (Yellow) and TN (Blue). **(B)** Graph shows fold change per individual participant for significant proteins conserved in both WT (Yellow) and TN (Blue). **(C)** TN specific proteins fold change per treatment. **(D)** WT specific increased secretion proteins with similar and differential secretion between the WT (Yellow) and TN (Blue). **(E)** Individual volunteers' close-up of similarly secreted WT-specific proteins, B2M and APOF. **(F)** Individual volunteers' close-up of differentially secreted WT-specific proteins, TMSB4X, APOC3 and LYZ. **(G)** WT-specific reduced secretion proteins between similarly secreted and differentially secreted proteins.

2.9 Discussion of results

Through identifying the secreted proteins in secretome-WT and pinpointing the differentially secreted proteins, APOC3 and LYZ are on the top list of proteins to investigate. APOC3 has recently been implicated in NLRP3 inflammasome activation and consequently activates a series of inflammatory pathways.[256] LYZ is a metabolite interconversion enzyme, as previously mentioned, thus it causes membrane disintegration and metabolite efflux leading to lyse membranes.

Gibani *et al.* 2019 showed no difference in infection between Sm-WT and Sm-TN. There were no effects on symptom progression, nor was there an effect in CFU count in blood.[56] The only significant difference in their study was a shorter duration of bacteremia in response to the toxin. This raised many questions, amongst which, if there are toxin induced signals that could aid in this phenotype. The Oxford vaccine group (OVG) proceeded to perform a cytokine screen. They assayed a range of cytokines and found no significant difference in cytokine levels. There was an increased secretion in interferon gamma induced protein (IP10), monokine induced by interferon-gamma (MIG) and interleukin-1 receptor antagonist protein (IL-1RA) in both Sm-WT and Sm-TN groups. Meanwhile IL-8 reported a significant reduced secretion in the Sm-TN.[56] This could not explain the Sm-WT specific phenotype.

The cytokine array is a specific approach with high specificity to an array of cytokines. Although thorough, the array does not consider other proteins that could contribute to *Salmonella* infection. This is a major advantage of our method of employing mass spectrometry to elucidate the toxin-induced secretome.

Mass spectrometry is a widely accepted unbiased analytical tool.[257] It identifies significant protein hits between groups and thus can provide a wide database proteins. Blood plasma has been used as a tool to identify biomarkers for several diseases and continues to be an ideal way to host responses. Human plasma consists of three main classes of proteins. The first class is the aforementioned high abundance proteins, this includes albumin and apolipoproteins. High abundance proteins are necessary for protein transport, homeostasis, innate immunity amongst other crucial roles.[176,258–261] The second class of proteins are tissue leakage proteins which do not have a function in circulation but are in the bloodstream to be transported elsewhere, examples include aspartate aminotransferases (ASAT), alanine aminotransferases (ALAT) both signify liver disease when their secretion is enhanced in the bloodstream.[262] Finally the least abundant class which consists of small proteins and cytokines that are usually at constant levels and are secreted when needed.

By employing immunodepletion, as a targeted proteomic strategy, we unmasked some of the lower abundance proteins, like tissue leakage proteins (class 2) and small proteins (class 3). To our surprise, no cytokines were detected. It is worth noting that despite removing many of the high abundance proteins, blood plasma has proteins that continue to mask smaller proteins, for example, cytokines and interleukins.[262] In addition, it has been reported that small proteins can bind to MARS-14 columns by non-specific binding and thus leading to loss of proteins in the process.[263,264] Despite this limitation, our approach identified toxin specific proteins, secretome-WT.

The mass spectrometry proteomic strategy most commonly used and therefore used in this study follows the triangular approach of protein identification. The triangular approach in essence involves using a small cohort of participants, ∼10s of participants, and performing shotgun proteomics on these samples. Shotgun proteomics involves fragmenting eluted peptides in order of intensity. This fragmentation can lead to random loss of some values across the samples. Studies have been recently aiming at minimising this and thus reported more consistent peptide identification.[265,266] Another drawback of the triangular approach is that all samples are pooled in together, excluding variances and outliers. This in turn makes it really difficult to identify if the protein that is significantly different is different within the group on a person-by-person basis.[262] Following protein identification of the small samples cohort, identified proteins are validated by immunoassays on much bigger samples. Bigger samples, ∼1000s of participants, are tested for the proteins of interest using immunoassays.[267] By identifying APOC3 and LYZ, from 20 samples per group, we are validating it *in vitro* which could then be validated on typhoid patients in endemic regions.

The small cohort in the triangular approach is due to the complexity of sample preparation which involves laborious procedures, such as, immunodepeletion. Geyer *et al.* 2016 proposed the idea of creating a faster automated workflow that would allow for quantification of proteins in plasma in larger cohorts, rectangular approach.[268] This approach was inspired by genome wide sequencing scientists who show a more efficient approach when large cohorts of samples are analysed together rather than the small cohort sequential pipelines.[269] The advantage of the rectangular approach is the merging of both shotgun and validation steps. Although this has not been achieved yet, the fast advancement in the proteomic field makes it probable in the near future.

In conclusion, human plasma samples were depleted of high abundance proteins and analysed by LC-MS/MS. Depleted plasma samples revealed that the human host responds to the toxin through release of a secretome (Secretome-WT). Secretome-WT proteins belong to several protein classes and exhibit important functions. Secretome-WT reported APOC3 and LYZ, which were differentially secereted between *S.* Typhi-WT (increased secretion) and *S.* Typhi-TN (reduced secretion). Thus, APOC3 and LYZ show the most

promise for validation experiments using *in vitro* cell culture experiments discussed in Chapter 3.

Chapter 3

Results Part II

The previous chapter revealed how *S.* Typhi-WT infected participants in the TYGER study responded to the toxin by releasing a secretome (henceforth secretome-WT). Through correlating the secretome-WT with the human proteome database and human secretome atlas, APOC3 and LYZ were identified as proteins of interest that were differentially secreted in *S.* Typhi-WT infected relative to *S.* Typhi-TN.

LYZ is expressed in all human cells and is present in all bodily secretions (**Fig.3.1A**). In 1922, Alexander Fleming discovered LYZ as an antibacterial agent.[270] LYZ is a naturally occurring human enzyme[271] conserved amongst several mammals and is considered part of the innate immune response.[272] *In vitro*, LYZ exhibited effectiveness against Gram positive bacteria and ineffective against some Gram negative bacteria *in vitro*.[273] However, LYZ can affect Gram negative *in vivo* responding to campylobacter bacteria, another gastroenteritis causing Gram negative bacteria.[274,275]

LYZ causes bacterial lysis through hydrolysis of the bacterial cell wall, thus bacteria becomes vulnerable to osmotic stress.[276,277] LYZ's primary activity works on peptidoglycans (PG), which is a major component of the bacterial cell wall. PGs is a polymer formed by β-1,4,glycosidic linkage between disaccharide N-acetylglucosamine (NAG)-N-acetylmuramic acid (NAM). β-1,4,glycosidic linkage provides the tensile strength of the PG and protects the bacteria from external factors aiding in bacterial survival. LYZ's enzymatic activity works by hydrolyzing the β-1,4,glycosidic linkage, and thus it is also known as 1,4-β-N-acetylmuramidase.[277]

LYZ's active site surrounds 6 residues of NAM and NAG and the Aspartate (Asp) and Glutamate (Glu) amino acids bind to the β-1,4,glycosidic linkage and cleaves it (**Fig.3.1A,B**). This is effective against Gram positive bacteria where PGs are exposed and once hydrolysed the bacteria becomes vulnerable to killing. LYZ enzymatic activity is not the only mode of its action. LYZ is also cationic which allows it to insert itself in the outer spanning the outer and inner membrane of Gram negative bacteria. This

forms auger-like structures creating a cylinder in the membrane that enhances bacterial vulnerability.[278,279]

Gram negative bacteria have two membranes, the inner membrane, and the outer membrane between both is PGs which LYZ acts upon. Gram negative bacteria also have lipopolysaccharide (LPS) which makes them immunogenic. LPS is an anionic molecule which allows it to bind to cationic molecules like LYZ. However when bound it deactivates the enzymatic properties of LYZ rendering it incapable of cleaving PG. *In vivo* studies showed effectiveness of LYZ against campylobacter bacteria, another gastroenteritis causing Gram negative bacteria, through perforating the bacterial membrane integrity leading to efflux of ions and lysis.[274,275]

In vivo results raised questions about the mechanism of action of LYZ *in vivo*, since its bacterial killing activity is not reported under normal *in vitro* conditions. LYZ cell wall permeabilization is attributed to its high positive charge, but it does not work on its own *in vivo*. LPS and PG are pathogen-associated molecular patterns (PAMPs) expressed by Gram negative bacteria. PAMPs are recognized by host's immune defences, namingly pattern recognition receptors (PRR).[280] Once activated by PAMPs, PRR stimulates a pro-inflammatory signal that recruits cytokines that inactivate some of these PAMPs(e.g. IL-1B) which in turn activate cell death pathways.[281] Cell death pathways produce gasdermin D (GASDMD) which in turn causes holes in the membrane, both host and bacterial membranes.[276,282,283] It is speculated that *in vivo* LYZ does not work alone, but has dual activity and interplay with components of the immune system (**Fig.3.1**), which might explain why it is effective against Gram negative bacteria, e.g. Campylobacter.

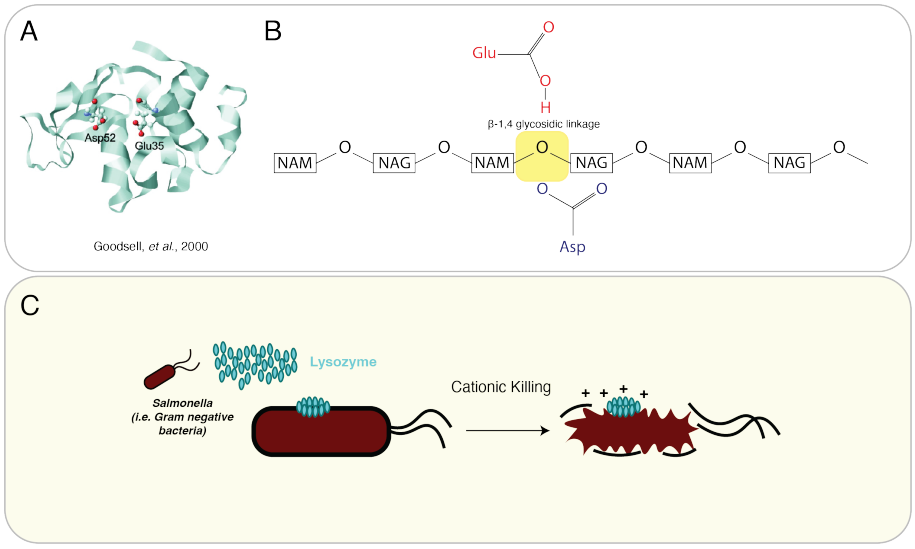

Figure 3.1: LYZ structure and function.(A) LYZ protein structure and active site highlighted[284] **(B)** Enzymatic activity of LYZ by hydrolysis of -1,4 glycosidic linkage. **(C)** Proposed mechanism of cationic killing exhibited by LYZ on Gram negative bacteria (e.g. *Salmonella*).

Little is known about Apolipoprotein C-III (APOC3) function. It is a 79 amino acid protein with a molecular weight of 8.8kDa. APOC3 is an apolipoprotein expressed and synthesised in the liver within hepatocytes and cells of the gastrointestinal tract[246,285,286] (**Fig.3.2**). APOC3 has an amphipathic helix which gives it both hydrophilic and hydrophobic residues. Hydrophobic residues allow for lipid binding which is necessary for some of the reported APOC3 functions.[287] In the blood plasma APOC3 is bound to high density lipoproteins (HDL), low density lipoprotein (LDL) and triglyceride-rich proteins (TRLs).[288,289] An increase in circulating APOC3 has been reported to be correlated with hypertriglyceridemia. APOC3 inhibits the lipoprotein lipase activity and interferes with lipoprotein endocytosis, which consequently increases the concentration of free lipids in the blood, thus hypertriglyceridemia.[290] In 2020, Zewinger *et al.* implicated APOC3 with NLRP3 inflammasome activation which promotes an inflammatory response that contributes to cell death pathways.[256] NLRP3 inflammasome activation was also reported as a host response to bacterial pathogens including *Salmonella*[291] amongst other pathogens (for example, *E. coli* and *streptococci*) that acts as an antibacterial[292,293] (**Fig.3.2**).

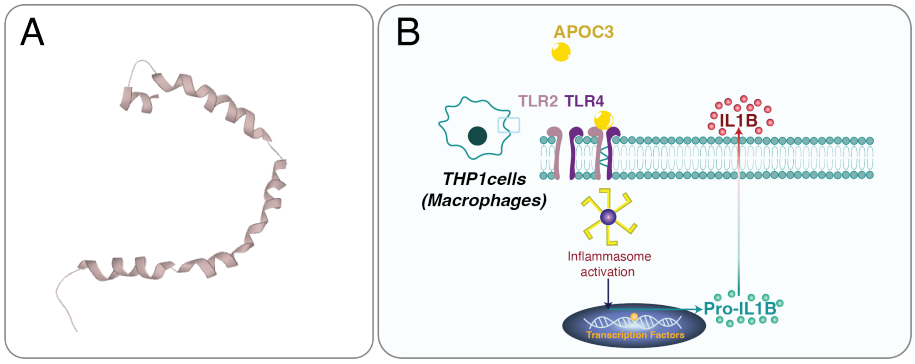

Figure 3.2: Apolipoprotein C3 (APOC3) structure and function. (A) APOC3 structure (uniprot, APOC3). (B) Proposed APOC3 function by Zewinger *et al.,* 2020, highlighting inflammasome activation.

A member of the apolipoprotein family, APOL3 has been reported to have detergent-like properties that lyse and kill *Salmonella* Typhimurium.[294] The bactericidal properties of APOL3 inactivates the LPS in the outer and inner membranes of *Salmonella* Typhimurium. This allows entry to the intermembrane space which causes bacterial membrane lysis. However, APOL3 does not work alone and was reported to work with inflammation induced proteins, such as, GBP1.[294] It is worth speculating that, similar to APOL3, APOC3 can exhibit bacterial killing properties with the aid of antimicrobial proteins such as LYZ. The aim of this chapter is to validate toxin regulation of APOC3 and LYZ in cultured cells and initiate experiments examining whether APOC3 and LYZ counteract *Salmonella in vitro*.

3.1 APOC3 is expressed in liver cells (HepG2) in a toxin-independent manner

The first focus was APOC3, which is known to be expressed in the liver and gastrointestinal tract. Consistent with this, unpublished RNA sequencing from the Oxford Vaccine Group performed on mRNA from peripheral blood mononuclear cells (PMBCs) from TYGER participants showed that APOC3 and APOF were not reported (**Fig.3.3A**). No significant differences between host responses *S.* Typhi WT and TN were identified (Gibani et al., unpublished). This included proteins identified in secretome-WT such as B2M, LYZ and TMSB4X (**Fig.3.3A**), which indicates that secretion of factors in secretome-WT were upregulated post-translationally. *Salmonella* is known to colonise the liver[295–297] making this tissue a possible source of APOC3 in the samples from TYGER participants. Thus, to validate APOC3 expression and secretion in responses to typhoid toxin, we sought to initially examine host responses to the toxin in cultured HepG2 liver cells.

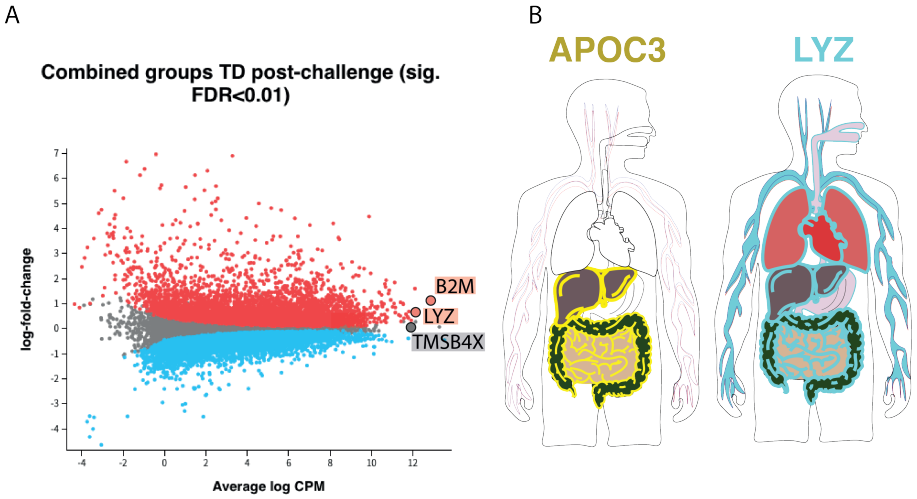

Figure 3.3: RNA sequencing data (Gibani unpublished) correlated with Secretome-WT.(A) RNA sequencing data (Gibani et al, unpublished) upregulated proteins (Red), downregulated proteins (Blue), and non-signifcant proteins (Gray). (B) Schematic showing presence of proteins of interest, APOC3 in yellow and LYZ in cyan.

HepG2 cells were incubated with the 20ng/μl purified typhoid toxin (Tx-WT) or the toxin mutant (Tx-HQ) for 2 hours. Tx-HQ lacks the functionality of the cdtB subunit due to a point mutation at histidine 160 to glutamate (H160Q), which attenuates nuclease activity.[226] After 2 hours, toxin was replaced with fresh media before incubation for 48 hours (**Fig.3.4A-C**) or 96 hours (**Fig.3.4D-F**). DNA damage was marked by an increase in histone-2AX phosphorylation (γH2AX) (cyan), which is enhanced in response to single- and double-strand DNA breaks.[298] In negative control cells, the proportion of γH2AX-positive cells in untreated cells was 0% at 48h and 25% at 96h, while Tx-HQ-treated cells was ~20% at 48h and 96h (**Fig.3.4A,B, D,E**). Treatment with the chemical inhibitor of

DNA polymerase aphidicolin (APH) that caused DNA replication stress induced γH2AX in 75% of cells at 48h (Figure 3.4A, B) and 100% of cells at 96h **Fig.3.4D,E**. Similarly, the Tx-WT induced a significant γH2AX DNA damage response, which mirrored the effect observed with APH **Fig.3.4A, B, D, E**. Despite differences in DDRs, APOC3 was expressed in all cells regardless of treatment or time-point and no significant differences were observed. This suggests that APOC3 is secreted from liver cells in a manner that is independent of DDRs and therefore the toxin. As a result, toxin responses in HepG2 cells do not explain the findings from proteomic experiments in TYGER samples and were removed from the possible cell lines that could be used to model APOC3 regulation by the toxin.

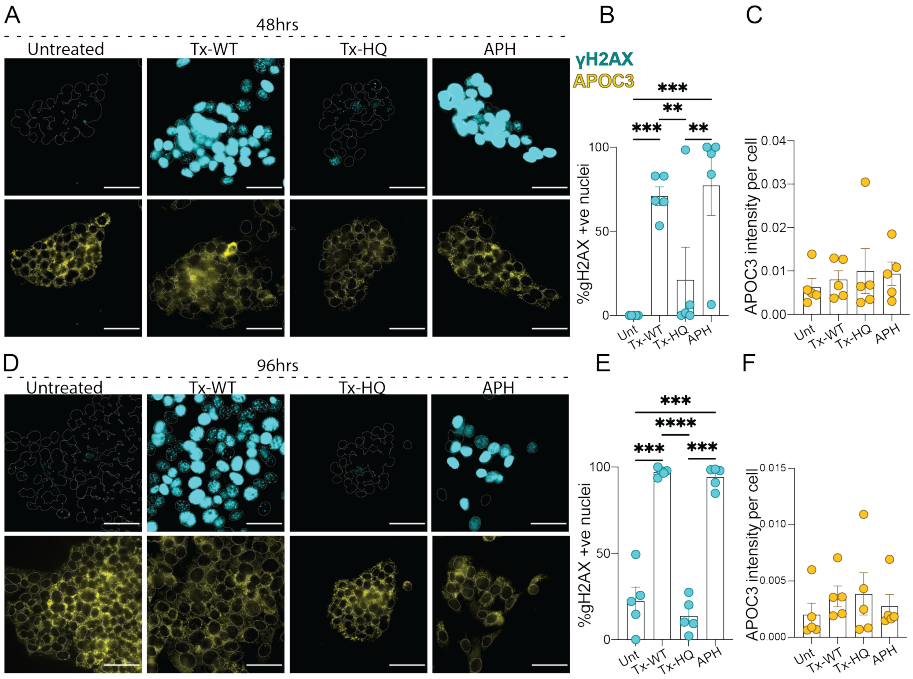

Figure 3.4: The typhoid toxin induces DNA damage response in HepG2 cells.(A) Immunofluorescence images of HepG2 cells responding to the toxin, DNA marked by γH2AX (cyan) and protein of interest APOC3 (yellow) at 48 hours following the toxin pulse (2hrs). **(B)** Quantification of percentage γH2AX positive nuclei at 48 hours post intoxication per image. **(C)** Quantification of APOC3 intensity per image at 48 hours post intoxication. **(D)** Immunofluorescence images of HepG2 cells responding to the toxin, DNA marked by γH2AX (cyan) and protein of interest APOC3 (yellow) at 96 hours following the toxin pulse (2 hours). **(E)** Quantification of percentage γH2AX positive nuclei at 96 hours post intoxication per image. **(F)** Quantification of APOC3 intensity per image at 96 hours post intoxication. *Scale bar = 50μm. One-way ANOVA statistical analysis was performed.*

3.2 Toxin induced DDRs are coincident with APOC3 expression in CACO-2 cells

Given that *Salmonella* is an enteric pathogen, gastrointestinal tract (GI) are amongst the first points of colonisation prior to entering the bloodstream and causing bacteraemia

in TYGER participants. Thus, *S.* Typhi would likely have intoxicated the GI, possibly inducing secretion of APOC3. Colorectal adenocarcinoma cells (CACO-2) are a common model for the human colon which aids in understanding intestinal absorption of drugs or in this case the infection of a pathogen.[299,300]

First, DRRs were characterised in CACO-2 cells that were intoxicated in the same manner as HepG2 cells (i.e. 2h intoxication before immunofluorescence of cells at 48h/96h). In negative control cells, ∼20% of untreated cells were γH2AX-positive while 60% were observed in Tx-HQ-treated. However, Tx-WT intoxicated cells showed 100% of γH2AX-positive cells **Fig.3.5A,C**. The relative difference between γH2AX-positive cells in the presence of TxHQ (60%) and TxWT (100%) suggests a significant but relatively modest difference. However, the immunofluorescence images in **Fig.3.5A** show a much more robust γH2AX response in TxWT-treated cells that was not reflected in the quantification in **Fig.3.5C,D**. This is due to the quantification method where cells with any observable γH2AX staining in the nuclei were defined as positive cells. There was certainly an increase of γH2AX foci with TxHQ relative to untreated (**Fig.3.5A-D**), which was likely due to residual nuclease activity in TxHQ and/or LPS contaminants in the recombinant toxin preparations as previously reported by our group.[226] In contrast to both untreated and TxHQ, cells intoxicated with TxWT revealed divergent γH2AX phenotypes (**Fig.3.5A,C**), which were not resolved in the quantification process. At 48 hours, γH2AX spanned the entire nucleus in a pan-γH2AX phenotype and there was also a RING phenotype (yellow arrow) characterised by accumulation of γH2AX at the edge of the nucleus. At 96 hours, however,γH2AX was observed in foci within nuclei (magenta arrow). The foci appeared more globular and distinctive compared to the pan-γH2AX staining or the RING phenotype observed at 48 hours. Thus, the data shows that TxWT induced divergent DDRs in CACO-2 cells over 96 hours.

It was previously reported that toxin-induced DNA damage causes cell cycle arrest.[226] To assay cell cycle progression, cells were incubated with a fluorescently labelled nucleoside analogue of thymidine (EdU) that incorporates into newly synthesised DNA during replication and thus marks cell cycle progression. At 48 and 96 hours, ∼50% of negative control cells, both untreated and Tx-HQ, were EdU positive suggesting cell cycle progression (**Fig.3.5A-D**). Alternatively, Tx-WT treated cells exhibited no EdU incorporation suggesting cell cycle arrest. This agrees with the observations on the robust γH2AX DDRs induced by TxWT (**Fig.3.5A,C**).

Aberrations in the morphology of cell nuclei can indicate cell cycle arrest and genomic instability.[301] Indeed, typhoid toxin belongs to a family of cytolethal distending toxins, which are known to cause nuclear distension.[302] Relative to negative control cells, nuclear distention was clearly apparent in TxWT-treated cells that exhibited an increase in size at 48 and 96 hours exemplified in the DAPI channel in **Fig.3.5A, B**. In addition, extra-

nuclear bodies known as micronuclei (orange arrow) formed in Tx-WT-treated cells and were not observed in negative controls (**Fig.3.5B**). Micronuclei are a marker of genomic instability where genetic material has not been properly incorporated into chromosomes after cell division due to defective repair and/or chromosomal aberrations.[303] The increased nuclear size, cell cycle arrest and micronuclei formation at 96 hours was also indicative of senescence.[304]

Having characterised TxWT-induced DDRs in CACO-2 cells, APOC3 was investigated in the same images (**Fig.3.5A-D**). In negative control cells, low levels of APOC3 was observed at 48 and 96 hours. To compare across all variables, APOC3-positive cells were marked positive if they show any staining of APOC3. At 48 hours, APOC3-positive cells were 20% in untreated and 5% in TxHQ-treated cells but this increased to 50% in Tx-WT treated cells (**Fig.3.5C**). This contrasts with observations in HepG2 cells where APOC3 was expressed independently of the toxin (**Fig.3.4**). At 96 hours in CACO-2 cells, APOC3 increased from 20% to 30% in untreated cells, which was also observed in TxHQ-treated cells while TxWT induced APOC3 expression in 80% of cells(**Fig.3.5D**). There was an interesting pattern in APOC3 expression in TxWT-treated cells where APOC3 was observed in fine puncta at 48 hours in both the nucleus and the cytoplasm (white arrow). At 96 hours however, APOC3 formed large puncta (foci) that appears predominantly localised in the nucleus or perinuclear region (cyan arrow) (**Fig.3.5B, D**). The significance of this is unknown but may indicate accumulation of APOC3-labelled lipids in the nucleus or perinuclear region.[287]

In summary, APOC3 expression in CACO-2 cells is augmented by toxin nuclease activity and is coincident with DDRs and cell cycle arrest.

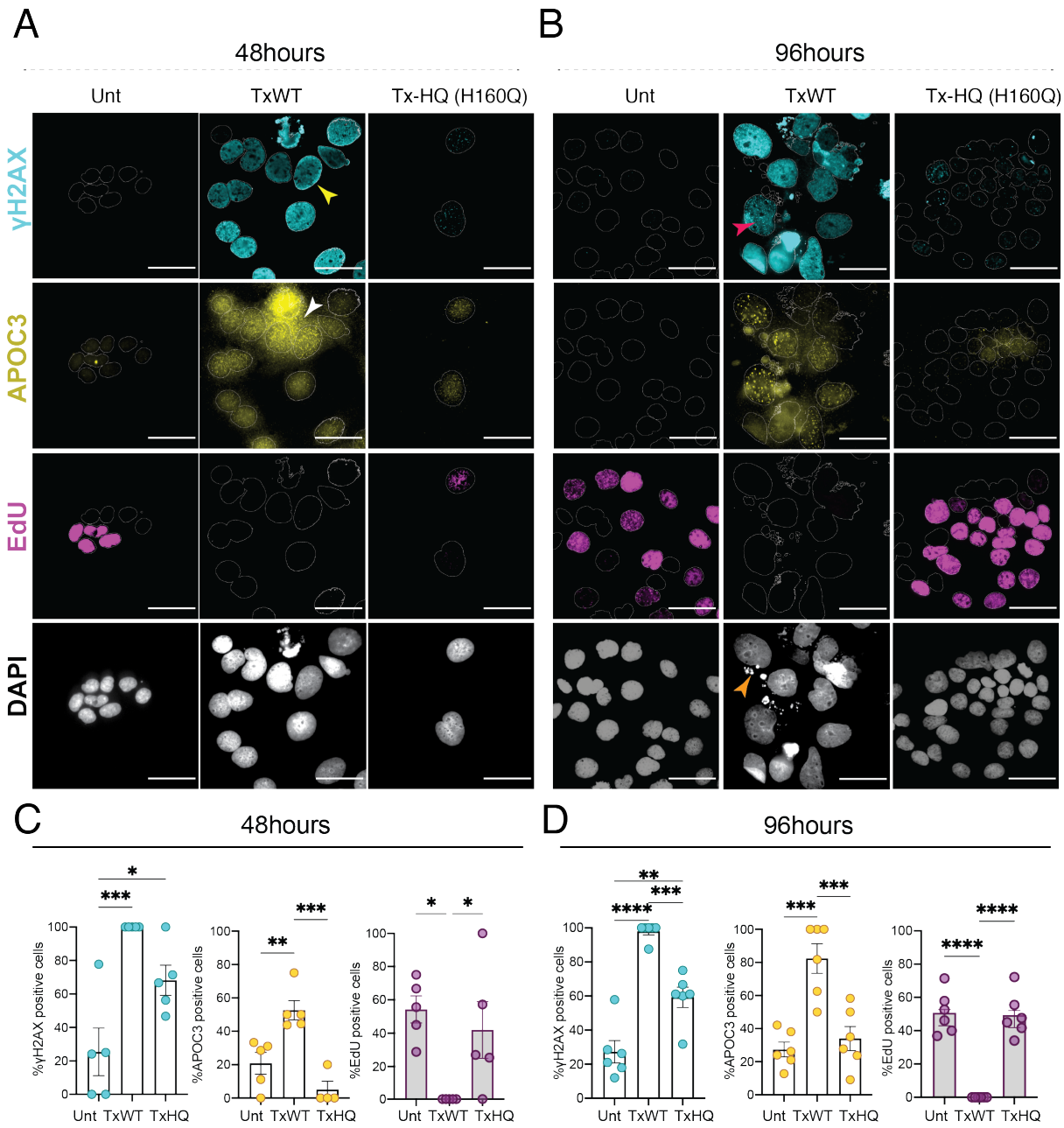

Figure 3.5: The typhoid toxin induces DNA damage, cell cycle arrest and APOC3 expression in CACO-2 cells. (A) Immunofluorescence images of CACO-2 cells untreated, treated with wild-type toxin (tx-WT) or treated with toxin mutant (tx-HQ) at 48 hours post intoxication, γH2AX (cyan), APOC3 (yellow) and EdU (magenta). Yellow arrows show RING reported cells. White arrow show small APOC3 foci **(B)**Immunofluorescence images of CACO-2 with respective treatments at 96 hours post intoxication, γH2AX (cyan), APOC3 (yellow) and EdU (magenta). Magenta arrow shows large γH2AX foci and orange arrow shows micronuclei. **(C)** Quantification of γH2AX (cyan), APOC3 (yellow) and EdU (magenta) positive nuclei at 48hours. **(D)** Quantification of γH2AX (cyan), APOC3 (yellow) and EdU (magenta) positive nuclei at 96hours. *Scale bar = 50μm*

3.3 *Salmonella* infection elicits DDRs and APOC3 expression

The next step was to investigate whether APOC3 was regulated in a toxin-dependent manner during *Salmonella* infection. In the absence of a schedule 5-compliant containment level 3 laboratory for studying wild-type *S.* Typhi, an alternative model for infection was required. The toxigenic non-typhoidal strain *Salmonella enterica* serovar Javiana (henceforth *S.* Javiana) encodes the toxin genes pltB, pltA and cdtB, which produce typhoid toxin during intracellular infections in an analogous fashion to *S.* Typhi.[97] *S.* Javiana is the 3rd most significant cause of *Salmonella*-borne gastroenteritis in the USA[152] and the toxin has been shown to suppress pathology, mediate immune evasion and promote pathogen dissemination in a mouse model.[139–141]

*S.*Javiana was used to infect CACO-2 cells using wild-type (Sm-WT) or the cdtB deficient strain (Sm-ΔcdtB) for 1h. Extracellular bacteria were killed by incubation with cell culture media containing the antibiotic gentamicin that does not penetrate mammalian cells thus allowing intracellular *Salmonella* to survive. In the untreated control, 30% of cells were γH2AX-positive(**Fig.3.6A,B;cyan**). In response to infection, CACO-2 cells infected with Sm-ΔcdtB exhibited a relative increase in γH2AX in ∼90% of cells at 48 hours which was also observed with Sm-WT in ∼70% of cells (**Fig.3.6A,B;cyan**). There was a significant increase in APOC3 expression in response to Sm-ΔcdtB at 48 hours, ∼60% of cells, but no significant response to Sm-WT (**Fig.3.6A, C;yellow**). It was noticeable that the DDRs with purified toxin at 48 hours (**Fig.3.5A, C**) were more robust than those observed for Sm-WT at 48 hours (**Fig.3.6A,C**). This suggests differences in toxin concentration, which may be partly due to delays with toxin expression and secretion during infection. Thus, the same infection experiment was repeated but the time-point extended to 96 hours.

At 96 hours post-infection, untreated CACO-2 cells were 20% γH2AX-positive while Sm-ΔcdtB-infected were 0% γH2AX-positive, thus indicating DNA repair between 48 hours and 96 hours with in Sm-ΔcdtB-infected (**Fig.3.7A**). In contrast, Sm-WT-infected cells were 100% γH2AX-positive (**Fig.3.7A**) relative to 70% at the 48 hour time point (**Fig.3.6A**), Sm-WT-infected cells exhibited enlarged nuclei as well the formation of budding micronuclei as indicated with the orange arrow in **Fig.3.7A**. This correlates with what was previously observed in CACO-2 cells intoxicated with purified toxin at 96 hours (**Fig.3.5B,D**) and further supports the view that typhoid toxin causes genomic instability.

Having established a *Salmonella* infection assay to assess the effects of typhoid toxin, the expression of APOC3 was investigated. Remarkably, APOC3 expression at 96 hours post-infection mirrored the DDR marked by γH2AX (**Fig.3.7A, C**). In negative control

cells, APOC3 was expressed in ∼20% of cells untreated and ∼5% in Sm-ΔcdtB-infected (**Fig.3.7C**). In contrast, Sm-WT-infected cells exhibited a significant increase in APOC3-positive cells, ∼80% of cells. Cells with a higher Sm-WT burden (white arrow) exhibited an increase in APOC3 expression all around the cell (**Fig.3.7B**).

With the purified toxin in **Fig.3.5**, APOC3 expression was coincident with cell cycle arrest. To assess whether toxigenic *Salmonella* exhibits similar phenotypes to that of the purified toxin during infection, EdU incorporation was examined in infected CACO-2 cells (**Fig.3.7B,C**). Untreated cells exhibit a lower EdU incorporation of ∼50% of cells EdU positive (**Fig.3.7B,C**) which was observed in previous experiments (**Fig.3.5B,D; magenta**). Meanwhile, Sm-ΔcdtB infected cells showed a decrease in EdU incorporation to ∼10% of cells. Considering this baseline decrease in EdU incorporation at 96 hours, 50%, Sm-WT infected cells reported a reduced EdU incorporation to ∼20%. This marks cell cycle arrest and consequently linking previous observations of senescence in response to infection, independently from the toxin. The decrease in EdU incorporation is not as drastic as the one described in **Fig.3.5**, however it remains significant in response to infection (**Fig.3.7B,C**).

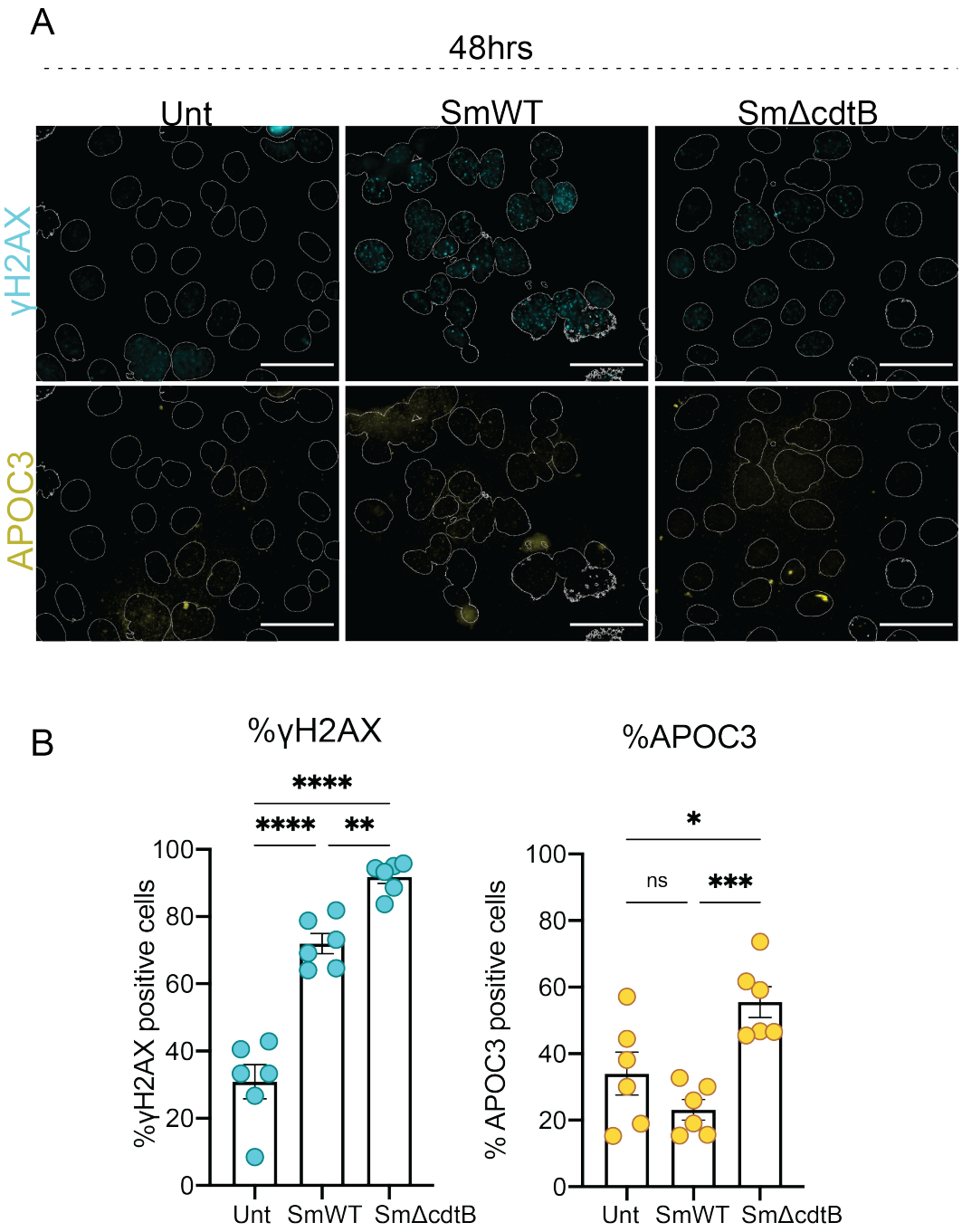

Figure 3.6: *Salmonella*-WT induces DNA damage and APOC3 expression at 48 hours post-infection.(A) Immunoflorescence images of γH2AX (cyan) and APOC3 (yellow) in response to *Salmonella* WT (SmWT) and *Salmonella* ΔcdtB (SmΔcdtB). **(B)** Quantification of percentage γH2AX nuclei (cyan) and percentage of APOC3 positive cells (yellow). *Scale bar = 50μm (n=1; each point represents a field of view)*

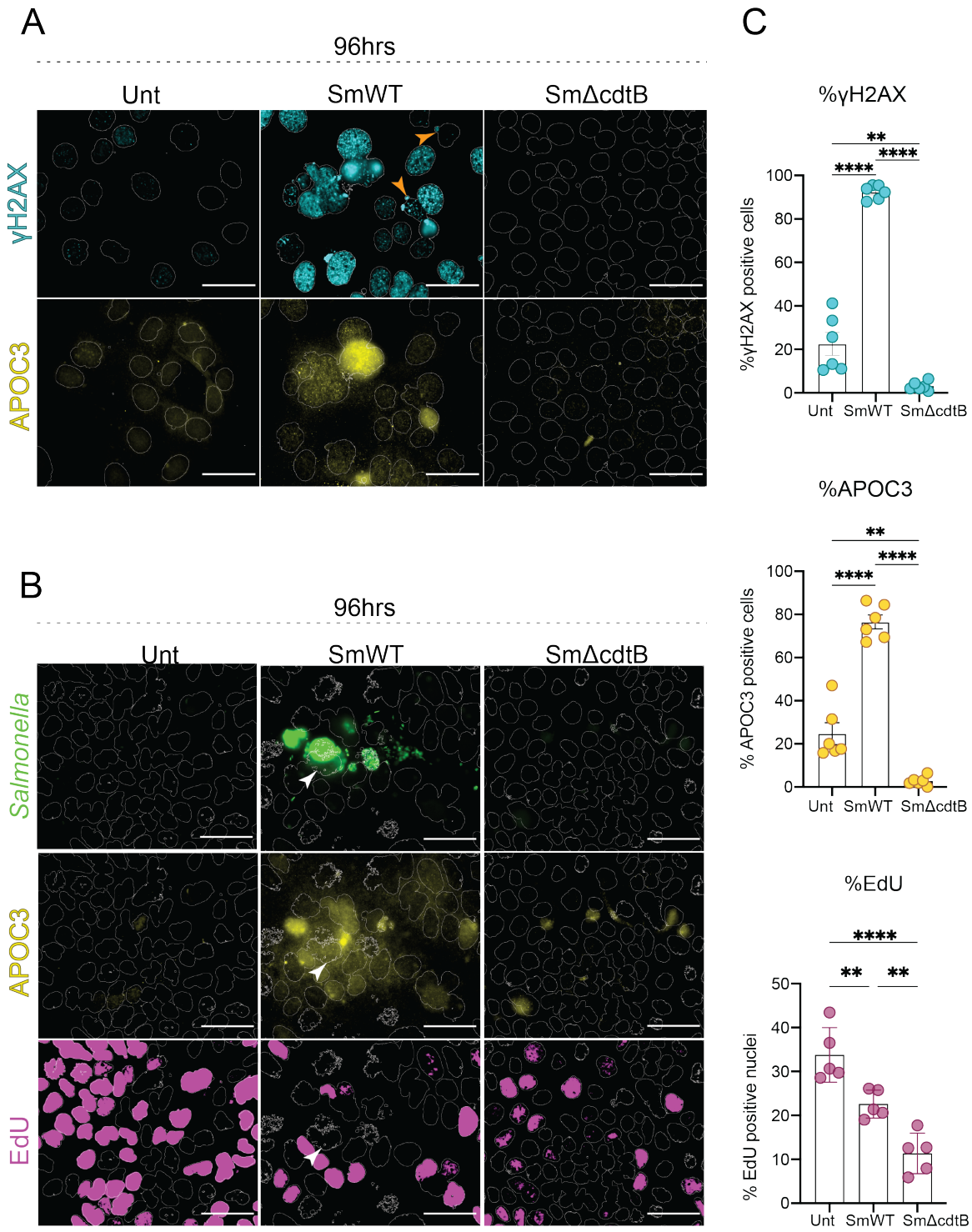

Figure 3.7: **(A)** Immunofluorescence images of γH2AX (cyan) and APOC3 (yellow) in response to *Salmonella* WT (SmWT) and *Salmonella* ΔcdtB (SmΔcdtB). **(B)** Immunofluorescence images of *Salmonella* (green), APOC3 (yellow) and EdU (magenta) in response to *Salmonella* after 96 hours post-infection. **(C)** Quantification of percentage γH2AX nuclei (cyan), percentage of APOC3 positive cells (yellow) and percentage of EdU positive nuclei (magenta). *Scale bar = 50μm (n=1; each point represents a field of view)*

3.4 APOC3 expression implicates DNA damage repair (DDR) machinery

In line with previous observation (**Fig.3.7**), APOC3 is produced in a toxigenic *Salmonella* dependent manner at 96 hours, coinciding with a DDR response. This further validates the toxin-dependent expression of APOC3 *in vitro* and implicates the DDR in APOC3 expression in CACO-2 following intoxication with purified toxin (**Fig.3.5**) or toxigenic *Salmonella* infection (**Fig.3.6, and 3.7**). However, APOC3 expression was associated with cell cycle arrest with purified typhoid toxin (Fig. 3.5) but not during infection with toxigenic *S.* Javiana (**Fig.3.7**). Thus, the contribution of DDRs to APOC3 expression was investigated in more detail.

When DNA damage occurs, the cell activates DNA repair machinery including ATM and ATR that are DNA repair kinases that activate a cascade of DNA repair proteins coordinating DNA repair. dsDNA breaks phosphorylates ATM kinase, meanwhile ssDNA breaks phosphorylates ATR, both activate a cascade of proteins that aid in respective DNA repair(**Fig.3.8A**).[305] In turn, inhibition of ATM and ATR would inhibit the phosphorylation of H2AX to γH2AX. To investigate the involvement of DNA repair machinery with APOC3 expression in CACO2 cells we inhibited both ATM and ATR by caffeine, an efficient ATM and ATR inhibitor.[306] In untreated cells, with 20% of γH2AX positive cells, the effect of ATM/ATR inhibition was not significantly observed. However, when incubating CACO-2 cells with ETP, a known inducer of double stranded DNA breaks, caffeine significantly reduced γH2AX from 60% to 40%. Similarly, Tx-WT treated cells showed a reduction in γH2AX positive cells from $\sim$90% to $\sim$20% post-caffeine (**Fig.3.8B,C**).

When APOC3 expression was examined in the same images as **Fig.3.8B,C**, no APOC3 was observed in untreated control cells (**Fig.3.8D**), which mirrored the observations with γH2AX (**Fig.3.8B**). Similarly, robust γH2AX signal observed with TxWT and ETP was mirrored by APOC3 expression (**Fig.3.8D**). However, the close proximity of each cell to one another made it difficult to quantify APOC3 expression per cell as was performed with γH2AX in **Fig.3.8C**.

To quantify APOC3 expression, the intensity of APOC3 per field of view was determined and used to calculate relative APOC3 intensities per cell identified by DAPI staining . Untreated cells exhibited minimal APOC3 levels before caffeine administration, $\sim$0.00025 intensity per cell, which was reduced to 0 intensity per cell after caffeine. In ETP treated cells, APOC3 intensity of 0.001 per cell was reduced to zero by caffeine went down to zero (**Fig.3.8D,E**). Meanwhile, APOC3 expression in Tx-WT treated cells was reduced from f $\sim$0.008 intensity/cell without caffeine to zero with caffeine (**Fig.3.8D,E**).This implicates ATM/ATR-mediated DDR in control of APOC3 expression in CACO-2 cells.

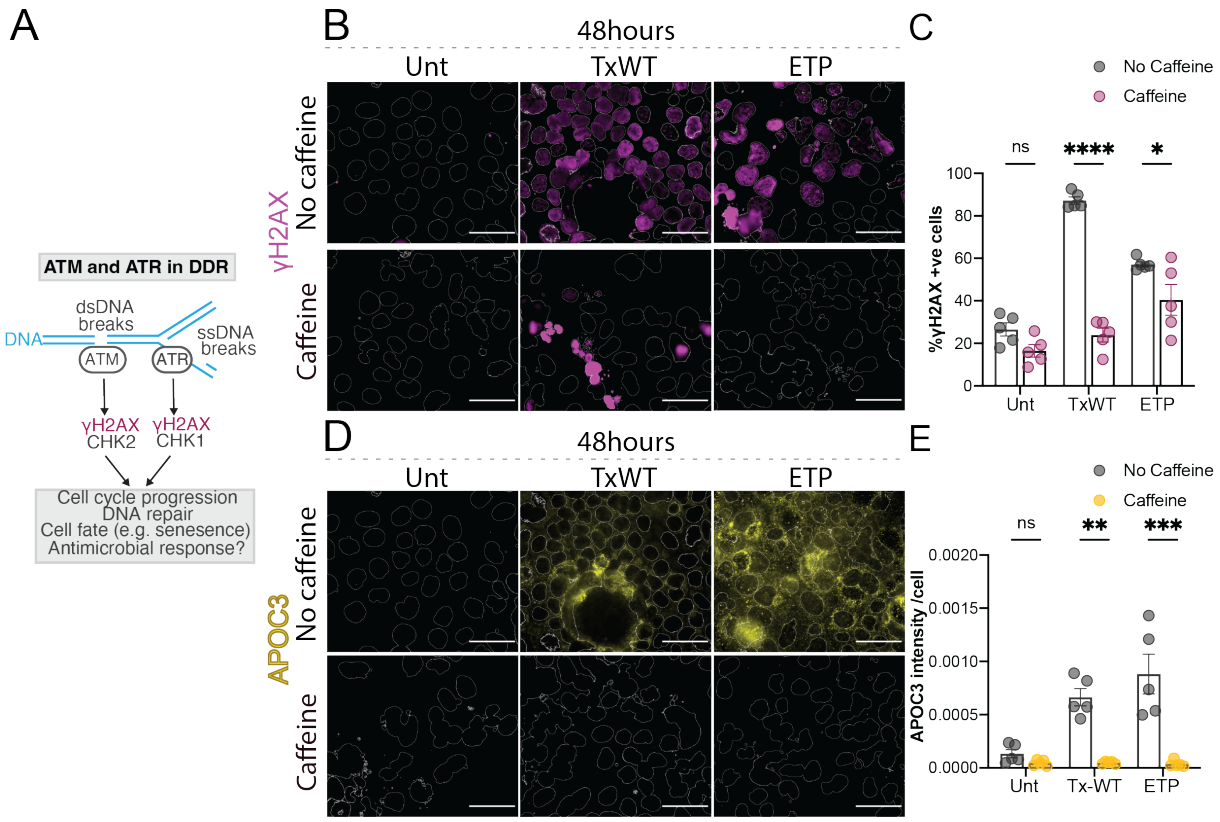

Figure 3.8: ATM and ATR inhibition by caffeine inhibits APOC3 expression in CACO-2 cells. **(A)** Schematic showing the role of ATM and ATR in DNA repair. **(B)** γH2AX expression (magenta) with and without caffeine treatment in CACO-2 cells at 48 hours chase. **(C)** Quantification of γH2AX expression in respective groups (no caffeine, gray; caffeine, magenta). **(D)** APOC3 expression (Yellow) with and without caffeine treatment in CACO-2 cells at 48 hours chase. **(E)** Quantification of APOC3 expression in respective groups (no caffeine, gray; caffeine, yellow). Scale bar = 50μm (n=1; each point represents a field of view)

3.5 Toxigenic *Salmonella* induce host secretion of APOC3

APOC3 was identified as a secreted host factor in human participants during infection by wild-type *S.* Typhi-WT but not *S.* Typhi-TN (**Fig. 2.10 and 2.13**). To test for APOC3 secretion *in vitro*, conditioned media (CM) was harvested from intoxication experiments in Fig 3.5 and infection experiments in (**Fig.3.6, and 3.7**) and APOC3 secretion assessed by ELISA (**Fig.3.9**).

When CM from intoxicated cells was analysed by ELISA (**Fig.3.9A**) untreated cells and Tx-HQ incubated cells showed low concentrations of APOC3 relative to cell number, both at ∼1pg/μl (**Fig.3.9B**). APH was used as a positive control for APOC3 secretion. APH is an inhibitor of DNA polymerase which inturn causes DNA replication stress and consequently DNA damage.[307] APH incubated cells showed relatively high concentrations

of APOC3, ∼3pg/μl. Tx-WT intoxicated cells exhibited similar concentration of APOC3 to that of APH treated cells, ∼3pg/μl (**Fig.3.9B**).

CM collected from Sm-WT and Sm-ΔctdB infected cells at 48 hours and 96 hours were added to APOC3 ELISA plates (**Fig.3.9**). At 48 hours, untreated cells exhibited low concentrations of APOC3, ∼200pg/μl relative to cell lysate optical density (OD). However, Sm-ΔctdB infected cells secreted a relatively high concentration of APOC3, ∼2000pg/μl (**Fig.3.9**). This is higher secretion than the untreated and the Sm-WT infected cells, ∼1500pg/μl (**Fig.3.9**). This trend was consistent with the increased APOC3 expression observed within Sm-ΔctdB-infected CACO-2 cells at 48 hours (**Fig.3.6**). However, APOC3 expression was significantly higher in Sm-WT infected cells at 96 hours (**Fig.3.7**), a trend also observed with APOC3 secretion at 96 hours (**Fig.3.9**): untreated and Sm-ΔcdtB infected cells showed a similar APOC3 secretion, Δ2000pg/μl. In contrast, Sm-WT infected cells secreted significantly more APOC3, ∼4000pg/μl (**Fig.3.9D**). This supports the hypothesis that CACO-2 cells express the APOC3, which is subsequently secreted it, which could explain why APOC3 was identified in the human plasma samples of TYGER participants.

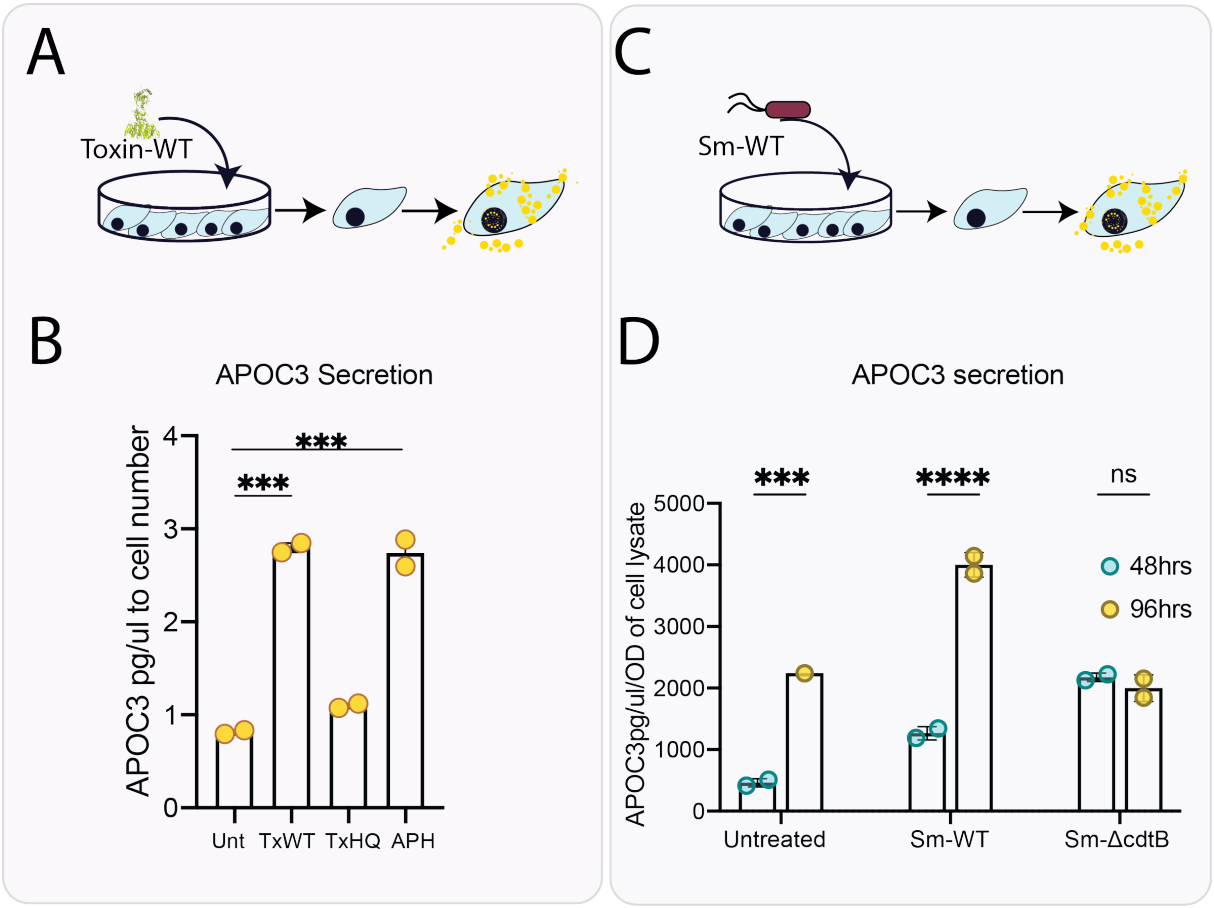

Figure 3.9: APOC3 secretion profile in conditioned media (CM) of intoxicated and infected cells using ELISA assay. (A) Schematic of hypothesised effect of toxin on CACO-2 cells secretory profile. **(B)** Concentration of APOC3 in response to Tx-WT compared to Tx-HQ, untreated (unt) and APH, normalised to cell number identified by ELISA assay *(n=2)*. **(C)** Schematic of proposed hypothesis of the response of CACO-2 cells to *Salmonella*-WT. **(D)** APOC3 concentration in response to *Salmonella*-WT, *Salmonella*-ΔcdtB and untreated cells at 48 hours (cyan) and 96 hours (yellow) identified by ELISA assay *(n=2). Error bars represent SEM.*

3.6 LYZ expression in intoxicated mononuclear THP1 cells

The next step was to investigate the expression of LYZ in response to the toxin. To identify the ideal modelling cell line we followed the same process of checking the cell line most likely to express LYZ and using it as a model.[246] In contrast to APOC3, which is restricted to the liver and GI, LYZ is found in all bodily secretions and is predominantly expressed in monocytes and macrophages,[308] which would be circulating in bacteraemic participants and potentially targeted by typhoid toxin. We started by investigating the effect of the toxin on monocytes using the THP1 cell lines derived from acute monocytic leukaemia (ATCC, THP1). THP1s can be differentiated into macrophages by 72h treatment with PMA during culture,[309] IFN-γ.[310] In the monocytic state, we observed that

by 48 hours THP1s were obliterated in response to TxWT and therefore no images could be taken (**Fig.3.10A**). To test the exhibited cell death, we used a live/dead assay which stains live cells with a calcein green dye that indicates intracellular esterase activity and dead cells with Ethidium homodimer red dye that is impermeable to living cells. Untreated cells and Tx-HQ treated cells exhibited 100% live cells, i.e. green fluorescence. Relative to negative controls, the proportion of live cells in THP1 monocytes treated with TxWT was reduced to ∼10% or to 15% with the positive control APH. Consistent with these observations, only 10% of untreated and Tx-HQ-treated cells were dead while 90% of Tx-WT treated monocytes were killed and ∼85% of APH-treated cells. (**Fig.3.10B**).

Experiment was then repeated on differentiated macrophages. THP1 cells were differentiated using PMA for three days to a macrophage state (M0), following protocols suggested by[309] (**Fig.3.10C**). The live/dead assay is suitable for determining cell viability in monocytic THP1 cell cultures, which grow in suspension. The assay is less effective for adherent THP1 macrophages that lose adherence during cell death and complicates interpretation. Thus, an alternative cell death assay was sought. Lactate dehydrogenase (LDH) is released into the cell culture medium during cell death and was assayed to determine cell death in macrophages at 1h, 4h, 24h, and 48h post-treatment (**Fig.3.10D-G**). Untreated macrophages LDH secretory profile was used as a baseline for other treatments while cell lysis by detergent was used as a positive control. There was no difference between treatments at 1h and 4h while a modest increase was observed at 24h with TxWT, TxHQ, and APH that exhibited 20% LDH secretion relative to the 0% in untreated. However, at 48 hours, while Tx-HQ- and APH-treated macrophages exhibited no difference in LDH release relative to the untreated control, LDH release increased to 90% in Tx-WT treated macrophages indicating high levels of cytotoxicity (**Fig.3.10D-G**).

While THP1 monocytes were killed by the toxin, macrophages survived the first 24h after which macrophages were observed undergoing toxin-dependent cell death at 48h (**Fig.3.10A-G**). Thus, LYZ expression was investigated in THP1 macrophages treated at 48h post-intoxication with TxWT (**Fig.3.10H**). Regardless of LDH release we observed surviving macrophages at 48 hours chase. LYZ was expressed in all THP1 macrophages regardless of treatment (**Fig.3.10I**). However, when treated with APH, DNA replication stress inducer, cells exhibited a slightly significant increase in LYZ expression upon quantification, with intensity of 0.02 intensity per image in APH treated compared to ∼0.01 intensity per image in Tx-HQ treated (**Fig.3.10J**). Although this suggested a possible implication of LYZ to a DNA damage induced phenotype, THP1s proved to be an ineffective model to test toxin-induced LYZ expression *in vitro*.

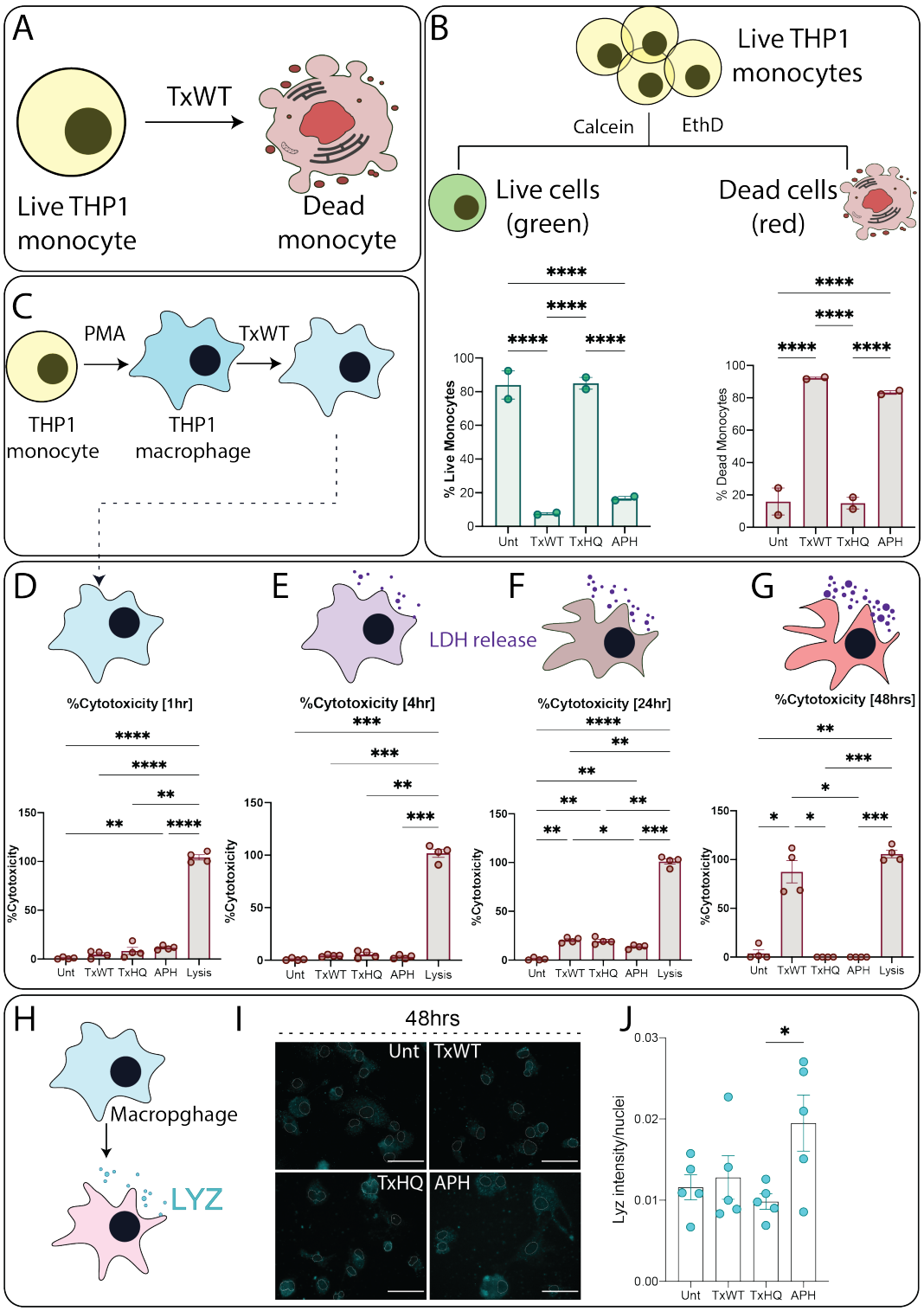

Figure 3.10: THP1 cells tested as an *in vitro* model for testing LYZ. (A) Schematic of observation of monocytes dying after intoxication *(data not shown, n=2).* **(B)** Monocytes assayed for cell death using Live/Dead flow cytometry kit. Bar charts show live cells (green bars) and dead cells (red bars) *(n=1; each point is a technical replicate).* **(C)** Schematic of experimental plan of PMA induced differentiation of THP1 monocytes to THP1 macrophages before intoxication. **(D)** - **(G)** Bar charts of %cytotoxicity, identified by LDH release, in intoxicated THP1 macrophages at 1hr (**D**; blue cell), 2hrs (**E**; purple cell), 24hrs (**F**; brown cell) and 48hrs (**G**; red cell) *(n=2, each point is a technical replicate).* **(H)** Schematic of LYZ release in macrophages. **(I)** Immunofluorescence images of LYZ (cyan) in THP1 macrophages at 48 hours chase. **(J)** Quantification of LYZ intensity per nuclei. *Error bars represent SEM (n=1; each point represents a field of view). Scale bar =50µm.*

3.7 LYZ expression in intoxicated CACO2 cells

According to the protein ATLAS,[247] THP1 cells express LYZ ∼50 times more than CACO-2 cells (normalised transcript expression values (nTPM) 489 compared to nTPM 9.5).[247] CACO-2 cells express LYZ but in trace amounts, making them a possible candidate to test toxin induced LYZ expression *in vitro*. Due to the low levels of naïve LYZ, this would allow for observing and detecting increased expression in response to the toxin in parallel with APOC3. CACO-2 cells were intoxicated with Tx-WT using our standard intoxication protocol, 2hrs pulse with the toxin and chased for 48hours. Untreated cells showed low levels of APOC3, as previously observed (**Fig.3.5**) and few LYZ puncta (**Fig.3.11A**). Meanwhile, Tx-WT treated cells induced LYZ expression in CACO-2 cells (**Fig.3.11A**). To quantify LYZ due to its low intensity, but globular phenotype, we used an algorithm on cell profiler to quantify the number of LYZ dots (or "puncta") per field of view. Quantification revealed ∼100 puncta per field of view in untreated controls and. ∼600 puncta in TxWT-treated cells (**Fig.3.11B**). There was no colocalization between APOC3 and LYZ, both would appear in similar regions, but would not superimpose on each other (**Fig.3.11**). The size of LYZ puncta was bigger and more globular than that of APOC3 at 48 hours (**Fig.3.11A**), consistent with previous APOC3 results at 48 hours (**Fig.3.5**).

3.8 LYZ is implicated in DDR

Fig.3.8 showed APOC3 was regulated by the DDR's ATM and ATR in CACO-2 cells. To investigate whether LYZ is controlled by the DDR as well, LYZ expression was examined in the presence of the ATR/ATM inhibitor caffeine (**Fig.3.11**). Untreated cells showed low levels of APOC3 and LYZ and subsequently no significant difference with caffeine treatment was observed (**Fig.3.11B, D**). Meanwhile, Tx-WT induction of APOC3 (**Fig.3.8D**) and LYZ was inhibited with caffeine (**Fig.3.11C**). Quantification showed a significant decrease in LYZ puncta per field of view following caffeine treatment of Tx-WT treated cells, from about 600 puncta to zero (**Fig.3.11D**).

This implicated the expression of both, APOC3 and LYZ, in CACO-2 cells with ATM and ATR. Both APOC3 and LYZ are part of the identified secretome-WT, which not only is specific to the WT infected participants, but it seems to be part of the DDR. This proposes that the typhoid toxin caused the secretion of a DDR-regulated secretome.

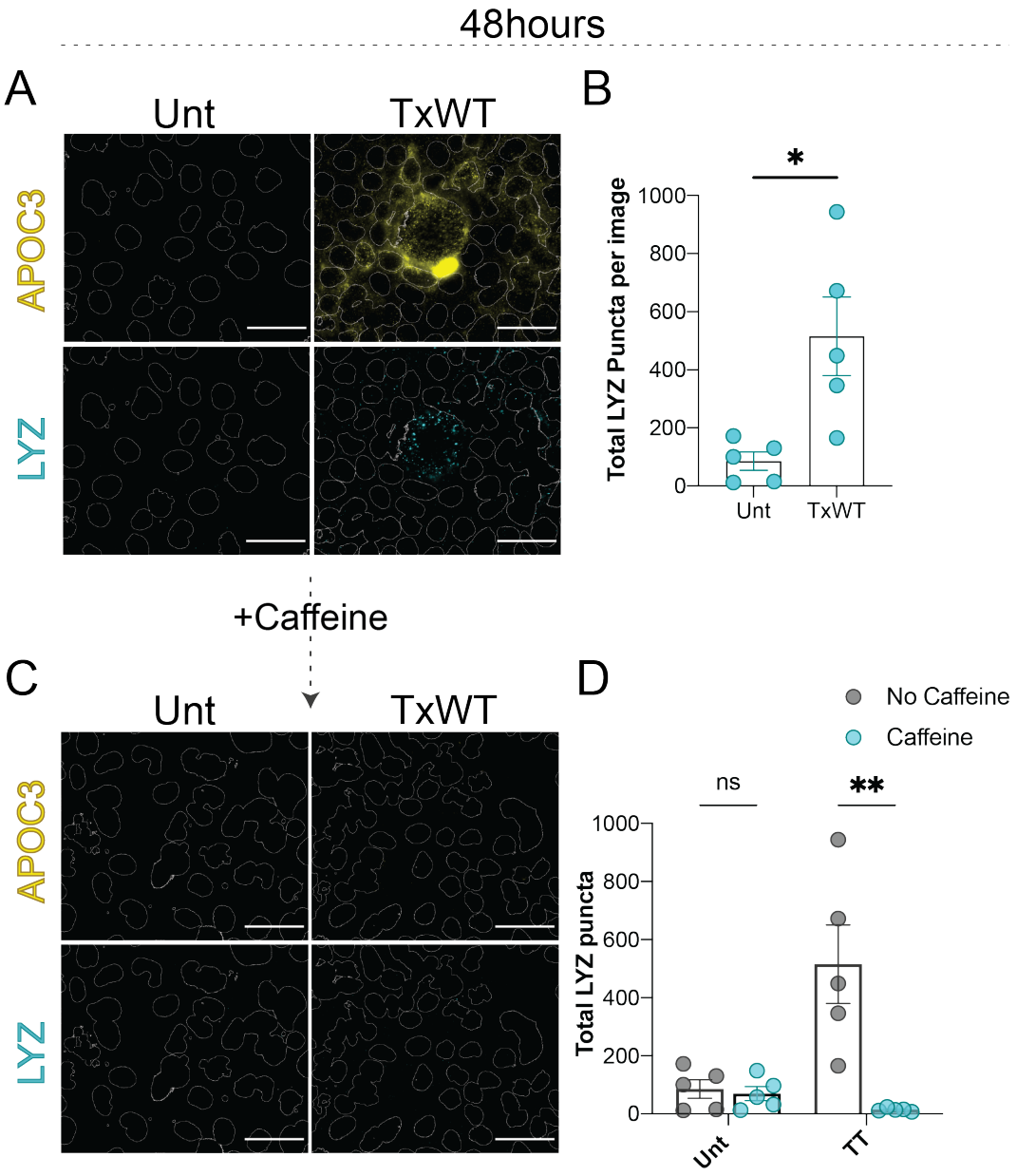

Figure 3.11: CACO-2 cells as a model for LYZ expression *in vitro*. **(A)** Immunofluorescence images of intoxicated CACO-2 cells at 48 hours post intoxication expressing APOC3 (yellow) and LYZ (cyan). **(B)** Quantification of average LYZ puncta per image. **(C)** Immunoflorescence images of caffeine incubated CACO-2 cells exhibit lack of LYZ (cyan) and APOC3 (yellow) expression. **(D)** Quantification of Total LYZ puncta per image before (gray) and after (cyan) caffeine treatment. *Error bars represent SEM. Scale bar = 50µm (n=1; each point represents a field of view)*

3.9 LYZ is secreted by intoxicated CACO-2 cells

Previous experiments showed LYZ expression in response to Tx-WT in CACO-2 cells. Next, LYZ secretion was tested by incubating CM harvested 96 hours post intoxication on pre-coated LYZ ELISA plates (**Fig.3.12A**). Absorbance measurements showed a concentration of ∼10ng/ml and 5ng/ml LYZ in CM collected from the negative control groups,

untreated and Tx-HQ-treated, respectively. Meanwhile, relative LYZ secretion increased to ∼30ng/ml in Tx-WT intoxicated cells ∼25ng/ml in APH treated cells (**Fig.3.12B**).

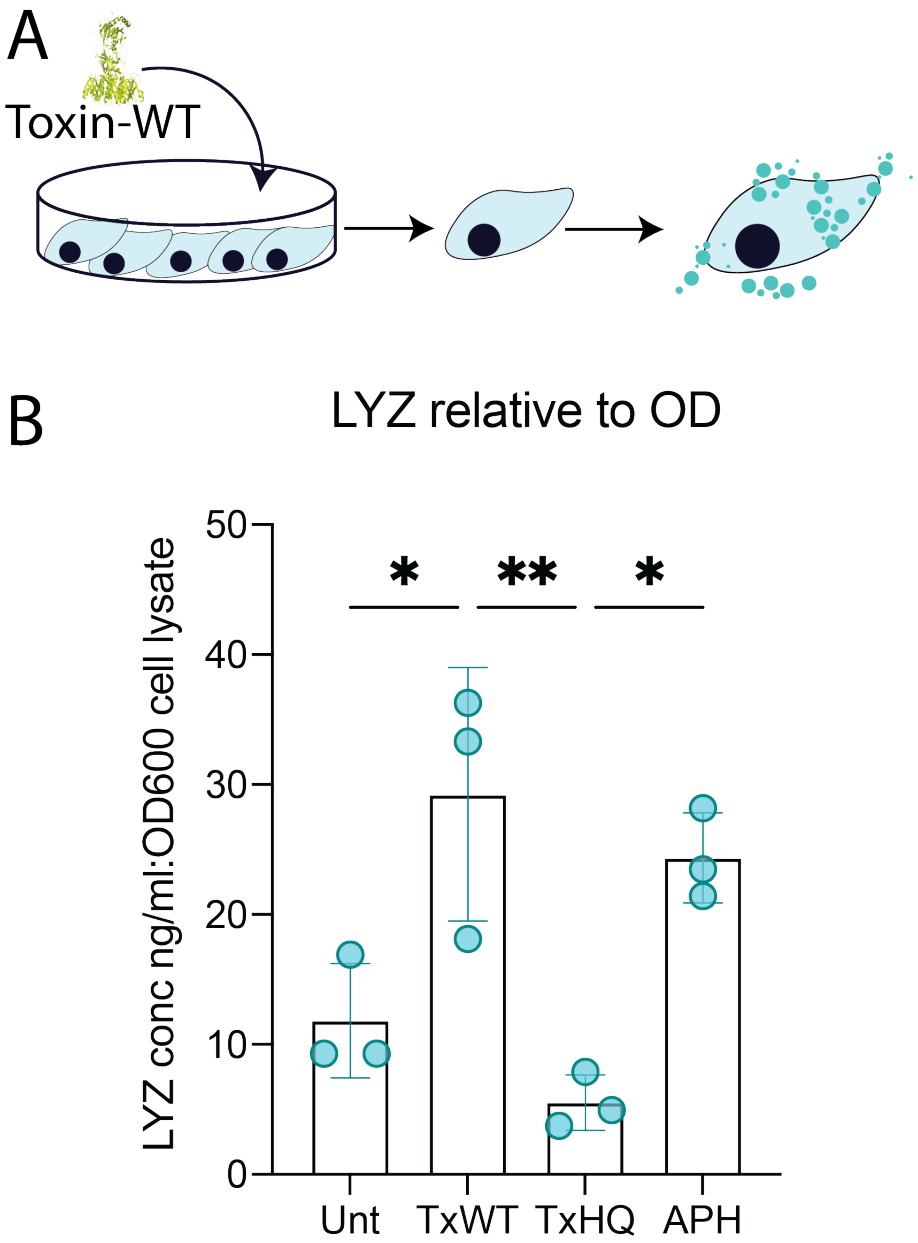

Figure 3.12: LYZ is secreted by CACO-2 cells. **(A)** Schematic representation of LYZ secretion in response to Tx-WT. **(B)** Bar chart of ELISA assay quantification of OD600 normalised to cell lysate in ng/ml. *(n=1). One-way ANOVA statistical test was performed.*

3.10 LYZ is expressed in mouse small intestine tissue sections

The expression and secretion of LYZ and APOC3 in CACO-2 cells (a gut epithelium model) supported the hypothesis that wild-type *S.* Typhi induced expression of APOC3 and LYZ during infection of the gut (**Fig.3.11,3.12**). To further validate secretome-

WT in human participants, a collaboration was established with Professor Teresa Frisan (University of Umeå) who has established a mouse infection model to study the typhoid toxin.[140] Nramp1+ Sv129 mice were infected with a placebo, 10^8 *S.* Typhimurium engineered with typhoid toxin (*S.* Typhimurium-TxWT) or the toxin-negative derivative (*S.* Typhimurium-TN) by gastric gavage before euthanisation at 5-days post infection. Fixed tissue sections enabled immunohistochemistry of APOC3 and LYZ during infection of the mouse intestinal epithelium and the raw images were transferred to our laboratory for image analysis (**Fig.3.13**). No APOC3 was observed. Nevertheless, LYZ was observed in non-infected and *S.* Typhimurium-TN, and though there was a relative increase in LYZ expression *S.* Typhimurium-TxWT during infection (**Fig.3.13A**), the findings were insignificant (**Fig.3.13**).

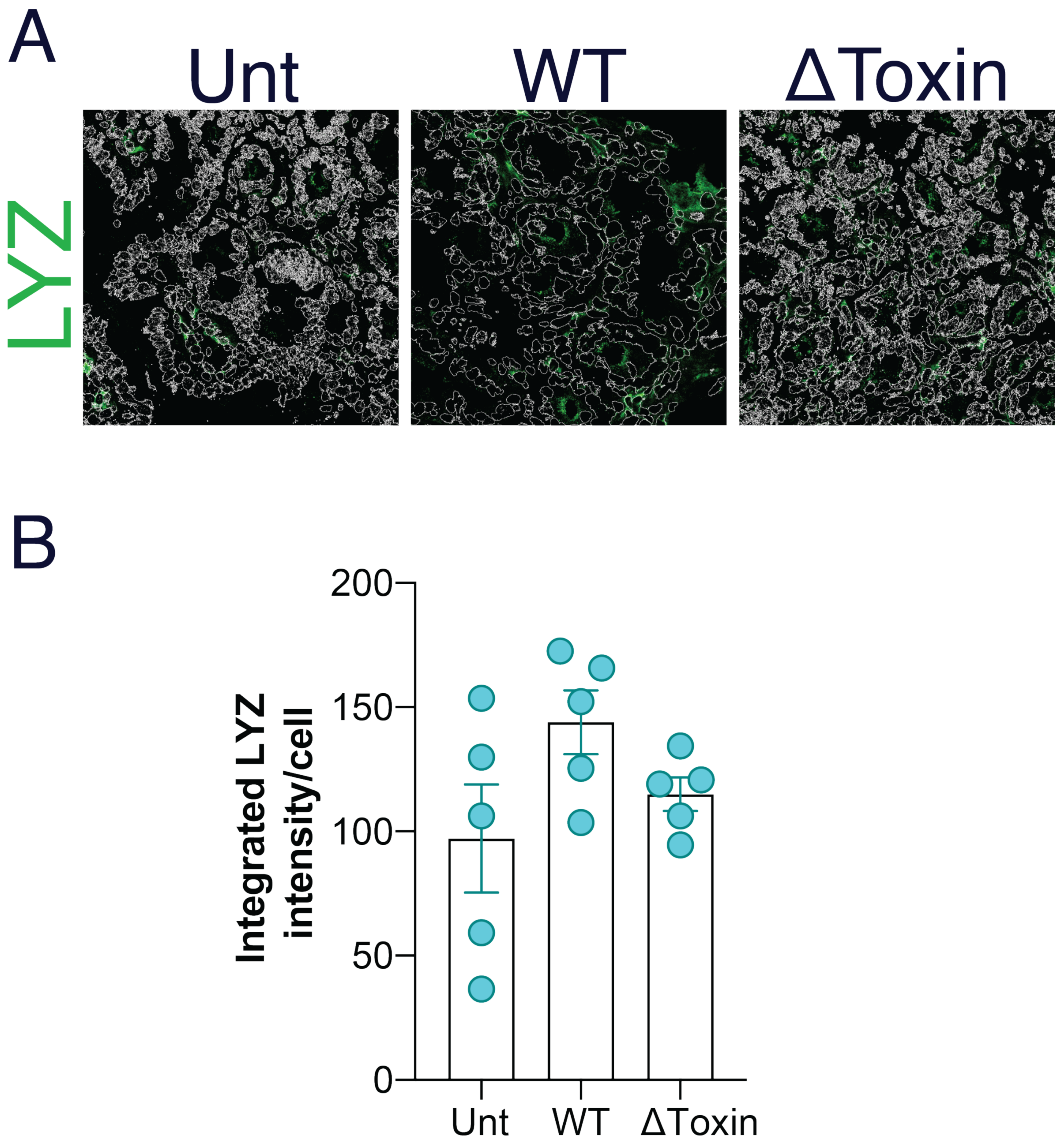

Figure 3.13: LYZ is expressed in mouse intestinal tissues in response to *Salmonella* infection. (A) Immunofluorescence images from Frisan Laboratory in Sweden processed by myself of mouse small intestine post ingestion of *Salmonella* WT or *Salmonella* ΔToxin. **(B)** Quantification of integrated LYZ intensity per cell, each point represents an average per image. *Error bars represent SEM (n=1)*

3.11 LYZ reduces the viability of *Salmonella*

In the TYGER study, the duration of bacteraemia was shorter in participants infected with *S.* Typhi WT than *S.* Typhi TN.[56] In Chapter 2, proteomic analysis of the plasma from participants with bacteraemia revealed toxin-induced secretome, which contained putative antimicrobials including APOC3 and LYZ, which may explain the shorter duration of bacteraemia in *S.* Typhi WT-infected participants. In this chapter, the secretion of APOC3 and LYZ from human cells was found augmented in a toxin-dependent manner validating the proteomic data in Chapter 2. Thus, the next step was to examine the antimicrobial properties of secretome-WT, which focussed on LYZ.

Gram-positive bacteria are bound by a single outer membrane that can be penetrated by LYZ resulting in cell death. Gram-negative bacteria have increased resistance to LYZ due to a cell wall comprising an inner and outer membrane.[311,312] LYZ can mediate bactericidal activities on Gram-negative bacteria through cationic pore forming activities and/or by working in cooperation with agents that can permeabilize the outer membrane, which allows LYZ access to the underlying peptidoglycan. For example, defensins are known to permeabilise the outer surface of bacteria to allow entry of excluded enzymes such as LYZ to further attack the bacteria.[313] This can be mimicked biochemically when cells are exposed to a mild osmotic shock in the presence of EDTA. Thus, I sought to investigate the antimicrobial properties of LYZ on *Salmonella* with a view to examining whether the lipid-binding properties of APOC3 enhance penetration of LYZ and therefore any bactericidal effects.

In an attempt to mimic that, *Salmonella* was permeabilized using Gaudet *et al.* 2021 permeabilization protocol.[294] *Salmonella* was incubated with EDTA and salts. EDTA neutralized LPS and salts cause osmotic pressure in the *Salmonella* causing a permeabilized OM for LYZ to function.

S. Javiana were non-permeabilized or permeabilized prior to incubation with LYZ and growth measured by OD 600nm readings every 30 minutes in a Tecan Sunrise plate reader at 37°C with shaking.

In the absence of permeabilization, untreated negative control *S.* Javiana (black line) grew exponentially in the first 5h reaching an OD600 of 0.6 after which no more growth was observed indicating stationary phase (**Fig.3.14A,C**). The addition of either chicken LYZ (LYZ-Chk; in **Fig.3.14A**) or human LYZ (LYZ-Hu in **Fig.3.14C**) reduced growth though not in a concentration dependent manner and findings with the lowest concentration of 20μg/ml (magenta line) were most consistent. This indicates that LYZ prevents growth of *Salmonella*. The same findings were also observed with permeablized *S.* Javiana incubated with LYZ-Chk in **Fig.3.14B** but not LYZ-Hu in **Fig.3.14C** where results

were inconclusive. During attempts to repeat the experiment, the Tecan Sunrise broke down and a Hidex sense plate reader was used instead. Due to time constraints, initial experiments were performed with permeablized *S.* Javiana incubated with LYZ-Chk (**Fig.3.14E**) or LYZ-Hu (**Fig.3.14F**). However, no differences on the growth of *S.* Javiana were observed.

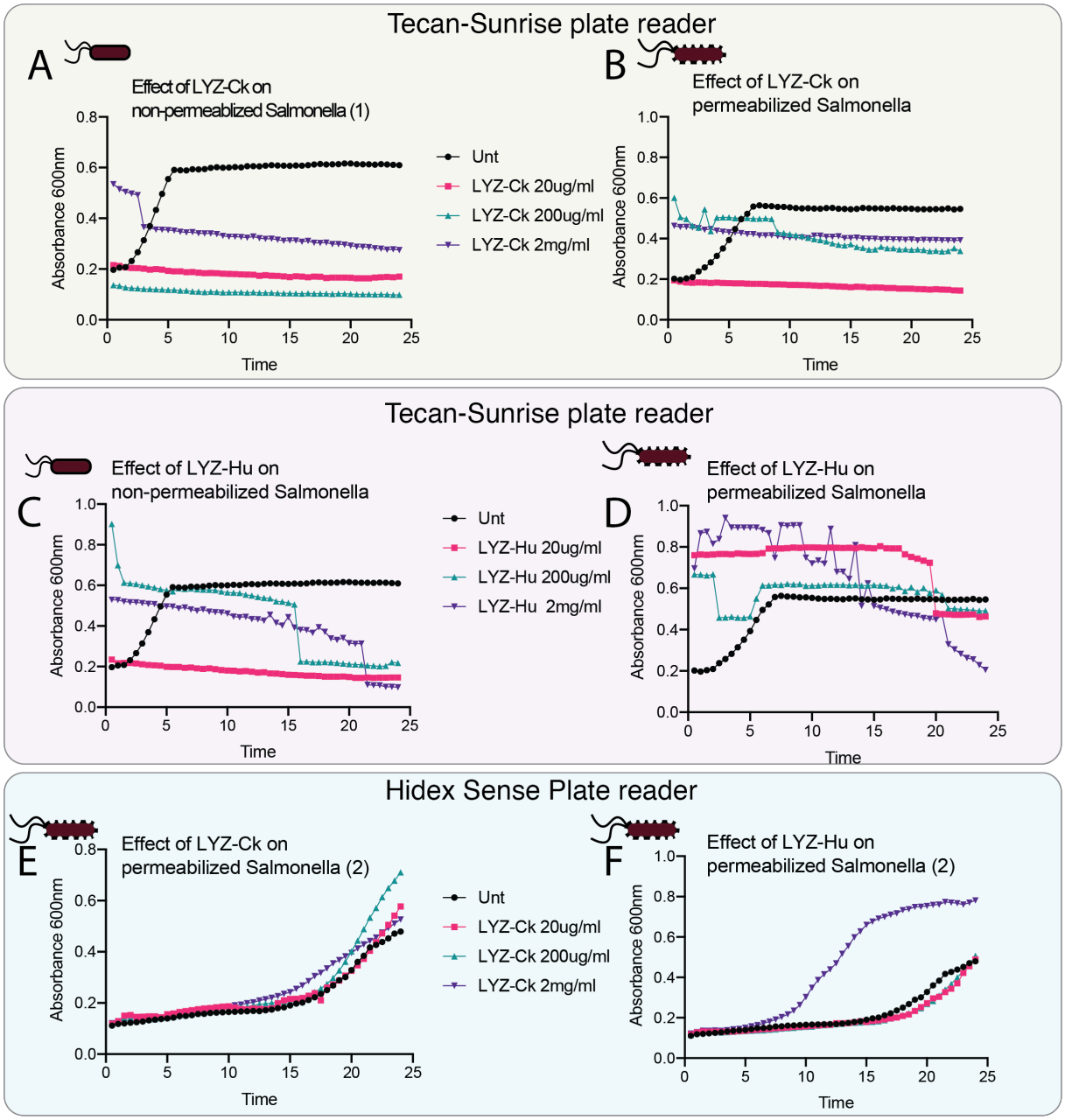

Figure 3.14: *Salmonella* Growth with LYZ treatment for 24 hours. (A)-(D) Tecan Sunrise plate reader performed experiments. **(A)** Non-permeabilized *Salmonella* incubated with three different concentrations of chicken LYZ (LYZ-Ck), 20μg/ml, 200μg/ml and 2mg/ml. **(B)** Permeabilized *Salmonella* incubated with LYZ-Ck. **(C)** Non-permeabilized *Salmonella* incubated with three different concentrations of human LYZ (LYZ-Hu), 20μg/ml, 200μg/ml and 2mg/ml. **(D)** Permeabilized *Salmonella* incubated with LYZ-Hu. (E)-(F) Hidex sense plate reader performed experiments. (E) Permeabilized Salmoenlla incubated with LYZ-Ck. (F) Permeabilized Salmoenlla incubated with LYZ-Hu. *Each point is the average of three technical replicates.*

Measuring bacterial growth in a plate reader enabled antimicrobial effects to be quantified but technical issues and time constraints due to repairs led to a change in strategy. To examine the effect of LYZ on *Salmonella* viability more directly, *S.* Javiana were grown to an OD of 0.5 before osmotic shock with EDTA buffer and incubation with LYZ then viability assayed by colony counting on LB agar plates (depicted in **Fig.3.15A**).

S. Javiana continued to grow in the absence of LYZ demonstrated by a uniform zone of growth and the lack of individual colonies (**Fig.3.15B**). Permeabilization itself reduced the growth rate of *S.* Javiana though bacterial growth increased between 2 hours and 4 hours indicating recovery (**Fig.3.15B**). This trend was also observed when serial dilutions were plated and resulting colony counts quantified (**Fig.3.15C**). In the presence of LYZ, 5μg/ml and 10μg/ml slowed the growth rate, which began to recover by 4 hours post-incubation (**Fig.3.15B,C**). In contrast, 1mg/ml and 2mg/ml resulted in loss of viability as LB could not support growth of *S.* Javiana at 4 hours.

The next step was investigating if the DDR secretome from intoxicated CACO-2 cells which secrete LYZ **Fig.3.12** could induce bacterial killing on permeabilized *Salmonella*. Our hypothesis was that other factors in the DDR secretome could permeabilize *S.* Javiana and subsequently allow for LYZ action, e.g. APOC3, defensins. Non-permeabilized *S.* Javiana were incubated with CM-WT and CM-HQ, and spotted on an Agar plate at different time points. As a negative control, *S.* Javiana were incubated with conditioned cell culture medium from untreated cells (i.e. untreated). As expected, the growth of non-permeabilised *S.* Javiana was indistinguishable when incubated with either untreated conditioned media (untreated), or conditioned media from cells treated with TxWT (CM-WT) or TxHQ (CM-HQ) (**Fig.3.15D,E**). However, the same observations were made with permeabilized *S.* Javiana providing no evidence of an antimicrobial DDR secretome. Indeed, if anything, the reverse trend was true as enhanced growth of *S.* Javiana was observed with CM-WT and CM-HQ relative to untreated (**Fig.3.15E**).

Looking at the previously shown LYZ ELISA results in **Fig.3.12**, it was noted that the concentration of LYZ in CM-WT was ∼15ng/ml (**Fig.3.15F**). This is 1500x lower than the lowest effective dose suggested in preliminary LYZ viability experiments (1g/ml) in **Fig.3.15E**. This may explain the unexpected effects observed in response to CM on *S.* Javiana.

In summary, purified LYZ can mediate bactericidal effects on *Salmonella* but only if the outer membrane is compromised to allow penetration of LYZ into the periplasmic space where its substrate peptidoglycan is accessible. However, the concentrations of LYZ in the DDR secretome appear insufficient to recapitulate the findings with purified LYZ. Thus, the findings do not currently support the hypothesis that the DDR secretome exerts antimicrobial effects through LYZ and APOC3.

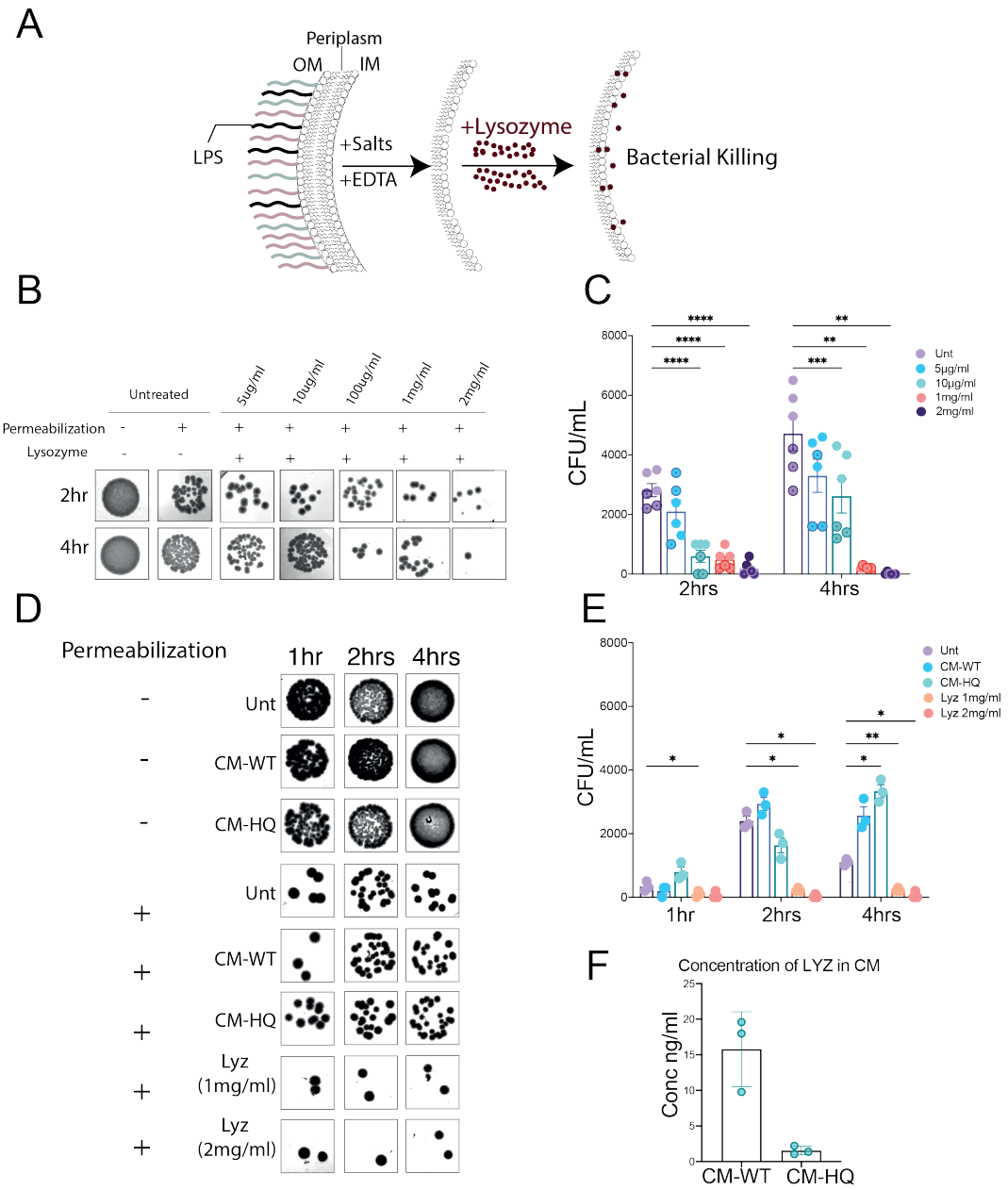

Figure 3.15: Permeabilization of *Salmonella* OM provides LYZ effectiveness in a dose dependent manner. **(A)** Schematic explaining the aim of permeabilization protocol. **(B)** Colony forming unit (CFU) images at timepoints post LYZ treatment. **(C)** Quantification of CFU counts at 2 and 4 hours with different concentrations of LYZ. **(D)** CFU images of *Salmonella* at different time points with different concentrations of LYZ and conditioned media (CM) collected from TxWT and TxHQ intoxicated CACO-2 cells. **(E)** Quantification of CFU counts at 1, 2, and 4 hours of incubation with LYZ concentrations, CM-WT or CM-HQ. **(F)** Bar chart showing concentration of LYZ in 1ml of collected CM before incubation on *Salmonella (n=1). **(B)** and **(D)** Representative images from n=2. **(C)** and **(E)** each point is a CFU colony and different shapes represent different biological repeats.*

3.12 Discussion of results

Protein secretion has been a major focus of the *Salmonella* host-pathogen interaction field for decades yet much of the attention has been placed on *Salmonella* secretion of virulence effector proteins or host cell secretion of cytokines. Once *Salmonella* colonises the gut epithelium studies have shown that secreted effector proteins aid in pathogen survival. However, the effectors can also alter the host secretome.[314] One of the first examples of a virulence effector to induce secretion of host proteins was SipB. SipB is a component of the T3SS translocon and membrane damage is thought to activate the inflammasome characterised by macrophage pyroptosis and secretion of IL-1 and IL-18.[315,316] Chapter 2 revealed that the typhoid toxin elicits release of a host secretome containing APOC3 and LYZ in human participants with typhoid. Chapter 3 suggests that the secretome is a host response to DNA damage controlled by ATM and ATR DNA repair kinases. This chapter advances the field by implicating a DDR secretome in response to *Salmonella* in participants with typhoid.

Chapter 2 utilised mass spectrometry to identify novel proteins that are produced in response to *Salmonella* infection in human participants. These proteins were hypothesised to play a role in *Salmonella* infection and associated symptoms. Amongst these proteins, APOC3 and LYZ showed the most promise as they exhibit differential secretion between secretome-WT and secretome-TN groups, in addition to their antibacterial properties.[256,317]

Chapter 3 identified CACO-2 as an efficient intestinal cell model to investigate toxin-induced APOC3 and LYZ expression. APOC3 and LYZ were both expressed in response to Tx-WT treatment of CACO-2 cells. Consistent with previous findings, the typhoid toxin induced a DDR marked by γH2AX signalling.[226] The toxin-induced DDR was also implicated with APOC3 and LYZ expression, suggesting that both proteins are implicated in DDR. It is also possible that secreted factors activate DDRs themselves, which is well-established in the senescence field where factors in SASP promote DDRs in bystander cells resulting cell-cycle arrest and senescence.[220] Consistent with this, APOC3 was found accumulating in the nucleus of intoxicated CACO-2 cells, which displayed γH2AX DDRs. APOC3 is an important regulator of lipid metabolism[290] and phosphoinositide lipids have been shown to recruit ATR to sites of DNA damage, thus, the lipids represent a component of the early DDR.[318] However, no colocalization between APOC3 and H2AX was observed suggesting that APOC3 is not involved in γH2AX production by recruitment of ATM/ATR. Thus, it remains to be established whether APOC3 accumulates in the nucleus or the perinuclear region, and whether lipids are bound to APOC3, and whether the nuclear accumulation of APOC3 is a result of nuclear dysfunction driven by micronuclei formation and genomic instability.

The use of CACO-2 cells has its limitations. CACO-2 cells are cancer cells and thus not an ideal model for healthy intestinal cells, which could be addressed using stem cell cultures or primary gut cells. CACO-2 cells were cultured in a monolayer which is another drawback as monolayer cells lacks the complexity of the intestinal epithelium.[319] Three-dimensional cultures of CACO-2 intestinal tubes is an emerging field of study that is currently being applied in our laboratory. It could be further used to investigate the toxin induced effects on a more complex system. An other drawback is that CACO-2 cells are p53 null.[320] P53 is an important regulator of senescence and so CACO-2 cells are unlikely to senesce.[321] As a result, the role of senescence in host secretory responses to typhoid toxin in cells and human participants have not been addressed.

This chapter shows bactericidal effects of LYZ on *Salmonella* fitting with the literature.[322] *Salmonella* permeabilization aided in observing dose dependent effects with LYZ (**Fig.3.15**). However, more experiments need to be carried out to ascertain the significance of APOC3 and LYZ in the shorter duration of bacteremia with wild-type *S.* Typhi reported in the TYGER study.

Chapter 4

Discussion

This study identified toxin-specific host protein signatures APOC3 and LYZ in human participants at the time of typhoid diagnosis. *In vitro* studies exploiting intoxicated cultured cells showed that expression of APOC3 and LYZ were induced by the DDR in a manner dependent on ATM/ATR and toxin nuclease activity, which resulted in secretion of APOC3 and LYZ. Secretion of APOC3 and LYZ was also observed during infection with the toxigenic NTS serovar *Salmonella* Javiana, which supports observations in human participants with typhoid whilst opening up the possibility that diverse serovars encoding typhoid toxin modulate the host secretome in a similar manner, e.g. *S.* Paratyphi A. The role of the secretome is still unclear but the data indicate that pathogen-induced DNA damage is sensed by ATM/ATR kinases, which elicits a host response via the secretome that counteracts *Salmonella* infection by reducing the duration of bacteraemia.

4.1 Lessons learned from proteomic analysis of host-pathogen interactions

Proteomics provides a powerful methodology to determine protein level changes in host-pathogen interactions, which can provide insight into the role of virulence factors including bacterial toxins.[323] For example, host proteome alterations in response to the toxin Listeriolysin O (LLO) of *Listeria monocytogenes* were identified by SILAC (stable isotope labelling by amino acids in cell culture) followed by LC-MS/MS of lysates of cultured cells.[324] This showed upregulation of the host ubiquitination system resulting in proteosome-dependent degradation of 149 host proteins. However, the study above exploited proteomic analysis of tissue culture models whereas this PhD study uses plasma from clinical samples, which is a valuable resource for studying typhoid host-pathogen interactions, vaccines and diagnostic markers. For example, plasma samples harvested from participants with typhoid fever following challenge with *S.* Typhi were used to screen 4,445 bacterial antigens in sera from 41 participants.[325] Proteomics-based identification of plasma proteins in chronic *S.* Typhi carriers identified albumin, proprotein convertase

subtilisin, furin, and haptoglobin, upregulated in chronic carriers.[326] While metabolomic profiling of plasma samples from chronic carriers identified glutaric acid and hexanoic acid.[327]To my knowledge, this PhD thesis advances the field by providing the first proteomic study of host responses to a bacterial toxin in a human infection challenge model.

Host secretomes in response to infection have also been analysed using proteomics.[323] For example, targeted analysis of macrophage secretions in response to TLR4 activation via heat-killed *E.* coli, TLR2 activation by heat-killed Staphylococcus aureus or TLR7 activation by live intracellular Burkholderia cenocepacia identified lysozyme-2 (LYZ-2) as an upregulated component of the secretome.[328] Does this suggest that increased secretion of LYZ during WT *S.* Typhi infection is due to PAMP recognition by TLRs? In this study, LYZ was found at a lower concentration in the TN *S.* Typhi infected relative to uninfected participants while WT *S.* Typhi infected participants showed an increased LYZ secretion in a toxin-dependent manner **Fig.2.13**. This suggests LYZ is not secreted in response to the PAMPs of TN *S.* Typhi. Our findings in CACO-2 cells suggest LYZ is upregulated in a manner dependent on DDRs in the *S.* Typhi-infected gut rather than TLR signalling in circulating mononuclear cells in the bloodstream of participants. Unpublished RNA sequencing of circulating leukocytes showed no difference in LYZ expression between WT and TN *S.* Typhi-infected participants suggesting that differences in secretion were not due to changes at the transcriptional level **Fig.3.3**.

The host secretome of *Salmonella* infected cells has been investigated *in vitro*. Cell culture supernatants of THP1 macrophages infected with *S.* Typhimurium for 1.5 hours were analysed by LC-MS/MS to determine the extracellular proteome.[329] The findings revealed that infected macrophages release exosomes that trigger TLRs, which in turn releases TNF-a and secretion of cytokines RANTES, IL-1ra, MIP-2, CXCL1, MCP-1, sICAM-1, GM-CSF, and G-CSF. When comparing the findings of Hui et al 2018[329] to the findings in this PhD thesis, we identify an array of host proteins in response to typhoid infection some of which are involved in inflammasome activation, for example, APOC3 **Fig.2.10**. While there is no direct overlap in the constituents, functional overlap in terms of innate immunity signalling is noteworthy.

4.2 DDR secretomes in response to bacterial infection

While DDRs to bacterial infection have been widely reported,[330] not much is known about interactions between host DDR secretomes and infection. Perhaps understandably, much of the attention has been focussed on the secretion of cytokines in response to infection. This is exemplified by interferon (IFN) and inflammasome responses. For example, the cytosolic DNA sensor cGAS senses cytosolic dsDNA originating from DNA

damage and synthesises cyclic GMP-AMP, which is detected by STING triggering type I IFN expression and NF-κB signalling.[331,332] Type I IFN expression is upstream of proinflammatory cytokines. The cGAS-dependent type I IFN response is known to be activated by the *E.* coli CDT, which causes DNA damage and consequently DDR, resulting in secretion of cytokines IL-1β,IL-6 and IL-8.[333] In this study, human participants infected with WT *S.* Typhi secreted LYZ and APOC3, which are implicated in degradation of bacteria and inflammasome activation, respectively. Thus, this PhD thesis demonstrates that host secretome responses to bacterial genotoxins is not limited to cytokines but includes divergent host proteins implicated in innate immune responses.

4.3 Role of ATM/ATR in innate immune responses to infection

DDR and innate immune responses were believed to be independent cellular functions, however recent evidence supports that there is more cross talk between them than once believed.[334–338] ATM is reported to activate immune responses through IFN and NF-κB stimulation,[339,340] and p53 phosphorylation and STING activation.[331,332] This study suggests that DDR secretome components, APOC3 and LYZ, are regulated by ATM and ATR, which were inhibited by caffeine *in vitro*. There are conflicting publications regarding the role of ATM in enhancing or inhibiting antimicrobial responses. Härtlova et al suggest that loss of ATM enhances both the antiviral and antibacterial effects, through augmenting STING activation and IFN production.[341] In their follow-up study, ATM knockout mice were more susceptible to *S.* pneumoniae, which they suggested could be due to the build up of ROS that hindered PRR-mediated recognition of PAMPs.[342,343] Further work is required to dissect the role of ATM/ATR in coordinating LYZ/APOC3 responses and whether these responses to *Salmonella* are antimicrobial.

4.4 Does DDR counteract or promote *Salmonella* infections?

How the DDR fits in with the *S.* Typhi disease model is still under investigation. In this study, we speculate that the DDR could be a host mechanism to counteract *Salmonella* infection. DNA damage via oncogenes activates p53, which prevents cell growth by cell cycle arrest and suppression of metabolism that limits nutrient supply.[344] Suppression of cell metabolism by p53 was also shown to inhibit the growth of the obligate intracellular pathogen *Chlamydia trachomatis* that activates DDRs during infection.[241,345] This PhD study shows toxin induced DNA damages in our CACO-2 model (**Fig.3.5**), coincident with toxin-induced APOC3 (**Fig.3.5**) and LYZ expression (**Fig.3.11**). Preliminary experiments with LYZ indicate antimicrobial properties towards *Salmonella* (**Fig.3.15**).

Intriguingly, the related protein APOL3 was recently shown to solubilise the outer membrane of *Salmonella* Typhimurium in a manner reminiscent of detergents.[294] It is interesting to speculate that APOC3 may functionally mimic APOL3 thereby providing enhanced access for LYZ to the peptidoglycan of *S.* Typhi. This remains to be investigated.

Recent studies suggest a role of the lipoprotein APOC3 in inflammasome activation by direct binding of TLR2/TLR4,[256] which are known to sense PAMP lipoproteins such as LPS from Gram-negative bacteria and lipoproteins of Gram-positives.[346] Inflammasomes are known to restrict *Salmonella* Typhimurium infections in the intestinal mucosa of mice through pyroptosis of infected cells, which recruits neutrophils and reduces pathogen dissemination.[347,348] Thus, APOC3 could potentiate inflammasome-mediated cell death in infected cells to reduce the duration of bacteraemia. *S.* Typhi have evolved mechanisms to counteract inflammasome activation. *S.* Typhimurium activates NLRC4 and NLRP3 inflammasome pathways through flagellin.[349] However, *Salmonella* has evolved to down-regulate flagellin[127,350,351] and produce effectors that inhibit inflammasome activation as *Salmonella* infection progresses.[352,353] For example, a regulator of flagellin in *S.* Typhi called tviA represses the expression of flagellin, which reduces pyroptosis.[354] Thus, secretion of APOC3 in response to virulence factors like typhoid toxin may sensitise infected cells to inflammasome activation. However, more investigations need to be carried out.

4.5 Does the study address a role for senescence?

Our study identified 54% of toxin specific proteins in secretome-WT to be implicated in senescence as reported in the SASP Atlas (**Fig.2.12**). APOC3 is a reported SASP[219] and its expression is impaired in ageing mice.[355] Meanwhile, LYZ is not a reported SASP, but rather reported antimicrobial protein. Both proteins of interest, APOC3 and LYZ were validated in CACO-2 cells which are p53-deficient. Thus, the CACO2 model shows that APOC3/LYZ are expressed in a p53-independent manner. P53 is a major regulator of senescence.[220,321] For example, p53 activates expression of p21, which inhibits cell-cycle progression to establish senescence.[321] Thus, the use of CACO-2 cells limits our ability to assess the significance of senescence *in vitro*.

4.6 Why would *S.* Typhi encode a toxin that promotes an anti-infective response?

This PhD study proposes that toxin-induced DDRs activate release of a host secretome that contributes to the rapid elimination of WT *S.* Typhi from the bloodstream of infected participants. Why would *S.* Typhi encode a virulence factor that reduces disease? Perhaps this is not necessarily the case. The phenotype of shorter bacteraemia in response to WT *S.* Typhi could be due to the *Salmonella* disseminating from the bloodstream more

rapidly within infected mononuclear cells, i.e. exiting the bloodstream to colonise systemic sites. Indeed, the toxin promotes *Salmonella* colonisation of systemic sites in mice, e.g. liver.[139,140] However, this does not fit with reduced pathology observed in human participants with typhoid infected with WT *S.* Typhi relative to TN *S.* Typhi.[56] Similarly, mice infected with toxigenic *S.* Typhimurium^{TOX} or *S.* Javiana have reduced host pathology relative to infections with toxin-negative mutant strains.[139,140] This suggests that the toxin limits infection in some manner to reduce pathology and protect the host, perhaps through activation of DDRs as proposed in this PhD study, which may fit with the stealth strategy of *S.* Typhi.

4.7 Proposed model: Human host secretome response to bacterial toxins.

This PhD thesis shows that typhoid toxin of *S.* Typhi triggers release of a host secretome into the bloodstream in human participants with bacteraemia at the time of typhoid diagnosis. APOC3 and LYZ are both reported in the secretome which potentially play an anti-infective role via APOC3-mediated inflammasome activation and/or LYZ-mediated degradation of *Salmonella*. In doing so, this study provokes closer inspection of the significant differences observed during bacteremia in the study by Gibani et al 2019.[56] My findings may suggest that a host DDR secretome in response to typhoid toxin mediates an anti-infective response, which counters bactereamia.

4.8 Future work

In the short term, we will address the hypothesis that APOC3 can work in synergy with LYZ to exhibit bacterial killing without the need for permeabilization with EDTA, i.e. via functional overlap with APOL3 . We will perform bacterial killing assays using purified LYZ and APOC3 to answer this question. We will be investigating the role of APOC3 in inflammasome activation in *Salmonella* infection models and its possible antibacterial properties. In addition, validation infection experiments will be carried out using *S.* Typhi instead of toxigenic *S.* Javiana. *S.* Typhi infections align with the pathogen model used in the TYGER study.

In the long-term. this PhD thesis provides a standing ground for future research to aid in understanding typhoid disease mechanisms. It proposes a complex secretome is involved and thus implicates several mechanisms in typhoidal disease, DNA damage, senescence, inflammasome activation. Future investigations recommend further examining the identified secretome-WT proteins and their implication in establishing bacteraemia. Proteins identified in this study can be validated in typhoid samples from endemic settings that could also investigate the effects of *S.* Typhi during the longer duration of disease *in vivo*, for example, severe typhoid, chronic carriage. Due to the outbreaks being reported in typhoid endemic regions, case studies are being devised to further understand the disease and create a database of plasma samples of typhoid diagnosed participants.[91,356,357] These case study plasma samples can be an important tool for identifying diagnostic proteins of interest, which include those stimulated by typhoid toxin. Thus, in the long term, it is possible that host proteins in plasma may be used to establish novel diagnostics to prevent typhoid.

Chapter 5

Materials & Methods

5.1 Plasma samples preparation

Plasma samples were obtained from human participants participating in the human infection challenge study.[56] Participants plasma was collected before infection (Baseline, D0) and at time of diagnosis post infection (TD). participants were infected with the WT- *Salmonella* Typhi (WT) or toxin-mutant *Salmonella* Typhi (TN). Forty samples were provided, twenty 100μl vials at baseline and twenty100μl vials at time of diagnosis. All samples were kept anonymous, participants were distinguished with barcodes and participant numbers, shown in **Table 5.1**.

5.1.1 Ethical Approval

This project was approved by the university ethics committee under the title "Investigating the host senescence responses triggered by the typhoid toxin during acute enteric fever", reference number 041178.

5.1.2 TYGER study ethical approval

Participant recruitment and sample collection was conducted and published by our collaborators in Oxford: Project OVG2016/03[TYGER]; Research Ethics Committtee reference 16/SC/0358; clinical trials.gov Reference NCT03067961.

Downloaded: 07/07/2021
Approved: 07/07/2021

Daniel Humphreys
Biomedical Science

Dear Daniel

PROJECT TITLE: Investigating the Host Senescence Responses triggered by the Typhoid Toxin during Acute Enteric Fever
APPLICATION: Reference Number 041178

On behalf of the University ethics reviewers who reviewed your project, I am pleased to inform you that on 07/07/2021 the above-named project was **approved** on ethics grounds, on the basis that you will adhere to the following documentation that you submitted for ethics review:

- University research ethics application form 041178 (form submission date: 20/06/2021); (expected project end date: 31/12/2021).
- Participant information sheet 1093789 version 1 (20/06/2021).
- Participant consent form 1093790 version 1 (20/06/2021).

If during the course of the project you need to deviate significantly from the above-approved documentation please inform me since written approval will be required.

Your responsibilities in delivering this research project are set out at the end of this letter.

Yours sincerely

Will Collier
Ethics Administrator
Biomedical Science

Please note the following responsibilities of the researcher in delivering the research project:

- The project must abide by the University's Research Ethics Policy: https://www.sheffield.ac.uk/rs/ethicsandintegrity/ethicspolicy/approval-procedure
- The project must abide by the University's Good Research & Innovation Practices Policy: https://www.sheffield.ac.uk/polopoly_fs/1.671066!/file/GRIPPolicy.pdf
- The researcher must inform their supervisor (in the case of a student) or Ethics Administrator (in the case of a member of staff) of any significant changes to the project or the approved documentation.
- The researcher must comply with the requirements of the law and relevant guidelines relating to security and confidentiality of personal data.
- The researcher is responsible for effectively managing the data collected both during and after the end of the project in line with best practice, and any relevant legislative, regulatory or contractual requirements.

Figure 5.1: Project ethical approval.

Table 5.1: Plasma Samples and corresponding Allocations

Barcode	Participant	Visit	Allocation
HIC-vac-8183-D00-Pl-Sh1	8183	D00	TN
HIC-vac-8199-D00-Pl-Sh1	8199	D00	WT
HIC-vac-8232-D00-Pl-Sh1	8232	D00	TN
HIC-vac-8273-D00-Pl-Sh1	8273	D00	TN
HIC-vac-8352-D00-Pl-Sh1	8352	D00	WT
HIC-vac-8414-D00-Pl-Sh1	8414	D00	WT
HIC-vac-8416-D00-Pl-Sh1	8416	D00	TN
HIC-vac-8424-D00-Pl-Sh1	8424	D00	TN
HIC-vac-8428-D00-Pl-Sh1	8428	D00	WT
HIC-vac-8450-D00-Pl-Sh1	8450	D00	WT
HIC-vac-8462-D00-Pl-Sh1	8462	D00	WT
HIC-vac-8542-D00-Pl-Sh1	8542	D00	WT
HIC-vac-8582-D00-Pl-Sh1	8582	D00	WT
HIC-vac-8612-D00-Pl-Sh1	8612	D00	TN
HIC-vac-8626-D00-Pl-Sh1	8626	D00	TN
HIC-vac-8648-D00-Pl-Sh1	8648	D00	TN
HIC-vac-8678-D00-Pl-Sh1	8678	D00	TN
HIC-vac-8822-D00-Pl-Sh1	8822	D00	WT
HIC-vac-8909-D00-Pl-Sh1	8909	D00	WT
HIC-vac-8951-D00-Pl-Sh1	8951	D00	TN
HIC-vac-8183-TD-Pl-Sh1	8183	TD	TN
HIC-vac-8199-TD-Pl-Sh1	8199	TD	WT
HIC-vac-8232-TD-Pl-Sh1	8232	TD	TN
HIC-vac-8273-TD-Pl-Sh1	8273	TD	TN
HIC-vac-8352-TD-Pl-Sh1	8352	TD	WT
HIC-vac-8414-TD-Pl-Sh1	8414	TD	WT
HIC-vac-8416-TD-Pl-Sh1	8416	TD	TN
HIC-vac-8424-TD-Pl-Sh1	8424	TD	TN
HIC-vac-8428-TD-Pl-Sh1	8428	TD	WT
HIC-vac-8450-TD-Pl-Sh1	8450	TD	WT
HIC-vac-8462-TD-Pl-Sh1	8462	TD	WT
HIC-vac-8542-TD-Pl-Sh1	8542	TD	WT
HIC-vac-8582-TD-Pl-Sh1	8582	TD	WT
HIC-vac-8612-TD-Pl-Sh1	8612	TD	TN
HIC-vac-8626-TD-Pl-Sh1	8626	TD	TN
HIC-vac-8648-TD-Pl-Sh1	8648	TD	TN
HIC-vac-8678-TD-Pl-Sh1	8678	TD	TN
HIC-vac-8822-TD-Pl-Sh1	8822	TD	WT
HIC-vac-8909-TD-Pl-Sh1	8909	TD	WT

5.1.3 Protein quantification:

Samples were quantified for protein concentration using micro BCA (*Thermoscientific, Cat. no. 23235*). Plasma samples are above the micro BCA sensitivity range (0.5μg/ml to 20μg/ml), with a theoretical concentration of 60-80mg/ml. Samples were diluted 1:1000, followed by a further dilution of 1:100, for a theoretical concentration of 0.6μg/ml; which in turn brings the samples down to the BCA sensitivity range. To establish a standard curve to interpolate unknown serum protein concentration bovine serum albumin (BSA) was used. BSA standards were prepared at the following concentrations. **Table 5.2**.

Table 5.2: BSA standard concentrations

Dilution Factor	Concentration
1x	50 μg/ml
2x	25 μg/ml
4x	12.5 μg/ml
5x	10 μg/ml
10x	5 μg/ml
20x	2.5 μg/ml

BCA solution was prepared as recommended by adding components A, B and C at a ratio of 25:24:1 respectively. 500μl of BCA solution was added to 475μl of water and 25μl of prepared standard solutions. Mixture was incubated at 37°C for 1 hour. Samples change color depending on protein concentration, a darker color indicates higher protein concentration.

Sample absorbance was measured using a spectrophotometer at 562nm and correlated to the standard curve to calculate protein concentration. Standard curve and unknown interpolation was carried out using GraphPad Prism *(Prism 9 for macOS Version 9.0.2 (134))*. Plasma samples protein concentrations were then noted down as shown in Table below

Table 5.3: Plasma samples protein concentration

Participant	Visit	Allocation	Protein concentration (μg/μl)	Volume loaded to ID column (μl)
8199	D0	WT	33.37	8.99
8352	D0		54.08	5.55
8414	D0		41.37	7.25
8428	D0		24.43	12.28
8450	D0		43.89	6.83
8462	D0		38.32	7.83
8542	D0		45.92	6.53
8582	D0		26.68	11.24
8822	D0		36.20	8.29
8909	D0		44.40	6.76
8199	TD		13.50	22.22
8352	TD		10.60	28.30
8414	TD		17.40	17.24
8428	TD		10.60	28.30
8450	TD		10.90	27.52
8462	TD		20.70	14.49
8542	TD		13.60	22.06
8582	TD		11.70	25.64
8822	TD		28.30	10.60
8909	TD		16.60	18.07
8183	D0	TN	32.90	9.12
8232	D0		22.08	13.59
8273	D0		53.14	5.65
8416	D0		30.55	9.82
8424	D0		26.78	11.20
8612	D0		36.20	8.29
8626	D0		27.73	10.82
8648	D0		25.84	11.61
8678	D0		33.84	8.86
8951	D0		30.55	9.82
8183	TD		17.20	17.44
8232	TD		14.80	20.27
8273	TD		23.40	12.82
8416	TD		17.70	16.95
8424	TD		13.60	22.06
8612	TD		14.40	20.83
8626	TD		12.30	24.39
8648	TD		24.40	12.30
8678	TD		16.00	18.75
8951	TD		15.60	19.23

5.1.4 Immunodepletion column

One of the biggest challenges facing proteomic analysis on plasma is the high abundance of specific proteins, for example, albumin on its own makes up about 55% of total plasma concentration. To tackle this obstacle, immunodepletion columns are employed to remove abundant proteins and allow for detecting lower abundance proteins that are of more interest.

Immunodepletion columns use affinity chromatography to remove the most abundant proteins from plasma. Multiple Affinity Removal Column Human-14 (MARS-14) (*Agilant; 5188-6559*) is designed to remove the 14 most abundant proteins in human plasma (albumin, IgG, antitrypsin, IgA, transferrin, haptoglobin, fibrinogen, α2-macroglobulin, α1-acid glycoprotein, IgM, apolipoprotein AI, apolipoprotein AII, complement C3 and transthyretin) which make up 94% of overall protein concentration.

Total Protein concentration was calculated by micro BCA interpolation using GraphPad Prism and samples were diluted to 300μg per 200μls of Buffer A (1.5μg/μl). Diluted plasma was passed through the column by manual injection gently without induction of bubbles or exerting excess force, that would rupture the column. Spin sample down at 1300 rpm for 5minutes to remove any particulates.

Dilute 8μL (or appropriate volume based on concentration) of plasma into 192μL Buffer A (proprietary solution). Spin at 1300 rpm for 5 minutes to remove particulates.Prepare Agilent spin cartridge by removing cartridge cap and dispensing with storage Buffer. Add 200 μL of diluted serum/plasma sample to spin cartridge and centrifuge for 1 minute at 100×g. Wash Agilent spin cartridge. Add 400 μL of Buffer A and centrifuge for 1 minute at 100×g. Collect Flow-Through containing low-abundant proteins for mass spec analysis (tube F1). Repeat wash Step in new tube. Collect Flow-Through containing low-abundant proteins for mass spectrometry analysis (tube F2). Elute high-abundant proteins from Agilent spin cartridges. Syringe 5ml of Buffer B through column and collect flow through in 15ml tube containing high-abundant proteins. Combine tubes F1 and F2 (F12). Fractions contain low-abundant proteins. To Re-equilibrate cartridge, syringe 5ml of Buffer A through column and collect waste flow through. Cartridge is ready to re-use.

5.1.5 Acetone precipitation of protein and inactivation of *Salmonella*

Cool the required volume of acetone to -20°C. Prepare F12 fraction (∼800μL) from immunodepletion column into acetone compatible tube (15ml falcon). Acetone precipitate by adding four times the sample volume of cold (-20°C) acetone to the tube. Mix by inverting the tube gently and incubate overnight at 20°C. The contents of the tube are now precipitated/inactivated. Samples can now be moved to Class 1 laboratory. Harvest

precipitated proteins by centrifugation for 10 minutes at 13000-15000×g at 4°C. Decant acetone supernatant carefully to avoid disrupting the precipitated protein pellet. Air dry protein pellet by allowing it to evaporate from the uncapped tube at room temperature for about 30minutes, avoid over-drying (pellet will be hard to resuspend if it overdrive). Resuspend dried pellet in 50ul of S-Trap solubilization buffer (5% SDS (*Cat.no. 05030-500ML-F*), 5mM Triethylammonium Bicarbonate Buffer (TEAB) buffer (*Cat.no. 90114*), pH 7.55) and store dried samples at -20°C.

5.1.6 Protein digestion by S-Trap

Samples in S-Trap solubilization buffer were reduced with 2μl Tris(2-carboxyethyl)phosphine hydrochloride (TCEP) (*Cat.no. 646547-10X1ML*) (0.5M) and heated at 70°C for 15 minutes. Next, it was cooled down for 5minutes at room temperature. Alkylate samples by adding twice the concentration of iodoacetamide (*Cat. no. I6125*) (to prevent reformation of disulfide bonds). Make up 0.5M iodoacetamide by weighing 0.09248g in 1ml of HPLC water (*Cat.no. W6-1*) and store away from light (must be made fresh). Pipette 4μl of 0.5M Iodoacetamide to sample. Keep in the dark for 30 minutes at room temperature.

Add 2.5μl of 12% phosphoric acid (*Cat. no. A242- 500*)to SDS lysate sample, to a final concentration of 1.2% phosphoric acid. Prepare S-Trap binding buffer (90% aqueous methanol (*900688-1L*), 0.1M TEAB, pH 7.1) and add 165μl to 25μl of sample lysate. Prepare S-Trap columns for elution by adding S-Trap columns (*Cat.no. C02-micro-80*) in 2ml eppendorfs.

Spin down sample lysates to ensure there is no condensation. Load 150μl of sample at a time to the S-Trap column avoiding poking white material at the bottom of column. Spin for 10 seconds at 4000×g at room temperature. Repeat the process until the sample is spun down. After two collections change the eppendorfs. Wash 3× with S-trap binding buffer (150μl per wash). Move the S-trap column to a clean 2ml eppendorf.

5.1.7 Trypsinization (Digestion)

Prepare trypsin (*Cat.no. 90058*) stock at 1μg/μl of 0.1% Trifluoroacetic acid (TFA) (*Cat.no. 108262*). Trypsin is added at 1μg per 10μg per protein, 1:10 w/w. Each sample has about 50μg proteins so 5μg per sample, therefore 5μl per sample. Add 5μl of 1μg/μl Trypsin to 25μl TEAB buffer and apply to S-Trap columns, avoiding air bubbles. Seal S-Traps with parafilm and incubate for 1 hour at 47∘C without any shaking. Elute digested proteins by adding, 40μl of 50mM TEAB and centrifuge at 4000×g for 10 seconds. Next, add 40μl of 0.2% aqueous formic acid, centrifuge at 4000 xg for 10 seconds. Finally, add 40% of 50% ACN containing 0.2% aqueous formic acid (*Cat.no. A117-50*) centrifuge at 4000×g for 10 seconds. Store at -20°C until ready for drying.

5.1.8 Sample drying

Samples were centrifuged in 1.5ml eppendorfs (with lids left open to allow evaporation) at 45°C for 90 minutes in a vacuum setting. Once dried, samples were resuspended in 0.5% formic acid. Samples were then moved to polypropylene vials (*Thermo Scientific, 160134*), labelled and injected in the Orbitrap.

5.2 Mass Spectrometry Analysis

5.2.1 LC-MS/MS analysis

18 μl per sample was analysed by nanoflow LC-MS/MS using an Orbitrap Elite (Thermo Fisher) hybrid mass spectrometer equipped with an easyspray source, coupled to an Ultimate RSLCnano LC System (Dionex). Xcalibur 3.0.63 (Thermo Fisher) and DCMSLink (Dionex) controlled the system. Peptides were desalted on-line using an Acclaim PepMap 100 C18 nano/capillary BioLC, 100A nanoViper 20 mm x 75 μm I.D. particle size 3 μm (Fisher Scientific) followed by separation using a 125-min gradient from 5 to 35% buffer B (0.5% formic acid in 80% acetonitrile) on an EASY-Spray column, 50 cm $\times$ 50 μm ID, PepMap C18, 2 μm particles, 100 Å pore size (Fisher Scientific). The Orbitrap Elite was operated with a cycle of one MS (in the Orbitrap) acquired at a resolution of 60,000 at m/z 400, with the top 20 most abundant multiply charged (2+ and higher) ions in a given chromatographic window subjected to MS/MS fragmentation in the linear ion trap. An FTMS target value of 1e6 and an ion trap MSn target value of 1e4 were used with the lock mass (445.120025) enabled. Maximum FTMS scan accumulation time of 500 ms and maximum ion trap MSn scan accumulation time of 100 ms were used. Dynamic exclusion was enabled with a repeat duration of 45 s with an exclusion list of 500 and an exclusion duration of 30 s.

5.2.2 MaxQuant Analysis

All raw mass spectrometry data were analysed with MaxQuant version 1.6.10.43. Data were searched against a human UniProt sequence database (May 2019) using the following search parameters: digestion set to Trypsin/P with a maximum of 2 missed cleavages, methionine oxidation and N-terminal protein acetylation as variable modifications, cysteine carbamidomethylation as a fixed modification, match between runs enabled with a match time window of 0.7 min and a 20-min alignment time window, label-free quantification enabled with a minimum ratio count of 2, minimum number of neighbours of 3 and an average number of neighbours of 6. A first search precursor tolerance of 20ppm and a main search precursor tolerance of 4.5 ppm was used for FTMS scans and a 0.5 Da tolerance for ITMS scans. A protein FDR of 0.01 and a peptide FDR of 0.01 were used for identification level cut-offs.

5.2.3 Perseus Bioinformatic Analysis

There is variation between plasma samples, due to the fundamental variation between human beings. The participants were not of similar age, but rather a spectrum of age between 18-60 years old. They were not given the same diet and there were several uncontrolled factors. This further incriminated the variation between every volunteer. Each post-infection sample (TD) was normalised to its respective pre-infection baseline (D0).

MaxQuant data output was loaded into perseus version 1.6.10.50 and all LFQ intensities were set as main columns. The Matrix was filtered removing any contaminants, identified by site and reverse sequences. LFQ intesnities were trasformed using Log2(x) default function. Rows were then filtered with a minimum value of 5 in each group only showing the default valid values. Data was visualized using Pearson correlation values and outliers omitted. Sample 8183 D0 was excluded from analysis using subtract function due to inconsistent Pearson correlation value. Missing values were then replaces with a width of 0.3 and down shift 1.8. Samples where then compared two at a time with D0 and TD of respective groups using studet t-test with permutation-based FDR calculation (FDR = 0.05) with an (S0) =0.1. Data was then exported to Microsoft excel and Graphpad prism and made into the figures discussed in Chapter 2. Raw data files can be found in this link: https://figshare.com/s/5bbfac2d2db54dc000d9.

5.3 Cell Culture

5.3.1 Cell maintenance

Cells were stored in cryopreservative media (10% DMSO (*Sigma-Aldrich, D2438*) and 90% complete media) at -80°C until they are revived in culture. Frozen cells are thawed in water-bath for 90 seconds and cultured in respective complete media. Table X summarises media composition and cell origins. Cells were maintained in a 37^{o}C humidified incubator with 5%CO2. Cells were passaged every 3 to 5 days depending on their doubling time. Trypsin (*Sigma Aldrich, T4049*) was used to detach adherent cells followed by neutralisation with FBS (*Sigma Aldrich, F7524*) containing media. Suspension cells were cultured in suspension and do not require the trypsin step. To ensure seeding cells are alive, 10μl of cell suspension is stained with trypan blue (*Sigma-Aldrich, T8154*) in 1:1 dilution, followed by cell counting of trypan blue negative cells.

Table 5.4: Cell culture media composition for each cell line

Cell	Origin	Media	Supplements**	Doubling Time
IMR90	Lungs of a 16-week female foetus.	Minimum Eagle Media (MEM)	15% FBS	∼30-40 hours
THP1	Acute monocytic leukaemia cells	RPMI-1640	10% FBS Serum	∼26 hours
CACO2	Colorectal adenocarcinoma cells	Gibco Dulbecco's Modified Eagle Medium (DMEM)	10% FBS	∼32 hours

*Added in maintenance culture only

**All media included PenStrep and Kanamycin antibiotics except in indicated antibiotic-free (Ab-free) media used for infections.

Table 5.5: Catalgue numbers of each media

Media	Company	Catalogue Number
MEM	ThermoFisher	32561037
RPMI-1640	ThermoFisher	R8758-500ML
DMEM	ThermoFisher	31966021

5.3.2 Cell counting

Cells were counted using a manual hemocytometer. Four replicates of cell counts were collected and averaged to minimise human errors. After detachment with Trypsin (*ThermoFisher T4049*) and incubation with Trypan Blue, 10μl of cells:trypan blue are added in a glass haemocytometer (*Hawksley, AC1000*). The haemocytometer comprises 4 chambers, trypan blue negative cells of each chamber are counted and halved.

$$No.of cells/ml = \frac{a+b+c+d}{2} \times 10^4$$

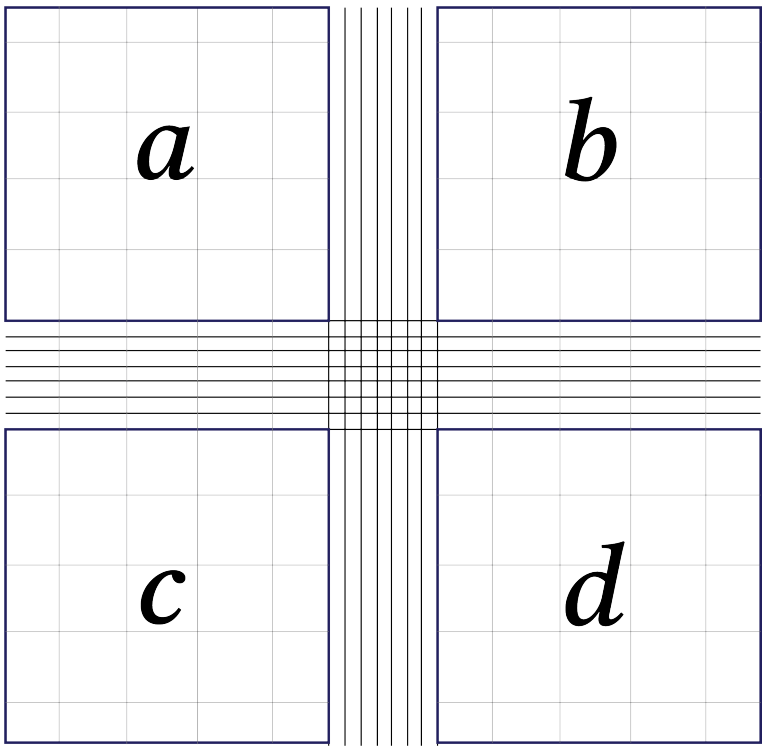

Figure 5.2: Hematocytometer organization and cell counting.

The volume of cell suspension needed to be diluted in the media for seeding was calculated as follows:

$$No.of cells/ml = \frac{\text{Number of cells to be seeded}}{\text{Counted number of cells/ml}}$$

Before seeding, glass coverslips (*VWR, 631-1578*) are added into cell culture wells for adherent cell lines. The calculated volume then is then diluted in enough complete growth media to be divided across the required number of culture plate wells.

5.3.3 Monocyte differentiation

THP1s are monocytes in suspension that can be differentiated into macrophages using Phorbol 12-myristate 13-acetate (PMA) (*Sigma-Aldrich, P8139*). PMA is added at 100ng/ml for 72 hours to ensure adherence and differentiation into M0 macrophages.

5.3.4 Intoxication

Toxin Purification

The typhoid toxin was purified by my PhD supervisor Dr. Daniel Humphreys from BL21 DE3 pETDuet-1 encoding pltB^{His} pltA^{Myc} and cdtB^{FLAG} using NiNTA agarose (Qiagen) affinity chromatography according to manufacturer instructions as previously in Ibler *et. al.*, 2019.[226] In brief, recombinant typhoid toxin was expressed from pETDuet-1 overnight in E.coli BL21 DE3 (69450, Merck Millipore) at 30°C following addition of 0.1

mM Isopropyl β-D-1-thiogalactopyranoside (Sigma- Aldrich). E.coli were harvested by centrifugation for 10 mins at 6000RCF and resuspended in lysis buffer containing 20 mM Tris-HCl, pH 8.0, 100 mM NaCl, 1 mM $MgCl_2$ (Sigma-Aldrich) and complete EDTA-free protease inhibitor cocktail (Roche) then lysed by passage through a Cell Disrupter at 30kPSI (Constant systems Ltd). The His-tagged PltB subunit was used to immobilise typhoid toxin on Ni-NTA agarose (Qiagen) and purify the toxin from the lysate using via affinity chromatography according to manufacturer instructions. The toxin was stored at 80°C in lysis buffer supplemented with 20% glycerol.

Toxin dilution

Previously purified toxin in Humphreys lab was used at 20ng/ml unless otherwise indicated.

Intoxication procedure

Cells were seeded overnight before intoxication, to allow for adherence of adherent cell lines. Growth media was aspirated off and replaced with media supplemented with toxin for 2 hours pulse, followed by three washes with sterile PBS (*Sigma-Aldrich, J60801.K3*) to remove any toxin, and chased in fresh complete media in Table 5.4 till the end of the experimental duration.

Caffeine treatment

Cells were seeded overnight as previously discussed. On the day of intoxication, cells are incubated with 10mM of caffeine for 30minutes before intoxication. Cells are then intoxicated with the WT toxin, as discussed above, or treated with Etoposide 10μM for 24 hours (topoisomerase inhibitor, Cayman Chemicals (12092)). Cells are fixed at 48 hours and prepared for staining.

5.3.5 Infection

Infection protocol

Cells were seeded overnight before infection, as described above. Meanwhile, *Salmonella* was grown overnight by collecting an inoculum of a colony in a streaked plate and resuspending it in LB agar with the appropriate antibiotic. Overnight culture is then diluted in 1:100 and left to grow till normalised OD600 1.0. *Salmonella* strains used were diluted to the required multiplicity of infection (MOI) and added to cells for 30 minutes. Gentamicin was then incubated at 50 μg/ml to eliminate extracellular bacteria for 90 minutes, then followed by a lower gentamicin concentration of 10μg/ml for the remaining duration of the experiment.

Bacterial strains used

Bacterial strains contain the pM975 plasmid which encode a green fluorescent protein (GFP). pM975 is encoded in the SPI-2 pathogenicity island thus only expressed when the *Salmonella* is inside the cell. Wild-Type (WT) strains express the typhoid toxin, while the ΔCdtB strain expresses the ΔCdtB null toxin.

Table 5.6: Bacterial strains used

Strain	Resistance
S. Javiana WT + pM975	Amp
S. Javiana Δ CdtB + pM975	Amp

Multiplicity of infection (MOI)

The number of bacteria in OD600 1.0 is estimated to be 8x108 bacteria per ml. As previously discussed OD600 was normalised to 1.0, to calculate MOI the following equation was used:

$$MOI = \frac{\text{Volume of Media x } (8 \text{ x } 10^4)}{\text{CNumber of seeded cells}}$$

5.3.6 Cell culture analysis

Conditioned media collection

Conditioned media was collected from treated cells at the end of the duration of the experiment. Using stripettes media was aspirated from cells into falcon tubes. Conditioned media was centrifuged at 6000 x g for 5minutes to pellet any floating cells. The supernatant is collected avoiding disrupting any formed pellet and passed through a sterile 0.2μm filter. Both techniques ensure conditioned media represents external proteins secreted off cells in response to treatment. Centrifugation removed floating cells that could be burst open in the filtration process which in turn would release internalised proteins into the conditioned media. Meanwhile filtration further removed any remaining cells in the media.

Fixation

Following conditioned media removal, cells are washed off three times with PBS, and 4% Paraformaldehyde (PFA) (*ThermoFisher, J61899*) was added for 10-15minutes. PFA was washed off three times with PBS and fixed cells on coverslips were stored at 4^{o}C until the start of immunostaining protocol.

EdU staining

Click-iT EdU Cell Proliferation Kit for Imaging, Alexa Fluor 647 dye (*Thermofisher, C10340*) was used as per manufacturer's instructions. EdU was added 24 hours before fixation. The incubation time was decided based on the average doubling time of all cells used, which was about 28 hours.

CellEvent Senescence associated β-Galactosidase Green detection Kit

CellEvent Senescence Green detection kit (Invitrogen, C10851) was used according to manufacturer's instructions. After fixation, samples were washed with 1% BSA (*Sigma-Aldrich, 3117332001*)in PBS to remove PFA. Next, staining solution is made up of a 1:1000 dilution of CellEvent senescence Green Probe and CellEvent senescence Buffer, respectively. Staining solution is added to samples for 2 hours in a 37^{o}C incubator without CO2 for 2hours. Following incubation, cells are washed with PBS twice before staining with immunostaining protocol.

Immunostaining

Samples in PBS are washed off and incubated with 3%BSA in 0.2%Triton X-100 in PBS (blocking solution) for 1 hour at room temperature. Samples are then incubated with primary antibody diluted appropriately in blocking solution, details in Table 5.7 for 1 hour at room temperature. Primary antibody is washed off with PBS. Secondary antibody is diluted 1:500 in 0.2% Triton X-100 in PBS for 30minutes at room temperature. Samples were then counterstained with DAPI (6μg/ml) in Triton X-100 in PBS. Samples were washed off in PBS, then water to remove any salt and avoid crystal formation, and left to dry for a minimum of 30 minutes. Coverslips were then mounted with VectaShield mounting agent (Vector Lab, H1200) and sealed with nail polish. Coverslips were imaged on the Nikon Widefield microscope.

Table 5.7: Primary antibodies Used

Antibody	Species	Dilution	Product code
γH2AX	Mouse monoclonal	1:1000	Merck/Sigma, 05-636
APOC3	Rabbit polyclonal	1:250	GeneTex, GTX129994
LYZ	Mouse polyclonal	1:250	ThermoFisher, MA1-82873
Anti-*Salmonella*	Rabbit polyclonal	1:1000	Abcam, ab35156

Table 5.8: Secondary antibodies Used

Antibody	Species	Dilution	Product code
594 Alexa Fluorophore	Donkey*anti-ms	1:500	Life Technologies, A21203
568 Alexa Fluorophore	Donkey**anti-Rb	1:500	Life Technologies, A11036
488 Alexa Fluorophore	Donkey*anti-ms	1:500	Invitrogen, A21202
488 Alexa Fluorophore	Goat**anti-Rb	1:500	Invitrogen, A11008

*Anti-ms (anti-mouse); **Anti-Rb (anti-Rabbit)

Live-Dead Assay

Live cells have ubiquitous intracellular esterase activity which can be determined by the enzymatic conversion of cell-permeant calcein AM (non-fluorescent) to calcein (intensely fluorescent). Calcein is a well retained polyanionic dye within live cells with excitation/emission ∼495nm/∼515nm (Green). Meanwhile, ethidium homodimer-1 (EthD-1) enters cells through damaged membranes and is excluded by the intact membrane of live cells, where it binds to nucleic acids which causes 40-fold enhancement in fluorescence upon binding. This produces a bright red fluorescence in dead cells with excitation/emission ∼495nm/∼635nm (Red).

Flow cytometry

Cells are collected in 1ml suspension, or scrapped and left in suspension (for adherent cells). Calcein is prepared at a 50μM working concentration. Ethidium homodimer-1 is at a working concentration of 2mM. Cells are washed off in PBS once and resuspended in 1ml PBS. Calcein and EthD-1 are added 2μl and 4μl respectively in 1ml. Sample is mixed thoroughly and incubated for 15-20minutes at room temperature away from light. Samples were analyzed within 1 hour using FACSCalibur Flow Cytometer (Beckman Coulter) with excitation wavelength of 488 nm for calcein and red fluorescence emission for EthD-1. Analysis was performed with FlowJo R Software. Data was gated for the right cell size based on the population with SSC and FSC. Flow cytometry technicians provided us with a pdf of the analysis, then we took the percentage of live and dead cells based on the gating and presented it in GraphPad prism where we performed the statistically analysis.

ELISA - Enzyme linked immunoassays

Protocols were followed as per manufacturer's instructions. Conditioned media was serially diluted with a factor of 5 to ensure efficient sensitivity.

Table 5.9: ELISA Kits used

ELISA Kit	Catalogue number
APOC3 Human ELISA Kit	ThermoFischer, EHAPOC3
Human LYZ ELISA Kit	Abcam, ab108880

5.4 Bacterial Killing Assay

5.4.1 Outer membrane permeabilization

Transient permeabilization of the outer membrane (OM) was adapted from Gaudet, et al., 2021[294] where they used EDTA to destabilise the LPS. Bacterial cultures were grown overnight, followed by culturing them to OD600 = 0.5 in LB Broth supplied with 2mM $CaCl_2$ and 2mM $MgCl_2$. After bacterial culture reaches the required OD, it is washed twice in 0.1M Tris-HCl pH 8.0 in 0.75M sucrose. It is then spun down at 13000 rpm for 1 minute, the supernatant is removed and the pellet is resuspended in 350μl of 0.1M Tris-HCl 0.75M sucrose pH 8.0 Buffer and 700μl of 1mM EDTA in H2O were added for 20minutes at RT. Following incubation, 50μl of 0.5M MgCl2 were added on ice for 5 minutes and bacteria was spun down for 1minute at 13000 rpm. Bacteria was then resuspended in 50mM MES pH 6.0 in 100mM potassium gluconate (KGl).

5.4.2 Colony forming unit (CFU) count

Bacteria was serially diluted and 5μl of bacterial suspension was spotted on antibiotic resistant Agar plates. Colonies were incubated on Agar plates at 37°C overnight and counted the following morning. Counting was performed on 30 colonies or less. No more than 30 colonies were counted to avoid human error.

5.4.3 Plate reader OD measurement

Sunrise ™ absorbance reader (Tecan, 30190079) was used to measure OD600 of bacterial culture at 37^{o}C treated with several treatments. Bacteria was initially grown overnight then inoculated for a day culture to a pre-logarithmic phase, OD600 0.5-0.8. Bacteria is then pelleted and diluted to OD600 0.1 in complete media supplemented with 100mM HEPES. HEPES ensures pH maintenance. Diluted bacteria is plated in a flat bottom 96-well plate (Corning, 3595) and incubated with respective treatment. Absorbance reader was set to measure OD600 every 30minutes at 37°^{o}C with occasional shaking.

Hidex Sense plate reader was used as an alternative to measure OD600 of bacterial culture at the same conditions as that used for the Tecan plate reader. 96 well plate covers were treated with 0.2% triton in 50% methanol to avoid perspiration. Plates were then incubated for 24 hours inside the Hidex plate reader.

5.5 Microscopy

5.5.1 Nikon Wide-field Live-cell system

Samples were fixed and stained on 13mm coverslips and mounted on glass slides as described. Samples were imaged on Nikon's Inverted Ti eclipse equipped with an Andor Zyla sCMOS camera (2560 x 2160; 6.5μm pixels). The microscope is equipped with 6 objective lens, Plan Apo 10x (NA 0.45); Plan Apo 20x (NA 0.75); Plan Fluor 40x oil (NA 1.3); Apo 60x oil (NA 1.4); Plan Apo 100x Ph oil (Na 1.45); Plan Apo VC 100x oil (NA 1.4). Images were captured using Plan Apo 20x lens randomly through the entire coverslip for quantitative analysis performed by cell profiler. Plan Fluor 40x oil lens was used for high resolution qualitative representative images carrried out in Fiji. Quad emission filters were used with SpectraX excitation, 395nm for blue, 470nm for green, 561nm for red and 640nm for far red.

5.5.2 Microscope image processing

For qualitative purposes images were processed using fiji 2.0.0-rc-69/1.52p, with a macro code created by Dr. Mohamed ElGhazaly to automate image processing. The macro code adjusts brightness and contrast and is normalised across all images. DAPI nuclei are outlined and overlapped with other channels and the images are then saved as a png file.

5.5.3 Cell Profiler image quantification

Cell profiler pipeline was created by Dr. Mohamed El Ghazaly to identify nuclei and quantify the intensity of signals per nuclei. Further pipelines were adjusted from the original pipeline to cater for more experiments.

5.6 Statistical Analysis

Statistical analysis was carried out by Graphpad Prism 9 version 9.0.2. Most analysis are t-test or ANOVA as indicated in figure legends. The significance is represented using *, $p < 0.05$ (*), $p < 0.01$(**), $p < 0.001$ (***), and $p < 0.0001$(****).

5.7 Figures and illustrations

All figures and schematics were done on Adobe Illustrator version 25.4.1, unless otherwise stated in the figure and figure legend.

Bibliography

[1] Rodolfo Notario, Noemi Borda, Telma Gambande, and Emma Sutich. Species and serovars of enteropathogenic agents associated with acute diarrheal disease in Rosario, Argentina. *Revista do Instituto de Medicina Tropical de Sao Paulo*, 38(1):5–7, 1996.

[2] I A Mikhail, E Fox, R L Haberberger, M H Ahmed, and E A Abbatte. Epidemiology of bacterial pathogens associated with infectious diarrhea in Djibouti. *Journal of clinical microbiology*, 28(5):956–961, 1990.

[3] M. K. Bhan, Rajiv Bahl, and Shinjini Bhatnagar. Typhoid and paratyphoid fever. *Lancet (London, England)*, 366(9487):749–762, 8 2005.

[4] Hongwei Shen, Jinjin Zhang, Yinghui Li, Sirou Xie, Yixiang Jiang, Yanjie Wu, Yuhui Ye, Hong Yang, Haolian Mo, Chaoman Situ, and Qinghua Hu. The 12 gastrointestinal pathogens spectrum of acute infectious diarrhea in a sentinel hospital, Shenzhen, China. *Frontiers in Microbiology*, 7(NOV):1926, 11 2016.

[5] Amir Saeed, Hadi Abd, and Gunnar Sandstrom. Microbial aetiology of acute diarrhoea in children under five years of age in Khartoum, Sudan. *Journal of Medical Microbiology*, 64(Pt 4):432, 2015.

[6] Isidore Juste O Bonkoungou, Kaisa Haukka, Monica Österblad, Antti J Hakanen, Alfred S Traoré, Nicolas Barro, and Anja Siitonen. Bacterial and viral etiology of childhood diarrhea in Ouagadougou, Burkina Faso. *BMC Pediatrics*, 13(1):1–6, 3 2013.

[7] Lin Hui Su, Cheng Hsun Chiu, Chishih Chu, and Jonathan T Ou. Antimicrobial resistance in nontyphoid Salmonella serotypes: A global challenge. *Clinical Infectious Diseases*, 39(4):546–551, 8 2004.

[8] Martine Guibourdenche, Peter Roggentin, Matthew Mikoleit, Patricia I. Fields, Jochen Bockemühl, Patrick A.D. Grimont, and François Xavier Weill. Supplement 2003-2007 (No. 47) to the White-Kauffmann-Le Minor scheme. *Research in Microbiology*, 161(1):26–29, 1 2010.

[9] Marie A. Chattaway, Gemma C. Langridge, and John Wain. Salmonella nomenclature in the genomic era: a time for change. *Scientific reports*, 11(1), 12 2021.

[10] Mark P Stevens, Tom J Humphrey, and Duncan J Maskell. Molecular insights into farm animal and zoonotic Salmonella infections. *Philosophical Transactions of the Royal Society B: Biological Sciences*, 364(1530):2708–2723, 9 2009.

[11] Bryan Coburn, Guntram A. Grassl, and B. B. Finlay. Salmonella, the host and disease: A brief review. *Immunology and Cell Biology*, 85(2):112–118, 2 2007.

[12] Nicholas A. Feasey, Gordon Dougan, Robert A. Kingsley, Robert S. Heyderman, and Melita A. Gordon. Invasive non-typhoidal salmonella disease: an emerging and neglected tropical disease in Africa. *The Lancet*, 379(9835):2489–2499, 6 2012.

[13] Arie H Havelaar, Martyn D Kirk, Paul R Torgerson, Herman J Gibb, Tine Hald, Robin J Lake, Nicolas Praet, David C Bellinger, Nilanthi R de Silva, Neyla Gargouri, Niko Speybroeck, Amy Cawthorne, Colin Mathers, Claudia Stein, Frederick J Angulo, Brecht Devleesschauwer, Gabriel O Adegoke, Reza Afshari, Deena Alasfoor, Janis Baines, Kalpana Balakrishnan, Wan Mansor Bin Hamza, Robert E Black, P Michael Bolger, Wanpen Chaicumpa, Alejandro Cravioto, Dörte Döpfer, John E Ehiri, Aamir Fazil, Catterina Ferreccio, Eric M Fèvre, Gillian Hall, Fumiko Kasuga, Karen H Keddy, Claudio F Lanata, Haicho Lei, Xiumei Liu, Ben Manyindo, George Nasinyama, Pierre Ongolo-Zogo, John I Pitt, Mohammad B Rokni, Banchob Sripa, Rolaf van Leeuwen, Philippe Verger, Arve Lee Willingham, Xiao Nong Zhou, Willy Aspinall, Robert Buchanan, Christine Budke, Marisa L Caipo, Hélène Carabin, Dana Cole, Roger M Cooke, John A Crump, Fadi El-Jardali, Christa Fischer-Walker, Thomas Fürst, Juanita A Haagsma, Aron J Hall, Olga Henao, Sandra Hoffmann, Helen Jensen, Nasreen Jessani, Marion P G Koopmans, Myron M Levine, Charline Maertens de Noordhout, Shannon Majowicz, Scott A McDonald, Sara Pires, Elaine Scallan, Banchob Sripa, M Kate Thomas, Linda Verhoef, Felicia Wu, and Marco Zeilmaker. World Health Organization Global Estimates and Regional Comparisons of the Burden of Foodborne Disease in 2010. *PLoS Medicine*, 12(12), 2015.

[14] European Food Safety Authority, , and European Centre for Disease Prevention Control. The European Union summary report on trends and sources of zoonoses, zoonotic agents and food-borne outbreaks in 2016. *EFSA Journal*, 15(12), 12 2017.

[15] Johanna L Leinert, Stefan Weichert, Alexander J Jordan, and Rüdiger Adam. Non-Typhoidal Salmonella Infection in Children: Influence of Antibiotic Therapy on Post-convalescent Excretion and Clinical Course-A Systematic Review. *Antibiotics (Basel, Switzerland)*, 10(10), 9 2021.

[16] D W Day, B K Mandal, and B C Morson. The rectal biopsy appearances in Salmonella colitis. *Histopathology*, 2(2):117–131, 1978.

[17] Hung Ming Chen, Yue Wang, Lin Hui Su, and Cheng Hsun Chiu. Nontyphoid Salmonella infection: Microbiology, clinical features, and antimicrobial therapy. *Pediatrics and Neonatology*, 54(3):147–152, 6 2013.

[18] A. Marijke Keestra-Gounder, Renée M. Tsolis, and Andreas J. Bäumler. Now you see me, now you don't: the interaction of Salmonella with innate immune receptors. *Nature Reviews Microbiology*, 13(4):206–216, 3 2015.

[19] Calman A MacLennan. Out of Africa: links between invasive nontyphoidal Salmonella disease, typhoid fever, and malaria. *Clinical infectious diseases : an official publication of the Infectious Diseases Society of America*, 58(5):648–650, 3 2014.

[20] R. K. Selander, P. Beltran, N. H. Smith, R. Helmuth, F. A. Rubin, D. J. Kopecko, K. Ferris, B. D. Tall, A. Cravioto, and J. M. Musser. Evolutionary genetic relationships of clones of Salmonella serovars that cause human typhoid and other enteric fevers. *Infection and Immunity*, 58(7):2262–2275, 1990.

[21] Christopher M. Parry, Tran Tinh Hien, Gordon Dougan, Nicholas J. White, and Jeremy J. Farrar. Typhoid Fever. *New England Journal of Medicine*, 347(22):1770–1782, 11 2002.

[22] Sean-Paul Nuccio and Andreas J. Bäumler. Evolution of the Chaperone/Usher Assembly Pathway: Fimbrial Classification Goes Greek. *Microbiology and Molecular Biology Reviews*, 71(4):551–575, 12 2007.

[23] Yasuhiro Hashimoto, Takayuki Ezaki, Na Li, and Hiroyuki Yamamoto. Molecular cloning of the ViaB region of Salmonella typhi. *FEMS microbiology letters*, 69(1):53–56, 12 1991.

[24] WHO — Typhoid Fever. *WHO*, 2018.

[25] R. Leon Ochiai, Xuanyi Wang, Lorenz Von Seidlein, Jin Yang, Zulfiqar A. Bhutta, Sojit K. Bhattacharya, Magdarina Agtini, Jacqueline L. Deen, John Wain, Deok Ryun Kim, Mohammad Ali, Camilo J. Acosta, Luis Jodar, and John D. Clemens. Salmonella paratyphi A rates, Asia. *Emerging Infectious Diseases*, 11(11):1764–1766, 2005.

[26] Eyal Meltzer and Eli Schwartz. Enteric fever: A travel medicine oriented view. *Current Opinion in Infectious Diseases*, 23(5):432–437, 10 2010.

[27] S. J. Olsen, S. C. Bleasdale, A. R. Magnano, C. Landrigan, B. H. Holland, R. V. Tauxe, E. D. Mintz, and S. Luby. Outbreaks of typhoid fever in the United States, 1960-99. *Epidemiology and Infection*, 130(1):13, 2 2003.

[28] Ohad Gal-Mor. Persistent Infection and Long-Term Carriage of Typhoidal and Nontyphoidal Salmonellae. 2018.

[29] Albert M. Vollaard, Soegianto Ali, Henri A.G.H. Van Asten, Suwandhi Widjaja, Leo G. Visser, Charles Surjadi, and Jaap T. Van Dissel. Risk factors for typhoid and paratyphoid fever in Jakarta, Indonesia. *Journal of the American Medical Association*, 291(21):2607–2615, 6 2004.

[30] Claire S Waddington, Thomas C Darton, and Andrew J Pollard. The challenge of enteric fever. *The Journal of infection*, 68 Suppl 1(SUPPL1), 1 2014.

[31] Asma Azmatullah, Farah Naz Qamar, Durrane Thaver, Anita K M Zaidi, and Zulfiqar A Bhutta. Systematic review of the global epidemiology, clinical and laboratory profile of enteric fever. *Journal of Global Health*, 5(2), 2015.

[32] Myron M. Levine, Robert E. Black, and Claudio Lanata. Precise estimation of the numbers of chronic carriers of salmonella typhi in santiago, chile, an endemic area. *Journal of Infectious Diseases*, 146(6):724–726, 1982.

[33] J. Brooks. The sad and tragic life of Typhoid Mary. *CMAJ: Canadian Medical Association Journal*, 154(6):915, 3 1996.

[34] Mary Mallon (Typhoid Mary). *American journal of public health and the nation's health*, 29(1):66–68, 1 1939.

[35] P. P. Mortimer. Mr N the milker, and Dr Koch's concept of the healthy carrier. *Lancet (London, England)*, 353(9161):1354–1356, 1999.

[36] Brock, Thomas D. (1988): Robert Koch. A Life in Medicine and Bacteriology: In: Scientific Revolutionaries: A Biographical Series. Science Tech. Publishers, Madison WI and J. Springer, Berlin, 364 pp., hard cover, 48 - DM. *European journal of protistology*, 25(1):85, 9 1989.

[37] D. S. Buchwald and M. J. Blaser. A review of human salmonellosis: II. Duration of excretion following infection with nontyphi Salmonella. *Reviews of infectious diseases*, 6(3):345–356, 1984.

[38] Geoffrey Gonzalez-Escobedo, Joanna M. Marshall, and John S. Gunn. Chronic and acute infection of the gall bladder by Salmonella Typhi: Understanding the carrier state. *Nature Reviews Microbiology*, 9(1):9–14, 1 2011.

[39] M. A. Mateen, Sheena Saleem, P. Chandrasekhar Rao, P. Sudhershan Reddy, and D. Nageshwar Reddy. Ultrasound in the diagnosis of typhoid fever. *Indian journal of pediatrics*, 73(8):681–685, 8 2006.

[40] Jennifer C van Velkinburgh and John S Gunn. PhoP-PhoQ-Regulated Loci Are Required for Enhanced Bile Resistance in Salmonella spp. *Infection and Immunity*, 67(4):1614, 4 1999.

[41] Caressa N. Tsai, Craig R. MacNair, My P.T. Cao, Jordyn N. Perry, Jakob Magolan, Eric D. Brown, and Brian K. Coombes. Targeting Two-Component Systems Uncovers a Small-Molecule Inhibitor of Salmonella Virulence. *Cell chemical biology*, 27(7):793–805, 7 2020.

[42] A. M. Prouty, W. H. Schwesinger, and J. S. Gunn. Biofilm formation and interaction with the surfaces of gallstones by Salmonella spp. *Infection and Immunity*, 70(5):2640–2649, 2002.

[43] R. Paul Wilson, Manuela Raffatellu, Daniela Chessa, Sebastian E. Winter, Çagla Tükel, and Andreas J. Bäumler. The Vi-capsule prevents Toll-like receptor 4 recognition of Salmonella. *Cellular Microbiology*, 10(4):876–890, 4 2008.

[44] Christopher M. Parry, Lalith Wijedoru, Amit Arjyal, and Stephen Baker. The utility of diagnostic tests for enteric fever in endemic locations. *http://dx.doi.org/10.1586/eri.11.47*, 9(6):711–725, 2014.

[45] Zulfiqar A. Bhutta. Current concepts in the diagnosis and treatment of typhoid fever. *BMJ*, 333(7558):78–82, 7 2006.

[46] Warren ; Coleman and Buxton. THE BACTERIOLOGY OF THE BLOOD IN TYPHOID FEVER.: AN ANALYSIS OF 1602 CASES.1. *The American Journal of the Medical Sciences*, 133(6):896, 1907.

[47] Robert H. Gilman, Miguel Terminel, Myron M. Levine, Pablo Hernandez-Mendoza, and Richard B. Hornick. RELATIVE EFFICACY OF BLOOD, URINE, RECTAL SWAB, BONE-MARROW, AND ROSE-SPOT CULTURES FOR RECOVERY OF SALMONELLA TYPHI IN TYPHOID FEVER. *The Lancet*, 305(7918):1211–1213, 5 1975.

[48] J. Wain, P. V.B. Bay, H. Vinh, N. M. Duong, T. S. Diep, A. L. Walsh, C. M. Parry, R. P. Hasserjian, V. A. Ho, T. T. Hien, J. Farrar, N. J. White, and N. P.J. Day. Quantitation of Bacteria in Bone Marrow from Patients with Typhoid Fever: Relationship between Counts and Clinical Features. *Journal of Clinical Microbiology*, 39(4):1571, 2001.

[49] A. FELIX and H. J. BENSTED. Proposed Standard Agglutinating Sera for Typhoid and Paratyphoid A and B Fevers. *Bulletin of the World Health Organization*, 10(6):919, 1954.

[50] Pak Leong Lim, Frankie C.H. Tam, Yuet Meng Cheong, and M. Jegathesan. One-Step 2-Minute Test To Detect Typhoid-Specific Antibodies Based on Particle Separation in Tubes. *Journal of Clinical Microbiology*, 36(8):2271, 1998.

[51] Zulfiqar Ahmed Bhutta and Naseem Mansurali. Rapid serologic diagnosis of pediatric typhoid fever in an endemic area: a prospective comparative evaluation of two dot-

enzyme immunoassays and the Widal test. *The American journal of tropical medicine and hygiene*, 61(4):654–657, 1999.

[52] Kamala Thriemer, Benedikt Ley, Joris Menten, Jan Jacobs, and Jef Van Den Ende. A Systematic Review and Meta-Analysis of the Performance of Two Point of Care Typhoid Fever Tests, Tubex TF and Typhidot, in Endemic Countries. *PLoS ONE*, 8(12), 12 2013.

[53] Shanta Dutta, Dipika Sur, Byomkesh Manna, Bhaswati Sen, Alok Kumar Deb, Jacqueline L. Deen, John Wain, Lorenz Von Seidlein, Leon Ochiai, John D. Clemens, and Sujit Kumar Bhattacharya. Evaluation of new-generation serologic tests for the diagnosis of typhoid fever: data from a community-based surveillance in Calcutta, India. *Diagnostic Microbiology and Infectious Disease*, 56(4):359–365, 12 2006.

[54] Ritesh Kumar, Alexander Gont, Theodore J. Perkins, Jennifer E.L. Hanson, and Ian A.J. Lorimer. Induction of senescence in primary glioblastoma cells by serum and TGFβ. *Scientific Reports*, 7(1), 12 2017.

[55] Abraham Majak Gut, Todor Vasiljevic, Thomas Yeager, and Osaana N. Donkor. Salmonella infection - prevention and treatment by antibiotics and probiotic yeasts: a review. *Microbiology (Reading, England)*, 164(11):1327–1344, 11 2018.

[56] Malick M. Gibani, Elizabeth Jones, Amber Barton, Celina Jin, Juliette Meek, Susana Camara, Ushma Galal, Eva Heinz, Yael Rosenberg-Hasson, Gerlinde Obermoser, Claire Jones, Danielle Campbell, Charlotte Black, Helena Thomaides-Brears, Christopher Darlow, Christina Dold, Laura Silva-Reyes, Luke Blackwell, Maria Lara-Tejero, Xuyao Jiao, Gabrielle Stack, Christoph J. Blohmke, Jennifer Hill, Brian Angus, Gordon Dougan, Jorge Galán, and Andrew J. Pollard. Investigation of the role of typhoid toxin in acute typhoid fever in a human challenge model. *Nature Medicine*, 25(7):1082–1088, 7 2019.

[57] John A. Crump, Maria Sjölund-Karlsson, Melita A. Gordon, and Christopher M. Parry. Epidemiology, clinical presentation, laboratory diagnosis, antimicrobial resistance, and antimicrobial management of invasive Salmonella infections. *Clinical Microbiology Reviews*, 28(4):901–937, 7 2015.

[58] Nicholas A. Feasey, Katherine Gaskell, Vanessa Wong, Chisomo Msefula, George Selemani, Save Kumwenda, Theresa J. Allain, Jane Mallewa, Neil Kennedy, Aisleen Bennett, Joram O. Nyirongo, Patience A. Nyondo, Madalitso D. Zulu, Julian Parkhill, Gordon Dougan, Melita A. Gordon, and Robert S. Heyderman. Rapid emergence of multidrug resistant, H58-lineage Salmonella typhi in Blantyre, Malawi. *PLoS neglected tropical diseases*, 9(4), 4 2015.

[59] Vanessa K. Wong, Stephen Baker, Derek J. Pickard, Julian Parkhill, Andrew J. Page, Nicholas A. Feasey, Robert A. Kingsley, Nicholas R. Thomson, Jacqueline A. Keane,

François Xavier Weill, David J. Edwards, Jane Hawkey, Simon R. Harris, Alison E. Mather, Amy K. Cain, James Hadfield, Peter J. Hart, Nga Tran Vu Thieu, Elizabeth J. Klemm, Dafni A. Glinos, Robert F. Breiman, Conall H. Watson, Samuel Kariuki, Melita A. Gordon, Robert S. Heyderman, Chinyere Okoro, Jan Jacobs, Octavie Lunguya, W. John Edmunds, Chisomo Msefula, Jose A. Chabalgoity, Mike Kama, Kylie Jenkins, Shanta Dutta, Florian Marks, Josefina Campos, Corinne Thompson, Stephen Obaro, Calman A. Maclennan, Christiane Dolecek, Karen H. Keddy, Anthony M. Smith, Christopher M. Parry, Abhilasha Karkey, E. Kim Mulholland, James I. Campbell, Sabina Dongol, Buddha Basnyat, Muriel Dufour, Don Bandaranayake, Take Toleafoa Naseri, Shalini Pravin Singh, Mochammad Hatta, Paul Newton, Robert S. Onsare, Lupeoletalalei Isaia, David Dance, Viengmon Davong, Guy Thwaites, Lalith Wijedoru, John A. Crump, Elizabeth De Pinna, Satheesh Nair, Eric J. Nilles, Duy Pham Thanh, Paul Turner, Sona Soeng, Mary Valcanis, Joan Powling, Karolina Dimovski, Geoff Hogg, Jeremy Farrar, Kathryn E. Holt, and Gordon Dougan. Phylogeographical analysis of the dominant multidrug-resistant H58 clade of Salmonella Typhi identifies inter- and intracontinental transmission events. *Nature genetics*, 47(6):632–639, 5 2015.

[60] Christopher J Harmer and Ruth M Hall. The A to Z of A/C plasmids. *Plasmid*, 80:63–82, 7 2015.

[61] Elizabeth A. McMillan, Charlene R. Jackson, and Jonathan G. Frye. Transferable Plasmids of Salmonella enterica Associated With Antibiotic Resistance Genes. *Frontiers in Microbiology*, 11:562181, 10 2020.

[62] Maria Hoffmann, James B. Pettengill, Narjol Gonzalez-Escalona, John Miller, Sherry L. Ayers, Shaohua Zhao, Marc W. Allard, Patrick F. McDermott, Eric W. Brown, and Steven R. Monday. Comparative sequence analysis of multidrug-resistant incA/C plasmids from salmonella enterica. *Frontiers in Microbiology*, 8(AUG), 8 2017.

[63] Elizabeth A. McMillan, Sushim K. Gupta, Laura E. Williams, Thomas Jové, Lari M. Hiott, Tiffanie A. Woodley, John B. Barrett, Charlene R. Jackson, Jamie L. Wasilenko, Mustafa Simmons, Glenn E. Tillman, Michael McClelland, and Jonathan G. Frye. Antimicrobial resistance genes, cassettes, and plasmids present in salmonella enterica associated with United States food animals. *Frontiers in Microbiology*, 10(APR), 2019.

[64] Mutsawashe Bwakura-Dangarembizi, Lindsay Kendall, Sabrina Bakeera-Kitaka, Patricia Nahirya-Ntege, Rosette Keishanyu, Kusum Nathoo, Moira J. Spyer, Adeodata Kekitiinwa, Joseph Lutaakome, Tawanda Mhute, Philip Kasirye, Paula Munderi, Victor Musiime, Diana M. Gibb, A. Sarah Walker, and Andrew J. Prendergast. A Randomized Trial of Prolonged Co-trimoxazole in HIV-Infected Children in Africa. *The New England journal of medicine*, 370(1):41, 1 2014.

[65] Wim L. Cuypers, Jan Jacobs, Vanessa Wong, Elizabeth J. Klemm, Stijn Deborggraeve, and Sandra van Puyvelde. Fluoroquinolone resistance in Salmonella: insights by whole-genome sequencing. *Microbial genomics*, 4(7), 7 2018.

[66] Samuel Kariuki and Robert S. Onsare. Epidemiology and genomics of invasive nontyphoidal salmonella infections in Kenya. *Clinical Infectious Diseases*, 61:S317–S324, 11 2015.

[67] Celina Jin, Malick M. Gibani, Shaun H. Pennington, Xinxue Liu, Alison Ardrey, Ghaith Aljayyoussi, Maria Moore, Brian Angus, Christopher M. Parry, Giancarlo A. Biagini, Nicholas A. Feasey, and Andrew J. Pollard. Treatment responses to Azithromycin and Ciprofloxacin in uncomplicated Salmonella Typhi infection: A comparison of Clinical and Microbiological Data from a Controlled Human Infection Model. *PLOS Neglected Tropical Diseases*, 13(12):e0007955, 12 2019.

[68] Duy Pham Thanh, Abhilasha Karkey, Sabina Dongol, Nhan Ho Thi, Corinne N. Thompson, Maia A. Rabaa, Amit Arjyal, Kathryn E. Holt, Vanessa Wong, Nga Tran Vu Thieu, Phat Voong Vinh, Tuyen Ha Thanh, Ashish Pradhan, Saroj Kumar Shrestha, Damoder Gajurel, Derek Pickard, Christopher M. Parry, Gordon Dougan, Marcel Wolbers, Christiane Dolecek, Guy E. Thwaites, Buddha Basnyat, and Stephen Baker. A novel ciprofloxacin-resistant subclade of H58 Salmonella Typhi is associated with fluoroquinolone treatment failure. *eLife*, 5(MARCH2016), 3 2016.

[69] K. H. Wong, J. C. Feeley, R. S. Northrup, and M. E. Forlines. Vi Antigen from Salmonella typhosa and Immunity Against Typhoid Fever I. Isolation and Immunologic Properties in Animals. *Infection and Immunity*, 9(2):348, 1974.

[70] K H Wong' And and John C Feeley2. Isolation of Vi Antigen and a Simple Method for Its Measurement. *Applied Microbiology*, 24(4):628, 10 1972.

[71] Myron M. Levine, Catterine Ferreccio, Robert E. Black, Carol O. Tacket, Rene Germanier, and Chilean Typhoid Committee. Progress in vaccines against typhoid fever. *Reviews of infectious diseases*, 11 Suppl 3:S552–S567, 1989.

[72] Shousun Chen Szu, Audrey L. Stone, Joan D. Robbins, Rachel Schneerson, and John B. Robbins. Vi capsular polysaccharide-protein conjugates for prevention of typhoid fever: Preparation, characterization, and immunogenicity in laboratory animals. *Journal of Experimental Medicine*, 166(5):1510–1524, 11 1987.

[73] Keith P. Klugman, Hendrik J. Koornhof, John B. Robbins, and Nancy N. Le Cam. Immunogenicity, efficacy and serological correlate of protection of Salmonella typhi Vi capsular polysaccharide vaccine three years after immunization. *Vaccine*, 14(5):435–438, 1996.

[74] L. Hessel, H. Debois, M. Fletcher, and R. Dumas. Experience with Salmonella typhi Vi capsular polysaccharide vaccine. *European journal of clinical microbiology & infectious diseases : official publication of the European Society of Clinical Microbiology*, 18(9):609–620, 1999.

[75] M R Saha, T Ramamurthy, P Dutta, and U Mitra. Emergence of Salmonella typhi Vi antigen-negative strains in an epidemic of multidrug-resistant typhoid fever cases in Calcutta, India., 2000.

[76] B Ivanoff, MM Levine, PH Lambert Bulletin of the World Health, and undefined 1994. Vaccination against typhoid fever: present status. *ncbi.nlm.nih.gov*, 1994.

[77] Myron M. Levine, Catterine Ferreccio, Paulina Abrego, Oriana San Martin, Edith Ortiz, and Stanley Cryz. Duration of efficacy of Ty21a, attenuated Salmonella typhi live oral vaccine. *Vaccine*, 17(SUPPL. 2), 10 1999.

[78] Jacob John, Carola J.C. Van Aart, and Nicholas C. Grassly. The Burden of Typhoid and Paratyphoid in India: Systematic Review and Meta-analysis. *PLoS Neglected Tropical Diseases*, 10(4), 4 2016.

[79] Manikandan Srinivasan, Kulandaipalayam Natarajan Sindhu, Sidhartha Giri, Nirmal Kumar, Venkata Raghava Mohan, Nicholas C. Grassly, and Gagandeep Kang. Salmonella Typhi Shedding and Household Transmission by Children With Blood Culture-Confirmed Typhoid Fever in Vellore, South India. *The Journal of Infectious Diseases*, 224(Supplement_5):S593–S600, 11 2021.

[80] Sarah Lindsay, Denise Garrett, and Duncan Steele. Evidence to Action: The 10th International Conference on Typhoid and Other Invasive Salmonelloses. *Clinical Infectious Diseases: An Official Publication of the Infectious Diseases Society of America*, 68(Suppl 1):S1, 2 2019.

[81] Celina Jin, Malick M. Gibani, Maria Moore, Helene B. Juel, Elizabeth Jones, James Meiring, Victoria Harris, Jonathan Gardner, Anna Nebykova, Simon A. Kerridge, Jennifer Hill, Helena Thomaides-Brears, Christoph J. Blohmke, Ly Mee Yu, Brian Angus, and Andrew J. Pollard. Efficacy and immunogenicity of a Vi-tetanus toxoid conjugate vaccine in the prevention of typhoid fever using a controlled human infection model of Salmonella Typhi: a randomised controlled, phase 2b trial. *The Lancet*, 390(10111):2472–2480, 12 2017.

[82] M Shakya, R Colin-Jones, K Theiss-Nyland, and et al. Phase 3 efficacy analysis of a typhoid conjugate vaccine trial in Nepal. *N Engl J Med*, 381:2209–2218, 2019.

[83] Vadrevu Krishna Mohan, Vineeth Varanasi, Anit Singh, Marcela F. Pasetti, Myron M. Levine, Ramasamy Venkatesan, and Krishna M. Ella. Safety and Immunogenicity of a Vi Polysaccharide-Tetanus Toxoid Conjugate Vaccine (Typbar-TCV) in Healthy

Infants, Children, and Adults in Typhoid Endemic Areas: A Multicenter, 2-Cohort, Open-Label, Double-Blind, Randomized Controlled Phase 3 Study. *Clinical Infectious Diseases*, 61(3):393–402, 8 2015.

[84] WHO. Typhoid vaccines: WHO position paper, March 2018—recommendations. *Vaccine*, 37:214–216, 2019.

[85] Mohammad Tahir Yousafzai, Sultan Karim, Sonia Qureshi, Momin Kazi, Hina Memon, Amber Junejo, Zohra Khawaja, Najeeb Ur Rehman, Muhammad Sajid Ansari, Rafey Ali, Ikram Uddin Ujjan, Heera Mani Lohana, Naveed M. Memon, Mudassar Hussain, Roohi Nigar, Naor Bar-Zeev, and Farah Naz Qamar. Effectiveness of typhoid conjugate vaccine against culture-confirmed Salmonella enterica serotype Typhi in an extensively drug-resistant outbreak setting of Hyderabad, Pakistan: a cohort study. *The Lancet Global Health*, 9(8):e1154–e1162, 8 2021.

[86] Evelina Tacconelli, Elena Carrara, Alessia Savoldi, Stephan Harbarth, Marc Mendelson, Dominique L. Monnet, Céline Pulcini, Gunnar Kahlmeter, Jan Kluytmans, Yehuda Carmeli, Marc Ouellette, Kevin Outterson, Jean Patel, Marco Cavaleri, Edward M. Cox, Chris R. Houchens, M. Lindsay Grayson, Paul Hansen, Nalini Singh, Ursula Theuretzbacher, Nicola Magrini, Aaron Oladipo Aboderin, Seif Salem Al-Abri, Nordiah Awang Jalil, Nur Benzonana, Sanjay Bhattacharya, Adrian John Brink, Francesco Robert Burkert, Otto Cars, Giuseppe Cornaglia, Oliver James Dyar, Alex W. Friedrich, Ana C. Gales, Sumanth Gandra, Christian Georg Giske, Debra A. Goff, Herman Goossens, Thomas Gottlieb, Manuel Guzman Blanco, Waleria Hryniewicz, Deepthi Kattula, Timothy Jinks, Souha S. Kanj, Lawrence Kerr, Marie Paule Kieny, Yang Soo Kim, Roman S. Kozlov, Jaime Labarca, Ramanan Laxminarayan, Karin Leder, Leonard Leibovici, Gabriel Levy-Hara, Jasper Littman, Surbhi Malhotra-Kumar, Vikas Manchanda, Lorenzo Moja, Babacar Ndoye, Angelo Pan, David L. Paterson, Mical Paul, Haibo Qiu, Pilar Ramon-Pardo, Jesús Rodríguez-Baño, Maurizio Sanguinetti, Sharmila Sengupta, Mike Sharland, Massinissa Si-Mehand, Lynn L. Silver, Wonkeung Song, Martin Steinbakk, Jens Thomsen, Guy E. Thwaites, Jos WM van der Meer, Nguyen Van Kinh, Silvio Vega, Maria Virginia Villegas, Agnes Wechsler-Fördös, Heiman Frank Louis Wertheim, Evelyn Wesangula, Neil Woodford, Fidan O. Yilmaz, and Anna Zorzet. Discovery, research, and development of new antibiotics: the WHO priority list of antibiotic-resistant bacteria and tuberculosis. *The Lancet Infectious Diseases*, 18(3):318–327, 3 2018.

[87] Sabina Dongol, Corinne N. Thompson, Simon Clare, Tran Vu Thieu Nga, Pham Thanh Duy, Abhilasha Karkey, Amit Arjyal, Samir Koirala, Nely Shrestha Khatri, Pukar Maskey, Sanjay Poudel, Vijay Kumar Jaiswal, Sujan Vaidya, Gordon Dougan, Jeremy J. Farrar, Christiane Dolecek, Buddha Basnyat, and Stephen Baker. The Microbiological and Clinical Characteristics of Invasive Salmonella in Gallbladders from Cholecystectomy Patients in Kathmandu, Nepal. *PLoS ONE*, 7(10), 10 2012.

[88] Geoffrey Gonzalez-Escobedo, Krista M.D. La Perle, and John S. Gunn. Histopathological analysis of Salmonella chronic carriage in the mouse hepatopancreatobiliary system. *PLoS ONE*, 8(12), 12 2013.

[89] Thomas C. Darton, Christoph J. Blohmke, Eleni Giannoulatou, Claire S. Waddington, Claire Jones, Pamela Sturges, Craig Webster, Hal Drakesmith, Andrew J. Pollard, and Andrew E. Armitage. Rapidly Escalating Hepcidin and Associated Serum Iron Starvation Are Features of the Acute Response to Typhoid Infection in Humans. *PLoS Neglected Tropical Diseases*, 9(9), 9 2015.

[90] R. B. Hornick, S. E. Greisman, T. E. Woodward, H. L. DuPont, A. T. Dawkins, and M. J. Snyder. Typhoid Fever: Pathogenesis and Immunologic Control. *New England Journal of Medicine*, 283(13):686–691, 9 1970.

[91] James E. Meiring, Matthew B. Laurens, Pratiksha Patel, Priyanka Patel, Theresa Misiri, Kenneth Simiyu, Felistas Mwakiseghile, J. Kathleen Tracy, Clemens Masesa, Yuanyuan Liang, Marc Henrion, Elizabeth Rotrosen, Markus Gmeiner, Robert Heyderman, Karen Kotloff, Melita A. Gordon, and Kathleen M. Neuzil. Typhoid vaccine acceleration consortium Malawi: A Phase III, randomized, double-blind, controlled trial of the clinical efficacy of typhoid conjugate vaccine among children in Blantyre, Malawi. *Clinical Infectious Diseases*, 68:S50–S58, 3 2019.

[92] Katherine Theiss-Nyland, Firdausi Qadri, Rachel Colin-Jones, K. Zaman, Farhana Khanam, Xinxue Liu, Merryn Voysey, Arifuzzaman Khan, Nazmul Hasan, Fahim Ashher, Yama G. Farooq, Andrew J. Pollard, and John D. Clemens. Assessing the Impact of a Vi-polysaccharide Conjugate Vaccine in Preventing Typhoid Infection Among Bangladeshi Children: A Protocol for a Phase IIIb Trial. *Clinical infectious diseases : an official publication of the Infectious Diseases Society of America*, 68(Suppl 2):S74–S82, 3 2019.

[93] Katherine Theiss-Nyland, Firdausi Qadri, Rachel Colin-Jones, K. Zaman, Farhana Khanam, Xinxue Liu, Merryn Voysey, Arifuzzaman Khan, Nazmul Hasan, Fahim Ashher, Yama G. Farooq, Andrew J. Pollard, and John D. Clemens. Assessing the Impact of a Vi-polysaccharide Conjugate Vaccine in Preventing Typhoid Infection Among Bangladeshi Children: A Protocol for a Phase IIIb Trial. *Clinical Infectious Diseases*, 68(Supplement_2):S74–S82, 3 2019.

[94] Jeongmin Song, Tim Willinger, Anthony Rongvaux, Elizabeth E. Eynon, Sean Stevens, Markus G. Manz, Richard A. Flavell, and Jorge E. Galán. A mouse model for the human pathogen salmonella typhi. *Cell Host and Microbe*, 8(4):369–376, 10 2010.

[95] Ramkumar Mathur, Hyunju Oh, Dekai Zhang, Sung Gyoo Park, Jin Seo, Alicia Koblansky, Matthew S. Hayden, and Sankar Ghosh. A mouse model of salmonella typhi infection. *Cell*, 151(3):590–602, 10 2012.

[96] John Wain, Deborah House, Afia Zafar, Stephen Baker, Satheesh Nair, Claire Kidgell, Zulfiqar Bhutta, Gordon Dougan, and Rumina Hasan. Vi antigen expression in Salmonella enterica serovar typhi clinical isolates from Pakistan. *Journal of Clinical Microbiology*, 43(3):1158–1165, 3 2005.

[97] Miryoung Song, Maroof Husain, Jessica Jones-Carson, Lin Liu, Calvin A. Henard, and Andrés Vázquez-Torres. Low-molecular-weight thiol-dependent antioxidant and antinitrosative defences in Salmonella pathogenesis. *Molecular Microbiology*, 87(3):609–622, 2 2013.

[98] Malick M. Gibani, Celina Jin, Sonu Shrestha, Maria Moore, Lily Norman, Merryn Voysey, Elizabeth Jones, Luke Blackwell, Helena Thomaides-Brears, Jennifer Hill, Christoph J. Blohmke, Hazel C. Dobinson, Philip Baker, Claire Jones, Danielle Campbell, Yama F. Mujadidi, Emma Plested, Lorena Preciado-Llanes, Giorgio Napolitani, Alison Simmons, Melita A. Gordon, Brian Angus, Thomas C. Darton, Vincenzo Cerundulo, and Andrew J. Pollard. Homologous and heterologous re-challenge with Salmonella Typhi and Salmonella Paratyphi A in a randomised controlled human infection model. *PLOS Neglected Tropical Diseases*, 14(10):e0008783, 10 2020.

[99] Masaki Miyake, Licheng Zhao, Takayuki Ezaki, Kenji Hirose, Abdul Quayum Khan, Yoshiaki Kawamura, Ryuichiro Shima, Miki Kamijo, Toshiyuki Masuzawa, and Yasutake Yanagihara. Vi-deficient and nonfimbriated mutants of Salmonella typhi agglutinate human blood type antigens and are hyperinvasive. *FEMS microbiology letters*, 161(1):75–82, 4 1998.

[100] A W M Van Der Velden, S W Lindgren, M J Worley, and F Heffron. Salmonella Pathogenicity Island 1-Independent Induction of Apoptosis in Infected Macrophages by Salmonella enterica Serotype Typhimurium. *Infection and Immunity*, 68(10):5702, 2000.

[101] J. E. Galán. Salmonella interactions with host cells: Type III secretion at work. *Annual Review of Cell and Developmental Biology*, 17:53–86, 2001.

[102] Jonas Jennewein, Jasmin Matuszak, Steffi Walter, Boas Felmy, Kathrin Gendera, Valentin Schatz, Monika Nowottny, Gregor Liebsch, Michael Hensel, Wolf Dietrich Hardt, Roman G. Gerlach, and Jonathan Jantsch. Low-oxygen tensions found in Salmonella-infected gut tissue boost Salmonella replication in macrophages by impairing antimicrobial activity and augmenting Salmonella virulence. *Cellular Microbiology*, 17(12):1833–1847, 12 2015.

[103] Bryan Coburn, Inna Sekirov, and B Brett Finlay. Type III Secretion Systems and Disease. *Clinical Microbiology Reviews*, 20(4):535, 10 2007.

[104] Wolf Dietrich Hardt, Li Mei Chen, Kornel E. Schuebel, Xosé R. Bustelo, and Jorge E. Galán. S. typhimurium Encodes an activator of Rho GTPases that induces membrane ruffling and nuclear responses in host cells. *Cell*, 93(5):815–826, 5 1998.

[105] Emma J McGhie, Richard D Hayward, and Vassilis Koronakis. Control of actin turnover by a salmonella invasion protein. *Molecular cell*, 13(4):497–510, 2 2004.

[106] Samantha Gruenheid and B Brett Finlay. Microbial pathogenesis and cytoskeletal function. *Nature*, 422(6933):775–781, 4 2003.

[107] Markus C Schlumberger and Wolf Dietrich Hardt. Salmonella type III secretion effectors: pulling the host cell's strings. *Current opinion in microbiology*, 9(1):46–54, 2 2006.

[108] Martin Lorkowski, Alfonso Felipe-López, Claudia A. Danzer, Nicole Hansmeier, and Michael Hensel. Salmonella enterica invasion of polarized epithelial cells is a highly cooperative effort. *Infection and immunity*, 82(6):2657–2667, 2014.

[109] V. Kuhle and M. Hensel. Cellular microbiology of intracellular Salmonella enterica: Functions of the type III secretion system encoded by Salmonella pathogenicity island 2. *Cellular and Molecular Life Sciences*, 61(22):2812–2826, 11 2004.

[110] Kieran McGourty, Teresa L. Thurston, Sophie A. Matthews, Laurie Pinaud, Luís Jaime Mota, and David W. Holden. Salmonella inhibits retrograde trafficking of mannose-6-phosphate receptors and lysosome function. *Science*, 338(6109):963–967, 11 2012.

[111] Katelyn Knuff and B. Brett Finlay. What the SIF Is Happening—The Role of Intracellular Salmonella-Induced Filaments. *Frontiers in Cellular and Infection Microbiology*, 7(JUL):335, 7 2017.

[112] Viktoria Liss, A. Leoni Swart, Alexander Kehl, Natascha Hermanns, Yuying Zhang, Deepak Chikkaballi, Nathalie Böhles, Jörg Deiwick, and Michael Hensel. Salmonella enterica Remodels the Host Cell Endosomal System for Efficient Intravacuolar Nutrition. *Cell Host and Microbe*, 21(3):390–402, 3 2017.

[113] Elliott Jennings, Teresa L.M. Thurston, and David W. Holden. Salmonella SPI-2 Type III Secretion System Effectors: Molecular Mechanisms And Physiological Consequences. *Cell Host and Microbe*, 22(2):217–231, 8 2017.

[114] Marcus Fulde, Kira van Vorst, Kaiyi Zhang, Alexander J. Westermann, Tobias Busche, Yong Chiun Huei, Katharina Welitschanski, Isabell Froh, Dennis Pägelow, Johanna Plendl, Christiane Pfarrer, Jörn Kalinowski, Jörg Vogel, Peter Valentin-Weigand, Michael Hensel, Karsten Tedin, Urska Repnik, and Mathias W. Hornef. SPI2 T3SS effectors facilitate enterocyte apical to basolateral transmigration of Salmonella-containing vacuoles in vivo. *Gut Microbes*, 13(1), 2021.

[115] Kathryn G. Watson and David W. Holden. Dynamics of growth and dissemination of Salmonella in vivo. *Cellular Microbiology*, 12(10):1389–1397, 10 2010.

[116] Ion Rusan Vladoianu, Hernán R Chang, and Jean Claude Pechère. Expression of host resistance to Salmonella typhi and Salmonella typhimurium: bacterial survival within macrophages of murine and human origin. *Microbial Pathogenesis*, 8(2):83–90, 2 1990.

[117] Geoffrey Gonzalez-Escobedo and John S. Gunn. Gallbladder epithelium as a niche for chronic salmonella carriage. *Infection and Immunity*, 81(8):2920–2930, 8 2013.

[118] John S. Gunn, Joanna M. Marshall, Stephen Baker, Sabina Dongol, Richelle C. Charles, and Edward T. Ryan. Salmonella chronic carriage: Epidemiology, diagnosis, and gallbladder persistence. *Trends in Microbiology*, 22(11):648–655, 11 2014.

[119] Taro Kawai and Shizuo Akira. The role of pattern-recognition receptors in innate immunity: Update on toll-like receptors. *Nature Immunology*, 11(5):373–384, 5 2010.

[120] Damien Bierschenk, Dave Boucher, and Kate Schroder. Salmonella-induced inflammasome activation in humans. *Molecular immunology*, 86:38–43, 6 2017.

[121] Doris L. Larock, Anu Chaudhary, and Samuel I. Miller. Salmonellae interactions with host processes. *Nature reviews. Microbiology*, 13(4):191, 3 2015.

[122] Patrick Kaiser and Wolf Dietrich Hardt. Salmonella Typhimurium diarrhea: Switching the mucosal epithelium from homeostasis to defense. *Current Opinion in Immunology*, 23(4):456–463, 8 2011.

[123] Nguyen Quoc Chanh, Paul Everest, Tran Tan Khoa, Deborah House, Simon Murch, Christopher Parry, Phillippa Connerton, Phan Van Bay, To Song Diep, Pietro Mastroeni, Nicholas J. White, Tran T. Hien, Vo Van Ho, Gordon Dougan, Jeremy J. Farrar, and John Wain. A clinical, microbiological, and pathological study of intestinal perforation associated with typhoid fever. *Clinical Infectious Diseases*, 39(1):61–67, 7 2004.

[124] H. Sprinz, E. J. Gangarosa, M. Williams, R. B. Hornick, and T. E. Woodward. Histopathology of the upper small intestines in typhoid fever - Biopsy study of experimental disease in man. *The American Journal of Digestive Diseases*, 11(8):615–624, 8 1966.

[125] M D Kraus, B Amatya, and Y Kimula. Histopathology of typhoid enteritis: morphologic and immunophenotypic findings. *Modern pathology : an official journal of the United States and Canadian Academy of Pathology, Inc*, 12(10):949–955, 10 1999.

[126] Sébastien P. Faucher, Roy Curtiss, and France Daigle. Selective capture of Salmonella enterica serovar Typhi genes expressed in macrophages that are absent

from the Salmonella enterica serovar Typhimurium genome. *Infection and Immunity*, 73(8):5217–5221, 8 2005.

[127] Sebastian E. Winter, Maria G. Winter, Ivan Godinez, Hee Jeong Yang, Holger Rüssmann, Helene L. Andrews-Polymenis, and Andreas J. Bäumler. A rapid change in virulence gene expression during the transition from the intestinal lumen into tissue promotes systemic dissemination of salmonella. *PLoS Pathogens*, 6(8):63–64, 8 2010.

[128] Quynh T. Tran, Gabriel Gomez, Sangeeta Khare, Sara D. Lawhon, Manuela Raffatellu, Andreas J. Bäumler, Dharani Ajithdoss, Soma Dhavala, and L. Garry Adams. The Salmonella enterica serotype Typhi Vi capsular antigen is expressed after the bacterium enters the ileal mucosa. *Infection and Immunity*, 78(1):527–535, 1 2010.

[129] Sebastian E. Winter, Manuela Raffatellu, Paul R. Wilson, Holger Rüssmann, and Andreas J. Bäumler. The Salmonella enterica serotype Typhi regulator TviA reduces interleukin-8 production in intestinal epithelial cells by repressing flagellin secretion. *Cellular Microbiology*, 10(1):247–261, 2008.

[130] Takeshi Haneda, Sebastian E. Winter, Brian P. Butler, R. Paul Wilson, Çagla Tükel, Maria G. Winter, Ivan Godinez, Renée M. Tsolis, and Andreas J. Bäumler. The capsule-encoding viaB locus reduces intestinal inflammation by a Salmonella pathogenicity island 1-independent mechanism. *Infection and Immunity*, 77(7):2932–2942, 7 2009.

[131] Manuela Raffatellu, Renato L. Santos, Daniela Chessa, R. Paul Wilson, Sebastian E. Winter, Carlos A. Rossetti, Sara D. Lawhon, Hiutung Chu, Tsang Lau, Charles L. Bevins, L. Garry Adams, and Andreas J. Bäumler. The capsule encoding the viaB locus reduces interleukin-17 expression and mucosal innate responses in the bovine intestinal mucosa during infection with Salmonella enterica serotype typhi. *Infection and Immunity*, 75(9):4342–4350, 9 2007.

[132] F. B. Mallory. A HISTOLOGICAL STUDY OF TYPHOID FEVER. *The Journal of Experimental Medicine*, 3(6):611, 11 1898.

[133] Xiao Lian Zhang, Victor Tunje Jeza, and Qin Pan. Salmonella Typhi: from a Human Pathogen to a Vaccine Vector. *Cellular and Molecular Immunology*, 5(2):91, 4 2008.

[134] Stefania Spanò, Juan E. Ugalde, and Jorge E. Galán. Delivery of a Salmonella Typhi exotoxin from a host intracellular compartment. *Cell Host Microbe*, 3(1):30–38, 1 2008.

[135] Jorge E Galán. Typhoid toxin provides a window into typhoid fever and the biology of salmonella typhi. *Proceedings of the National Academy of Sciences of the United States of America*, 113(23):6338–6344, 2016.

[136] Casey C. Fowler and Jorge E. Galán. Decoding a Salmonella Typhi Regulatory Network that Controls Typhoid Toxin Expression within Human Cells. *Cell Host and Microbe*, 23(1):65–76, 1 2018.

[137] Casey C. Fowler, Gabrielle Stack, Xuyao Jiao, Maria Lara-Tejero, and Jorge E. Galán. Alternate subunit assembly diversifies the function of a bacterial toxin. *Nature Communications*, 10(1), 12 2019.

[138] Erik Haghjoo and Jorge E. Galán. Salmonella typhi encodes a functional cytolethal distending toxin that is delivered into host cells by a bacterial-internalization pathway. *Proc. Natl Acad. Sci. USA*, 101(13):4614–4619, 3 2004.

[139] Rachel A. Miller, Michael I. Betteken, Xiaodong Guo, Craig Altier, Gerald E. Duhamel, and Martin Wiedmann. The Typhoid Toxin Produced by the Nontyphoidal Salmonella enterica Serotype Javiana Is Required for Induction of a DNA Damage Response In Vitro and Systemic Spread In Vivo. *mBio*, 9(2), 3 2018.

[140] Lisa Del Bel Belluz, Riccardo Guidi, Ioannis S. Pateras, Laura Levi, Boris Mihaljevic, Syed Fazle Rouf, Marie Wrande, Marco Candela, Silvia Turroni, Claudia Nastasi, Clarissa Consolandi, Clelia Peano, Toma Tebaldi, Gabriella Viero, Vassilis G. Gorgoulis, Thorbjørn Krejsgaard, Mikael Rhen, and Teresa Frisan. The Typhoid Toxin Promotes Host Survival and the Establishment of a Persistent Asymptomatic Infection. *PLoS Pathogens*, 12(4), 4 2016.

[141] Océane C.B. Martin, Anna Bergonzini, Maria Lopez Chiloeches, Eleni Paparouna, Deborah Butter, Sofia D.P. Theodorou, Maria M. Haykal, Elisa Boutet-Robinet, Toma Tebaldi, Andrew Wakeham, Mikael Rhen, Vassilis G. Gorgoulis, Tak Mak, Ioannis S. Pateras, and Teresa Frisan. Influence of the microenvironment on modulation of the host response by typhoid toxin. *Cell Rep*, 35(1), 4 2021.

[142] Sylvie Y. Pérès, Olivier Marchès, France Daigle, Jean Philippe Nougayrède, Frédéric Hérault, Christian Tasca, Jean De Rycke, and Eric Oswald. A new cytolethal distending toxin (CDT) from Escherichia coli producing CNF2 blocks HeLa cell division in G2/M phase. *Molecular Microbiology*, 24(5):1095–1107, 1997.

[143] Jun Okuda, Hisao Kurazono, and Yoshifumi Takeda. Distribution of the cytolethal distending toxin A gene (cdtA) among species of Shigella and Vibrio, and cloning and sequencing of the cdt gene from Shigella dysenteriae. *Microbial pathogenesis*, 18(3):167–172, 1995.

[144] Leslie D. Cope, Sheryl Lumbley, Jo L. Latimer, Julia Klesney-Tait, Marla K. Stevens, Linda S. Johnson, Maria Purven, Robert S. Munson, Teresa Lagergard, Justin D. Radolf, and Eric J. Hansen. A diffusible cytotoxin of Haemophilus ducreyi. *Proceedings of the National Academy of Sciences of the United States of America*, 94(8):4056–4061, 4 1997.

[145] Motoyuki Sugai, Toru Kawamoto, Sylvie Y. Pérès, Yoko Ueno, Hitoshi Komatsuzawa, Tamaki Fujiwara, Hidemi Kurihara, Hidekazu Suginaka, and Eric Oswald. The cell cycle-specific growth-inhibitory factor produced by Actinobacillus actinomycetemcomitans is a cytolethal distending toxin. *Infection and Immunity*, 66(10):5008–5019, 1998.

[146] Vincent B. Young, Kimberly A. Knox, and David B. Schauer. Cytolethal distending toxin sequence and activity in the enterohepatic pathogen Helicobacter hepaticus. *Infection and Immunity*, 68(1):184–191, 2000.

[147] Benoît J. Pons, Julien Vignard, and Gladys Mirey. Cytolethal Distending Toxin Subunit B: A Review of Structure–Function Relationship. *Toxins*, 11(10), 10 2019.

[148] Lingquan Deng, Jeongmin Song, Xiang Gao, Jiawei Wang, Hai Yu, Xi Chen, Nissi Varki, Yuko Naito-Matsui, Jorge E. Galán, and Ajit Varki. Host adaptation of a bacterial toxin from the human pathogen salmonella typhi. *Cell*, 159(6):1290–1299, 12 2014.

[149] Casey C. Fowler, Gabrielle Stack, Xuyao Jiao, Maria Lara-Tejero, and Jorge E. Galán. Alternate subunit assembly diversifies the function of a bacterial toxin. *Nature Communications 2019 10:1*, 10(1):1–10, 8 2019.

[150] Xiang Gao, Lingquan Deng, Gabrielle Stack, Hai Yu, Xi Chen, Yuko Naito-Matsui, Ajit Varki, and Jorge E. Galán. Evolution of host adaptation in the Salmonella typhoid toxin. *Nature Microbiology*, 2(12):1592–1599, 12 2017.

[151] Henk C den Bakker, Andrea I Moreno Switt, Gregory Govoni, Craig A Cummings, Matthew L Ranieri, Lovorka Degoricija, Karin Hoelzer, Lorraine D Rodriguez-Rivera, Stephanie Brown, Elena Bolchacova, Manohar R Furtado, and Martin Wiedmann. Genome sequencing reveals diversification of virulence factor content and possible host adaptation in distinct subpopulations of Salmonella enterica. *BMC Genomics*, 12(1), 12 2011.

[152] Lorraine D. Rodriguez-Rivera, Barbara M. Bowen, Henk C. Den Bakker, Gerald E. Duhamel, and Martin Wiedmann. Characterization of the cytolethal distending toxin (typhoid toxin) in non-typhoidal Salmonella serovars. *Gut Pathogens*, 7(1), 7 2015.

[153] Rachel A. Miller and Martin Wiedmann. The cytolethal distending toxin produced by nontyphoidal Salmonella serotypes javiana, montevideo, oranienburg, and mississippi induces DNA damage in a manner similar to that of serotype Typhi. *mBio*, 7(6), 1 2016.

[154] A. Gaballa, R. A. Cheng, A. S. Harrand, A. R. Cohn, and M. Wiedmann. The Majority of Typhoid Toxin-Positive Salmonella Serovars Encode ArtB, an Alternate Binding Subunit . *mSphere*, 6(1), 2 2021.

[155] Ezat H. Mezal, Ashley Sabol, Mariam A. Khan, Nawab Ali, Rossina Stefanova, and Ashraf A. Khan. Isolation and molecular characterization of Salmonella enterica serovar Enteritidis from poultry house and clinical samples during 2010. *Food Microbiology*, 38:67–74, 2014.

[156] Wen Sen Lee, Shio Shin Jean, Fu Lun Chen, Szu Min Hsieh, and Po Ren Hsueh. Lemierre's syndrome: A forgotten and re-emerging infection. *Journal of Microbiology, Immunology and Infection*, 53(4):513–517, 8 2020.

[157] Dragana Nešić, Yun Hsu, and C. Erec Stebbins. Assembly and function of a bacterial genotoxin. *Nature*, 429(6990):429–433, 5 2004.

[158] Cherilyn A. Elwell and Lawrence A. Dreyfus. DNase I homologous residues in CdtB are critical for cytolethal distending toxin-mediated cell cycle arrest. *Molecular Microbiology*, 37(4):952–963, 2000.

[159] M. Lara-Tejero and J. E. Galan. A bacterial toxin that controls cell cycle progression as a deoxyribonuclease I-like protein. *Science (New York, N.Y.)*, 290(5490):354–357, 10 2000.

[160] Teresa Frisan, Ximena Cortes-Bratti, and Monica Thelestam. Cytolethal distending toxins and activation of DNA damage-dependent checkpoint responses. *International Journal of Medical Microbiology : IJMM*, 291(6-7):495–499, 2 2002.

[161] Teresa Frisan, Ximena Cortes-Bratti, Esteban Chaves-Olarte, Bo Stenerlöw, and Monica Thelestam. The Haemophilus ducreyi cytolethal distending toxin induces DNA double-strand breaks and promotes ATM-dependent activation of RhoA. *Cell. Microbiol.*, 5(10):695–707, 10 2003.

[162] C. Elwell, K. Chao, K. Patel, and L. Dreyfus. Escherichia coli CdtB Mediates Cytolethal Distending Toxin Cell Cycle Arrest. *Infection and Immunity*, 69(5):3418, 2001.

[163] Ximena Cortes-Bratti, Christina Karlsson, Teresa Lagergård, Monica Thelestam, and Teresa Frisan. The Haemophilus ducreyi Cytolethal Distending Toxin Induces Cell Cycle Arrest and Apoptosis via the DNA Damage Checkpoint Pathways. *Journal of Biological Chemistry*, 276(7):5296–5302, 2 2001.

[164] Ximena Cortes-Bratti, Teresa Frisan, and Monica Thelestam. The cytolethal distending toxins induce DNA damage and cell cycle arrest. *Toxicon*, 39(11):1729–1736, 2001.

[165] D. C. Hassane, R. B. Lee, M. D. Mendenhall, and C. L. Pickett. Cytolethal distending toxin demonstrates genotoxic activity in a yeast model. *Infection and immunity*, 69(9):5752–5759, 2001.

[166] Xiangqun Mao and Joseph M. DiRienzo. Functional studies of the recombinant subunits of a cytolethal distending holotoxin. *Cell. Microbiol.*, 4(4):245–255, 2002.

[167] Y. Fedor, J. Vignard, M. L. Nicolau-Travers, E. Boutet-Robinet, C. Watrin, B. Salles, and G. Mirey. From single-strand breaks to double-strand breaks during S-phase: a new mode of action of the Escherichia coli cytolethal distending toxin. *Cell Microbiol*, 15(1):1–15, 1 2013.

[168] Jean Philippe Nougayrède, Stefan Homburg, Frédéric Taieb, Michèle Boury, Elzbieta Brzuszkiewicz, Gerhard Gottschalk, Carmen Buchrieser, Jörg Hacker, Ulrich Dobrindt, and Eric Oswald. Escherichia coli induces DNA double-strand breaks in eukaryotic cells. *Science*, 313(5788):848–851, 8 2006.

[169] Teresa Frisan. Bacterial genotoxins: The long journey to the nucleus of mammalian cells. *Biochimica et Biophysica Acta - Biomembranes*, 1858(3):567–575, 2016.

[170] Eleonora García Véscovi, Fernando C. Soncini, and Eduardo A. Groisman. Mg2+ as an extracellular signal: Environmental regulation of Salmonella virulence. *Cell*, 84(1):165–174, 1 1996.

[171] JS Gunn JC Velkinburgh. PhoP-PhoQ-regulated loci are required for enhanced bile resistance in Salmonella spp. *Infect Immun*, 67:1614–1622, 1999.

[172] John S. Gunn. Mechanisms of bacterial resistance and response to bile. *Microbes and Infection*, 2(8):907–913, 7 2000.

[173] Martin W. Bader, Sarah Sanowar, Margaret E. Daley, Anna R. Schneider, Uhnsoo Cho, Wenqing Xu, Rachel E. Klevit, Hervé Le Moual, and Samuel I. Miller. Recognition of antimicrobial peptides by a bacterial sensor kinase. *Cell*, 122(3):461–472, 8 2005.

[174] Jeongjoon Choi and Eduardo A. Groisman. Acidic pH sensing in the bacterial cytoplasm is required for Salmonella virulence. *Molecular microbiology*, 101(6):1024, 9 2016.

[175] Elizabeth L. Hohmann, Carmen A. Oletta, and Samuel I. Miller. Evaluation of a phoP/phoQ-deleted, aroA-deleted live oral Salmonella typhi vaccine strain in human volunteers. *Vaccine*, 14(1):19–24, 1996.

[176] Ronald Chang and John B. Holcomb. Choice of fluid therapy in the initial management of sepsis, severe sepsis, and septic shock. *Shock (Augusta, Ga.)*, 46(1):17, 7 2016.

[177] Hélène Hodak and Jorge E. Galán. A Salmonella Typhi homologue of bacteriophage muramidases controls typhoid toxin secretion. *EMBO Reports*, 14(1):95–102, 1 2013.

[178] R. Young. Bacteriophage holins: deadly diversity - PubMed, 2002.

[179] I. N. Wang, D. L. Smith, and R. Young. Holins: the protein clocks of bacteriophage infections. *Annual review of microbiology*, 54:799–825, 2000.

[180] Stefania Spanò, Xiaoyun Liu, and Jorge E. Galán. Proteolytic targeting of Rab29 by an effector protein distinguishes the intracellular compartments of human-adapted and broad-host Salmonella. *Proceedings of the National Academy of Sciences of the United States of America*, 108(45):18418–18423, 11 2011.

[181] Shu-Jung Chang, Yu-Ting Hsu, Yun Chen, Yen-Yi Lin, Maria Lara-Tejero, and Jorge E Galan. Typhoid toxin sorting and exocytic transport from Salmonella Typhi-infected cells. *eLife*, 11, 5 2022.

[182] Shu-Jung Chang, Sheng Chih Jin, Xuyao Jiao, and Jorge E Galán. Unique features in the intracellular transport of typhoid toxin revealed by a genome-wide screen. *PLOS Pathogens*, 15(4):e1007704, 4 2019.

[183] Billy Tsai, Yihong Ye, and Tom A. Rapoport. Retro-translocation of proteins from the endoplasmic reticulum into the cytosol. *Nature Reviews Molecular Cell Biology*, 3(4):246–255, 2002.

[184] Roger D. Kornberg. Chromatin structure: a repeating unit of histones and DNA. *Science (New York, N.Y.)*, 184(4139):868–871, 1974.

[185] G. Arents and E. N. Moudrianakis. Topography of the histone octamer surface: repeating structural motifs utilized in the docking of nucleosomal DNA. *Proceedings of the National Academy of Sciences of the United States of America*, 90(22):10489–10493, 1993.

[186] Katerina Gurova, Han Wen Chang, Maria E. Valieva, Poorva Sandlesh, and Vasily M. Studitsky. Structure and function of the histone chaperone FACT – resolving FACTual issues. *Biochimica et biophysica acta. Gene regulatory mechanisms*, 1861(9):892–904, 9 2018.

[187] Marcus Buschbeck and Sandra B. Hake. Variants of core histones and their roles in cell fate decisions, development and cancer. *Nature Reviews Molecular Cell Biology 2017 18:5*, 18(5):299–314, 2 2017.

[188] Katrien Vermeulen, Dirk R. Van Bockstaele, and Zwi N. Berneman. The cell cycle: a review of regulation, deregulation and therapeutic targets in cancer. *Cell proliferation*, 36(3):131–149, 6 2003.

[189] Amit Deshpande, Peter Sicinski, and Philip W. Hinds. Cyclins and cdks in development and cancer: a perspective. *Oncogene*, 24(17):2909–2915, 4 2005.

[190] Naoko Ohtani, Kimi Yamakoshi, Akiko Takahashi, and Eiji Hara. The p16INK4a-RB pathway: molecular link between cellular senescence and tumor suppression. *The journal of medical investigation : JMI*, 51(3-4):146–153, 8 2004.

[191] Sophie E. Polo and Stephen P. Jackson. Dynamics of DNA damage response proteins at DNA breaks: a focus on protein modifications. *Genes Dev.*, 25(5):409–433, 3 2011.

[192] Karlene A. Cimprich and David Cortez. ATR: an essential regulator of genome integrity. *Nat. Rev. Mol. Cell Biol.*, 9(8):616–627, 8 2008.

[193] Bunsyo Shiotani and Lee Zou. Single-Stranded DNA Orchestrates an ATM-to-ATR Switch at DNA Breaks. *Molecular cell*, 33(5):547, 3 2009.

[194] Christopher L. Brooks and Wei Gu. p53 ubiquitination: Mdm2 and beyond. *Molecular cell*, 21(3):307–315, 2 2006.

[195] Jayne Loughery, Miranda Cox, Linda M. Smith, and David W. Meek. Critical role for p53-serine 15 phosphorylation in stimulating transactivation at p53-responsive promoters. *Nucleic Acids Research*, 42(12):7666, 8 2014.

[196] Marc S. Wold. Replication protein A: a heterotrimeric, single-stranded DNA-binding protein required for eukaryotic DNA metabolism. *Annu Rev. Biochem*, 66:61–92, 1997.

[197] Vitaly M. Vassin, Rachel William Anantha, Elena Sokolova, Shlomo Kanner, and James A. Borowiec. Human RPA phosphorylation by ATR stimulates DNA synthesis and prevents ssDNA accumulation during DNA-replication stress. *Journal of Cell Science*, 122(22):4070–4080, 11 2009.

[198] Felix E. Kemmerich, Peter Daldrop, Cosimo Pinto, Maryna Levikova, Petr Cejka, and Ralf Seidel. Force regulated dynamics of RPA on a DNA fork. *Nucleic Acids Research*, 44(12):5837, 7 2016.

[199] Luis Ignacio Toledo, Matthias Altmeyer, Maj Britt Rask, Claudia Lukas, Dorthe Helena Larsen, Lou Klitgaard Povlsen, Simon Bekker-Jensen, Niels Mailand, Jiri Bartek, and Jiri Lukas. ATR prohibits replication catastrophe by preventing global exhaustion of RPA. *Cell*, 155(5):1088–1103, 11 2013.

[200] Alexis R. Barr, Samuel Cooper, Frank S. Heldt, Francesca Butera, Henriette Stoy, Jörg Mansfeld, Béla Novák, and Chris Bakal. DNA damage during S-phase mediates the proliferation-quiescence decision in the subsequent G1 via p21 expression. *Nature Communications 2017 8:1*, 8(1):1–17, 3 2017.

[201] Solveig A.S. Walles, Rong Zhou, and Eva Liliemark. DNA damage induced by etoposide; a comparison of two different methods for determination of strand breaks in DNA. *Cancer Letters*, 105(2):153–159, 8 1996.

[202] Thomas W. Glover, Carol Berger, Jane Coyle, and Barbara Echo. DNA polymerase alpha inhibition by aphidicolin induces gaps and breaks at common fragile sites in human chromosomes. *Human genetics*, 67(2):136–142, 7 1984.

[203] Brandon J. Lamarche, Nicole I. Orazio, and Matthew D. Weitzman. The MRN complex in double-strand break repair and telomere maintenance. *FEBS letters*, 584(17):3682–3695, 9 2010.

[204] Raquel Cuella-Martin, Catarina Oliveira, Helen E. Lockstone, Suzanne Snellenberg, Natalia Grolmusova, and J. Ross Chapman. 53BP1 Integrates DNA Repair and p53-Dependent Cell Fate Decisions via Distinct Mechanisms. *Molecular cell*, 64(1):51–64, 10 2016.

[205] Myriam Cuadrado, Barbara Martinez-Pastor, Matilde Murga, Luis I. Toledo, Paula Gutierrez-Martinez, Eva Lopez, and Oscar Fernandez-Capetillo. ATM regulates ATR chromatin loading in response to DNA double-strand breaks. *The Journal of Experimental Medicine*, 203(2):297, 2 2006.

[206] Konark Mukherjee, Seetharaman Parashuraman, Manoj Raje, and Amitabha Mukhopadhyay. SopE Acts as an Rab5-specific Nucleotide Exchange Factor and Recruits Non-prenylated Rab5 on Salmonella-containing Phagosomes to Promote Fusion with Early Endosomes. *Journal of Biological Chemistry*, 276(26):23607–23615, 6 2001.

[207] Ruchi Kumari and Parmjit Jat. Mechanisms of Cellular Senescence: Cell Cycle Arrest and Senescence Associated Secretory Phenotype. *Frontiers in Cell and Developmental Biology*, 9:485, 3 2021.

[208] Masataka Haneda, Eiji Kojima, Akihiko Nishikimi, Tadao Hasegawa, Izumi Nakashima, and Ken-Ichi Isobe. Protein phosphatase 1, but not protein phosphatase 2A, dephosphorylates DNA-damaging stress-induced phospho-serine 15 of p53. *Wiley Online Library*, 567(2-3):171–174, 6 2004.

[209] Nicholas R. Helps, Hazel M. Barker, Stephen J. Elledge, and Patricia T.W. Cohen. Protein phosphatase 1 interacts with p53BP2, a protein which binds to the tumour suppressor p53. *FEBS Letters*, 377(3):295–300, 12 1995.

[210] S. J. Lee, C. J. Lim, J. K. Min, J. K. Lee, Y. M. Kim, J. Y. Lee, M. H. Won, and Y. G. Kwon. Protein phosphatase 1 nuclear targeting subunit is a hypoxia inducible gene: Its role in post-translational modification of p53 and MDM2. *Cell Death and Differentiation*, 14(6):1106–1116, 6 2007.

[211] Adrián Campos and Andrés Clemente-Blanco. Cell Cycle and DNA Repair Regulation in the Damage Response: Protein Phosphatases Take Over the Reins. *International Journal of Molecular Sciences*, 21(2), 1 2020.

[212] Katsutoshi Oda, Hirofumi Arakawa, Tomoaki Tanaka, Koichi Matsuda, Chizu Tanikawa, Toshiki Mori, Hiroyuki Nishimori, Katsuyuki Tamai, Takashi Tokino, Yusuke Nakamura, and Yoichi Taya. p53AIP1, a potential mediator of p53-dependent

apoptosis, and its regulation by ser-46-phosphorylated p53. *Cell*, 102(6):849–862, 9 2000.

[213] Jian Yu, Lin Zhang, Paul M. Hwang, Kenneth W. Kinzler, and Bert Vogelstein. PUMA induces the rapid apoptosis of colorectal cancer cells. *Mol Cell*, 7(3):673–682, 3 2001.

[214] Katsunori Nakano and Karen H. Vousden. PUMA, a novel proapoptotic gene, is induced by p53. *Mol Cell*, 7(3):683–694, 3 2001.

[215] Brandon J. Aubrey, Gemma L. Kelly, Ana Janic, Marco J. Herold, and Andreas Strasser. How does p53 induce apoptosis and how does this relate to p53-mediated tumour suppression? *Cell Death & Differentiation 2018 25:1*, 25(1):104–113, 11 2017.

[216] Tsukasa Shibue, Kiyoshi Takeda, Eri Oda, Hiroshi Tanaka, Hideki Murasawa, Akinori Takaoka, Yasuyuki Morishita, Shizuo Akira, Tadatsugu Taniguchi, and Nobuyuki Tanaka. Integral role of Noxa in p53-mediated apoptotic response. *Genes Dev*, 17(18):2233–2238, 9 2003.

[217] Alejandra Hernandez-Segura, Simone Brandenburg, and Marco Demaria. Induction and validation of cellular senescence in primary human cells. *Journal of Visualized Experiments*, 2018(136):1–10, 2018.

[218] Slavica Dodig, Ivana Čepelak, and Ivan Pavić. Hallmarks of senescence and aging, 10 2019.

[219] Nathan Basisty, Abhijit Kale, Ok Hee Jeon, Chisaka Kuehnemann, Therese Payne, Chirag Rao, Anja Holtz, Samah Shah, Vagisha Sharma, Luigi Ferrucci, Judith Campisi, and Birgit Schilling. A proteomic atlas of senescence-associated secretomes for aging biomarker development. *PLoS biology*, 18(1):e3000599, 1 2020.

[220] Daniel Muñoz-Espín and Manuel Serrano. Cellular senescence: From physiology to pathology. *Nature Reviews Molecular Cell Biology*, 15(7):482–496, 2014.

[221] Antony Cougnoux, Guillaume Dalmasso, Ruben Martinez, Emmanuel Buc, Julien Delmas, Lucie Gibold, Pierre Sauvanet, Claude Darcha, Pierre Déchelotte, Mathilde Bonnet, Denis Pezet, Harald Wodrich, Arlette Darfeuille-Michaud, and Richard Bonnet. Bacterial genotoxin colibactin promotes colon tumour growth by inducing a senescence-associated secretory phenotype. *Gut*, 63(12):1932–1942, 12 2014.

[222] Tobias Eggert, Katharina Wolter, Juling Ji, Chi Ma, Tetyana Yevsa, Sabrina Klotz, José Medina-Echeverz, Thomas Longerich, Marshonna Forgues, Florian Reisinger, Mathias Heikenwalder, Xin Wei Wang, Lars Zender, and Tim F. Greten. Distinct Functions of Senescence-Associated Immune Responses in Liver Tumor Surveillance and Tumor Progression. *Cancer cell*, 30(4):533–547, 10 2016.

[223] Yossi Ovadya, Tomer Landsberger, Hanna Leins, Ezra Vadai, Hilah Gal, Anat Biran, Reut Yosef, Adi Sagiv, Amit Agrawal, Alon Shapira, Joseph Windheim, Michael Tsoory, Reinhold Schirmbeck, Ido Amit, Hartmut Geiger, and Valery Krizhanovsky. Impaired immune surveillance accelerates accumulation of senescent cells and aging. *Nature communications*, 9(1), 12 2018.

[224] Rohit Sharma. Perspectives on the dynamic implications of cellular senescence and immunosenescence on macrophage aging biology. *Biogerontology*, 22(6):571–587, 12 2021.

[225] Leane Perim Rodrigues, Vitória Rodrigues Teixeira, Thuany Alencar-Silva, Bianca Simonassi-Paiva, Rinaldo Wellerson Pereira, Robert Pogue, and Juliana Lott Carvalho. Hallmarks of aging and immunosenescence: Connecting the dots. *Cytokine & growth factor reviews*, 59:9–21, 6 2021.

[226] Angela E M Ibler, Mohamed ElGhazaly, Kathryn L Naylor, Natalia A Bulgakova, Sherif F. El-Khamisy, and Daniel Humphreys. Typhoid toxin exhausts the RPA response to DNA replication stress driving senescence and Salmonella infection. *Nature Communications*, 10(1):1–14, 2019.

[227] Riccardo Guidi, Lina Guerra, Laura Levi, Bo Stenerlöw, James G. Fox, Christine Josenhans, Maria G. Masucci, and Teresa Frisan. Chronic exposure to the cytolethal distending toxins of Gram-negative bacteria promotes genomic instability and altered DNA damage response. *Cellular Microbiology*, 15(1):98–113, 1 2013.

[228] Bruce J. Shenker, Lisa M. Walker, Ali Zekavat, Robert H. Weiss, and Kathleen Boesze-Battaglia. The Cell-Cycle Regulatory Protein p21CIP1/WAF1 Is Required for Cytolethal Distending Toxin (Cdt)-Induced Apoptosis. *Pathogens 2020, Vol. 9, Page 38*, 9(1):38, 1 2020.

[229] Miao Qian, Shuyang Cao, Tao Wang, Xiangming Xu, and Quan Zhang. Apoptosis triggered by cytolethal distending toxin B subunit of Helicobacter hepaticus is aggravated by autophagy inhibition in mouse hepatocytes. *Biochemical and Biophysical Research Communications*, 598:40–46, 4 2022.

[230] Xiao Ling Li, Murugan Subramanian, Matthew F. Jones, Ritu Chaudhary, Deepak K. Singh, Xinying Zong, Berkley Gryder, Sivasish Sindri, Min Mo, Aaron Schetter, Xinyu Wen, Swetha Parvathaneni, Dickran Kazandjian, Lisa M. Jenkins, Wei Tang, Fathi Elloumi, Jennifer L. Martindale, Maite Huarte, Yuelin Zhu, Ana I. Robles, Susan M. Frier, Frank Rigo, Maggie Cam, Stefan Ambs, Sudha Sharma, Curtis C. Harris, Mary Dasso, Kannanganattu V. Prasanth, and Ashish Lal. Long Noncoding RNA PURPL Suppresses Basal p53 Levels and Promotes Tumorigenicity in Colorectal Cancer. *Cell Reports*, 20(10):2408–2423, 9 2017.

[231] Suzzanne F. Bradley and Carol A. Kauffman. Aging and the response to Salmonella infection. *Exp. Gerontol.*, 25(1):75–80, 1990.

[232] Jae Sung Lim, Hyon E Choy, Sang Chul Park, Jung Min Han, Ik-Soon Jang, and Kyung A Cho. Caveolae-mediated entry of Salmonella typhimurium into senescent nonphagocytotic host cells. *Aging Cell*, 9(2):243–251, 4 2010.

[233] Ames WR and Robins M. Age and Sex as Factors in the Development of the Typhoid Carrier State, and a Method for Estimating Carrier Prevalence. *American journal of public health and the nation's health*, 33(3):221–230, 3 1943.

[234] Hana Blazkova, Katerina Krejcikova, Pavel Moudry, Teresa Frisan, Zdenek Hodny, and Jiri Bartek. Bacterial intoxication evokes cellular senescence with persistent DNA damage and cytokine signalling. *Journal of Cellular and Molecular Medicine*, 14(1-2):357–367, 2010.

[235] Mohamed ElGhazaly, Mark O Collins, Angela E M Ibler, and Daniel Humphreys. Typhoid toxin hijacks Wnt5a to potentiate TGFβ-mediated senescence and Salmonella infections. *bioRxiv*, page 2022.10.05.510870, 1 2022.

[236] Sarah L. Mathiasen, Laura Gall-Mas, Ioannis S. Pateras, Sofia D.P. Theodorou, Martin R.J. Namini, Morten B. Hansen, Océane C.B. Martin, Chella Krishna Vadivel, Konstantinos Ntostoglou, Deborah Butter, Michael Givskov, Carsten Geisler, Arne N. Akbar, Vassilis G. Gorgoulis, Teresa Frisan, Niels Ødum, and Thorbjørn Krejsgaard. Bacterial genotoxins induce T cell senescence. *Cell Rep*, 35(10), 6 2021.

[237] Ascel Samba-Louaka, Jorge M. Pereira, Marie Anne Nahori, Veronique Villiers, Ludovic Deriano, Mélanie A. Hamon, and Pascale Cossart. Listeria monocytogenes dampens the DNA damage response. *PLoS Pathog.*, 10(10):e1004470, 10 2014.

[238] Elsa Leitão, Ana Catarina Costa, Cláudia Brito, Lionel Costa, Rita Pombinho, Didier Cabanes, and Sandra Sousa. Listeria monocytogenes induces host DNA damage and delays the host cell cycle to promote infection. *Cell Cycle*, 13(6):928–940, 3 2014.

[239] Julien Mambu, Emilie Barilleau, Laetitia Fragnet-Trapp, Yves Le Vern, Michel Olivier, Guillaume Sadrin, Olivier Grépinet, Frédéric Taieb, Philippe Velge, and Agnès Wiedemann. Rck of Salmonella Typhimurium Delays the Host Cell Cycle to Facilitate Bacterial Invasion. *Frontiers in Cellular and Infection Microbiology*, 10:656, 11 2020.

[240] Jie Yu Liu, George P. Souroullas, Brian O. Diekman, Janakiraman Krishnamurthy, Brandon M. Hall, Jessica A. Sorrentino, Joel S. Parker, Garrett A. Sessions, Andrei V. Gudkov, and Norman E. Sharpless. Cells exhibiting strong p16 INK4a promoter activation in vivo display features of senescence. *Proceedings of the National Academy of Sciences of the United States of America*, 116(7):2603–2611, 2 2019.

[241] Christine Siegl, Bhupesh K. Prusty, Karthika Karunakaran, Jörg Wischhusen, and Thomas Rudel. Tumor suppressor p53 alters host cell metabolism to limit Chlamydia trachomatis infection. *Cell Reports*, 9(3):918–929, 2014.

[242] William E. Woodward. Volunteer studies of typhoid fever and vaccines. *Transactions of the Royal Society of Tropical Medicine and Hygiene*, 74(5):553–556, 1980.

[243] N. Leigh Anderson and Norman G. Anderson. The human plasma proteome: history, character, and diagnostic prospects. *Molecular & cellular proteomics : MCP*, 1(11):845–867, 2002.

[244] VA Piettre. On the separation of proteins of the serum. *Rendus de l'Académie des Sciences*, 1920.

[245] Maurice Landy. Enhancement of the immunogenicity of typhoid vaccine by retention of the V antigen. *American Journal of Epidemiology*, 58(2):148–164, 1953.

[246] Mathias Uhlén, Linn Fagerberg, Bjö M. Hallström, Cecilia Lindskog, Per Oksvold, Adil Mardinoglu, Åsa Sivertsson, Caroline Kampf, Evelina Sjöstedt, Anna Asplund, Ing Marie Olsson, Karolina Edlund, Emma Lundberg, Sanjay Navani, Cristina Al Khalili Szigyarto, Jacob Odeberg, Dijana Djureinovic, Jenny Ottosson Takanen, Sophia Hober, Tove Alm, Per Henrik Edqvist, Holger Berling, Hanna Tegel, Jan Mulder, Johan Rockberg, Peter Nilsson, Jochen M. Schwenk, Marica Hamsten, Kalle Von Feilitzen, Mattias Forsberg, Lukas Persson, Fredric Johansson, Martin Zwahlen, Gunnar Von Heijne, Jens Nielsen, and Fredrik Pontén. Tissue-based map of the human proteome. *Science*, 347(6220), 1 2015.

[247] Mathias Uhlén, Max J. Karlsson, Andreas Hober, Anne Sophie Svensson, Julia Scheffel, David Kotol, Wen Zhong, Abdellah Tebani, Linnéa Strandberg, Fredrik Edfors, Evelina Sjöstedt, Jan Mulder, Adil Mardinoglu, Anna Berling, Siri Ekblad, Melanie Dannemeyer, Sara Kanje, Johan Rockberg, Magnus Lundqvist, Magdalena Malm, Anna Luisa Volk, Peter Nilsson, Anna Månberg, Tea Dodig-Crnkovic, Elisa Pin, Martin Zwahlen, Per Oksvold, Kalle von Feilitzen, Ragna S. Häussler, Mun Gwan Hong, Cecilia Lindskog, Fredrik Ponten, Borbala Katona, Jimmy Vuu, Emil Lindström, Jens Nielsen, Jonathan Robinson, Burcu Ayoglu, Diana Mahdessian, Devin Sullivan, Peter Thul, Frida Danielsson, Charlotte Stadler, Emma Lundberg, Göran Bergström, Anders Gummesson, Bjørn G. Voldborg, Hanna Tegel, Sophia Hober, Björn Forsström, Jochen M. Schwenk, Linn Fagerberg, and Åsa Sivertsson. The human secretome. *Science Signaling*, 12(609), 11 2019.

[248] Aleksandra Makowiecka, Natalia Malek, Ewa Mazurkiewicz, Ewa Mrówczyńska, Dorota Nowak, and Antonina Joanna Mazur. Thymosin $\beta 4$ Regulates Focal Adhesion Formation in Human Melanoma Cells and Affects Their Migration and Invasion. *Frontiers in Cell and Developmental Biology*, 7:304, 12 2019.

[249] Krishnanand Padmanabhan, Hanna Grobe, Jonathan Cohen, Arad Soffer, Adnan Mahly, Orit Adir, Ronen Zaidel-Bar, and Chen Luxenburg. Thymosin β4 is essential for adherens junction stability and epidermal planar cell polarity. *Development (Cambridge)*, 147(23), 12 2020.

[250] Shean Jaw Chiou, Chan Chi Wang, Yan Shen Tseng, Yen Jung Lee, Shih Chieh Chen, Chi Hsien Chou, Lea Yea Chuang, Yi Ren Hong, Chi Yu Lu, Chien Chih Chiu, and Michel Chignard. A novel role for β2-microglobulin: a precursor of antibacterial chemokine in respiratory epithelial cells. *Scientific Reports 2016 6:1*, 6(1):1–12, 8 2016.

[251] Shean Jaw Chiou, Huey Jiun Ko, Chi Ching Hwang, and Yi Ren Hong. The Double-Edged Sword of Beta2-Microglobulin in Antibacterial Properties and Amyloid Fibril-Mediated Cytotoxicity. *International Journal of Molecular Sciences*, 22(12), 6 2021.

[252] W. M. Johnson and H. Lior. A new heat-labile cytolethal distending toxin (CLDT) produced by Escherichia coli isolates from clinical material. *Microbial Pathogenesis*, 4(2):103–113, 1988.

[253] Barbara Masschalck and Chris W. Michiels. Antimicrobial properties of lysozyme in relation to foodborne vegetative bacteria. *Critical reviews in microbiology*, 29(3):191–214, 2003.

[254] Xinxing Wang, Donna M. Driscoll, and Richard E. Morton. Molecular Cloning and Expression of Lipid Transfer Inhibitor Protein Reveals Its Identity with Apolipoprotein F. *Journal of Biological Chemistry*, 274(3):1814–1820, 1 1999.

[255] Jan Borén, Chris J. Packard, and Marja Riitta Taskinen. The Roles of ApoC-III on the Metabolism of Triglyceride-Rich Lipoproteins in Humans. *Frontiers in Endocrinology*, 11:474, 7 2020.

[256] Stephen Zewinger, Jochen Reiser, Vera Jankowski, Dalia Alansary, Eunsil Hahm, Sarah Triem, Mira Klug, Stefan J Schunk, David Schmit, Rafael Kramann, Christina Körbel, Emmanuel Ampofo, Matthias W Laschke, Simina-Ramona Selejan, Anna Paschen, Tobias Herter, Susanne Schuster, Günther Silbernagel, Martina Sester, Urban Sester, Gunter Aßmann, Robert Bals, Gerhard Kostner, Willi Jahnen-Dechent, Michael D Menger, Lucia Rohrer, Winfried März, Michael Böhm, Joachim Jankowski, Manfred Kopf, Eicke Latz, Barbara A Niemeyer, Danilo Fliser, Ulrich Laufs, and Thimoteus Speer. Apolipoprotein C3 induces inflammation and organ damage by alternative inflammasome activation. *Nature Immunology*.

[257] Ruedi Aebersold and Matthias Mann. Mass-spectrometric exploration of proteome structure and function. *Nature*, 537(7620):347–355, 9 2016.

[258] Shaza B. Zaghlool, Sapna Sharma, Megan Molnar, Pamela R. Matías-García, Mohamed A. Elhadad, Melanie Waldenberger, Annette Peters, Wolfgang Rathmann, Johannes Graumann, Christian Gieger, Harald Grallert, and Karsten Suhre. Revealing the role of the human blood plasma proteome in obesity using genetic drivers. *Nature Communications 2021 12:1*, 12(1):1–13, 2 2021.

[259] Marcus A. Rothschild, Murray Oratz, and Sidney S. Schreiber. Serum albumin. *Hepatology (Baltimore, Md.)*, 8(2):385–401, 1988.

[260] Robert W Mahley, Thomas L Innerarity, Stanley C Rall, and Karl H Weisgraber. I I revzezo Plasma lipoproteins: apolipoprotein structure and function. *Journal Lipid Research*, 25:1277–1294, 1984.

[261] Marek H. Dominiczak and Muriel J. Caslake. Apolipoproteins: Metabolic role and clinical biochemistry applications. *Annals of Clinical Biochemistry*, 48(6):498–515, 11 2011.

[262] Philipp E Geyer, Eugenia Voytik, Peter V Treit, Sophia Doll, Alisa Kleinhempel, Lili Niu, Johannes B Müller, Marie-Luise Buchholtz, Jakob M Bader, Daniel Teupser, Lesca M Holdt, and Matthias Mann. Plasma Proteome Profiling to detect and avoid sample-related biases in biomarker studies. *EMBO Molecular Medicine*, 11(11), 11 2019.

[263] Chengjian Tu, Paul A. Rudnick, Misti Y. Martinez, Kristin L. Cheek, Stephen E. Stein, Robbert J.C. Slebos, and Daniel C. Liebler. Depletion of abundant plasma proteins and limitations of plasma proteomics. *Journal of Proteome Research*, 9(10):4982–4991, 10 2010.

[264] Elisa Bellei, Stefania Bergamini, Emanuela Monari, Luca Isaia Fantoni, Aurora Cuoghi, Tomris Ozben, and Aldo Tomasi. High-abundance proteins depletion for serum proteomic analysis: concomitant removal of non-targeted proteins. *Amino acids*, 40(1):145–156, 1 2011.

[265] Paola Picotti and Ruedi Aebersold. Selected reaction monitoring-based proteomics: workflows, potential, pitfalls and future directions. *Nature methods*, 9(6):555–566, 6 2012.

[266] Tatjana Sajic, Yansheng Liu, and Ruedi Aebersold. Using data-independent, high-resolution mass spectrometry in protein biomarker research: perspectives and clinical applications. *Proteomics. Clinical applications*, 9(3-4):307–321, 4 2015.

[267] Philipp E Geyer, Lesca M Holdt, Daniel Teupser, and Matthias Mann. Revisiting biomarker discovery by plasma proteomics. *Molecular Systems Biology*, 13(9):942, 9 2017.

[268] Philipp E. Geyer, Nils A. Kulak, Garwin Pichler, Lesca M. Holdt, Daniel Teupser, and Matthias Mann. Plasma Proteome Profiling to Assess Human Health and Disease. *Cell Systems*, 2(3):185–195, 3 2016.

[269] Andrew D. Skol, Laura J. Scott, Gonçalo R. Abecasis, and Michael Boehnke. Joint analysis is more efficient than replication-based analysis for two-stage genome-wide association studies. *Nature genetics*, 38(2):209–213, 2 2006.

[270] A Fleming and By A lexander F leming. On a remarkable bacteriolytic element found in tissues and secretions. *Proceedings of the Royal Society of London. Series B, Containing Papers of a Biological Character*, 93(653):306–317, 5 1922.

[271] R. T. Ellison and T. J. Giehl. Killing of gram-negative bacteria by lactoferrin and lysozyme. *Journal of Clinical Investigation*, 88(4):1080–1091, 1991.

[272] Sriram Varahan, Vijayalakshmi S. Iyer, William T. Moore, and Lynn E. Hancock. Eep confers lysozyme resistance to enterococcus faecalis via the activation of the extracytoplasmic function sigma factor SigV. *Journal of Bacteriology*, 195(14):3125–3134, 2013.

[273] Brian C. Cunningham, Mark Ultsch, Abraham M. De Vos, Michael G. Mulkerrin, Karl R. Clauser, and James A. Wells. Dimerization of the extracellular domain of the human growth hormone receptor by a single hormone molecule. *Science (New York, N.Y.)*, 254(5033):821–825, 1991.

[274] K. D. May, J. E. Wells, C. V. Maxwell, and W. T. Oliver. Granulated lysozyme as an alternative to antibiotics improves growth performance and small intestinal morphology of 10-day-old pigs. *Journal of animal science*, 90(4):1118–1125, 4 2012.

[275] J. E. Wells, E. D. Berry, N. Kalchayanand, L. A. Rempel, M. Kim, and W. T. Oliver. Effect of lysozyme or antibiotics on faecal zoonotic pathogens in nursery pigs. *Journal of applied microbiology*, 118(6):1489–1497, 6 2015.

[276] Stephanie A. Ragland and Alison K. Criss. From bacterial killing to immune modulation: Recent insights into the functions of lysozyme. *PLoS Pathogens*, 13(9), 9 2017.

[277] Lien Callewaert and Chris W. Michiels. Lysozymes in the animal kingdom. *Journal of Biosciences 2010 35:1*, 35(1):127–160, 2 2010.

[278] Melanie Derde, Valérie Lechevalier, Catherine Guérin-Dubiard, Marie Françoise Cochet, Sophie Jan, Florence Baron, Michel Gautier, Véronique Vié, and Françoise Nau. Hen egg white lysozyme permeabilizes Escherichia coli outer and inner membranes. *Journal of Agricultural and Food Chemistry*, 61(41):9922–9929, 10 2013.

[279] Xiaolin Zhang, Anmin Jiang, Hao Yu, Youyi Xiong, Guoliang Zhou, Meisong Qin, Jinfeng Dou, and Jianfei Wang. Human Lysozyme Synergistically Enhances Bactericidal Dynamics and Lowers the Resistant Mutant Prevention Concentration for Metronidazole to Helicobacter pylori by Increasing Cell Permeability. *Molecules 2016, Vol. 21, Page 1435*, 21(11):1435, 10 2016.

[280] Jie Liu, James A. Platts-Mills, Jane Juma, Furqan Kabir, Joseph Nkeze, Catherine Okoi, Darwin J. Operario, Jashim Uddin, Shahnawaz Ahmed, Pedro L. Alonso, Martin Antonio, Stephen M. Becker, William C. Blackwelder, Robert F. Breiman, Abu S.G. Faruque, Barry Fields, Jean Gratz, Rashidul Haque, Anowar Hossain, M. Jahangir Hossain, Sheikh Jarju, Farah Qamar, Najeeha Talat Iqbal, Brenda Kwambana, Inacio Mandomando, Timothy L. McMurry, Caroline Ochieng, John B. Ochieng, Melvin Ochieng, Clayton Onyango, Sandra Panchalingam, Adil Kalam, Fatima Aziz, Shahida Qureshi, Thandavarayan Ramamurthy, James H. Roberts, Debasish Saha, Samba O. Sow, Suzanne E. Stroup, Dipika Sur, Boubou Tamboura, Mami Taniuchi, Sharon M. Tennant, Deanna Toema, Yukun Wu, Anita Zaidi, James P. Nataro, Karen L. Kotloff, Myron M. Levine, and Eric R. Houpt. Use of quantitative molecular diagnostic methods to identify causes of diarrhoea in children: a reanalysis of the GEMS case-control study. *The Lancet*, 388(10051):1291–1301, 9 2016.

[281] Dina M. Tawfik, Jacqueline M. Lankelma, Laurence Vachot, Elisabeth Cerrato, Alexandre Pachot, W. Joost Wiersinga, and Julien Textoris. Comparison of host immune responses to LPS in human using an immune profiling panel, in vivo endotoxemia versus ex vivo stimulation. *Scientific Reports 2020 10:1*, 10(1):1–10, 6 2020.

[282] Jolanta Lukasiewicz and Czeslaw Lugowski. Editorial: O-specific polysaccharide confers lysozyme resistance to extraintestinal pathogenic Escherichia coli. *Virulence*, 9(1):919, 1 2018.

[283] Patrizia Ferraboschi, Samuele Ciceri, and Paride Grisenti. Applications of Lysozyme, an Innate Immune Defense Factor, as an Alternative Antibiotic. *Antibiotics (Basel, Switzerland)*, 10(12), 12 2021.

[284] D S Goodsell. Lysozyme. *RCSB Protein Data Bank*, 9 2000.

[285] Ko Willems Van Dijk, Patrick C.N. Rensen, Peter J. Voshol, and Louis M. Havekes. The role and mode of action of apolipoproteins CIII and AV: synergistic actors in triglyceride metabolism? *Current opinion in lipidology*, 15(3):239–246, 6 2004.

[286] Peter J Thul, Lovisa Akesson, Mikaela Wiking, Diana Mahdessian, Aikaterini Geladaki, Hammou Ait Blal, Tove Alm, Anna Asplund, Lars Björk, Lisa M Breckels, Anna Bäckström, Frida Danielsson, Linn Fagerberg, Jenny Fall, Laurent Gatto, Christian Gnann, Sophia Hober, Martin Hjelmare, Fredric Johansson, Sunjae Lee, Cecilia Lindskog, Jan Mulder, Claire M Mulvey, Peter Nilsson, Per Oksvold, Johan Rockberg,

Rutger Schutten, Jochen M Schwenk, Asa Sivertsson, Evelina Sjöstedt, Marie Skogs, Charlotte Stadler, Devin P Sullivan, Hanna Tegel, Casper Winsnes, Cheng Zhang, Martin Zwahlen, Adil Mardinoglu, Fredrik Pontén, Kalle Von Feilitzen, Kathryn S Lilley, Mathias Uhlén, and Emma Lundberg. A subcellular map of the human proteome. *Science*, 356(6340), 5 2017.

[287] Wen Qin, Meenakshi Sundaram, Yuwei Wang, Hu Zhou, Shumei Zhong, Chia Ching Chang, Sanjay Manhas, Erik F. Yao, Robin J. Parks, Pamela J. McFie, Scot J. Stone, Zhenghui G. Jiang, Congrong Wang, Daniel Figeys, Weiping Jia, and Zemin Yao. Missense Mutation in APOC3 within the C-terminal Lipid Binding Domain of Human ApoC-III Results in Impaired Assembly and Secretion of Triacylglycerol-rich Very Low Density Lipoproteins: EVIDENCE THAT ApoC-III PLAYS A MAJOR ROLE IN THE FORMATION OF LIPID P. *Journal of Biological Chemistry*, 286(31):27769–27780, 8 2011.

[288] Miek C. Jong, Marten H. Hofker, and Louis M. Havekes. Role of ApoCs in lipoprotein metabolism: functional differences between ApoC1, ApoC2, and ApoC3. *Arterioscle-rosis, thrombosis, and vascular biology*, 19(3):472–484, 1999.

[289] Christina Khoo, Hannia Campos, Helena Judge, and Frank M. Sacks. Effects of estrogenic oral contraceptives on the lipoprotein B particle system defined by apolipoproteins E and C-III content. *Journal of Lipid Research*, 40(2):202–212, 2 1999.

[290] Jinxiong Wei, Jennifer Noto, Elena Zaika, Judith Romero-Gallo, Pelayo Correa, Wael El-Rifai, Richard M. Peek, and Alexander Zaika. Pathogenic bacterium Helicobacter pylori alters the expression profile of p53 protein isoforms and p53 response to cellular stresses. *Proc. Natl Acad. Sci. USA*, 109(38):E2543–E2550, 9 2012.

[291] Yan Qu, Shahram Misaghi, Kim Newton, Allie Maltzman, Anita Izrael-Tomasevic, David Arnott, and Vishva M. Dixit. NLRP3 recruitment by NLRC4 during Salmonella infection. *Journal of Experimental Medicine*, 213(6):877–885, 5 2016.

[292] Xingyin Liu, Rong Lu, Shaoping Wu, Yong Guo Zhang, Yinglin Xia, R. Balfour Sartor, and Jun Sun. Wnt2 inhibits enteric bacterial-induced inflammation in intestinal epithelial cells. *Inflammatory Bowel Diseases*, 18(3):418–429, 3 2012.

[293] Alessandro Costa, Rahul Gupta, Giacomo Signorino, Antonio Malara, Francesco Cardile, Carmelo Biondo, Angelina Midiri, Roberta Galbo, Patrick Trieu-Cuot, Salvatore Papasergi, Giuseppe Teti, Philipp Henneke, Giuseppe Mancuso, Douglas T. Golenbock, and Concetta Beninati. Activation of the NLRP3 inflammasome by group B streptococci. *Journal of immunology (Baltimore, Md. : 1950)*, 188(4):1953–1960, 2 2012.

[294] Ryan G. Gaudet, Shiwei Zhu, Anushka Halder, Bae Hoon Kim, Clinton J. Bradfield, Shuai Huang, Dijin Xu, Agnieszka Mamiñska, Thanh Ngoc Nguyen, Michael Lazarou,

Erdem Karatekin, Kallol Gupta, and John D. MacMicking. A human apolipoprotein L with detergent-like activity kills intracellular pathogens. *Science (New York, N.Y.)*, 373(6552), 7 2021.

[295] Daniel A. Saltzman, Emmanuel Katsanis, Charles P. Heise, Diane E. Hasz, Vladimir Vigdorovich, Sandra M. Kelly, Roy Curtiss, Arnold S. Leonard, and Peter M. Anderson. Antitumor mechanisms of attenuated Salmonella typhimurium containing the gene for human interleukin-2: A novel antitumor agent? *Journal of Pediatric Surgery*, 32(2):301–306, 1997.

[296] Manja Barthel, Siegfried Hapfelmeier, Leticia Quintanilla-Martínez, Marcus Kremer, Manfred Rohde, Michael Hogardt, Klaus Pfeffer, Holger Rüssmann, and Wolf Dietrich Hardt. Pretreatment of mice with streptomycin provides a Salmonella enterica serovar Typhimurium colitis model that allows analysis of both pathogen and host. *Infection and immunity*, 71(5):2839–2858, 5 2003.

[297] K. P. Nickerson, S. Senger, Y. Zhang, R. Lima, S. Patel, L. Ingano, W. A. Flavahan, D. K.V. Kumar, C. M. Fraser, C. S. Faherty, M. B. Sztein, M. Fiorentino, and A. Fasano. Salmonella Typhi Colonization Provokes Extensive Transcriptional Changes Aimed at Evading Host Mucosal Immune Defense During Early Infection of Human Intestinal Tissue. *EBioMedicine*, 31:92–109, 5 2018.

[298] Tanya T. Paull, Emmy P. Rogakou, Vikky Yamazaki, Cordula U. Kirchgessner, Martin Gellert, and William M. Bonner. A critical role for histone H2AX in recruitment of repair factors to nuclear foci after DNA damage. *Current biology : CB*, 10(15):886–895, 8 2000.

[299] Richard B. Van Breemen and Yongmei Li. Caco-2 cell permeability assays to measure drug absorption. *Expert opinion on drug metabolism & toxicology*, 1(2):175–185, 8 2005.

[300] Per Artursson, Katrin Palm, and Kristina Luthman. Caco-2 monolayers in experimental and theoretical predictions of drug transport. *Advanced drug delivery reviews*, 46(1-3):27–43, 3 2001.

[301] Patrick G. Pilié, Chad Tang, Gordon B. Mills, and Timothy A. Yap. State-of-the-art strategies for targeting the DNA damage response in cancer. *Nature Reviews Clinical Oncology 2018 16:2*, 16(2):81–104, 10 2018.

[302] Rasika N. Jinadasa, Stephen E. Bloom, Robert S. Weiss, and Gerald E. Duhamel. Cytolethal distending toxin: A conserved bacterial genotoxin that blocks cell cycle progression, leading to apoptosis of a broad range of mammalian cell lineages. *Microbiology*, 157(7):1521–1875, 7 2011.

[303] Lidiya Luzhna, Palak Kathiria, and Olga Kovalchuk. Micronuclei in genotoxicity assessment: from genetics to epigenetics and beyond. *Frontiers in Genetics*, 4(JUL), 2013.

[304] Hong Zhao and Zbigniew Darzynkiewicz. Biomarkers of Cell Senescence Assessed by Imaging Cytometry. *Methods in molecular biology (Clifton, N.J.)*, 965:83, 2013.

[305] Alexandre Maréchal and Lee Zou. DNA Damage Sensing by the ATM and ATR Kinases. *Cold Spring Harbor Perspectives in Biology*, 5(9), 9 2013.

[306] David Cortez. Caffeine inhibits checkpoint responses without inhibiting the ataxia-telangiectasia-mutated (ATM) and ATM- and Rad3-related (ATR) protein kinases. *The Journal of biological chemistry*, 278(39):37139–37145, 9 2003.

[307] Robert Sheaff, Diane Ilsley, and Robert Kuchta. Mechanism of DNA polymerase alpha inhibition by aphidicolin. *Biochemistry*, 30(35):8590–8597, 9 1991.

[308] I. Torsteinsdóttir, L. Håkansson, R. Hällgren, B. Gudbjörnsson, N. G. Arvidson, and P. Venge. Serum lysozyme: a potential marker of monocyte/macrophage activity in rheumatoid arthritis. *Rheumatology*, 38(12):1249–1254, 12 1999.

[309] Tregei Starr, Timothy J. Bauler, Preeti Malik-Kale, and Olivia Steele-Mortimer. The phorbol 12-myristate-13-acetate differentiation protocol is critical to the interaction of THP-1 macrophages with Salmonella Typhimurium. *PLOS ONE*, 13(3):e0193601, 3 2018.

[310] E. W. Baxter, A. E. Graham, N. A. Re, I. M. Carr, J. I. Robinson, S. L. Mackie, and A. W. Morgan. Standardized protocols for differentiation of THP-1 cells to macrophages with distinct M(IFNγ+LPS), M(IL-4) and M(IL-10) phenotypes. *Journal of immunological methods*, 478, 3 2020.

[311] Jonathan M. Stokes, Craig R. Macnair, Bushra Ilyas, Shawn French, Jean Philippe Côté, Catrien Bouwman, Maya A. Farha, Arthur O. Sieron, Chris Whitfield, Brian K. Coombes, and Eric D. Brown. Pentamidine sensitizes Gram-negative pathogens to antibiotics and overcomes acquired colistin resistance. *Nature Microbiology*, 2, 3 2017.

[312] Thomas Clairfeuille, Kerry R. Buchholz, Qingling Li, Erik Verschueren, Peter Liu, Dewakar Sangaraju, Summer Park, Cameron L. Noland, Kelly M. Storek, Nicholas N. Nickerson, Lynn Martin, Trisha Dela Vega, Anh Miu, Janina Reeder, Maria Ruiz-Gonzalez, Danielle Swem, Guanghui Han, Daniel P. DePonte, Mark S. Hunter, Cornelius Gati, Sheerin Shahidi-Latham, Min Xu, Nicholas Skelton, Benjamin D. Sellers, Elizabeth Skippington, Wendy Sandoval, Emily J. Hanan, Jian Payandeh, and Steven T. Rutherford. Structure of the essential inner membrane lipopolysaccharide-PbgA complex. *Nature*, 584(7821):479–483, 8 2020.

[313] Robert I. Lehrer, Charles L. Bevins, and Tomas Ganz. Defensins and Other Antimicrobial Peptides and Proteins. *Mucosal Immunology*, page 95, 2005.

[314] Edward A. Miao and Jayant V. Rajan. Salmonella and Caspase-1: A complex interplay of detection and evasion. *Frontiers in Microbiology*, 2(APR), 2011.

[315] Susan L. Fink and Brad T. Cookson. Caspase-1-dependent pore formation during pyroptosis leads to osmotic lysis of infected host macrophages. *Cellular Microbiology*, 8(11):1812–1825, 11 2006.

[316] Madeleine A. Wemyss and Jaclyn S. Pearson. Host Cell Death Responses to Non-typhoidal Salmonella Infection. *Frontiers in immunology*, 10:1758, 2019.

[317] W. T. Oliver and J. E. Wells. Lysozyme as an alternative to growth promoting antibiotics in swine production. *Journal of Animal Science and Biotechnology*, 6(1), 8 2015.

[318] Jie Wang, Lixia Kang, Di Song, Lu Liu, Shuai Yang, Lingling Ma, Zhixiang Guo, Huaxia Ding, Hui Wang, and Bo Yang. Ku70 Senses HTLV-1 DNA and Modulates HTLV-1 Replication. *The Journal of Immunology*, 199(7):2475–2482, 10 2017.

[319] Nicole J. Darling, Claire L. Mobbs, Ariana L. González-Hau, Matthew Freer, and Stefan Przyborski. Bioengineering Novel in vitro Co-culture Models That Represent the Human Intestinal Mucosa With Improved Caco-2 Structure and Barrier Function. *Frontiers in Bioengineering and Biotechnology*, 8:992, 8 2020.

[320] Ramesh M. Ray, Sujoy Bhattacharya, and Leonard R. Johnson. Mdm2 inhibition induces apoptosis in p53 deficient human colon cancer cells by activating p73- and E2F1-mediated expression of PUMA and Siva-1. *Apoptosis : an international journal on programmed cell death*, 16(1):35–44, 1 2011.

[321] Mahmut Mijit, Valentina Caracciolo, Antonio Melillo, Fernanda Amicarelli, and Antonio Giordano. Role of p53 in the Regulation of Cellular Senescence. *Biomolecules*, 10(3), 3 2020.

[322] B. Masschalck, R. Van Houdt, E. G.R. Van Haver, and W. C. Michiels. Inactivation of Gram-Negative Bacteria by Lysozyme, Denatured Lysozyme, and Lysozyme-Derived Peptides under High Hydrostatic Pressure. *Applied and Environmental Microbiology*, 67(1):339, 2001.

[323] Arjun Sukumaran, Elizabeth Woroszchuk, Taylor Ross, Jennifer Geddes-McAlister, A Sukumaran, E Woroszchuk, T Ross, and J Geddes-McAlister. Proteomics of host-bacterial interactions: new insights from dual perspectives. *Can. J. Microbiol. Downloaded from cdnsciencepub*, 67:213–225, 2021.

[324] Julien Karim Malet, Francis Impens, Filipe Carvalho, Mélanie Anne Hamon, Pascale Cossart, and David Ribet. Rapid remodeling of the host epithelial cell proteome by the listeriolysin O (LLO) pore-forming toxin. *Molecular and Cellular Proteomics*, 17(8):1627–1636, 8 2018.

[325] Thomas C. Darton, Liqing Zhou, Christoph J. Blohmke, Claire Jones, Claire S. Waddington, Stephen Baker, and Andrew J. Pollard. Blood culture-PCR to optimise typhoid fever diagnosis after controlled human infection identifies frequent asymptomatic cases and evidence of primary bacteraemia. *Journal of Infection*, 74(4):358–366, 4 2017.

[326] Abhai Kumar, Smita Singh, Suneel Kumar Ahirwar, and Gopal Nath. Proteomics-based identification of plasma proteins and their association with the host–pathogen interaction in chronic typhoid carriers. *International Journal of Infectious Diseases*, 19(1):59–66, 2 2014.

[327] Elin Näsström, Pär Jonsson, Anders Johansson, Sabina Dongol, Abhilasha Karkey, Buddha Basnyat, Nga Tran Vu Thieu, Tan Trinh Van, Guy E Thwaites, Henrik Antti, and Stephen Baker. Diagnostic metabolite biomarkers of chronic typhoid carriage. *PLOS Neglected Tropical Diseases*, 12(1):e0006215, 1 2018.

[328] Zia A Khan, Hana Farhangkhoee, Jeffery L Mahon, Lynda Bere, John R Gonder, Bosco M Chan, Shashi Uniyal, and Subrata Chakrabarti. Endothelins: Regulators of Extracellular Matrix Protein Production in Diabetes:. *https://doi.org/10.3181/00379727-231-2311022*, 8 2017.

[329] Winnie W. Hui, Kamil Hercik, Sayali Belsare, Navatha Alugubelly, Beata Clapp, Carlos Rinaldi, and Mariola J. Edelmann. Salmonella enterica serovar Typhimurium alters the extracellular proteome of macrophages and leads to the production of proinflammatory exosomes. *Infection and Immunity*, 86(2), 2 2018.

[330] Darja Žgur-Bertok. DNA Damage Repair and Bacterial Pathogens. *PLoS Pathogens*, 9(11), 11 2013.

[331] John K. Won and Samuel F. Bakhoum. The cytosolic DNA-sensing cGAS–sting pathway in cancer. *Cancer Discovery*, 10(1):26–39, 1 2020.

[332] Gilles Berger, Mickaël Marloye, and Sean E. Lawler. Pharmacological Modulation of the STING Pathway for Cancer Immunotherapy. *Trends in Molecular Medicine*, 25(5):412–427, 5 2019.

[333] Benoît J. Pons, Aurélie Pettes-Duler, Claire Naylies, Frédéric Taieb, Catherine Bouchenot, Saleha Hashim, Patrick Rouimi, Maxime Deslande, Yannick Lippi, Gladys Mirey, and Julien Vignard. Chronic exposure to Cytolethal Distending Toxin (CDT)

promotes a cGAS-dependent type I interferon response. *Cellular and Molecular Life Sciences*, 78(17-18):6319–6335, 9 2021.

[334] Karen J. MacKenzie, Paula Carroll, Carol Anne Martin, Olga Murina, Adeline Fluteau, Daniel J. Simpson, Nelly Olova, Hannah Sutcliffe, Jacqueline K. Rainger, Andrea Leitch, Ruby T. Osborn, Ann P. Wheeler, Marcin Nowotny, Nick Gilbert, Tamir Chandra, Martin A.M. Reijns, and Andrew P. Jackson. CGAS surveillance of micronuclei links genome instability to innate immunity. *Nature*, 548(7668):461–465, 8 2017.

[335] Shane M. Harding, Joseph L. Benci, Jerome Irianto, Dennis E. Discher, Andy J. Minn, and Roger A. Greenberg. Mitotic progression following DNA damage enables pattern recognition within micronuclei. *Nature*, 548(7668):466–470, 8 2017.

[336] Haipeng Liu, Haiping Zhang, Xiangyang Wu, Dapeng Ma, Juehui Wu, Lin Wang, Yan Jiang, Yiyan Fei, Chenggang Zhu, Rong Tan, Peter Jungblut, Gang Pei, Anca Dorhoi, Qiaoling Yan, Fan Zhang, Ruijuan Zheng, Siyu Liu, Haijiao Liang, Zhonghua Liu, Hua Yang, Jianxia Chen, Peng Wang, Tianqi Tang, Wenxia Peng, Zhangsen Hu, Zhu Xu, Xiaochen Huang, Jie Wang, Haohao Li, Yilong Zhou, Feng Liu, Dapeng Yan, Stefan H.E. Kaufmann, Chang Chen, Zhiyong Mao, and Baoxue Ge. Nuclear cGAS suppresses DNA repair and promotes tumorigenesis. *Nature*, 563(7729):131–136, 11 2018.

[337] Hui Jiang, Xiaoyu Xue, Swarupa Panda, Ajinkya Kawale, Richard M Hooy, Fengshan Liang, Jungsan Sohn, Patrick Sung, and Nelson O Gekara. Chromatin-bound cGAS is an inhibitor of DNA repair and hence accelerates genome destabilization and cell death. *EMBO J*, 38(21), 11 2019.

[338] Christian Zierhut, Norihiro Yamaguchi, Maria Paredes, Ji Dung Luo, Thomas Carroll, and Hironori Funabiki. The Cytoplasmic DNA Sensor cGAS Promotes Mitotic Cell Death. *Cell*, 178(2):302–315, 7 2019.

[339] Gillian Dunphy, Sinéad M. Flannery, Jessica F. Almine, Dympna J. Connolly, Christina Paulus, Kasper L. Jønsson, Martin R. Jakobsen, Michael M. Nevels, Andrew G. Bowie, and Leonie Unterholzner. Non-canonical activation of the DNA sensing adaptor STING by ATM and IFI16 mediates NF-κB signaling after nuclear DNA damage. *Mol Cell*, 71(5):745–760, 9 2018.

[340] Prabhat K. Purbey, Philip O. Scumpia, Peter J. Kim, Ann Jay Tong, Keisuke S. Iwamoto, William H. McBride, and Stephen T. Smale. Defined Sensing Mechanisms and Signaling Pathways Contribute to the Global Inflammatory Gene Expression Output Elicited by Ionizing Radiation. *Immunity*, 47(3):421–434, 9 2017.

[341] Anetta Härtlova, Saskia F. Erttmann, Faizal A.M. Raffi, Anja M. Schmalz, Ulrike Resch, Sharath Anugula, Stefan Lienenklaus, Lisa M. Nilsson, Andrea Kröger, Jonas A.

Nilsson, Torben Ek, Siegfried Weiss, and Nelson O. Gekara. DNA Damage Primes the Type I Interferon System via the Cytosolic DNA Sensor STING to Promote Anti-Microbial Innate Immunity. *Immunity*, 42(2):332–343, 2 2015.

[342] Saskia F. Erttmann, Anetta Härtlova, Marta Sloniecka, Faizal A.M. Raffi, Ava Hosseinzadeh, Tomas Edgren, Reza Rofougaran, Ulrike Resch, Maria Fällman, Torben Ek, and Nelson O. Gekara. Loss of the DNA Damage Repair Kinase ATM Impairs Inflammasome-Dependent Anti-Bacterial Innate Immunity. *Immunity*, 45(1):106–118, 7 2016.

[343] Andrew Lopez, Randilea Nichols Doyle, Carina Sandoval, Karly Nisson, Vivian Yang, and Oliver I. Fregoso. Viral Modulation of the DNA Damage Response and Innate Immunity: Two Sides of the Same Coin. *Journal of Molecular Biology*, 434(6):167327, 3 2022.

[344] Christine Siegl and Thomas Rudel. Modulation of p53 during bacterial infections. *Nature Reviews Microbiology 2015 13:12*, 13(12):741–748, 11 2015.

[345] Erik González, Marion Rother, Markus C. Kerr, Munir A. Al-Zeer, Mohammad Abu-Lubad, Mirjana Kessler, Volker Brinkmann, Alexander Loewer, and Thomas F. Meyer. Chlamydia infection depends on a functional MDM2-p53 axis. *Nature Communications*, 5, 11 2014.

[346] Laura Oliveira-Nascimento, Paola Massari, and Lee M. Wetzler. The role of TLR2 ininfection and immunity. *Frontiers in Immunology*, 3(APR):79, 2012.

[347] Leigh A. Knodler, Shauna M. Crowley, Ho Pan Sham, Hyungjun Yang, Marie Wrande, Caixia Ma, Robert K. Ernst, Olivia Steele-Mortimer, Jean Celli, and Bruce A. Vallance. Noncanonical inflammasome activation of caspase-4/caspase-11 mediates epithelial defenses against enteric bacterial pathogens. *Cell host & microbe*, 16(2):249–256, 8 2014.

[348] Mikael E. Sellin, Anna A. Müller, Boas Felmy, Tamas Dolowschiak, Médéric Diard, Aubry Tardivel, Kendle M. Maslowski, and Wolf Dietrich Hardt. Epithelium-intrinsic NAIP/NLRC4 inflammasome drives infected enterocyte expulsion to restrict Salmonella replication in the intestinal mucosa. *Cell host & microbe*, 16(2):237–248, 8 2014.

[349] Anna M. Gram, John A. Wright, Robert J. Pickering, Nathaniel L. Lam, Lee M. Booty, Steve J. Webster, and Clare E. Bryant. Salmonella Flagellin Activates NAIP/NLRC4 and Canonical NLRP3 Inflammasomes in Human Macrophages . *The Journal of Immunology*, 206(3):631–640, 2 2021.

[350] Lisa A. Cummings, W. David Wilkerson, Tessa Bergsbaken, and Brad T. Cookson. In vivo, fliC expression by Salmonella enterica serovar Typhimurium is heterogeneous,

regulated by ClpX, and anatomically restricted. *Molecular Microbiology*, 61(3):795–809, 8 2006.

[351] Edward A. Miao, Irina A. Leaf, Piper M. Treuting, Dat P. Mao, Monica Dors, Anasuya Sarkar, Sarah E. Warren, Mark D. Wewers, and Alan Aderem. Caspase-1-induced pyroptosis is an innate immune effector mechanism against intracellular bacteria. *Nature Immunology*, 11(12):1136–1142, 12 2010.

[352] Zhongde Ye, Elaine O. Petrof, David Boone, Erika C. Claud, and Jun Sun. Salmonella effector AvrA regulation of colonic epithelial cell inflammation by deubiquitination. *American Journal of Pathology*, 171(3):882–892, 2007.

[353] Gaëlle Le Negrate, Benjamin Faustin, Kate Welsh, Markus Loeffler, Maryla Krajewska, Patty Hasegawa, Sohini Mukherjee, Kim Orth, Stan Krajewski, Adam Godzik, Donald G. Guiney, and John C. Reed. Salmonella secreted factor L deubiquitinase of Salmonella typhimurium inhibits NF-kappaB, suppresses IkappaBalpha ubiquitination and modulates innate immune responses. *Journal of immunology (Baltimore, Md. : 1950)*, 180(7):5045–5056, 4 2008.

[354] Sebastian E. Winter, Maria G. Winter, Vidya Atluri, Victor Poon, Everton L. Romão, Renée M. Tsolis, and Andreas J. Bäumler. The flagellar regulator TviA reduces pyroptosis by Salmonella enterica serovar Typhi. *Infection and Immunity*, 83(4):1546–1555, 2015.

[355] Sachiko Araki and Sataro Goto. Dietary restriction in aged mice can partially restore impaired metabolism of apolipoprotein A-IV and C-III. *Biogerontology*, 5(6):445–450, 11 2004.

[356] Sidhartha Giri, Venkata Raghava Mohan, Manikandan Srinivasan, Nirmal Kumar, Vinoth Kumar, Pavithra Dhanapal, Jayalakshmi Venkatesan, Annai Gunasekaran, Dilip Abraham, Jacob John, and Gagandeep Kang. Case-Control Study of Household and Environmental Transmission of Typhoid Fever in India. *The Journal of Infectious Diseases*, 224(Supplement_5):S584–S592, 11 2021.

[357] Elizabeth J. Klemm, Sadia Shakoor, Andrew J. Page, Farah Naz Qamar, Kim Judge, Dania K. Saeed, Vanessa K. Wong, Timothy J. Dallman, Satheesh Nair, Stephen Baker, Ghazala Shaheen, Shahida Qureshi, Mohammad Tahir Yousafzai, Muhammad Khalid Saleem, Zahra Hasan, Gordon Dougan, and Rumina Hasan. Emergence of an extensively drug-resistant Salmonella enterica serovar typhi clone harboring a promiscuous plasmid encoding resistance to fluoroquinolones and third-generation cephalosporins. *mBio*, 9(1), 1 2018.